Generation of a Geological database for the Liquefaction hazard assessment in Kathmandu valley

By

Birendra Kumar Piya

March 2004

Generation of a Geological database for Liquefaction hazard assessment in Kathmandu valley

By

Birendra Kumar Piya

Thesis submitted to the International Institute for Geo-information Science and Earth Observation in partial fulfilment of the requirements for the degree of Master of Science in Earth Resources and Environmental Geoscience with the specialisation in Natural Hazard Studies.

Degree Assessment Board

Prof. Dr. F.D. (Freek) van der Meer **(Chairman)**
Prof. Dr. S.B. Kroonenberg **(External Examiner), Delft University**
Dr. C.J. (Cees) van Westen **(First Supervisor)**
Dr. T. (Tsehaie) Woldai **(Second Supervisor)**
Dr. P. M. (Paul) van Dijk **(Internal Examiner)**

ITC

INTERNATIONAL INSTITUTE FOR GEO-INFORMATION SCIENCE AND EARTH OBSERVATION
ENSCHEDE, THE NETHERLANDS

I certify that although I may have conferred with others in preparing for this assignment, and drawn upon a range of sources cited in this work, the content of this thesis report is my original work.
Signed …………………….

Disclaimer

This document describes work undertaken as part of a programme of study at the International Institute for Geo-information Science and Earth Observation. All views and opinions expressed therein remain the sole responsibility of the author, and do not necessarily represent those of the institute.

Acknowledgements

This research study has become possible as a result of the opportunity offered to me by the International institute for Geoinformation Science and Earth Observation (ITC), which nominated me for the second time to continue my studies for M.Sc, after obtaining a PM degree in Earth Resources and Environmental Geosciences (EREG) with specialisation on Natural Hazard Studies. For this, I am very much indebted to ITC. Further, I would like to express my hearty gratitude to the Netherlands Government for providing me a fellowship (NFP) without which the study was impossible.

My sincere and very much respectful gratitude goes to my supervisor Dr. Cees van Westen who encouraged me to apply for the second time to complete the M.Sc course and to involve me in SLARIM research project of ITC in Lalitpur, Nepal. Though my contribution is less in this project, it is of significance. He supervised my work with enthusiasm and devotion, I am very much grateful to him for his continuous guidance, criticism and valuable suggestions.

My sincere and respectful gratitude goes to my second supervisor Dr. T (**Tsehaie)** Woldai, who guided, advised and assisted me during my work. I am very much grateful to him for his continuous guidance, comments and for his valuable suggestions.

My sincere and respectful gratitude goes to the Program Director, Dr. P.M. (Paul) van Dijk who also kept eyes on me throughout the time as a guardian and encouraged me in my work.

My sincere and respectful gratitude goes to Professor Dr. F.D. (Freek) van der Meer, the head of the ESA department, to Drs. R. P.G.A (Robert) Voskuil, the student advisor and all other staff members of Earth Resources and Environmental Geosciences (EREG), and Earth System Analysis (ESA) for their continuous support and guidance.

My sincere thanks go to Dr. D.G. (David) Rossiter for his guidance in geostatistics.

I wish to express my sincere thanks and appreciation to Aiko Mulder, the cluster manager for his valuable help and assistance.

Thanks go to all ITC staff members for their help in one or other way.

I wish to express my thanks to my colleagues in my office (DMG) and to Consultancies, Soil test lab, Balaju; ESLA Soil test lab, Bashundhara; East drilling company; ITECO consultants; Nepal Geological Society and Geotech consultant Kathmandu for helping me to provide necessary data.

My thanks go to all my colleagues (M-Sc students) in the clusters 5.056: Angela Isabel-Cuba; Arturo Garrido Perez-Mexico; Ana Fonseco Escalante-Costarica; Jeewan Guragain-Nepal; Jenifer Otieno-Kenya; Jamali Hmbaruti-Tanzania; Maria Pérerra-Portugal; Syarif Budhiman-Indonesia; Marlina Purwadi-Indonesia; Maulida Suaib-Indonesia; Njoku Damian-Nigeria; Mohammad Abudaya-Palestine; Oyungerel Bayanjargal-Mongolia; Pablo Andrada de Palomera-Argentina; Tesfaya Kassa Mekonnen-Ethiopia and Umut Destegul-Turkey; who gave me company and helped in my work in one or other way and especially making the cluster like a homely environment.

Lastly but not the least, I wish to thank my dear wife Rajani Piya, who supported and helped me in my study by taking care of everything in my absence at home. My lovely thanks go to my daughter Rubiniya Piya and son, Rubin Piya for their patience in missing me. My thanks also go to all other members of my family for their kind support in many ways.

Abstract

As part of the ITC research project on "Strengthening Local Authorities in Risk Management (SLARIM)" the city of Lalitpur was selected as one of the case study cities for the development of a methodology for urban risk assessment, evaluation, and management.

Kathmandu valley is underlain by thick lacustrine sediments mainly composed of clay, locally called Kalimati (meaning black clay). It is a deposit of the so-called "Paleo-Kathmandu Lake" which was formed between 2 to 2.5 Ma B.P. The lacustrine materials are on top of coarse sand and gravel beds, which were formed by the so-called "Proto-Bagmati River system" of the valley. The thickness of lake sediment is found to be up to 304 m in the borehole at Harisiddhi south- eastern part of Lalitpur city,

The Quaternary materials in the Kathmandu valley are mainly lacustrine and fluvial in origin and are composed of clayey, silty, sandy and gravelly sediments. The maximum thickness of the sediments is found in the central and southern part of the valley (550 m at Bhrikutimandap, and greater than 457 m at Harisiddhi). The sedimentation process in the valley has taken place through series of stages. In this study, nine stages of sediment deposition have been differentiated based on the deepest borehole in the central part of the valley that has reached up to the bedrock.

A number of experts have already worked on the description and classification of these basin fill sediments from different aspects. Although at least 250 deep drillholes over 100 meters thickness and more than 100 shallow boreholes between 45 m to 100 m have made within the valley for different purposes, no one yet has compiled the detailed data and presented them in either digital or in an analogue form. Therefore in this research an attempt has been made to use borehole data in the generation of a subsurface geological database. The database stores all information described in the borehole log sheets such as lithological description, N-values, and other geotechnical information. Data files are named corresponding to the location of drilling sites so that one can easily refer to the required data.

A number of lithological cross sections and fence diagrams are also drawn that help to give a clear picture of the sediment distribution within the basin.

Kathmandu valley could be susceptible to liquefaction during a strong earthquake, due to its liquefiable soils (sand and silts), high groundwater level and potential strong earthquake motions in the region. The occurrence of liquefaction during the 1934 Bihar-Nepal earthquake has also been reported in some parts of the valley. Hence an attempt also has been made to prepare a liquefaction susceptibility map for the valley. A qualitative method was used for most of the area, supplemented by a quantitative analysis for certain boreholes with sufficient geotechnical information, following the method of Seed and Idriss (1971) and Iwasaki et al. (1984). The results of the qualitative and quantitative methods have been compared, and also a comparison has been made with earlier liquefaction susceptibility maps for the valley. The map is intended to give a general indication of liquefaction potential, and for the actual development purposes a more detailed site-specific investigation will be required.

Keywords: Urban risk assessment, Subsurface geological database, Borehole logs, Lithological cross sections, Fluvio-lacustrine sediments, Liquefaction susceptibility map, Earthquake intensity.

Table of Contents

List of Figures

LIST OF TABLES

List for Abbreviations / Acronyms

AGSO	Australian Geological Survey Organization
CBS	*Central bureau of statistics*
DMG	*Department of Mines and Geology*
DOI	Department of Irrigation
EGP	Environmental Geology Project
ENPHO	Environment and Public Health Organization
GIS	Geographic Information System
GSI	*Geological Survey of India*
HFF	Horizontal frontal fault
HMGN	His Majesty's Government of Nepal
JW	JICA Wells
JICA	Japan International Cooperation Agency
KVERMP	Kathmandu valley Earthquake Risk management Project.
KV	Kathmandu valley
MBT	Main Boundary Thrust
MCT	Main Central Thrust
MOHPP	Ministry of housing and physical planning
NWSC	*Nepal Water Supply and Sewerage Corporation*
NSET	National Society for Earthquake Technology
PGA	Peak Ground Acceleration
SLARIM	Strengthening Local authorities for Risk management
UNDP	United Nation Development Project
UTM	Universal Transverse Mercator
USCS	Unified Soil Classification System
UNCHS	United Nations Centre for Human Settlements
WHO	World Health Organization

1. Introduction

1.1. Background

The study area Kathmandu valley (KV) is situated between latitude 27^0 32'N to 27^0 49'16" N and longitude $85^0$13'28" E to $85^0$31'53" E. The location map of the study area is shown in Figure 1.1. The valley contains three main historical cities: Kathmandu (the capital of Kingdom of Nepal), Lalitpur and Bhaktapur, and parts of the city centres (enlisted as world heritage sites by UNESCO). Kathmandu valley is a fast growing city with a population of approximately 1.8 million people (CBS, 2001). The settlement within the valley is developing haphazardly without proper planning.

Kath

The valley is filled by thick lacustrine and fluvial deposits, more than 550 m thick, which is Pliocene to Pleistocene in age (Yoshida and Gautam 1988). It has a roughly circular outline having an EW diameter of 30 Km and 25 Km in NS direction and is surrounded by the lesser Himalayas ranging from 2000 to 2800 meters above mean sea level. The basin is in the middle of the lesser Himalayas and bounded by the Phulchauki and Chandragiri hills to the South and Shivapuri hills to the North. The average altitude of the valley floor is 1,340 m above mean sea level with the lowest part having an elevation of 1,220 m at the southern end of the valley (Sakai, 2001).

The Kathmandu valley is characterized by a warm and temperate climate having average monthly maximum temperatures of 30 to 32^0 Celsius in summer (April) and average monthly minimum temperature of 3 to 1^0 Celsius in winter (January). The average rainfall measured from 1990 to 1999 is 1436.8 mm per year. The Bagmati, Bishnumati and Manahara rivers drain the Kathmandu valley with an outlet in the southeast of the valley through the Chobhar gorge, which flows dissecting the mountain of the lesser Himlaya range in the southeast before it finally join the Ganges River in India.

Kathmandu valley lies in a very active seismic zone. Several big earthquakes have impacted the city in the past. There have been numerous devastating earthquakes within living memory such as in 1934, 1960, and 1988. There were also significant historical earthquakes recorded in 1833 and in 1255. Due to lack of instruments and technical know how, these earthquakes were not recorded instrumentally in Nepal. According to reports, huge damage and casualties had occurred due to these events. Normally there are frequent small to medium size earthquakes occurring in different parts of the country with localized effect. Earthquakes are an unavoidable part of Nepal's future, just as they have been a part of its past. Nepal however, is becoming increasingly vulnerable to earthquakes with each passing year. This is due to the increasing population, uncontrolled urban development, and a construction practice that has actually deteriorated over the last century.

Scientists (Haresh Shaha, Chairman World Seismic safety Initiative WSSI, an exclusive interview to the times of India, Wednesday September 5, 2001 and R.Bilham et al., 2001) have predicted a great earthquake of magnitude greater than 8 Richter scale to occur in future in this part affecting many people. The earthquake of 1934 with magnitude of 8.4 Richter scale that caused huge losses in Kathmandu and its surroundings is still fresh in the memory of the people of Nepal. The official record shows that in Kathmandu valley alone 4,296 people were killed and 55,739 houses were completely or partly destroyed (Rana, 1935). Rana has also reported about the occurrence of liquefaction in some of the places in Kathmandu valley in his book entitled “Great earthquake of Nepal” (Rana, 1935).

Looking at the urbanization of Kathmandu valley now, if a similar earthquake as that of 1934 was to occur today, the scenario would be devastating, and the fatalities would be very high. For that earthquake scenario, the Japan International Cooperation Agency (JICA, 2002) estimated up to 59,000 houses destroyed, 20,000 deaths and 59,000 seriously injured. Another study carried out in the framework of the Kathmandu Valley Earthquake Risk Management Project (Dixit et.al., 1999) estimate a total of 40,000 deaths, 95,000 injuries and 600,000 or more homeless for the same scenario earthquake. This situation has created the necessity for carrying out a detailed seismic hazard assessment of the city and an awareness building measures to the people of Kathmandu valley regarding the earthquake safety. It is also important to carryout more earthquake vulnerability reduction programs in Kathmandu valley.

For such an earthquake vulnerability program, data concerning the subsurface geology as well as geological structures is very important. Knowledge on such features plays a key role in the generation of damaging phenomena during an earthquake. A good knowledge of the subsurface soil conditions is very important for the assessment of local site response for sensitivity analysis (Destegul, 2004), building vulnerability analysis (Guragain, 2004), road and infrastructures vulnerability analysis (Tung, 2004; Islam, 2004) etc. As Kathmandu valley is extremely vulnerable to damaging earthquakes, it is highly important that the local authorities take their responsibility in the vulnerability reduction process so that the future loss of lives and damage can be minimized. The current research fits well into the on going ITC-SLARIM research whose purpose is to strengthen local authorities in medium sized cities in risk management for seismic and flood hazard.

With SLARIM 2002 (“Strengthening Local Authorities in Risk management”) ITC aims to develop a methodology for spatial information systems for municipalities, so that it allows the local authorities to evaluate the risk of natural disasters in their municipality in order to implement strategies for vulnerability reduction. In the SLARIM Project Lalitpur city was chosen as a case study. Seven M.Sc students including the author with different subjects are involved in this research project. The success of the project depends upon the collection and management of trustworthy spatial data using RS and GIS tools. The collection of existing borehole data and its proper management and preparation for Liquefaction hazard map forms the primary basis of the current research.

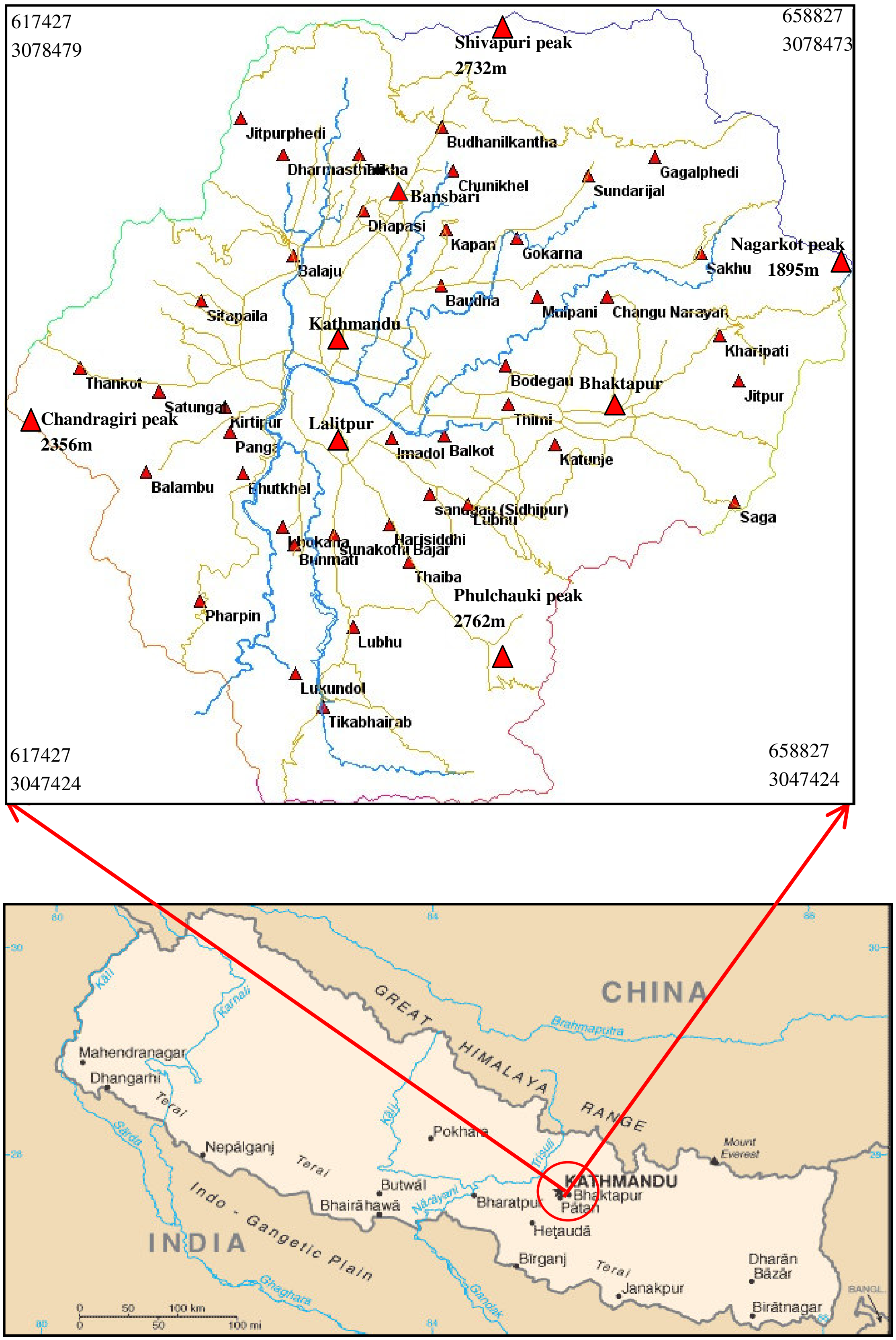

Figure 1.1: Location map of the study area

1.2. Earthquake threats and its mitigation measures in Kathmandu Valley

The Kathmandu valley area is potentially prone to Earthquake hazard as it is located in an active seismic zone. Several big earthquakes have impacted the city in the past. There have been numerous devastating earthquakes within living memory such as in 1934, 1960, and 1988. There were also significant historical earthquakes recorded in 1833 and in 1255. Huge damage and casualties have occurred due to these events. Although there have been reports on major earthquake events and damages caused by them in the valley during the last 8 centuries, for most intensity, magnitude, epicenter and actual records of damages are not recorded or mentioned in any existing literatures so far known. The Table 1.1 indicates the distribution of earthquakes in the study area for which the intensity, magnitude and epicenter were recorded. The data was collected from different sources. Similarly, the frequency of earthquake events in Nepal for magnitude greater than 5 Richter scale is shown in Figure 1.2.

Table 1.1: Distribution of earthquake near Kathmandu (Source: JICA 2002, UNDP/UNCHS 1994, Pandey, M.R. et al.., 2001)

Date	Magnitude	Intensity	Latitude	Longitude	Epicenter dist. (Km)	Assumed PGA (gal)
1255/6/7	7.7(assumed)	X	NA	NA	Near KTM	NA
1408	NA	X	NA	NA	Near KTM	NA
1681	7 (assumed)	IX	NA	NA	Near KTM	NA
1810	NA	IX	NA	NA	NA	NA
1833	7		28	85	38	137
1833/8/26	7	X	27	85	84	75
1833/10/4	7	IX	27	85	151(Kalaiya)	47
1833/10/18	7	VIII	27	84	India	NA
1866/23/05	7	X	27.7	85.3	Kathmandu	NA
1869/7/7	7		28	85	45	121
1934/1/15	8.4	IX-X	27.55	87	177 (North of Chainpur)	188
1936/5/27	7	NA	28.50	83.5	199	38
1954/9/4	6.5	NA	28.30	83.8	163	34
1988/8/20	6.5		26.75	86.62	167 (Udayapur)	36

Note: NA here represents data not available

From Table 1.1, it is evident that major destruction in the Kathmandu valley has taken place during the earthquake in 1833 and 1934. The records on Table 1.2 shows that, in 1833, a 7 Richter scale in magnitude earthquake caused the damage of 18000 houses, 43 people death and 30 injured (JICA, 2002). In reality there were much more casualties. Similarly in the 1934 earthquake 12,397 houses collapsed, and 43,342 houses were partially damaged, the death toll were 4296 within the Kathmandu valley alone (Rana, 1935). The earthquake of 1934 is also known as the Bihar-Nepal earthquake, the epicenter of which was located some 177 Km East of Kathmandu at a place North of Chainpur. The latter epicenter however is rather debatable. As shown in Figure 1.3 (Rana, 1935), most of the damages in 1934 occurred in the southern part of the valley such as in Bungamati, Khokana, Lubhu, Sunakothi, and Bhaktapur (see Figure 1.1 for location). Rana reported in his book ("Nepalko Maha Bhukampa – The great earthquake of Nepal") that 99 percent of houses were damaged or destroyed in those villages. Whereas in Kathmandu city 70 percent of the houses were damaged or destroyed. Even the present royal palace was heavily damaged and the then King had to loose 2 of his daughters (Rana, 1935). On the other hand, not much damaged was accounted in Gokarna, Sundarijal and Kirtipur area. According to him, earthquake induced fissures were developed in some streets and fields, which were 10 to 15 m deep and water ejected through those fissures. The rivers were flooded with black color mud, and at some places hot water with sand was also ejected. The scene of destruction in Kathmandu valley by 1934 earthquake is given in plates (1-14).

Auden and Ghosh (1935) measured the intensity of 1934 earthquake and prepared an intensity distribution map (Figure 1.4). The intensity map prepared by them and damage map (Figure 1.3) prepared by Rana (1935) were correlated. According to Pandey and Molnar (1988), the population and number of houses in 1920 in the Kathmandu valley were 306,909 and 66,440 respectively. Whereas according to the 1991 census the population of Kathmandu valley was 1,105,379 and according to that of 2001 it was 1,653,951. If we compare the present population with that of 1920, we find that the population has increased by almost 5 times or more. The population distribution of different cities according to the national censuses of 1991 and 2001 is given in Table 1.3. From the table we can find out that, from 1920 till 2001 the population has increased with 1,350,042. Similarly, the urbanized area in Kathmandu valley has extensively increased from that of 1920. We can compare the urban area in Lalitpur city from two images (IKONOS-2001, and CORONA-1967) as shown in Figure 1.6 and 1.7. We can see that there has been a tremendous increase in urban area in the last decades. The chart in Figure 1.5 below shows the population increased since 1800. The red triangles indicate major earthquakes that occurred.

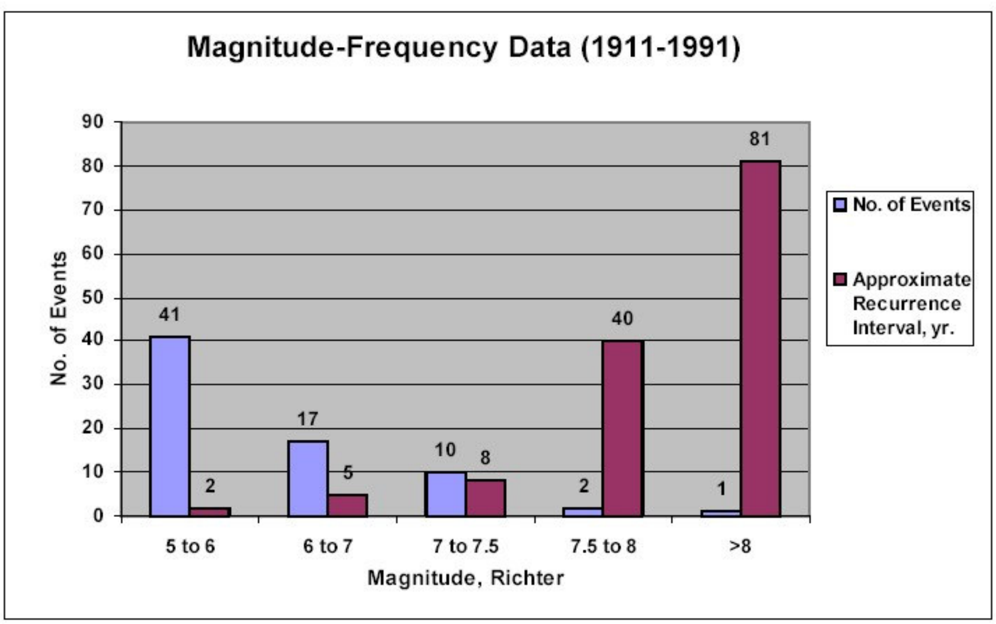

Figure 1.2: Magnitude Frequency data (Source: N-SET)

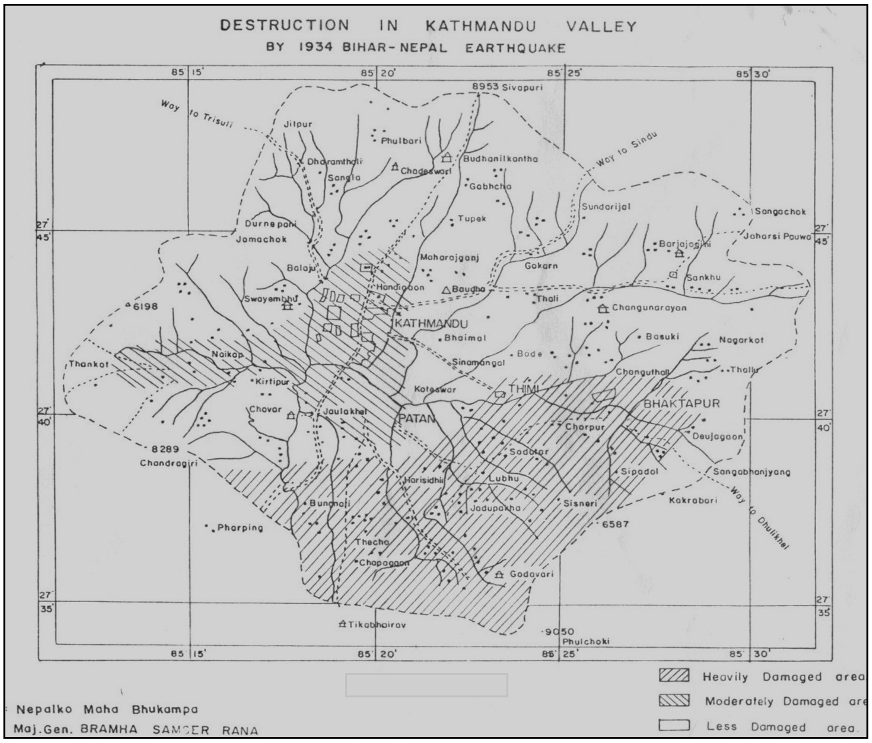

Figure 1.3: Damage map of Kathmandu valley by 1934 Bihar-Nepal Earthquake (Source: Pandey et al., DMG)

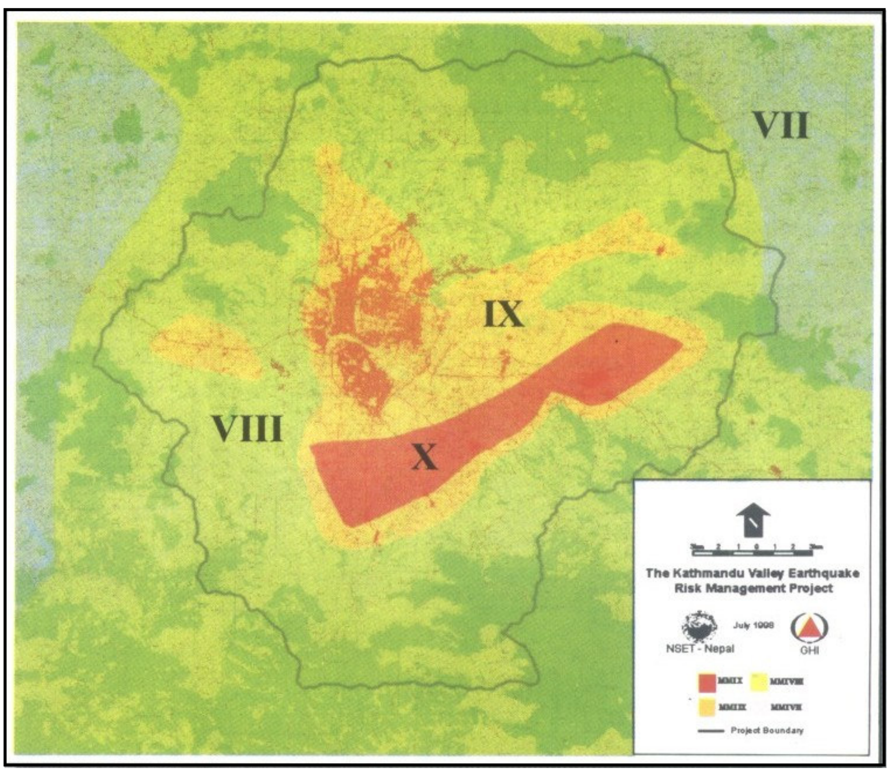

Figure 1.4: Intensity distribution map of the valley for 1934 earthquake (M-8.4) (Source: N-SET)

Table 1.2: Damage made by past and recent earthquakes in Kathmandu valley (source: JICA, 2002 N-SET, 2002; Rana, 1935);

Year	Date	Earthquake Epicenter	Human		Building/Temples	
			Death	Injuries	Collapsed	Damaged
1988	21 Aug	Udayapur	8	71	650	1814
1934	15 Jan	Bihar/ Nepal	4296	NA	12,397	43,342
1837`	17 Jan	NA	NA	NA	NA	NA
1833	26 Aug	NA	43	30	18,000	NA
	25 Sept	NA	NA	NA	NA	NA
1823	NA	NA	NA	NA	NA	NA
1810	May	NA	Moderate		Many buildings and Temples collapsed	
1767	Jun	NA	NA	NA	NA	NA
1681	NA	NA	Many	NA	Many buildings and Temples collapsed	
1408	NA	NA	Heavy		Many buildings and Temples collapsed	
1260	NA	NA	Heavy	NA/wide spread famine and epidemic	NA	NA
1255	07 Jun	NA	One third of the total population including King Abhaya Malla Killed		Many buildings and Temples collapsed.	

Table 1.3: Population distribution in Kathmandu valley in 1920, 1991 and 2001(Source: CBS, 2001)

District	1920 Total	1991 census			2001 census		
		Male	Female	Total	Male	Female	Total
Lalitpur	306909	130,326	126,760	257,086	171,822	164,855	336,677
Bhaktapur		86,818	86,134	172,952	115,487	111,373	226,860
Kathmandu		351,316	324,025	655,341	581,361	512,053	1,093,414
Total		568,460	536,919	1,105,379	868,670	788,281	1,656,951

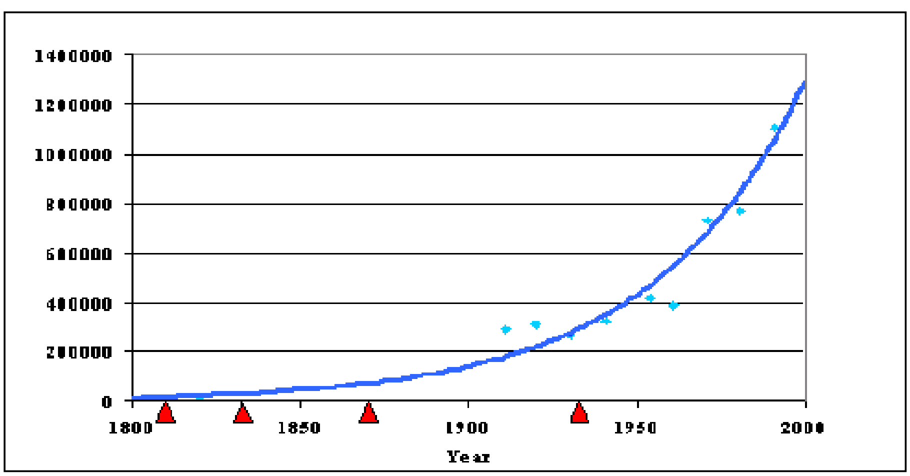

Figure 1.5: The trend of population increase in Kathmandu valley (Source N-SET)

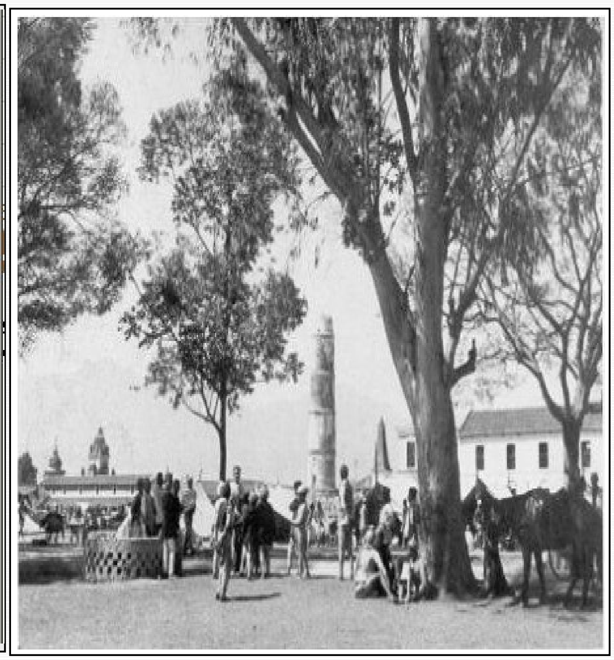

Plate1.1: The historical monument Bhimsen tower before an earthquake (Source: N-SET)

Plate 1.2: The historical monument Bhimsen tower after an earthquake (Source: N-SET)

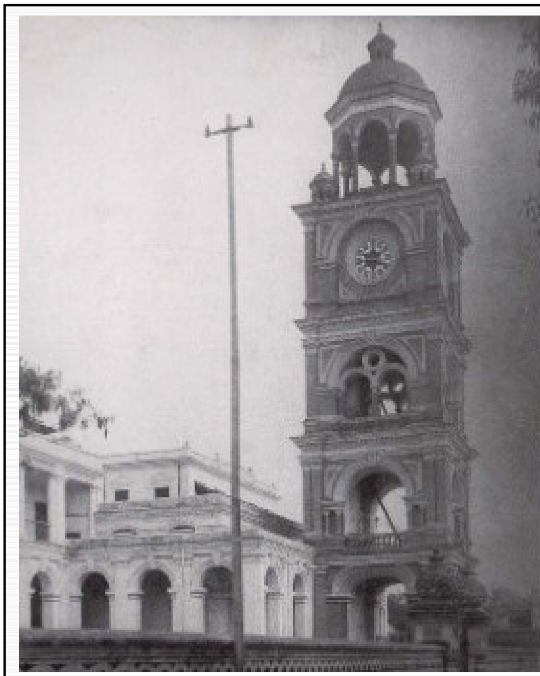

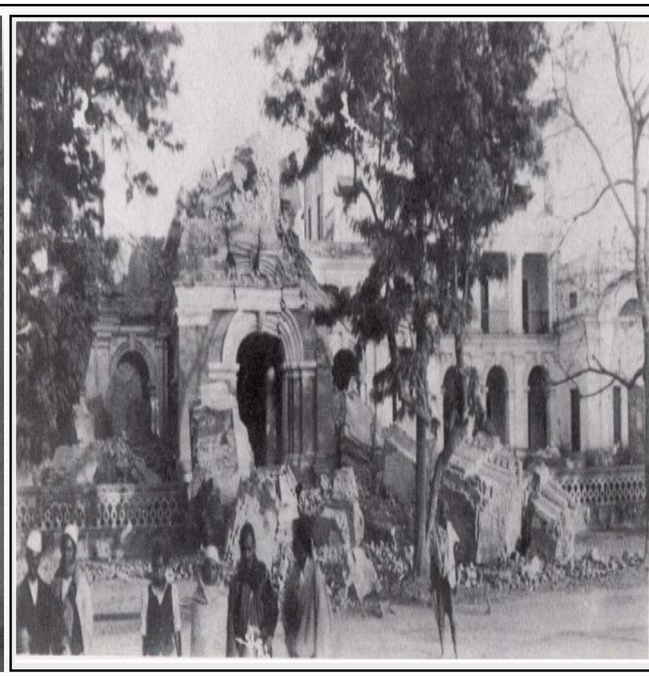

Plate 1.3: Historical monument Ghantaghar (Clock tower) before an earthquake of 1934 (Source: N-SET)

Plate 1.4: Historical monument Ghantaghar (Clock tower) after an earthquake of 1934 (Source: N-SET)

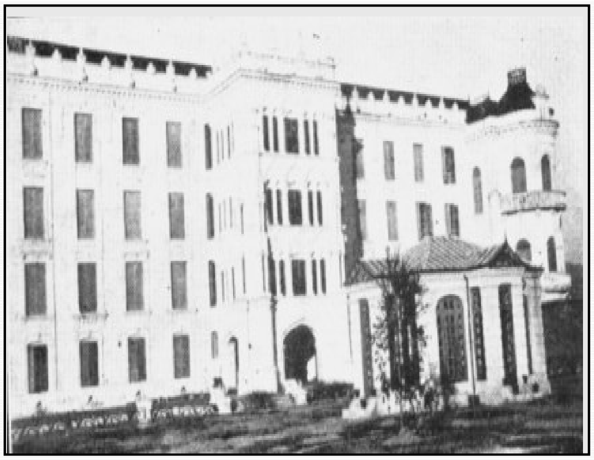

Plate 1.5: Sheetal Niwas (Now Ministry of Foreign affairs) before an earthquake (Rana, 1935)

Plate1 6: Sheetal Niwas (Now Ministry of Foreign affairs) after an earthquake (Rana, 1935).

Plate 1.7: Gol Baithak (Now Nepal National Bank) before the earthquake of 1934 (Rana, 1935)

Plate 1.8: Gol Baithak (Now Nepal National Bank) after the earthquake of 1934 (Rana, 1935)

Plate 1.9: Severe damage of the houses in 1934 earthquake (JICA, 2002)

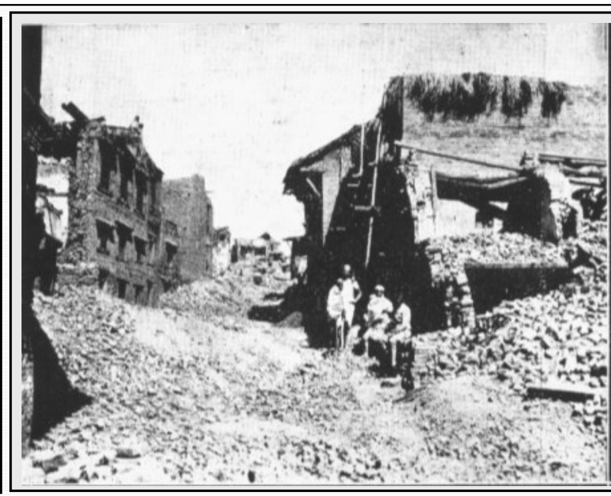

Plate 1.10: A damaged scene in a street of Bhaktapur city by 1934 earthquake (Rana, 1935)

Plate 1.11: A famous Bhairab Temple in Bhaktapur before an earthquake (Rana, 1935)

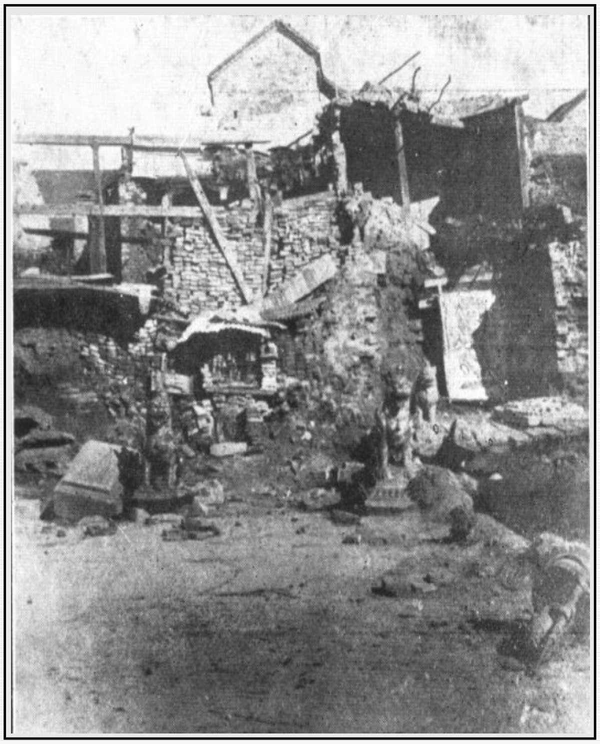

Plate 1.12: A famous Bhairab Temple in Bhaktapur after an earthquake (Rana, 1935)

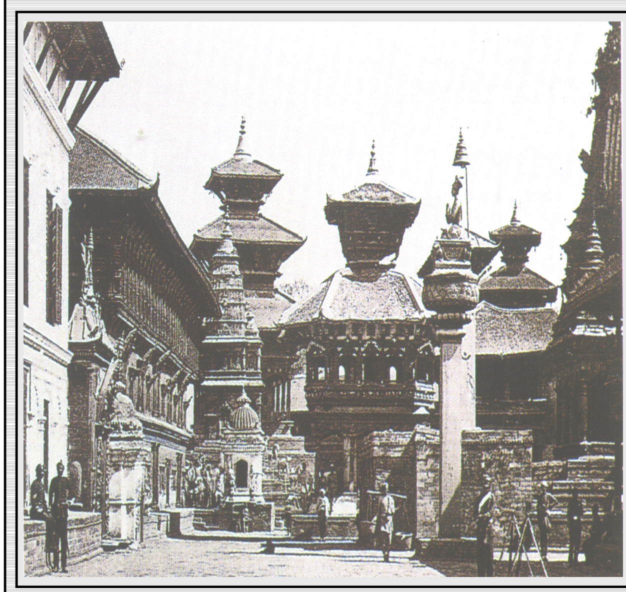

Plate 1.13: Bhaktapur Durbar square area before an earthquake of 1934 (Seismology section, DMG)

Plate 1.14: Bhaktapur Durbar square area after an earthquake of 1934 (Seismology section, DMG)

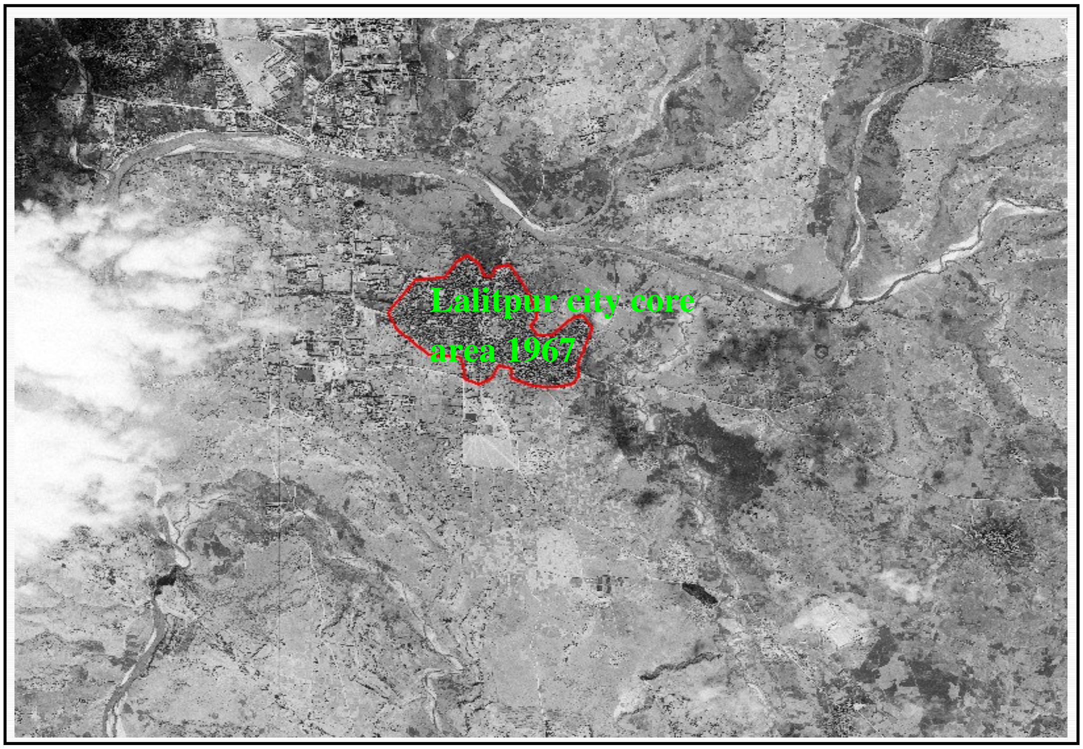

Figure 1.6: Urban area in 1967 in Lalitpur city (Corona image 1967).

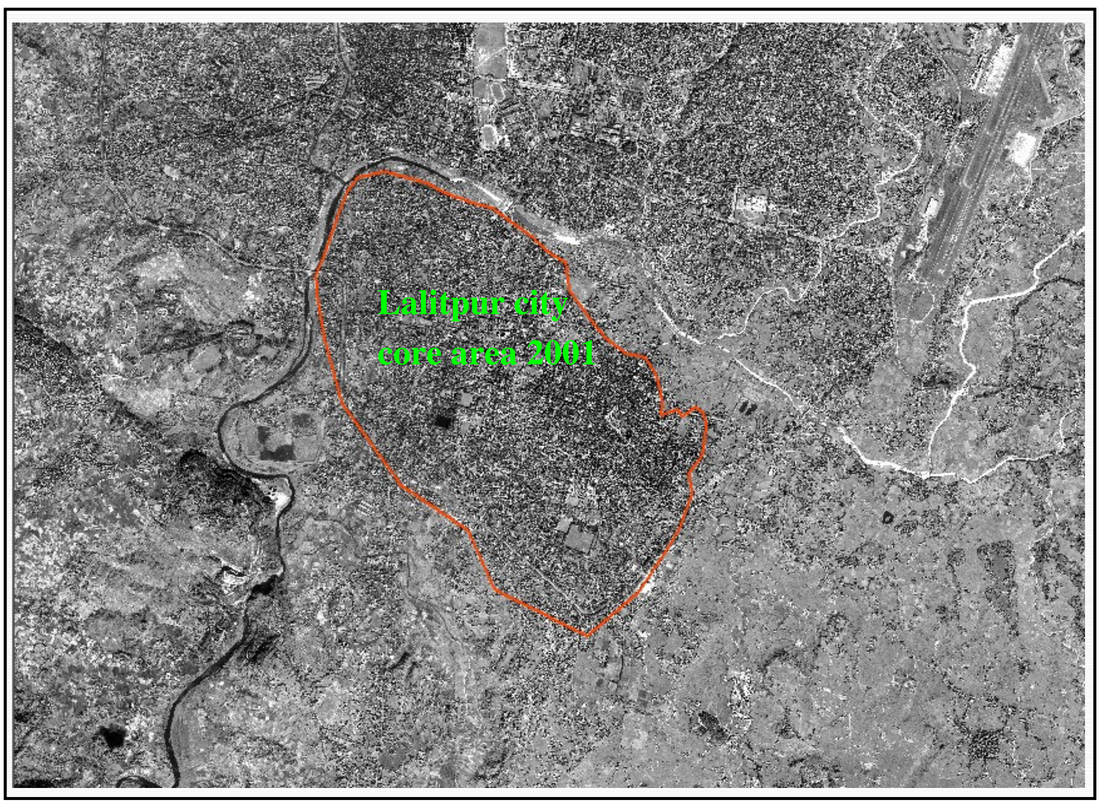

Figure 1.7: Urban area in 2001 in Lalitpur city (IKONOS image 2001)

Looking at the urbanization of Kathmandu valley now (See plate 15-16), if a similar earthquake like that of 1833 or 1934 was to occur today, the scenario will be totally devastating and the fatalities would be very high. This situation has created the necessity for carrying out a detailed seismic hazard assessment of the city and an awareness building measures, to the people of Kathmandu valley regarding the earthquake safety. Despite this growing risk, there was no institution, government or otherwise, concerned with this issue and working towards mitigating the earthquake risk till the early nineties. Presently, only the non-governmental Organization N-SET (National Society for Earthquake Technology) is working for earthquake awareness in Nepal (http://www.nset.org.np/home.htm).

The National Society for Earthquake Technology (N-SET) was established in 1993 as a professional society to confront this problem. It was officially registered with His Majesty's Government of Nepal as a non-government, non-profit organisation in 1994. Since then, NSET has been involved in the Kathmandu Valley Earthquake Risk Management Project (KVERMP) that subsequently led to the development and implementation of the Kathmandu Valley Earthquake Risk Management Action Plan in 1998. Since its establishment, it is giving a considerable contribution towards the preparedness and mitigation of Earthquake hazard in Nepal. It has been actively involved in bringing awareness about the need for earthquake vulnerability reduction to the people and schoolchildren by means of seminars, publication, workshops and exhibitions. It is also involved in training the local masons for building earthquake resistance houses and retrofitting the existing buildings. In the initiation of NSET, Nepal is marking national earthquake safety day on 16 January each year since 1998.

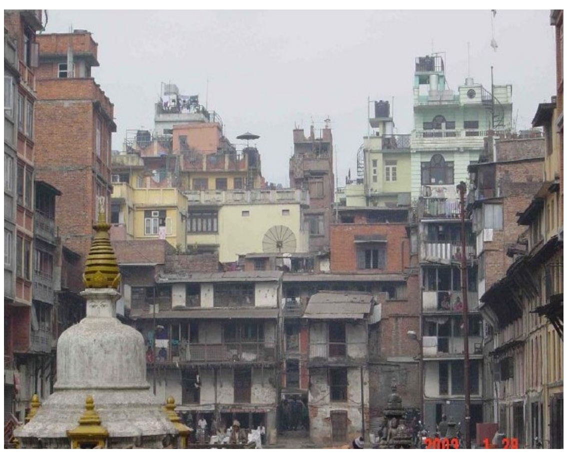

Plate15: Disorganised urbanization in Kathmandu valley (Source: N-SET)

Plate16: Disorganised urbanization in Kathmandu valley (Source: N-SET)

Besides this, a basic seismic hazard mapping and risk assessment for Nepal has been carried out by UNDP/UNCHS (Habitat) in 1994 with the collaboration of His majesty Government of Nepal. It also produced a Liquefaction susceptibility map and a seismic hazard map for Kathmandu Valley separately.

The Japan International Cooperation Agency (JICA, 2002) carried out a detailed study on Earthquake Disaster Mitigation in the Kathmandu valley in 2001. They prepared a series of vulnerability maps for buildings and infrastructures. Including liquefaction susceptibility map. In this way, initiatives have been taken by national and internationals organizations for the reduction of earthquake vulnerability in the cities of Kathmandu valley.

1.3. Problem definition

As described earlier, the Kathmandu valley is potentially prone to damaging earthquakes, as it is located in an active seismic zone. Because of the haphazard urbanization and increasing population in the Kathmandu valley now, it has become very essential to carry out studies on different aspects of the earthquake hazard leading to long term earthquake vulnerability reduction program. For such a program, it is needed to know the expected losses and for loss estimation, we need to know various seismic hazards. Kathmandu valley earthquake risk management project (KVERMP/N-SET) has carried out loss estimation in Kathmandu valley in case of the earthquake as that of 1934 for the population and different infrastructures as given in Table 1.4.

Table 1.4: Potential Impact due to scenario earthquake in Kathmandu Valley (KVERMP estimates for IX MMI)

Impact	Extent
Deaths	>40,000
Injuries	>95,000
Building destroyed/collapsed	>60 %
Homeless Population	>700,000
Bridges impassable	>50 %
Road length damaged	>10 %
Water supply pipe damaged	>95 %
Telephone exchange building	Most
Telephone lines	>60 %
Electric substations	Most
Electric lines	40 %

Liquefaction is one of the main effects of an earthquake that is responsible to structural failure and damage to roads, pipelines and infrastructures. In Kathmandu valley in spite of weak subsurface condition, many tall buildings have been built and the number is constantly rising. Most of these buildings (Except commercial, governmental and organizational buildings) have been constructed without adequate research on the subsurface sediment conditions (see Plates 15, 16) and hence may run a high risk that they are not properly designed to withstand the particular accelerations at the site. Looking at this situation, the study on subsurface geology is very important, as it helps for the study of seismic hazard and hence for the earthquake vulnerability reduction program. For the study of subsurface geology, the generation of a geological database is important which can be done by the collection of borehole data. One other potential source of useful information for subsurface information, geophysical measurements, are completely lacking for the Kathmandu valley.

Reports from previous major earthquakes, such as the one from 1934, give evidence that substantial damage to buildings and infrastructures can occur in Kathmandu valley as a result of widespread liquefaction (see Figures 1.8 and 1.9). Therefore, it is very essential to carryout a detailed mapping project of liquefaction hazard assessment in Kathmandu valley. To carry out a reliable liquefaction hazard assessment, borehole data with geotechnical information are important. A complete inventory of borehole data with geotechnical information for Kathmandu valley is missing. Although UNDP/UNHCS/HMGN (1994) have made a generalized liquefaction hazard map for Kathmandu valley with limited data sources, in this work, an attempt is made to prepare a new liquefaction hazard map using more borehole information.

The Kathmandu valley is filled by thick lacustrine and fluvial sediments from Pliocene to Pleistocene age. Different experts have studied the basin-fill sediments of the valley since the early sixties (Sharma and Singh, 1966; Yoshida and Igarashi, 1984; Dongol, 1985, 87; Shrestha et al. 1998; Sakai et al., 2001). A considerable number of drill holes also have been made in different parts of the valley for different purposes. The deepest drill hole (577 m) made so far is by the Department of Mines and Geology (DMG) for gas exploration that reaches to the bedrock in the central part of the valley. The previous studies on the basin fill faced several problems on the stratigraphic division and nomenclature of the formations due to lack of proper information on subsurface geology and insufficient description and definition of each formation. Different names were given to similar type of formations. This is mainly due to lack of structured borehole data, as this data, which has been collected by different organizations since 1960 has never been properly integrated. This is why it is required to collect all those primary data from the source organizations and organize it in a proper data base system including a geographical component related to the location of the boreholes. The properly established database can help the persons who are interested to carryout further research in that particular area thus helping him to save his money and time.

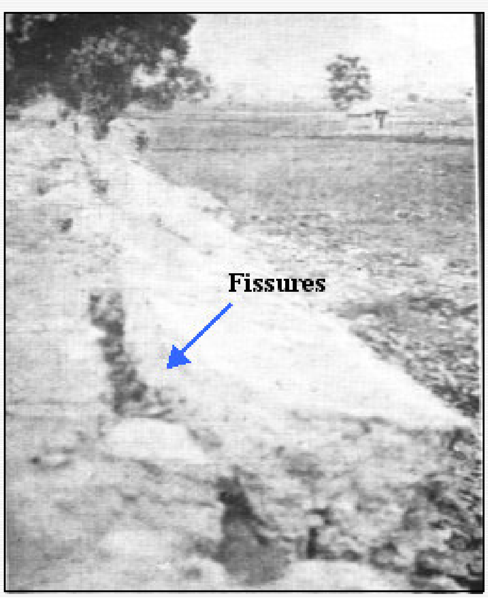

Figure 1.8: Fissures due to earthquake of 1934 along the way to Balaju

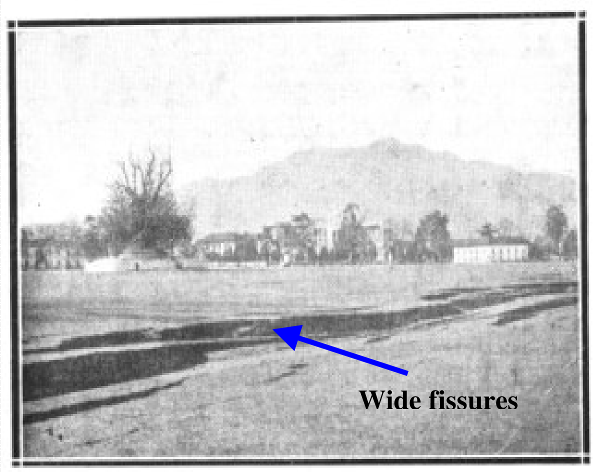

Figure 1.9: Fissures due to earthquake of 1934 in Tundikhel, the main city centre.

To date, the actual number of drill holes made in Kathmandu Valley is not known. It is believed that more than 300 deep drill holes have been made in the area by different organizations. Yet not a single organization has made an attempt to manage the complete borehole log information. The borehole information is limited in the hands of concerned organization that carried out the drilling project. As such, accessibility of such data to the professionals who are interested to carry out research work is limited. In this study, collection of these borehole data and managing them in a proper database system is the prior objective. Similarly, development of the subsurface models by using GIS software is very informative to all the geologists, hydrogeologists and geotechnical engineers, as it can give a clear picture of the subsurface in the form of 2D and 3D view, which can be useful for various purposes in the field of geology, geohydrology, geochemistry and geophysics. So the study is also dealing with the generation of GIS layer models and the generation of lithological cross sections and fence diagrams. So far, the information of 185 deep boreholes with a depth range from 35 m to 575 m and 328 shallow boreholes with depth range less than 30 m have been collected with their proper location and altitude for this study purpose. Finally, in this research, an attempt is made to prepare the Liquefaction Susceptibility map with the help of the available borehole data.

1.4. Research Objectives

(A). As mentioned in the previous section, there is no integrated database for subsurface information available for the Kathmandu valley. The available borehole data are concentrated in private organizations (consulting companies) and some government organizations, which do not tend to be very open in exchanging data. Hence, it is necessary to integrate all the available data in one place to make easy access to all researchers. Therefore, the main objective of this research is the **"Generation of a Geological Database for Kathmandu valley".**

Some of the sub-objectives that follow from this objective are:

- Generation of standardized borehole logs and digitizing them
- Location of all boreholes in the map
- Generation of lithological cross-sections
- Generation of fence diagrams
- Reconstruction of the geological evolution of the Kathmandu valley
- Development of layer models in GIS

(B). The main objective for the use of the integrated borehole database is in seismic hazard assess ment. The site response modeling has been carried out by Umut Destegul (Destegul, 2004) as mentioned in the previous section, liquefaction is expected to be one of the major effects of an earthquake with similar intensities as the one of 1934 (Rana, 1935) in Kathmandu valley. Hence, it is necessary to prepare a more detailed liquefaction susceptibility map, than the ones presently available. Therefore, my second objective of the research is to prepare a "**Liquefaction Susceptibility Map of Kathmandu Valley".**

1.5. Research Questions

From the general statement of the main objectives, the following research questions are derived:

- How many stages of lake deposit have actually developed in the valley?
- Are there any evidences for neo-tectonic activities, and for substantial displacements of the basin-fill along recent faults?
- Where were the main sources of sediment deposition in the valley?
- Is it possible to generate a simplified layer model for the subsurface conditions in Kathmandu valley?
- What is the liquefaction potential of the various sediments in Kathmandu valley?
- What is the minimum PGA value required to trigger liquefaction phenomena in Kathmandu Valley?
- Is there any other suitable methodology to carry out liquefaction hazard assessment with limited geo-technical data?
- What is the comparison of various methods for liquefaction susceptibility mapping? Do they correlate?
- How to go from point wise information on liquefaction susceptibility to map information? Can it be done using interpolation or through unit mapping?
- Is there an explanation for the intensity pattern of the 1934 earthquake as described by Auden and Ghosh, 1935? How should the various qualitative methods for classification of liquefaction susceptibility be used in actual loss estimations? Are there vulnerability function made for these classes?

1.6. Flow chart for the methodology

The research involves two types of objectives. Preparation of geological database and preparation of liquefaction susceptibility map. According to this target research methodology has been outlined. The detail approach used in the present study is shown in the flow chart (Figure 1.10). Further, objective wise flow chart and description to the methodology is also given in the successive chapters.

According to this scheme,

The available spatial data is well organized in spreadsheet and in Access and imported to ILWIS and Rockworks99/2002. The necessary analysis was carried out for the generation of GIS layer models, lithological cross sections, fence diagram etc, respectively. The analysis for liquefaction susceptibility was carried out in spreadsheet itself. The imageries such as Ikonos, Corona, aerial photographs and Dem were used for the generation of stereo-pairs in order to generate geomorphological map of the valley. Other information such as geology, structures, drainage etc. was obtained from the available maps and was used for the analysis purposes. Finally, a complete report was prepared.

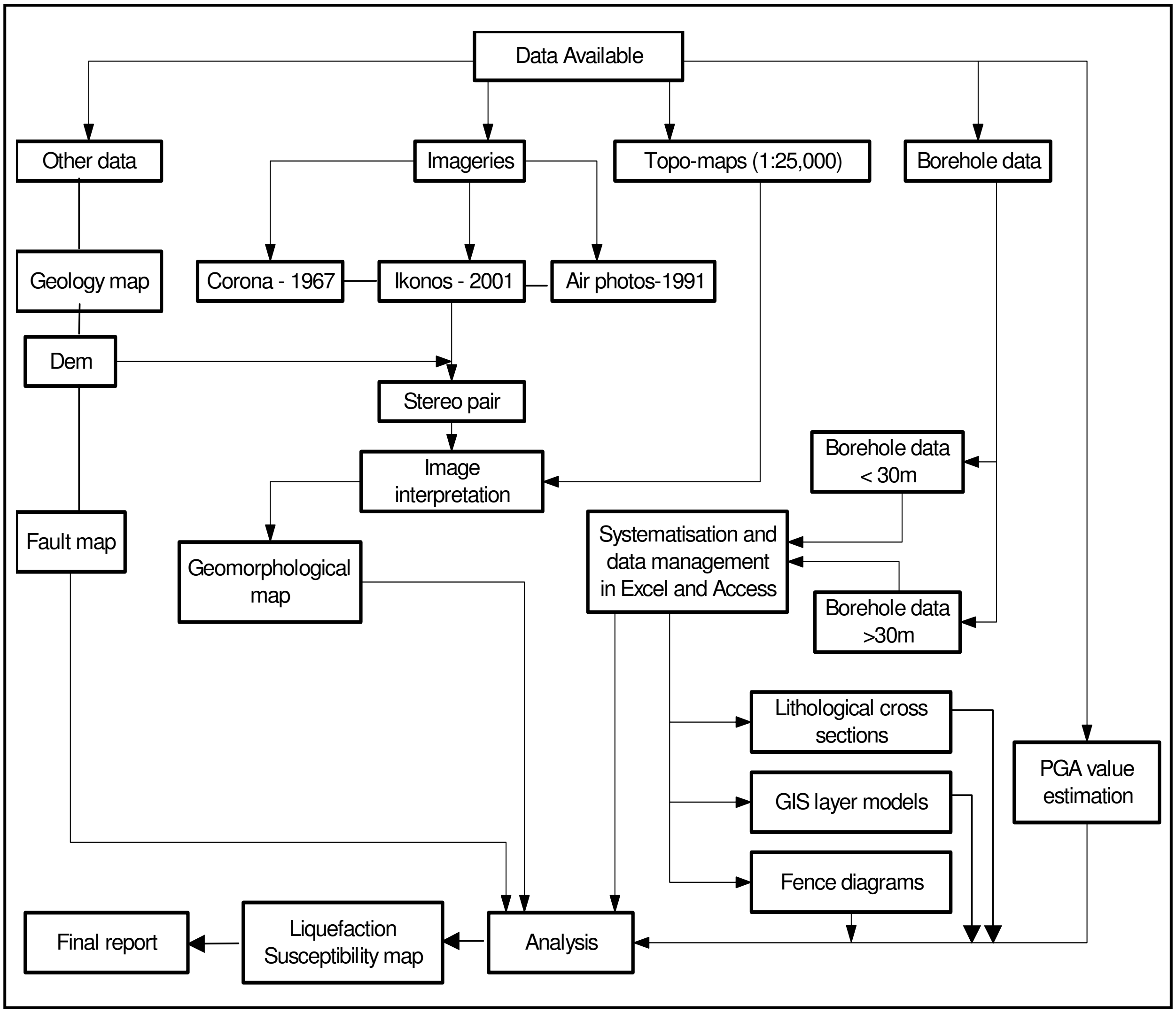

Figure 1.10: Flow Chart for methodology

1.7. Structure of the Rreport

The thesis is divided into the following chapters:

- Chapter one gives a general context of the study including the, introduction of the study area, the earthquake threats in Kathmandu valley and mitigation practice, problem definition, research objectives, research questions and flow charts etc.
- Chapter two deals with the General Geology, Structure (Tectonics) of the study area.
- Chapter three deals with liquefaction hazard assessment – overview of the methods.
- Chapter four explains about the generation of geological database processing of data and techniques. It also deals with the generation of the layer models, lithological cross sections, fence diagrams and stratigraphic projections using ILWIS 3.2 version and Rockworks99/2002.

- Chapter five deals with the liquefaction hazard assessment for Kathmandu valley.
- Chapter six gives the conclusion and recommendations of the research.

2. Geology of the study area

This chapter deals with a description of the tectonic situation of Kathmandu valley and its surroundings, general geological setting of the study area and focused on the evolution of the basin sediments within the valley.

2.1. Tectonic Setting

The Hindu Kingdom of Nepal is sandwiched between Peoples' Republic of China in the North and India in the South, East and West. Nepal is situated in the center of the long Himalayan concave chain, and is almost rectangular in shape with about 870 km length in the NWW-SEE and 130 to 260 Km in N-S. Direction. Nepal is divided in to 3 major tectonic zones as shown in the Figure 2.1. They are the Main central thrust (MCT), Main Boundary Thrust (MBT), Himalayan Frontal Fault (HFF). A cross section of the Nepal Himalayas running from SSW to NNE is shown in Figure 2.2.

According to Nakata (1982), many active faults are distributed along the major tectonic boundaries. He classified the active faults into (i) Main central active fault system, (ii) The active faults in the lower Himalaya (iii) The main boundary active fault system (iv) The active fault system along the Himalayan frontal thrust. These faults were produced by the collision of the Indian plate with the Eurasian plate. The MBT is interpreted as very active fault system and is dipping towards the North (Figures 2.1, 2.3). According to Sakai (2001), the Kathmandu complex occupies the core of the synclinorium, the axes of which trends in WNW-ESE direction. The main fold axis lies on the line connecting the peaks of Phulchauki (2,765 m) and Chandragiri (2,550 m). Many longitudinal faults run parallel to the fold axes, and the northern and southern margins of the basins are bounded by the Kalphu Khola fault and Chandragiri fault respectively, (See Figure 2.4). Both active faults cutting the late Pleistocene sediments. Saijo et al. (1995) and Yagi et al. (2000) also reported the existence of active faults in the Southwestern part of Kathmandu basin, such as the Chobhar Fault and Chandragiri Fault. According to Saijo et al. (1995), these active faults are cutting the late Pleistocene sediments and have a vertical displacement rate of 1 mm/yr. The active fault system in Kathmandu valley is shown in the Figure 2.4.

Sakai. (2001), reported a fault named Danuwaargaon fault in the southern margin of the Kathmandu valley and stated that it was very active in the late Pleistocene and hence might have been responsible for the draining of the Paleo lake of Kathmandu. Sakai (2001) and Saijo (1995) both believe that, the Chandragiri Fault and Chobhar Fault in the South may have played an important role for the basin development of the valley in the late Pliocene period. According to Sakai (2001), and Saijo et al., (1995), The Kalphu-Khola Fault and Chandragiri Fault both cut the late Pleistocene sediments. The Chandragiri Fault on the other hand is a thrust fault along which the rocks of the Lesser Himalaya in the South override the Quaternary sediments of the basin (Saijo et al. 1995, Nakata et al.1984). In this research, an attempt was made to trace the displacement zone with the help of borehole logs but no clear evidence of major displacement was found.

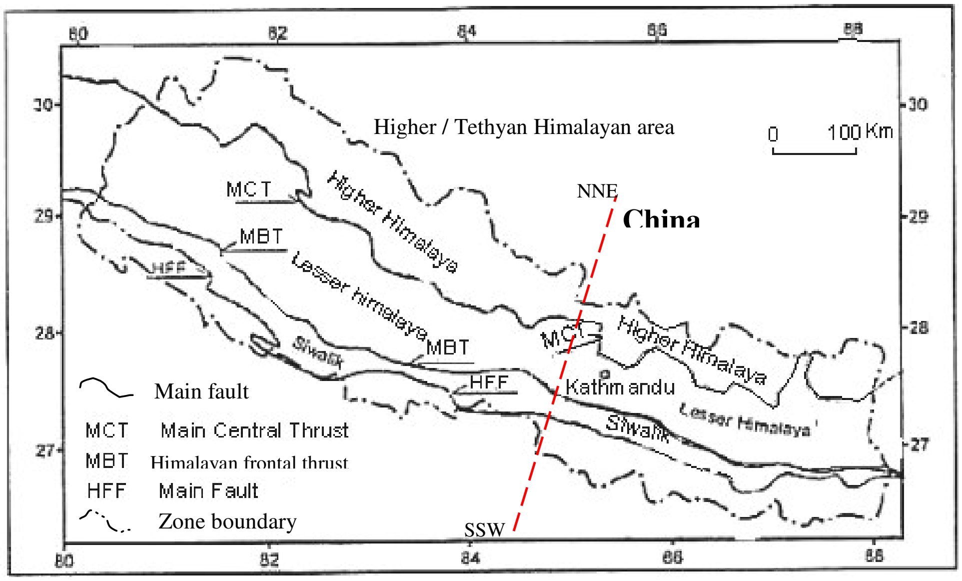

Figure 2.1: The Geo technical zones of Nepal and surroundings (JICA, 2002 and UNDP/ UNCHS, 1994)

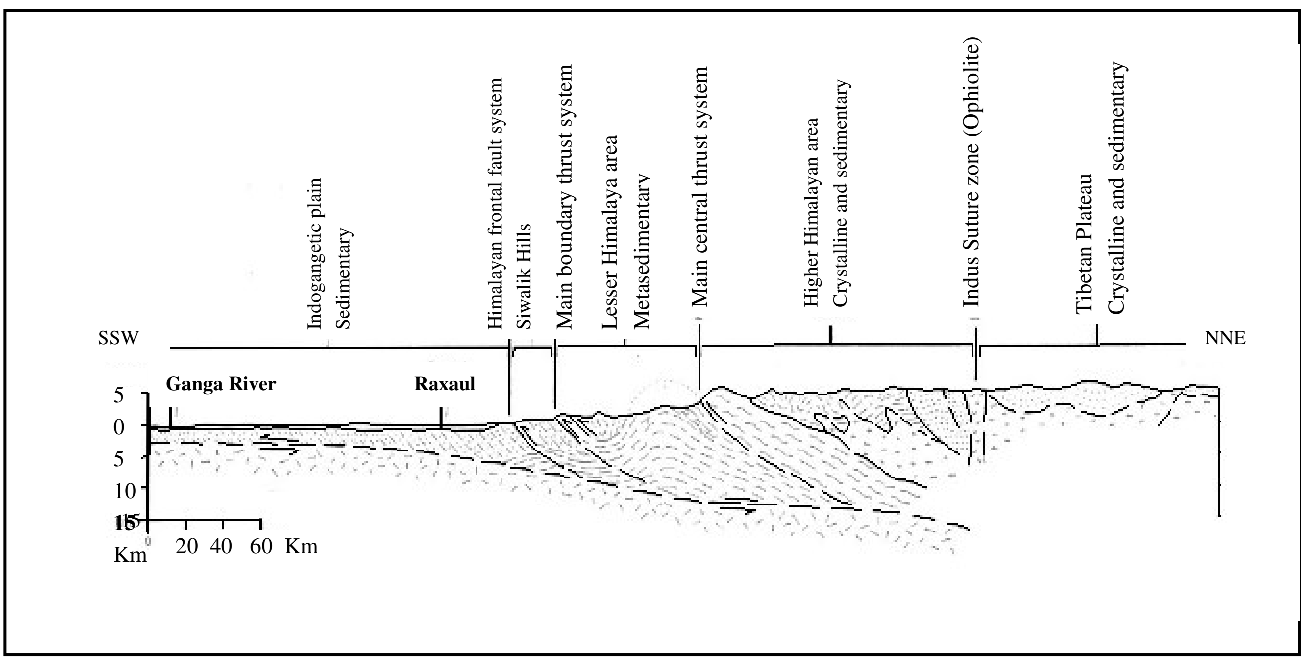

Figure 2.2: Approximate cross section location from South towards North
Source: UNDP/UNCHS, based primarily on Seeber et al.1981, and Vaidya, (1981)

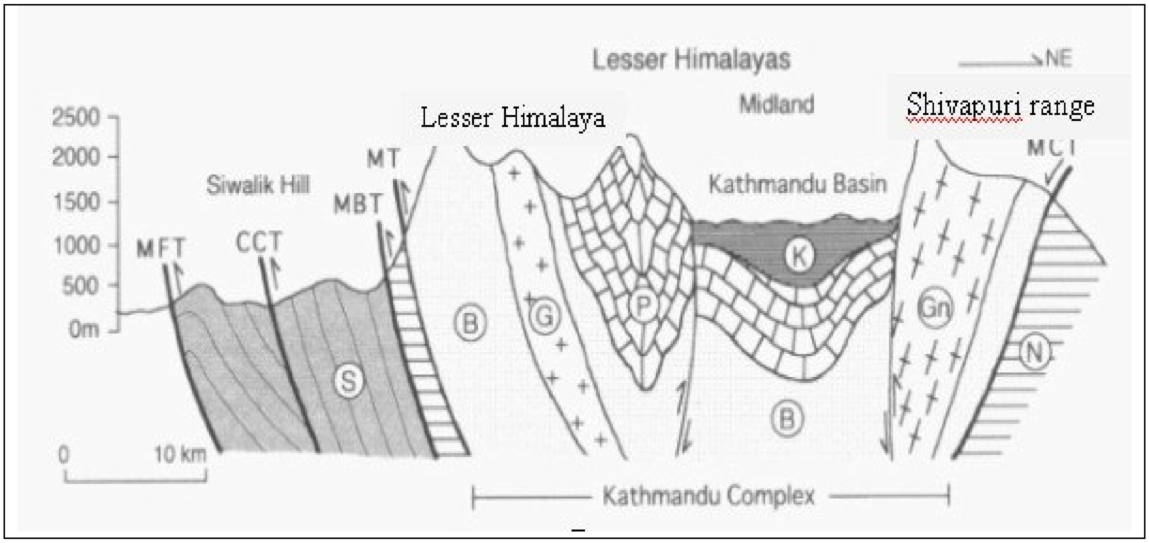

Figure 2.3: A profile of Kathmandu valley region and the tectonics (Modified after Stocklin and Bhatterai 1981) and the position of Kathmandu basin.
S=Siwalik group, B=Bhimphedi group, P=Phulchauki group, N=Nuwakot group, G=Granite, Gn=Gneiss and Granite complex, K=Kathmandu basin group, MFT=Main Frontal Thrust, MBT=Main Boundary Thrust, CCT= Central Churia Thrust, MT= Mahabharat Thrust, MCT= Main Central Thrust.

This might be due to the heterogeneous distribution of the lacustrine sediments within the valley and the far away location of the boreholes from the fault zone. From the study of the boreholes that have touched the bedrock, however, the existence of steep slopes in the bedrock topography could be deduced. Borehole B19 for example located at a distance of about 300 m from the nearest rock outcrop at Pashupatinath (with an altitude 1324 mmsl) touches the bedrock level at an elevation of 1204 mmsl this gives a total height difference of 120 m at that distance indicating a rather steeper slope. Similarly, the well B15 that touches the bedrock at an altitude of 1098 mmsl is at a distance of 500 m from the nearest outcrop at Swayambhu (Heritage site) with an altitude of 1320 mmsl. That gives the difference in height of 222 m, which also indicates a steep slope. Similarly two boreholes B2 and BB1, which are separated by distance of 475 m touch the bedrocks at an altitude of 1292 mmsl and 1092 mmsl respectively thus, giving the difference in height of 200 m (see Figure 2.4 for name of the places).

These examples might give an indication of neo-tectonic activity with in the basin fill sediments. Despite all these little can be said on the neotectonic of the Kathmandu valley. More detail study is necessary to affirm the neotectonic behaviour in the Kathmandu basin using modern techniques.

2.2. Geological Setting

Kathmandu valley is surrounded by high rising mountain ranges, such as Shivapuri (2732 m) in the North and Phulchauki (2762 m) in the South (see Figure1.1 Chapter 1). The Kathmandu valley comprises of quaternary sediments on top of basement rocks.

2.2.1. The basement rocks

The basement geology of the Kathmandu area has been described in detail by Stöcklin and Bhattarai (1977). The basement rock consists of Phulchauki group and Bhimphedi group of the Kathmandu complex of Stocklin and Bhattarai (1977) and is formed by Precambrian to Devonian rocks (See Table 2.1).

The rocks of Phulchauki group and Bhimphedi group together form the so called Kathmandu Complex, and tectonically interpreted as thrust mass (allochthonous). The rocks of Kathmandu complex along with the underlying para-autochthonous Nawakot Complex constitute the Mahabharat Synclinorium. The axis of this synclinorium passes along the Phulchauki-Chandragiri range, South of the Kathmandu Valley. Within the Kathmandu valley, the basement rocks are intersected by numerous fault systems (Figure 2.4). As mentioned above, the Kathmandu complex has been divided into the Bhimphedi Group and Phulchauki Group. The Bhimphedi Group consists of relatively high-grade meta sediments of Precambrian age. It comprises of approximately 8 Km thick successions of rocks, divided into six formations (Table 2.1). Similarly, the Phulchauki Group comprises of the unmetamorphosed or weakly metamorphosed sediments containing fossils of the early middle Palaeozoic age. It consists of about 5-6 km thick sequence of rocks, divided into five formations (Table 2.1). The rocks consists of intensely folded and faulted meta-sediments such as phyllites, schists, slates, limestone and marbles covering the southern, eastern and western part and intrusions of acid and basic rocks (Granite & Gneiss) known as Shivapuri injection complex in the northern part of the valley. Some isolated rock outcrops of Tistung Formation and Chandragiri Formation can also be observed in some parts of the valley basin such as in Balkhu, Pashupatinath, Swayambhu and Chobhar (See Figure 2.4). The Bhimphedi group of the Kathmandu complex mainly lies outside the watershed boundary of the Kathmandu valley; therefore, the source rocks of the basin fill sediments are limited to the Phulchauki group and Shivapuri injection complex. The geological succession of the Kathmandu valley is given in Table 2.2.

2.2.2. Quaternary Sediments

The Basement rocks of the Kathmandu valley is covered by thick semi-consolidated fluvio-lacustrine sediments of Pliocene to Pleistocene age. The basin is filled by thick semi-consolidated fluvio-lacustrine sediments. The maximum depth of the valley sediment is more than 550 m on the basis of borehole log DMG6 located at the central part of the valley. These thick sediments are mainly derived from the surrounding hills by the ancient drainage channel system.

The sediments consist of,

- Arenaceous sediments composed of fine to coarse-grained sand with a small quantity of rock fragments, which are believed to have been supplied from the northern gneiss rocks.
- Argillaceous sediments composed of clay and silt resulting from the erosion of limestone and phyllite, which are exposed in the eastern, southern and western mountainous areas.

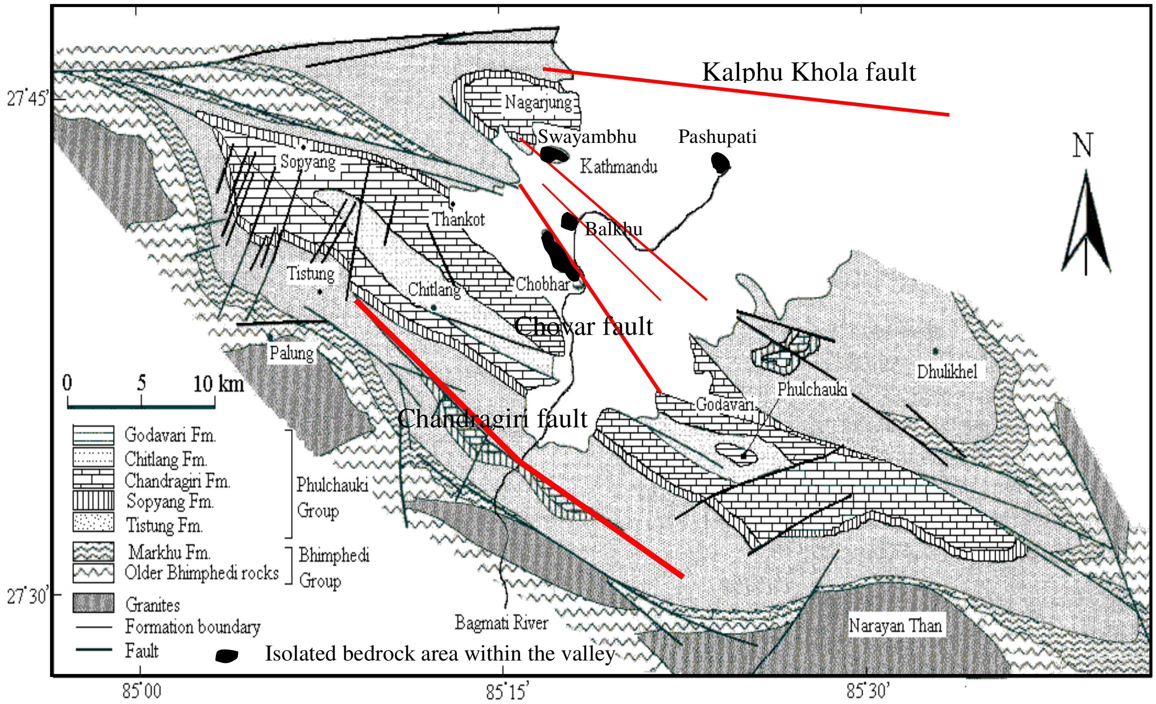

Figure 2.4: Simplified geological map of Kathmandu area (after Stöcklin 1980, new Fault lines redrawn by author, 2004)

Table 2.1: Stratigraphic sequences of basement rocks of Kathmandu Basin (Source: Stöcklin and Bhattarai, 1977)

Unit			Main Lithology	Approx. Thickness (m)	Age
Kathmandu complex	Phulchauki Group	e) Godavari Limestone	Limestone, dolomite	300	Devonian
		d) Chitlang Formation	Slate	1,000	Silurian
		c) Chandragiri Limestone	Limestone	2,000	Cambrian to - Ordovician
		b) Sopyang Formation	Slate, calc-phyllite	200	? Cambrian
		a) Tistung Formation	Metasandstone, Phyllite	3,000	E. Cambrian or Lower Pre-cambrian
	T r a n s i t i o n				
	Bhimphedi Group	f) Markhu Formation	Marble, schist	1,000	Precambrian
		e) Kulekhani Formation	Quartzite, schist	2,000	Precambrian
		d) Chisapani Quartzite	Quartzite	400	Precambrian
		c) Kalitar Formation	Schist, quartzite	2,000	Precambrian
		b) Bhainsedobhan Marble	Marble	800	Precambrian
		a) Raduwa Formation	Garnet-schist.	1,000	Precambrian

Table 2.2: Geological Succession of the Kathmandu Valley (modified after Stocklin and Bhattarai 1977)

Cenozoic	Holocene		Fan Gravel, Soil, Talus, Fluvial deposits (gravel, sand, silt)
	Pleistocene		Lake deposits (gravel, sand, silt, clay, peat, lignite & diatomite),
	Late Pliocene-Early Pleistocene		Fluvial deposits (boulder, gravel, sand, silt)
---	---------------------	--	------Unconformity--
Lower Paleozoic	Devonian	**Phulchauki Group**	Godavari Limestone - limestone, dolomite
	Silurian		Chitlang Formation - slate
	Cambrian-Ordovician		Chandragiri Limestone - limestone, phyllite
	Cambrian		Sopyang Formation - slate, calcareous phyllite
	Early Cambrian		Tistung Formation - meta sandstone, phyllites
---	---------------------	--	------Unconformity--
Pre-Cambrian		**Bhimphedi Group**	Markhu Formation - marble, schist
			Kulekhani Formation - quartzite, schist
Intrusion			Metamorphic - Sheopuri gneiss
			Igneous Rocks - pegmatite, granite, basic intrusive

- Lignite and diatomite from the lake sediments.
- Agglomerate of boulders and gravel with a clayey and silty matrix in the southern basin derived as debris flow from the southern hill.

Previous Geological and Geomorphological investigations have divided the fluvio-lacustrine sediments of Kathmandu valley into various formations and geomorphic surfaces (Yamanaka 1982; Yoshida and Igarashi 1984; Dongol 1985; Sakai 2001). The classification and modifications introduced by different authors and their correlations are shown in Table 2.3. The table shows that there has been a subsequent modification in the classification system of the valley sediments from the beginning. In the earlier classification made by Yoshida and Igarashi (1984) for example, they classified the basin fill sediments into three groups and seven stratigraphic units as shown in the Table 2.3. In the classification of Dongol (1985, 1987), Patan Formation, Thimi Formation and Gokarna Formation of Yoshida and Igarashi (1984) are combined into Kalimati clays, which are mainly distributed in the central part of the valley. Similarly, all the terrace formations and the upper part of the Lukundol Formation of Yoshida and Igarashi (1984) are included by Dongol (1985, 1987) into Champi-Itahari gravel, Nakhu khola mudstone and Keshari Nayakhandi lignite. On the other hand most part of the Lukondol Formation are included them into the Tarebhir basal gravel. Thus, Dongol (1985, 1987) made a more simplified classification.

Shrestha et al. (1998) made another classification (see Table 2.3) on which the geological map displayed in Figure 2.5 is based. They divided the entire valley sediments into six formations: Basal boulder bed, Lukundal, Kobgaon, Chapagaon, Kalimati, Tokha and Gokarna Formations in ascending order. Infact, in their classification the basal boulder bed, Lukundol Formation and Kobgaon Formation are related to the Lukundol Formation defined by Yoshida and Igarashi (1984), and the rest are related to the Terrace deposits and other younger deposits (Table 2.3). According to Sakai (2001), based on his field experience the Kobgaon Formation of Shrestha et al. (1998) is not different from the Lukundol Formation, as this formation is exposed only at some places close to the Lukundol Formation and its field characteristics is similar to that of the Lukundol Formation. So in the geological map, the Kobgaon Formation shown in Figure 2.5 can be considered as Lukundol Formation also.
Thus, when we explore the literature we find various views of the authors in classifying the sediments with in the valley. There is ambiguity in the naming of the formations. Different formation names are given to similar type of deposits. This has created a lot of confusion and difficulties in the research work. So a precise classification system is required so that everyone can follow it in a same way.

The classification of Yoshida and Igarashi (1984) and other workers as described above are basically based on the surficial evidences that were obtained from fieldwork observations only without adequate knowledge of borehole information. On the other hand Sakai (2001), has proposed a new classification system, which is based both on the field observations and borehole information, which seems more convincing.

Sakai (2001) made a detailed study on the valley fill sediment deposits during the Paleo-Kathmandu Lake project. They drilled three boreholes in different places of Kathmandu (Rabi Bhawan, Trichandra College and at Pulchok), one of which (at Rabibhawan) had reached up to the bedrock level (see borehole log Paleo1 in annex containing in CD) and carried out detailed investigations. Based on the drill core study and field observations, he proposed a different classification schemes for the sediments of the entire valley (see Table 2.3). His classification system is very much convincing and is correlated with the findings in this research.

2.3. General Classification of basin fill sediments based on previous studies and borehole logs information

From the lithological cross sections and fence diagrams drawn along different directions (Chapter 4), we find that the lithology of the valley fill generally varies from South towards North. Based on the variation of lithology we can divide the sediments within the valley basin into 3 main groups: A southern, central and northern group:

2.3.1. The Southern

The southern part of the valley is occupied by many hilly terraces formed during late Pliocene to middle Pleistocene (Yoshida and Igarashi, 1984). The sediments in the southern part are well exposed along the terraces and riverbeds, and can be subdivided into three formations: Tarebhir Formations, Lukundol Formation and the Itaiti Formation in ascending order.

Table 2.3: Correlation of stratigraphy of the Kathmandu basin sediments by different workers.

Yoshida & Igarashi (1984) Yoshida & Gautam (1988)			Dongol 1985, 1987	Shrestha et al. (1998)	Sakai et al. (2001)		Sakai 2001	
							Southern part	Central part
Patan Formation			Kalimati Clays	Gokarna fm Tokha fm Kalimati fm Chapagaon fm			Itaiti Fm	Kalimati Fm
Thimi Formation								
Gokarna Formation								
Boregaon terrace deposit			Champi-Itahari gravel		Lukundol Formation	Upper member		
Chapagaon terrace deposit								
Pyangaon terrace deposit								
Lukundol Formation	Member	VIII						
		VII						
		VI						
		V	Nakhu Khola mudstone & Keshari nayakhandi lignite	Lukundol fm & Kobgaon fm		Middle member	Lukundol fm	Basal lignite member
		IV						
		III						
		II						
		I	Tarebhir basal gravel	Basal boulder bed		Lower member	Tarebhir Fm	Bagmati Fm

2.3.1.1. Tarebhir Formation

It is the oldest basin fill sediments (Sakai 2001), which is unconformably overlying the Pre-Cambrian Tistung Formation. The formation is mainly composed of boulders and cobbles with minor amount of lenticular sand beds, which were fluvial in origin and were derived from the Chandragiri and Phulchauki hill in the south by the ancient river system (Figure 2.6). The thickness of this formation varies from less than 1 m at Tokalmat area to 350 m at Dukuchap area (Sakai, 2001). The top of this formation in the southern part is marked by a 14 m thick boulder and cobble bed. The age of this formation is believed to be from late Pliocene to early Pleistocene (Yoshida and Igarashi, 1984).

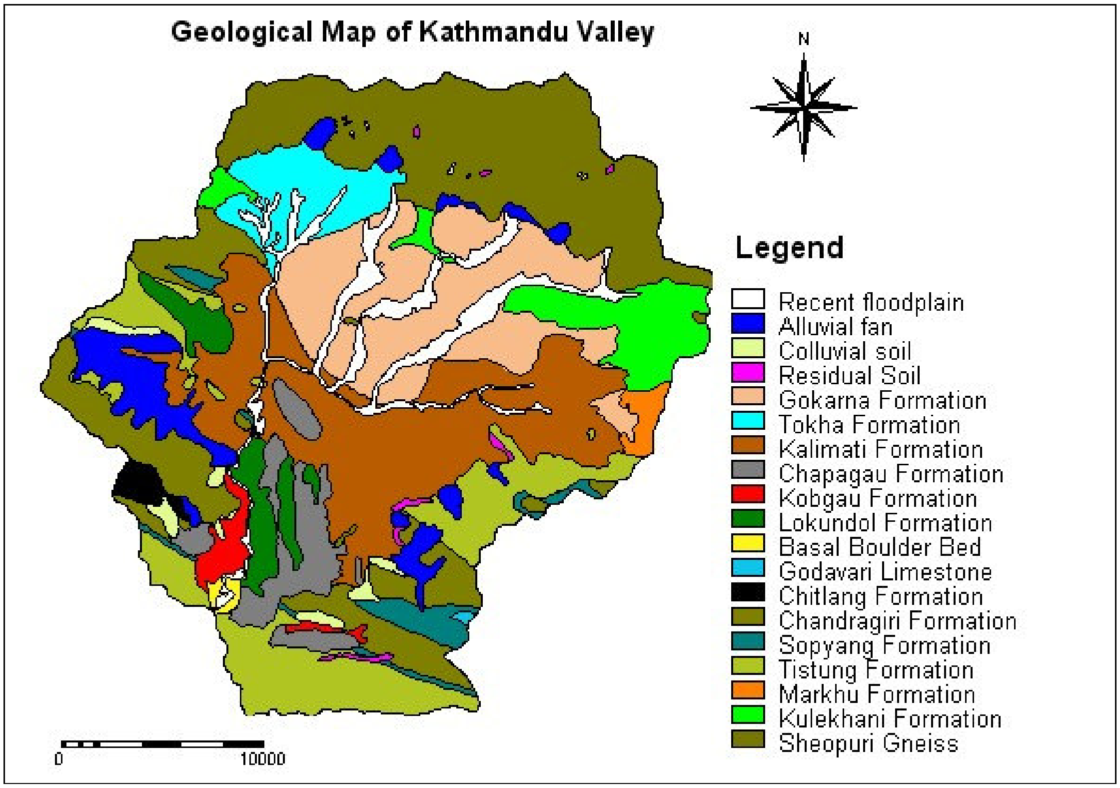

Figure 2.5: Geological Map of Kathmandu Valley, Source: Department of Mines and Geology (DMG)

2.3.1.2. Lukundol Formation

The Lukundol Formation is a mud dominant sequence of marginal lacustrine facies, which is conformably overlying the Tarebhir Formation (Figure 2.6). The formation is named after the Lukundol village that lies South of the Kathmandu valley. The formation consists of black to grey organic mud, rhythmite of sand and silt, coarse-grained sand and granules. Common occurrence of lignite beds ranging in thickness from 1 to 50 cm and vertebrate fossils such as ancient elephant, crocodile, deer, and artiodactile are characteristic features of this formation (Sakai 2001). These fossils are believed to have been formed in marginal lacustrine facies deposited in swamp and lake of shallow water deposit, where many animals were living and aquatic plants also flourished. The formation attains a total thickness of 115 m (Sakai, 2001). This formation is correlated with Kaseri-Nayakhandi lignite and Nakhu Khola mudstone of Dongol (1987), and members II, III, IV and V of Yoshida and Gautam (1988), see Table 2.3. In the central part, the formation is correlated with the Kalimati Formation (Basal lignite member) of Sakai (2001). The age of this formation is believed to be from early to middle Pleistocene (Yoshida and Igarashi, 1984).

2.3.1.3. Itaiti Formation

It is a cliff forming thick gravel dominant sequence resting on the Lukundol Formation. This formation comprises alternating sequence of gravel, fine sand and silty clay with carbonacious mud in ascending order. The base of this formation consists of pebble and cobble beds of meta-sandstone derived from the southern hills and rests on the top of the Lukundol Formation (see Figure 2.6). The Itaiti Formation is correlated with Terrace deposit of Yoshida and Igarashi (1984). The age of this formation is believed to be middle Pleistocene (Yoshida and Igarashi 1984).

2.3.2. Central

The compilation of large number of borehole data obtained from the Kathmandu basin sediment show that, the basin fills sediments in the central part of the Kathmandu basin can be roughly divided into three parts (Figure 2.7): - Lower part, Middle part and the Upper part. Sakai (2001), defined them as Bagmati Formation, Kalimati Formation and Patan Formation respectively.

2.3.2.1. The Lower part

The lower part of the sediments in the central group is given the name of Bagmati Formation by Sakai (2001). The name of Bagmati Formation is derived from the Bagmati River, which was very active before the appearance of lake and was responsible for the deposition of the sediments in most part of the valley. It consists of mainly medium to coarse sand, gravels and boulders that can be observed in the borehole logs distributed in this part (Figure 2.7). The sediments of this formation were derived from the surrounding hills particularly from the Shivapuri hill in the northern part of the valley and brought by Proto-Bagmati river system of Hagen (1968). The thickness of this formation varies from a few metres up to 135 m (P14b, Yak and Yeti hotel). In some of the boreholes such as in Bal2, B15, P01, Naik2, Jp1, the Bagmati Formation is missing which suggests that deposition was being controlled by the subsurface topography.

2.3.2.2. The middle part

The middle part of the sediments in the central group is given the name Kalimati Formation by Sakai (2001), which was derived from the local name known as “Kalimati” meaning black clay. It consists predominantly of dark grey carbonacious and diatomacious beds of open lacustrine facies (Sakai, 2001), Diatomacious beds were predominantly accumulated in marginal parts of the Lake and some landslide dammed ponds (Dill et al., 2001). This type of sediment is extensively distributed beneath the central portion of the Kathmandu valley, see Figures 2.7 and 2.8.

The formation was formed during the lacustrine period between 2,500,000 to 29,000 years B.P. (Yoshida and Igarashi 1984). The entire sequence is represented by a change in sedimentary facies. The lower part of it at some places contains lignite and bituminous pebbly mud showing a marginal lacustrine facies of shallow water depth designated as basal lignite member (Sakai 2001). In some places as shown in the cross section (Figure 2.7), varying thickness of medium to coarse-grained sand is interbedded. The thickness of this formation varies from few meters up to more than 300 m at borehole B1 (Harisiddhi). The formation is correlated with the Lukundol Formation in the southern part.

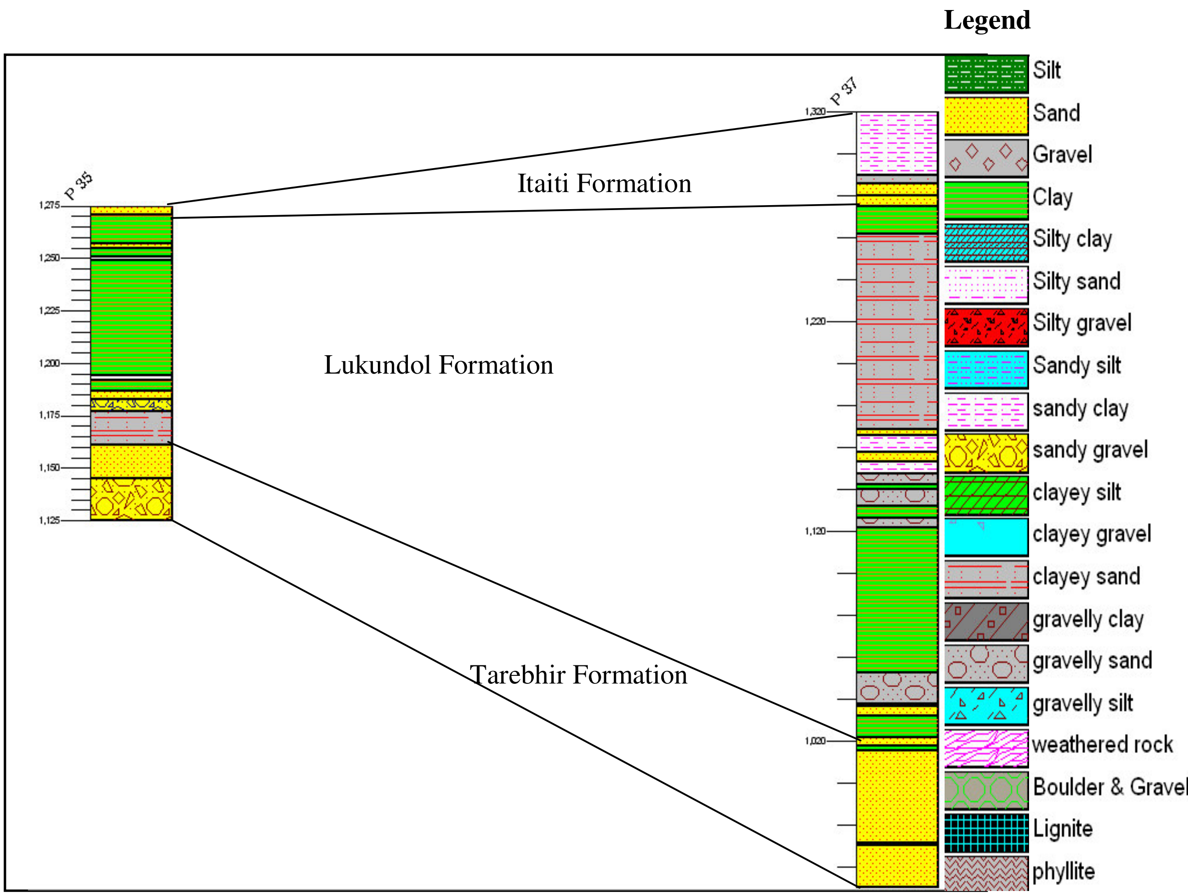

Figure 2.6: Lithologs in southern part with its formation names

2.3.2.3. The upper part

The upper part called Patan Formation (Sakai 2001, and Yoshida and Igarashi, 1984) is mainly distributed in and around the Kathmandu and Patan city and consists of mainly fine to medium sand and silt intercalated with clays and fine gravels in some places (Figure 2.7). It is fluvial in origin. The sediments of this formation that overlie the Kalimati Formation may have been developed after the lake started drying up and fluvial process became active. The age of this formation is determined as 19,000 BP to 10,000 BP (Yoshida and Igarashi, 1984). The thickness of this formation ranges from few meters up to more than 50 m in borehole BB1 (Bansbari).

A schematic cross section of deposits in the Kathmandu basin is shown in Figure 2.9 that helps to understand more about the sediments with in the valley. The section is taken for the eastern part of the valley running from Sundarijal in the North to Itaiti village in the South. The vertical scale is somehow exaggerated.

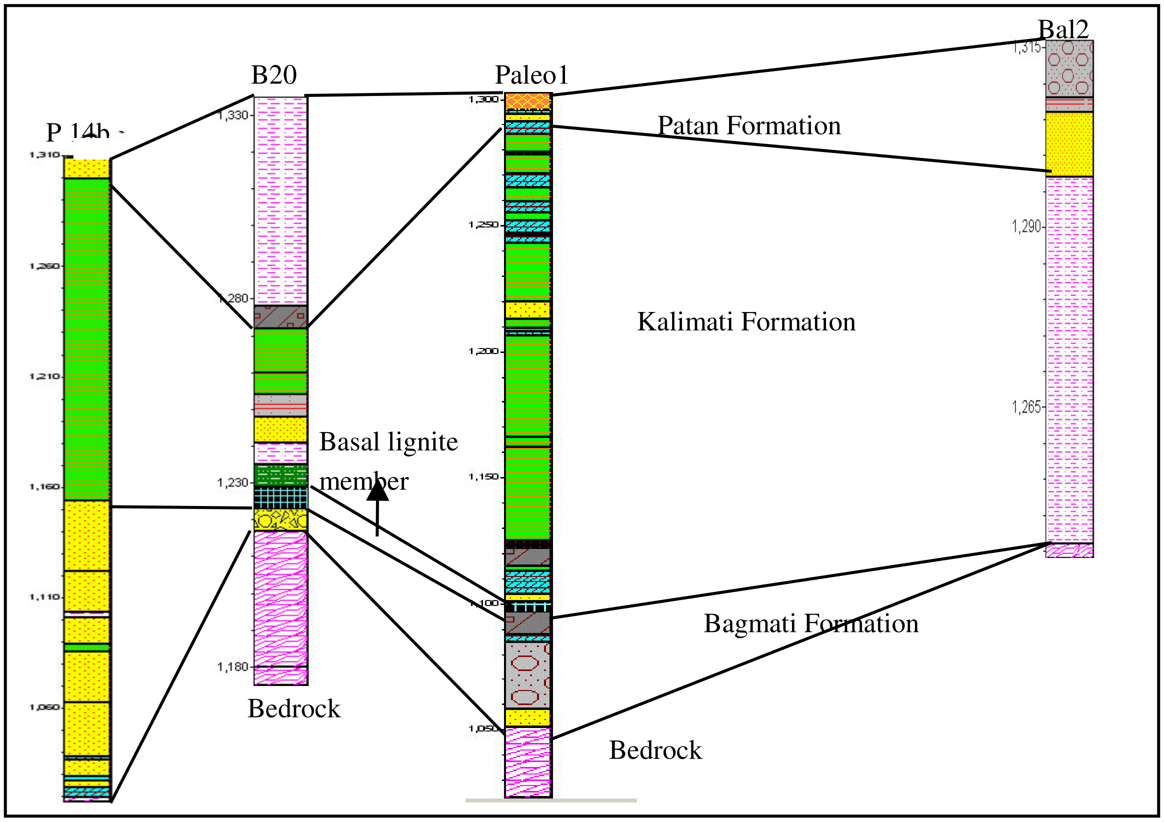

Figure 2.7: Lithologs in the central part of the valley and the formation names (For legend Please refer Figure 2.8)

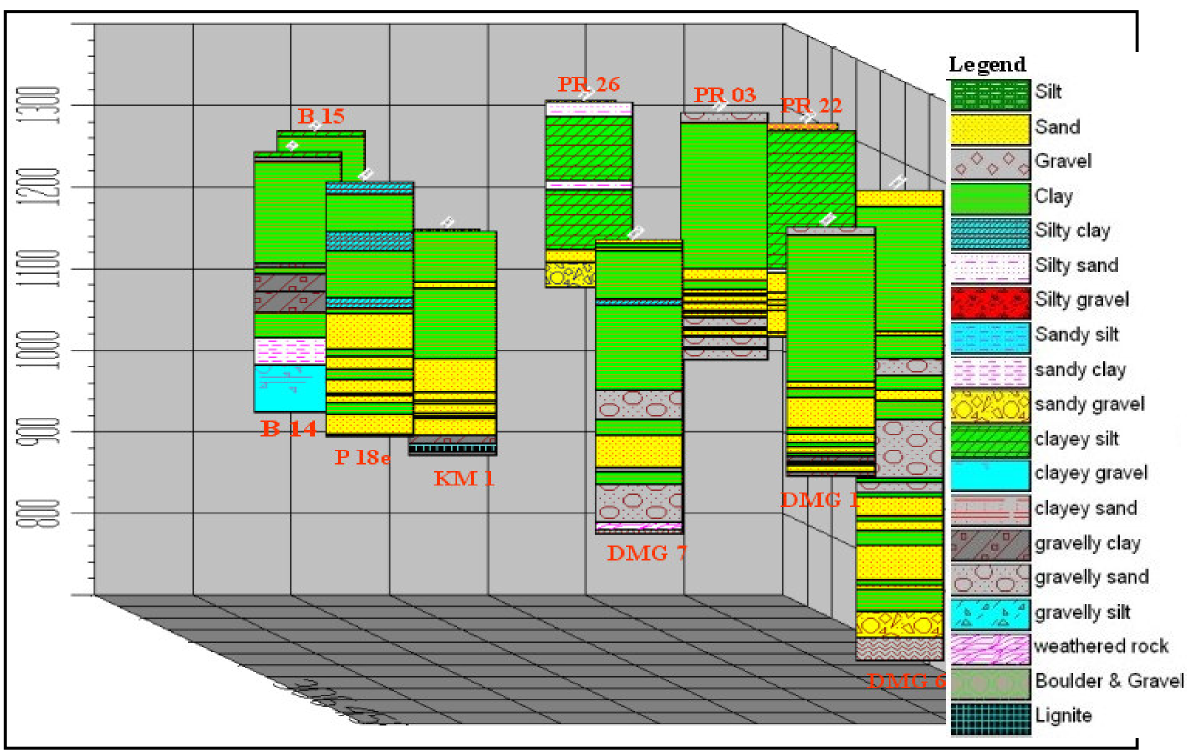

Figure 2.8: Distribution of boreholes in the central part of the valley, showing abundance of clay deposits

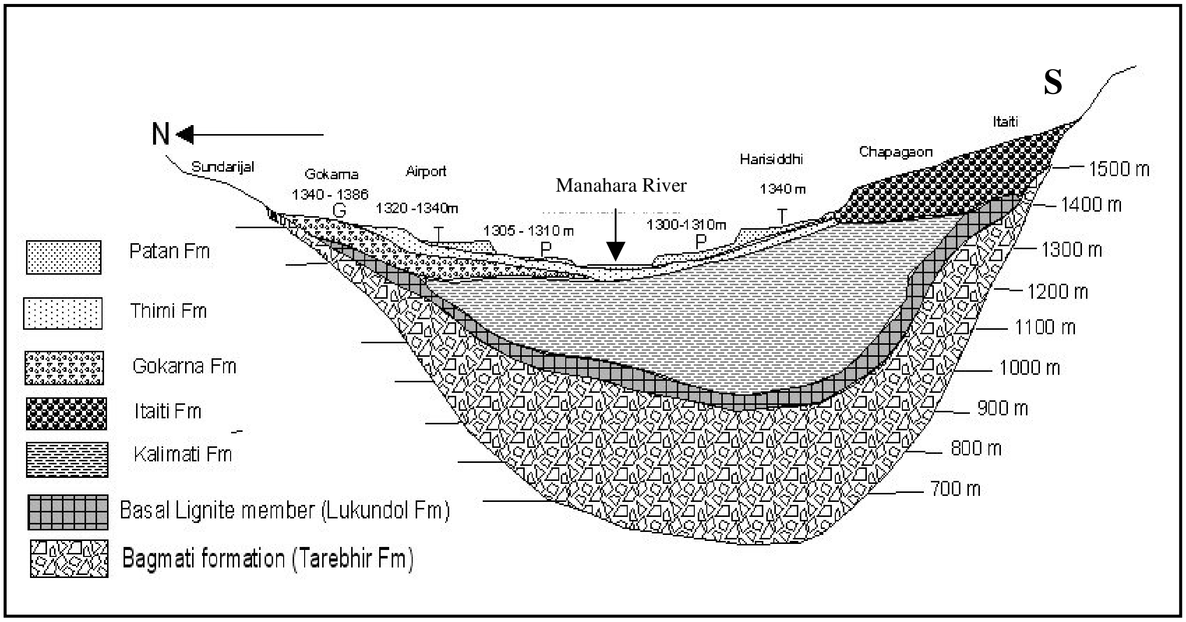

Figure 2.9: Schematic geological cross section of the basin fills sediments of KV showing strati graphic relationship of each formation (After Sakai 2001, vertical scale is exaggerated)

2.3.3. The Northern

Previous workers have reported that terrace-forming sands from fluvio-deltaic or fluvio-lacustrine origins are extensively distributed in the northern and northeastern part of the Kathmandu valley (see Figure 2.11), these are named as Gokarna Formation and Thimi Formation (Natori et al.1980a; Yoshida and Igarashi, 1984; Sakai, 2001). According to these authors, Thimi Formation is younger than the Gokarna Formation. The age of the latter formation is determined as 28,000 to 30,000 years BP and the age of the Thimi Formation is determined as 23,000 to 28,000 years BP (Yoshida and Igarashi, 1984). The extensive borehole data located in the northern part of the valley (see Figure 2.10), especially in the southern half of the northern group indicate the distribution of thick sequence of sandy and silty sediments without clay, which is regarded as the continuation of Thimi and Gokarna Formation (Sakai, 2001). From the lithological cross section drawn from South to North, it is evident that the Kalimati Formation diminishes its thickness and pinches out in the area to the North of Dhapasi and Bansbari. Similar features are also evident in the eastern part in the Mulpani village area (See Figure 2.11), which is considered to be the northern marginal line of the lake. In the northern marginal part of the Kathmandu valley, the basin fill sediments change their sedimentary facies to gravely braided river and fan deposits.

The general classification of the unconsolidated sediments of Kathmandu basin is shown in Figure 2.11. The classification is based on the borehole information.

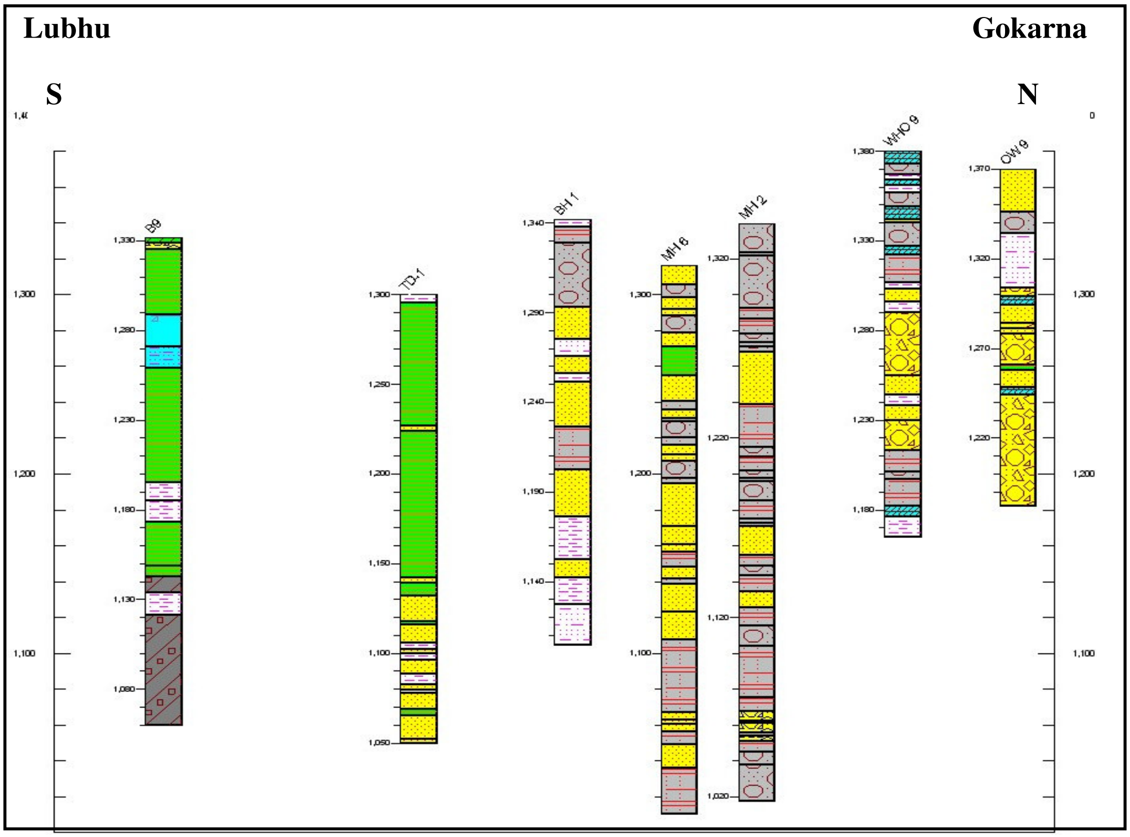

Fig. 2.10: Lithological Cross Section, South to North (refer previous figures for legend)

The Figure 2.12 shows the expansion of the lake area during the lacustrine period, which was prepared by digitizing the borehole locations lying in outermost regions with clay contents more than 10 m thick. The boreholes lying beyond that boundary do not contain any clay sediments. According to this figure, the main lake seems to be spread over the central part of the valley covering more than one-third part of the catchments boundary area. The occurrence of two separated isolated small lakes can also be noticed to the West (after Naikap village) and to the Northeast (Indrayani-Sankhu village) of the large main lake with in the valley.

The draining of the lake following erosion by rivers is indicated by the erosion features, which can be observed in some places over the Kalimati Formation in the borehole logs (Figure 2.13). For example the boundary between the lacustrine clay and the fluvial sand in well P14b (Hotel yak and Yeti), P01 and P03a (bottlers Nepal Balaju) is observed at 10.5 m, 9 m, and 33 m respectively below the ground surface which is at an altitude of 1269 m, 1305 m and 1300 m above mean sea level respectively, thus indicating the altitude of erosion surfaces lying between 1269 m and 1305 m above mean sea level. Similarly in well DMG5, DMG6, and DMG7, it lies at a depth of 5, 20 and 14 m respectively (altitude of 1269, 1274 and 1280 m above the mean sea level respectively), thus indicating the erosion surface lying between 1269 and 1280 m above mean sea level in this case. It is believed that the lake water from the valley was drained some 10,000 years B.P. (Yoshida and Igarashi. 1984). Until then there was believed to be the existence of lake still in some parts of Kathmandu valley, especially in the central portion.

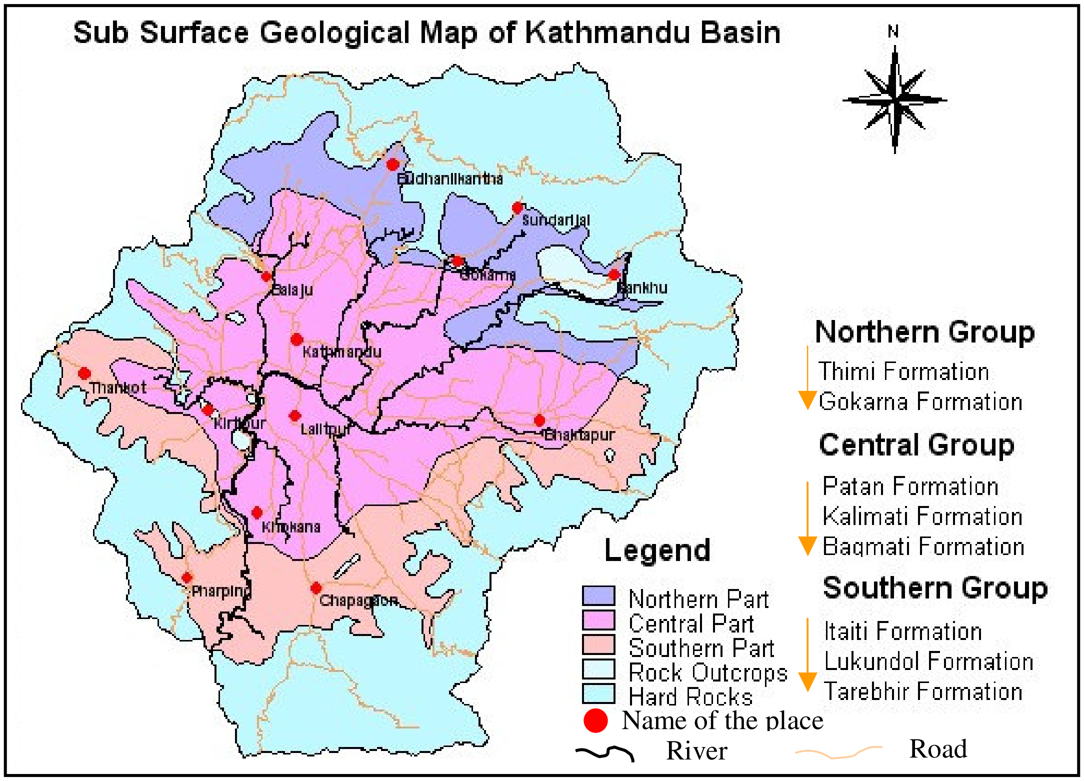

Figure 2.11: Subsurface Geological map of Kathmandu basin, (Classification is based on borehole information).

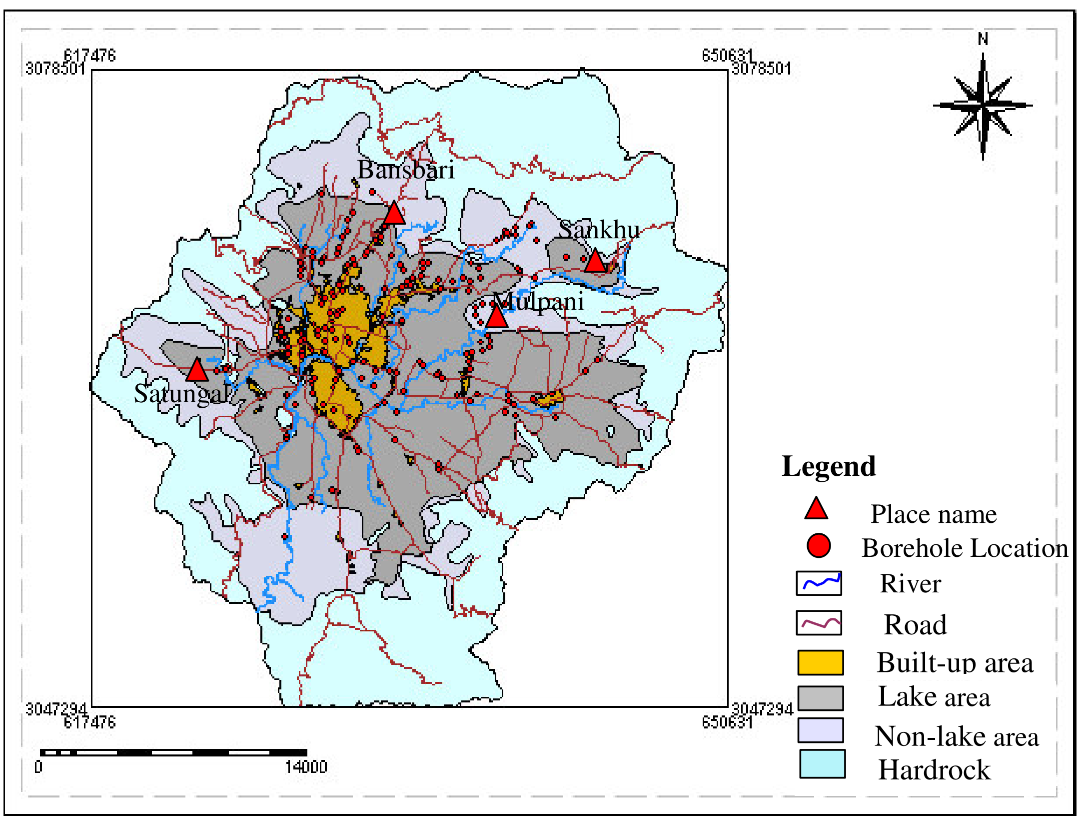

Figure 2.12: The map showing borehole locations and the area covered by the ancient lake

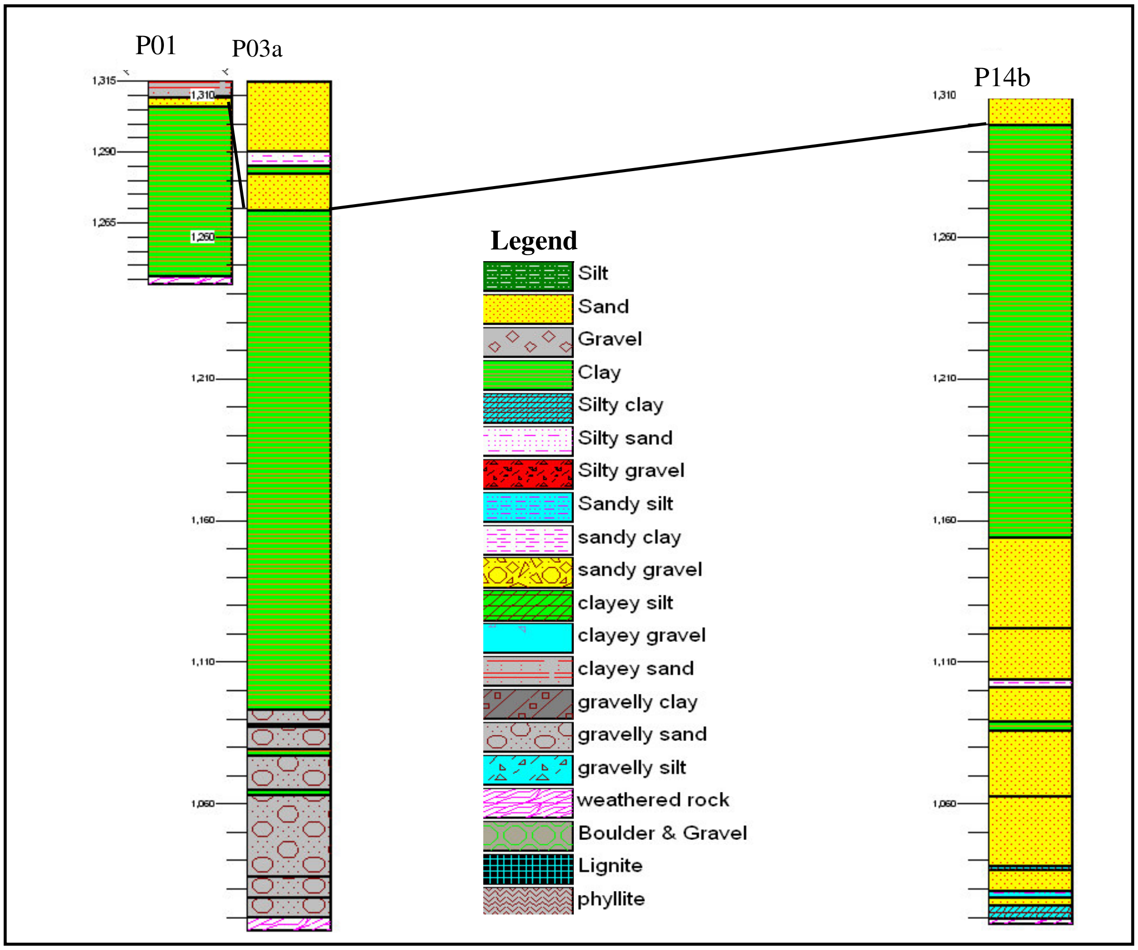

Figure 2.13: Lithologs showing erosional features of clayey sediments as evidenced by the difference in elevation of the top of the lake sediments.

2.4. Sedimentation Processes and Bedrock Topography

The sedimentation processes in the basin of Kathmandu valley are still not known in detail. There are many views about the sedimentation process in Kathmandu valley. The faults running parallel to the Kalphu Khola Fault (Figure 2.4) seem to have segmented the basin and produced a faulted topography with horst and graben structure (Sakai, 2001). According to Sakai two of the faults existing in the southern part of the valley, Chandragiri Fault and Chobhar Fault are active faults cutting the colluvial slopes and terraces of the late Pleistocene. On the other hand, Kalphu Khola Fault is an active fault cutting the late Pleistocene gneissic boulder beds to the North-west of the valley (Nakata et al., 1984). Hence, it can be said that the sedimentation of the Kathmandu basin group must have been controlled by these faults. The main source of the sedimentation in the basin however is the surrounding mountains from where the sediments were carried by the ancient drainage system. The southern sediments were derived from the southern hills such as Chandragiri and Phulchauki consist of meta sedimentary rocks (Argillacious type), while the northern sediments were derived from the northern Shivapuri, hills comprising of intrusive rock (gneiss and granites). The unconsolidated sediments that occupy the Kathmandu valley consist of fluvial-lacustrine sequences with much local variations. Overall, the sediments in the northern part of the valley are generally poorly sorted, thin to medium-bedded highly micaceous coarse sands, gravel and silts interbeded with clays in some places. These become increasingly common towards the northern margin. In the southern half, the sediments mainly consist of a thick sequence of cohesive sediments consisting of dark grey to black highly plastic clay and silts that is usually overlain and underlain by sequences of coarse sediments. The black plastic clay (locally called Kalimati) is exposed at the surface in some places and is rich in organic matter, which is also proven by the occurrence of natural gas within the valley. It is also characterized by the mineral vivianite. Diatomacious sediments and abundance plant fossils within the clay deposits are also reported in some of the boreholes along with spots of vivianite (Sakai et al., 2001). This clay is assumed Pliocene to Pleistocene in age by Yoshida and Igarashi (1984). Its thickness is greatest along the central part of the valley starting from Satungal towards Lalitpur and Bhaktapur. The clay thickness also increases quite a bit towards Bungamti and Harisidhi area in the South (see lithological cross sections, in Chapter 4).

Besides this, the valley comprises of alluvial deposits in river channels, flood plains, and fans, which are of Holocene age (Yoshida and Igarashi, 1984). The sediments in this area have been described as highly micaceous coarse grained sand and silt and have been derived from bedrock areas. Numerous well-developed alluvial fans are also present along the valley rim with steep upper slopes that flatten and widen progressively towards the valley (see geological map Figure 2.5). Many of these fans are deeply dissected and consist of gravels interbedded with clay layers suggesting the deposition into lacustrine environment.

Although not much is known about the bedrock topography and the origin of the sediments, the following discussion has been made based on the study of the borehole logs and the available literature. It is known from the drill hole data that, 36 out of 185 wells have reached the bedrock level, ranging in depth from 48 m from the surface in PR16 (Nursing campus, Sanepa) to 545 m in borehole DMG6 (Bhrikutimandap). The other boreholes are still in soft sediment deposits. Besides this the exposure of basement rock is either encountered at shallow depth or is exposed as an outcrop at Chobhar, Swayambhu, Pashupatinath, Balkhu and Patan (See Figure 2.4). All these evidences indicate that there are many buried ridges in the bottom of the valley that extend NW-SE (Sharma and Singh, 1966). The bedrock elevation reached by boreholes (see Table A. in annex part) suggests an undulating topography with steep relief. The 3 D view of the bedrock topography with the presence of ancient drainage channels is shown in Figure 2.17.

From the study of borehole logs, it can be concluded that the sediment distribution in the valley is far from uniform. However, it is reasonable to consider that in the pre-lake formation, drainage systems originating in the northern slope of the Shivapuri hill and termed as “Proto Bagmati River” by Hagen (1968) were very active. These river systems were responsible for the deposition of coarse-grained sediments (gravels, and coarse sand) below the lake deposits in the entire valley. These sediment deposits are known as Bagmati Formation in the central part and Tarebhir Formation in the southern part of the basin as described in section 2.3. The formation covers the basement rock of the Kathmandu complex as defined by Stocklin and Bhatterai (1977). The thickness of this formation in the borehole logs varies from a few meters up to 135 m (P14b, Yak and Yeti hotel). However the influence of the proto Bagmati river in well B24, B25, (Sanepa area), in well Bal2 and P01 (Balaju area) and in well Naik1, and Naik2 (Naikap area) seems to be negligible as no evidence of this type of deposit is found in them (see Figure 2.16 for location of these boreholes). The influence of proto Bagmati river system appears more in the northern and central part than in the southern part of the valley. According to Yoshida and Igarashi (1984), this deposition took place some 2.5 Ma before i.e. during middle to late Pliocene period.

Sakai et al. (2001) claim the lake in the valley to have originated around 2.5 Ma BP. After that several stages of deposition and erosion of the sediment has taken place. Sakai (2001) identified seven stages of depositional environment using the sediments obtained from borehole Paleo-1, drilled under the so-called Paleo-climatic study project in 2001. According to him the appearance of the lake in the Kathmandu valley is indicated by the occurrence of the marginal lacustrine sediments named as basal lignite member of the Kalimati Formation containing lignite bed (see Well B20 (Katunje), KM1 (Kalimati), and WHO8 (Bungamati), in Figure 2.14). Except in these wells and in Paleo-1 (Rabibhawan), WHO1 (Mahankal Chaur), and in WHO3 (Bansbari), the occurrence of lignite over the Bagmati Formation is not common. Along with the appearance of the lake fine sediments started to be deposited in the basin. The deposition of fine sediments is interrupted many times by the fluvial activity that brought coarse sediments such as sand and gravel along with it and was deposited over the clay. This indicates that the lake could not remain quiet for long period in the beginning. This alternative cycle of lacustrine environment and fluvial activity remained continuous for a successive period. Then a quieter lacustrine environment continued unhindered for a long period of time (middle to late Pleistocene period). This is called as an open lacustrine period. Very thick deposit of clay as shown in Figure 2.8 was deposited during this period and in this period the lake spread and occupied the maximum area of the valley and attained the maximum depth in its history (see Figure 2.12). However, it is to be noted that the entire sedimentation process was being controlled by the rough topography of the ancient basin, which was controlled, by the active Chandragiri Fault and Chobhar Faults in the South (Sakai, 2001). From the borehole logs, it is evident that the deepest part of the lake occurs at and around Bhrikutimandap (The current exhibition centre) where the bedrock was encountered at a depth of 545 m below the surface as can be seen in Figure 2.15. Another deep well DMG5 exists at Hyumat tole (name of the place), Kathmandu that reaches the bedrock at 445 m below the surface. Similarly, boreholes DMG8 at Shankhamul and B1 at Harisiddhi, drilled up to the depth of 455 m and 457 m respectively below the surface still do not meet the bedrock indicating that the lake was deeper in those area. Sakai (2001) estimated the average sedimentation rate of the upper part of the Kalimati Formation to be about 104 mm per 1000 year. According to him, the lake of Kathmandu valley was drained by 11,000-10,000 B.P. He claims that the active fault system (Chandragiri and Chobhar Faults) in the South must be responsible for the draining out of water from the lake. However, a detail study has still to prove this theory.

There are different stories among the people of Kathmandu valley about the draining of the lake, which is quite different from that of the experts (Geological view). These thoughts are based on the religious myths. Hindus believe that, lord Krishna drained the lake by cutting the gorge at Chobhar South of Kathmandu valley with his weapon known as “Sudarshan Chakra” (Sudarshan is other name of lord Krishna and Chakra is wheel according to Hindu mythology) who came to Kathmandu valley with other cow herders (Krishna’s friends) from Dwarika (A place in India which is believed to have been sunk in the ocean) and made the place inhabitable. On the other hand, Buddhists claim that, the Bodhisattva Manjushri came to Nepal from Tibet for meditation at a place called Nagarjun hill. Then he cut the mountains at Chobhar with one blow of his sword and the lake water was drained. However, these are only myths.

As it is already discussed and observed in the borehole logs, we can say that, the depositional environment of the sediments within the valley varies from place to place which was strongly controlled by the topographic situation. The changes in depositional environments of the sediments based on the deepest borehole of the valley are described below.

The deepest borehole in Kathmandu valley is shown in Figure 2.15. The left figure indicates the borehole log with lithological information and the right one indicates the borehole log with stratigraphic sequence. The number in bracket indicates thickness of each formation or deposits. From Figure 2.15 we see that, prior to the appearance of the lake; proto-Bagmati river system of Hagen (1968) was active within the basin that transported the coarse sediments from the northern Shivapuri hill. This sediment is characterised by coarse sand to gravel beds. The thickness of this Bagmati Formation (Sakai, 2001) in this borehole is up to 32 m as shown in the Figure 2.15. Then the appearance of lake began which is indicated by the deposition of greenish grey clay more than 27 m thick. Later as the lake began to lower down the process of clay deposition was interrupted by fluvial activity for a considerable period of time. 54 m thick, medium to coarse-grained sand was deposited during this period. Gradually the lake began to rise and its activity increased for other short period of time depositing about 18 m thick clay sediments. After this the lake again lowered down and its activity is diminished which was taken up by the fluvial activity that went to continue for long period of time, that deposited more than 136 m thick deposits of sand to gravelly sand with intercalation of few meters of clay deposits at certain interval. This time might be considered as the most turbulent condition of the fluvial activity.

Again, the river activity slowed down and the lake began to rise gradually that resulted in the deposition of 54 m thick sticky clay followed further by fluvial activity with deposition of 21 m thick gravelly sand. This alternate process of deposition of coarse material and fine materials before the deposition of long sequence of clay deposits might have been occurred until the beginning of the middle Pleistocene period. After this, the quietest period of lacustrine environment began that went for a long period of time during which it deposited greater than 187 m thick deposit of clay. In this time, the lake seems to have reached its most matured stage.

During this time, the lake might have occupied a maximum area of the valley. This situation might have been remained in the valley until 29,000 year B.P (Yoshida and Igarashi, 1984) and in some places in the central part of the valley until 11,000 years B.P. After this period, the lake is believed to have drained. The fluvial process became active again and began depositing the coarse material over the Kalimati clay. The erosion process became active, terraces were formed and gradually the lake became dry. According to Yoshida and Igarashi (1984), this happened about 10,000 years B.P. Thus in the central part of the valley we find nine stages of deposition processes, which is different from other places with in the valley. In some places, such as in boreholes B25, B 24, B13, P14b, P01, PR16, and in P3a we find only two or three stages of deposition processes (see Figure 2.16 for location).

Thus, based on study of depositional environment in borehole DMG6, I have named different stages of the depositional environment of the sediments in the basin as given below.

- Post lake,
- Shallow lake (stage3)
- Fluvio-deltaic (stage3)
- Deep lake (stage)
- Fluvio-deltaic (stage2)
- Shallow lake (stage 2)
- Fluvio-deltaic (stage1)
- Shallow lake (stage1)
- Protobagmati River

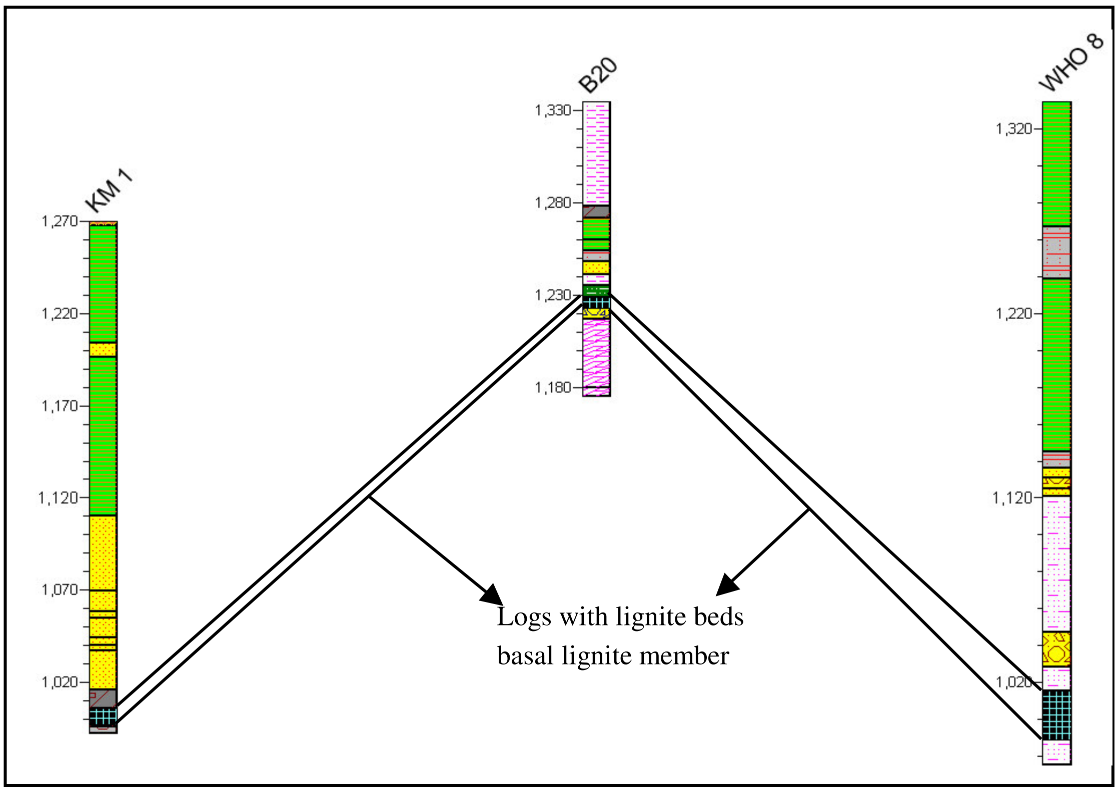

Figure 2.14: Lithologs with lignite beds

A combination of topographical data of the outcropping hard rock with an interpolation of the drilled depth of deep boreholes led to a digital elevation model of the bedrock without the Quaternary sediments as shown in Figure 2.17.

The model of bedrock topography created indicates that, the ancient Bagmati River did not flow through the present courses i.e., through Bagmati gorge at Gokarneswar via Pashupati, but from Sundarijal to the southeast before joining with Manohara. In the southern part of the valley, the joined

Bagmati/Manohara River was flowing directly to the southwest towards Dakshinkali gorge, passing through the East of Lalitpur city and North of Harisiddhi and from there towards Khokna, Bungamati, and to the South.

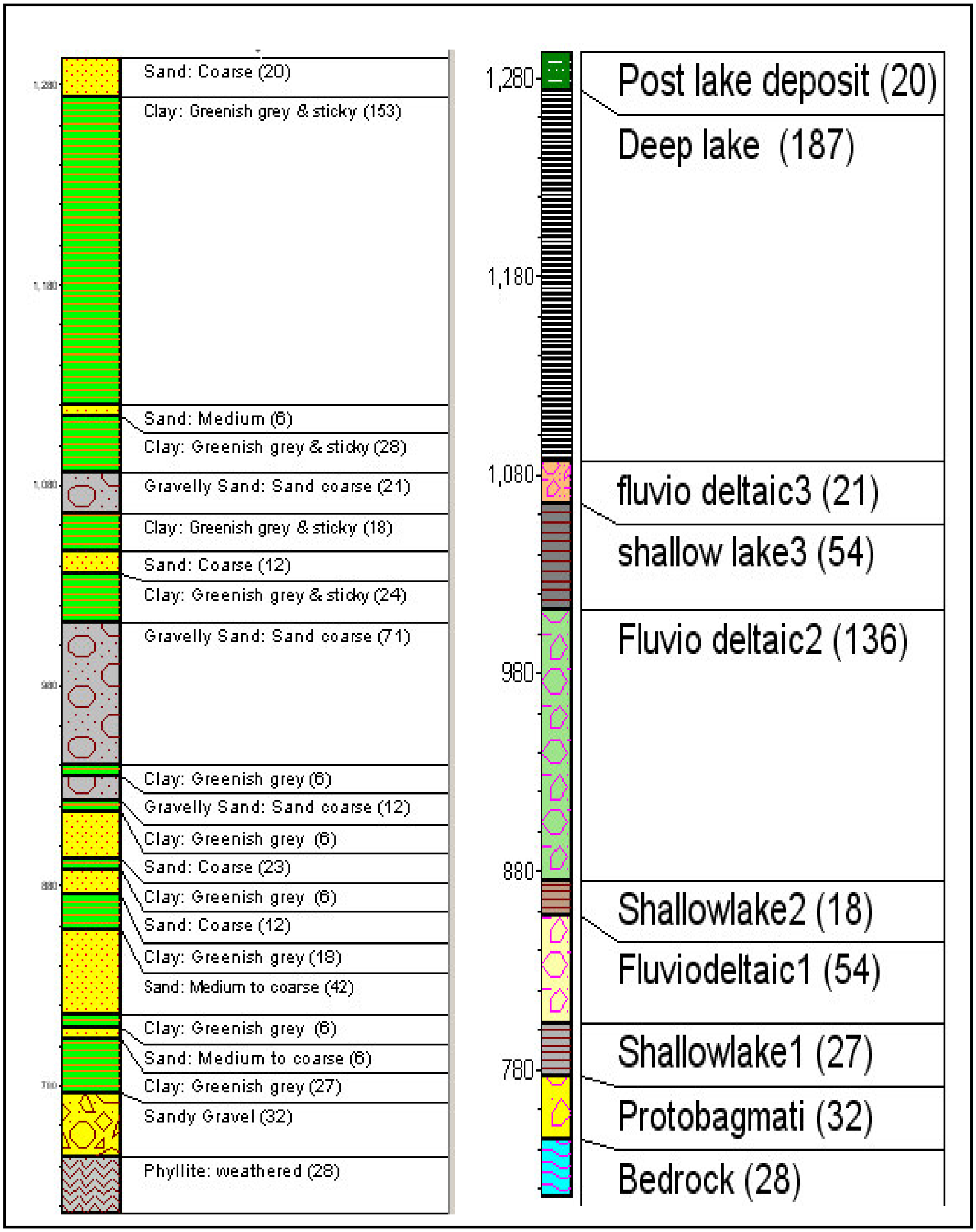

Figure 2.15: The lithological log and stratigraphic log of the deepest borehole in Kathmandu valley.

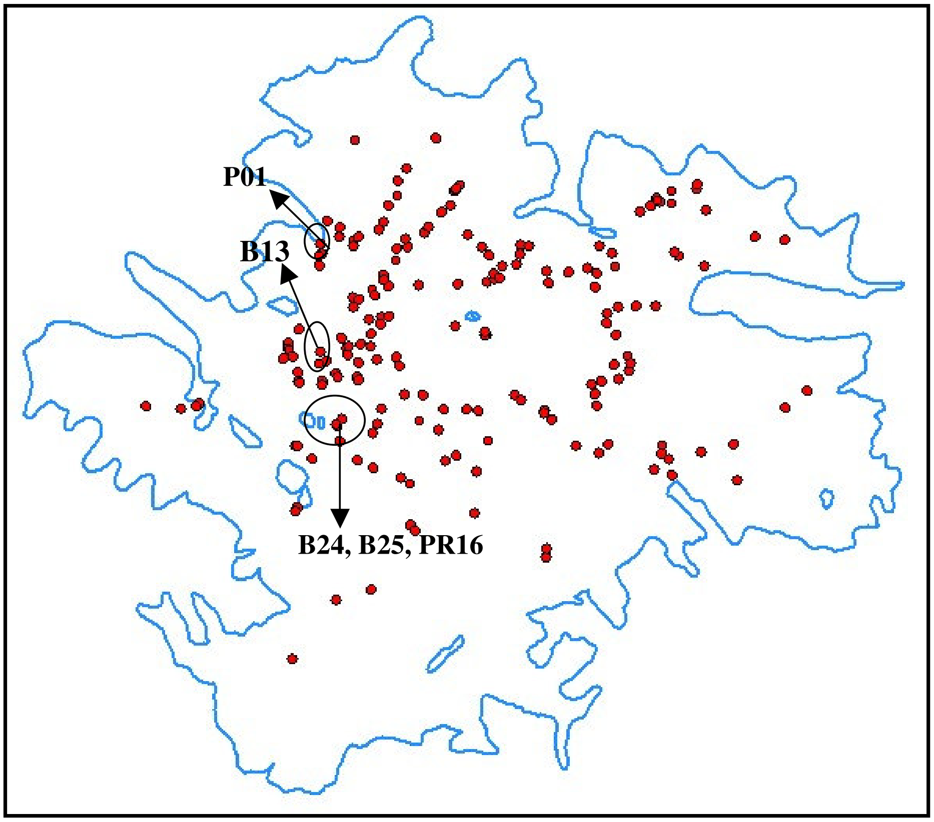

Figure 2.16: Boreholes location map

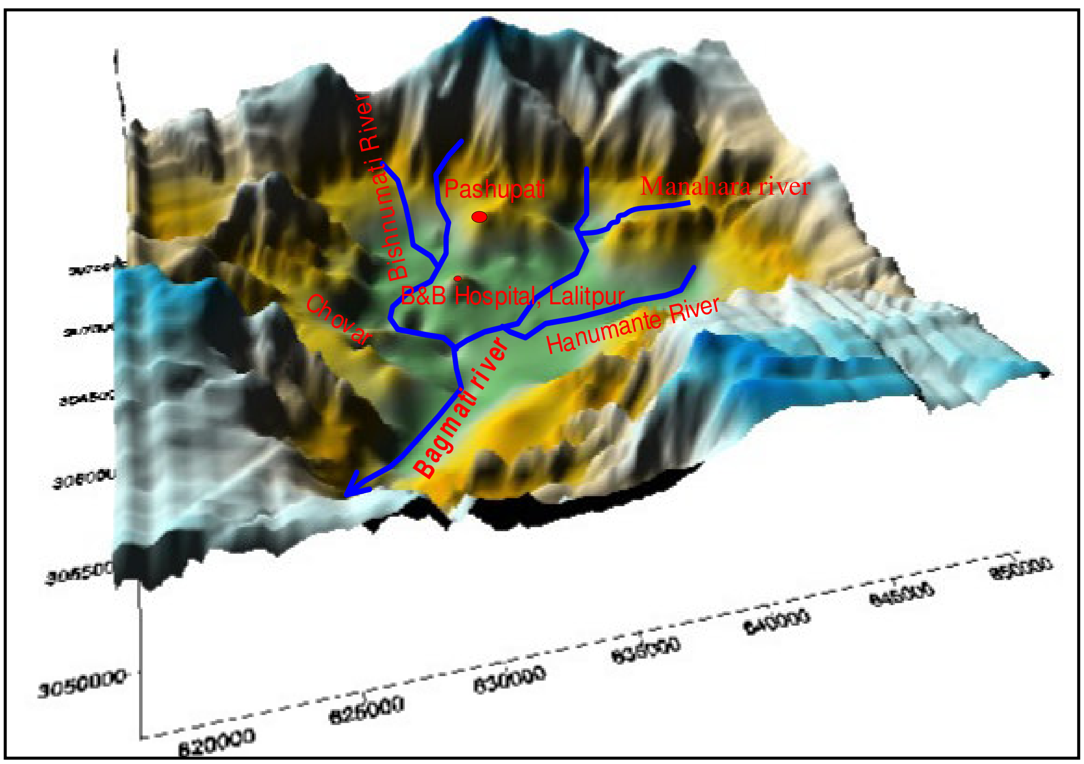

Figure 2.17: The model of bedrock topography, with ancient drainage channel

The model shows deeply incised channels from the surrounding mountains towards the centre of the Valley, several depressions of the bottom floor in the area of Tokha (NW), Southeast of Sundarijal (NE), Satungal (W) and in the centre of the Valley can also be seen, which leads to the following assumptions:

a) Old drainage channels existed with a different direction than that of the present
b) A system of several depressions (local lakes?) occurred, mainly towards the margins of the Valley, where they were blocked from the centre by highly competent ridges, the depressions were also common in the central part of the valley forming lakes.
c) These lakes had overflows and connections to the main drainage system.

There is no concrete explanation about the lake level changes yet, but Sakai et al., (2001) believe that climatic conditions such as, change in seasonal wet and dry cycles may be the important factors. According to them heavy rainfall of 300 to 400 mm per month has the potential to cause the lake level rise by few meters if the basin outlet is plugged. The terrace formation may have been associated with the lake fluctuation, which may have been accelerated due to damming effect at the outlet as a result of mass movement such as landslides (Sakai et al., 2000).

2.5. Ground Level Conditions of Kathmandu Valley

ENPHO (Environment and Public Health Organization) carried out a hydrogeological investigation in the Kathmandu Valley in 1999. The water table was measured in the 40 dug wells situated at different parts of the Valley. From the ground level, the shallowest water table in the dug wells was found in the Bungmati area situated in the South where the water level was only 0.5 m below the ground surface while the deepest water level was found in Nepal Lever Office in New Baneswor where the water level was 10.45 m below the ground. The maximum water level fluctuation was 3.8 meters in Pulchowk.

Similarly, the Environmental Geology project of DMG (1998) carried out investigation on water tables of dugwells and deep wells in Kathmandu valley. A total of 82 representative dug wells were selected for water table measurements. The water table measurements were made in July, August, September and November 1997. In general the depth of the water table is depending on the topographical position of the dug well, about 5-9 m deep in the north-eastern part of the Valley near Sankhu, where the wells are located at higher altitudes and not deeper than 2 m below ground in the western, central and eastern part. Towards the South, the depth of the water table is shallow in the valleys with depths of about 1 m, and deeper on the ridges at higher altitudes. The water table data of dug wells as measured by the project is given in annex in Excel file (file name water table data).

It is found that, the depth to water table in the month of July, vary from 0.71 m to 5.3 m, in august, the variation range from it was from 0 m to 6.22 m, while in September, it was between 0 m to 8.18 m below the ground surface at different places. Similarly, for November, it fluctuates from 0 m to 8.32 m below the ground surface. The two years data (as given in annex in CD enclosed herewith) show that the water table in the dug wells lie between 0 to 10 m below the ground surface. Generally, the water table in dug wells of Kathmandu valley rises during and after the rainy season and in winter and dry season, it is rather low. The study of water table in this research became important, because it is a key factor for the cause of the occurrence of liquefaction phenomena in a strong motion, which will be dealt in the following chapter.

3. Liquefaction Hazard Assessment: Overview of the methods

3.1. Introduction

Liquefaction is one of the most interesting but complex and controversial topics in earthquake engineering. Its devastating effects in Alaska (USA) and Niigata (Japan) as a result of the 1964 earthquake of magnitudes 9.2 and 7.5 Richter scale drew the attention of the geological engineers of the world and compelled them to think about it. Both earthquakes produced spectacular examples of liquefaction-induced damage including ground failures, bridge and building foundation failures and floatation of buried structures (Kramer, 1996). Since then hundreds of researchers around the world has been studying this hazard. The term liquefaction was originally coined by Mogami and Kubo, 1953 (cited from Kramer, 1996). The generation of excess pore pressure under undrained loading condition is a hallmark of all liquefaction phenomena. When cohesionless soils are saturated with water and rapid loading occurs under undrained condition, the tendency for densification causes excess pore pressure to increase and effective stress to decrease hence liquefaction results.

Liquefaction is caused by earthquake shaking. Before going to the liquefaction hazard assessment, it is important to know that:

- What strength of Earthquake motion and under what conditions of the ground surface causes liquefaction?
- What are the effects of liquefaction and how it can be mitigated?
- What are the guidelines for the preparation of Liquefaction hazard map?
- What are the applications of liquefaction hazard map?

Different experts have various ways of defining liquefaction. Some definitions are given below,

Liquefaction is defined as:

- A phenomenon in which the strength and stiffness of a soil is reduced by earthquake shaking or other rapid loading (ABAG's Report, "Real dirt on Liquefaction", 2001).

- The capacity of relatively loose saturated sandy soil to lose a large proportion of its strength under seismic shaking (UNDP / UNCHS/HABITAT, 1994).

- Processes by which sediments below the water table temporarily loose strength and behave as a viscous liquid rather than solid mainly caused by seismic waves (Hazus99-SR2Technical Manual).

Liquefaction occurs in saturated soils, in which the space between individual particles is completely filled with water. Its effects are most commonly observed in low-lying areas near bodies of water such as rivers, lakes, bays, and oceans (ABAG's Report, "Real dirt on Liquefaction", 2001).

Liquefaction occurs in Cohesionless sand deposited in fluvial environment. Areas of high liquefaction potentials are alluvial floodplains, deltaic deposits, estuaries deposit, colluvial and aeolian deposit, artificial fill etc. Areas of medium liquefaction potentials are alluvial fans, channel deposits, and beaches. Areas of coarse deposits and rock debris do not undergo liquefaction (L.S Srivastava, un-publ. report). The susceptibility to liquefaction depends on the density of the sand and intensity of ground motion (amplitude and duration).

According to Kramer (1996), two types of liquefaction exist.

Flow Liquefaction: - It occurs when the shear stress required for static equilibrium of a soil mass (The static shear stress) is greater than the shear strength of the soil in its liquefied state. When liquefaction occurs in such case the strength of the soil decreases and the ability of soil deposit to support for the structure is reduced.

Flow liquefaction failures are characterized by the sudden nature of their origin, the speed with which they develop and the large distance cover over which the liquefied materials often move.

Cyclic mobility: It occurs when the static shear stress is less than the shear strength of the liquefied soil. It produces unacceptably large permanent deformation during earthquake shaking, which is also known as lateral spreading. It can occur on very gently sloping ground or on virtually flat ground adjacent to bodies of water.

Flow liquefaction occurs much less frequently than cyclic mobility but its effects are usually far more severe. Besides these two types, Ground oscillation, loss of bearing strength and sand boils are common phenomena of Liquefaction.

Conditions for Liquefactions

For the liquefaction to occur in any place the following conditions should be met.

- The soil must be susceptible to liquefaction (i.e. the soil should be loose, water-saturated, sandy soil typically between 0 and 10 meters below the ground surface).
- Ground shaking must be strong enough to cause susceptible soils to liquefy.
- Ground water should lie within 15 meter deep inside the surface.

3.2. Factors affecting the liquefaction susceptibility

Liquefaction susceptibility is a function of the geotechnical properties and topographic position of the unit and is independent of the region's expected seismicity. Factors affecting liquefaction susceptibility include sedimentation process, age of deposit, water table depth, geologic history, grain size distribution, depth of burial, density state, proximity to a free face and ground slope (Youd and Perkins, 1978). They are briefly described below.

3.2.1. Grain Size

Both field and laboratory data show that loosely packed cohesionless sands that are clean without clay or silt can readily liquefy and form great number of clastic dykes, sills and sand blows. According to Valera et al., 1994 (cited in Obermeier, 1996) the threshold magnitude for sand to liquefy is 5.5 where as for gravel deposit is 7. Laboratory and insitu observation in recent years showed that non-plastic silts might also liquefy (Ishihara, 1985). Coarse silts with bulky particle shape, which are non-plastic and cohesionless, are fully susceptible to liquefaction. Whereas finer silts with flaky or plate like particles generally exhibit sufficient cohesion to inhibit liquefaction (Ishihara, 1993). Clays remain non-susceptible to liquefaction, although sensitive clays exhibit deformation-softening behaviour similar to that of liquefied soil (Kramer 1996). Fine-grained soils that satisfy each of the following four Chinese criteria (Wang, 1979) may be considered susceptible to significant strength loss:

- Fraction finer than 0.005 mm ≤ 15%
- Liquid Limit (LL) ≤ 35%
- Natural water content ≥ 0.9LL
- Liquidity index ≤ 0.75.

When clay is contained in the sand and the cohesion is high, liquefaction does not usually occur, and if it does, the displacement is small. Therefore, there is little settlement of ground, and damage is slight. The presence of even a small amount of cohesion from clay or silt sized material can impede particle rearrangement during cyclic straining and greatly increase resistance to cyclic loading.

As little as 5% clay or silt sized material in a sand deposit can make liquefaction significantly less likely than for the same sand deposit lacking fine grains (national research council, 1985, p. 103). Generally, coarse-grained material such as coarse sand and Gravel do not go liquefaction but under very strong seismic shaking and close to the source of the quake, gravel also liquefies. For example during the 1983 Borah Peak, Idaho earthquake M-7.3 extensive liquefaction occurred. During this earthquake large amount of gravel bearing sand were vented on to the ground surface. Significant lateral spreading also occurred (Andrus et al., 1991, cited in Obermeier, 1996). In general, gravel rich deposits are more densely packed than sands and high gravel content increases internal friction resistance making liquefaction more difficult. Liquefaction susceptibility is also influenced by gradation. Well-graded soils are generally less susceptible to liquefaction than poorly graded soil. The filling of voids between larger particles by smaller particles in a well-graded soil results in lower volume change potential under drained conditions and consequently lower excess pore pressure under undrained condition. Field evidence indicates that most liquefaction failures occur in uniformly graded soils. Similarly, particle shape also influences the liquefaction susceptibility. Soils with rounded particle shapes are known to densify more easily than soils with angular grains. Since particles rounding frequently occur in fluvial and alluvial environment, liquefaction susceptibility is often high in those areas.

3.2.2. Relative density

The arrangement or packing of sand grains has a profound effect on sediment liquefaction susceptibility. Susceptibility of the same sand can be changed from very high to non-susceptible simply because of a change in packing. The state of looseness or denseness of cohesion less sediment is generally measured in place by the Standard penetration test (SPT). SPT blow-count values in granular deposits principally reflect states of relative density and static vertical effective stress, which are the factors mainly controlling liquefaction susceptibility.

The Table 3.1 shows the relation between blow count and relative density in terms ranging from very loose to very dense. Sands that are moderately dense or looser liquefy in many field situations. Dense sands require exceptionally strong shaking and very dense sands probably rarely generate residual pore pressure large enough to form fluidisation features (Seed et al. 1983).

Table 3.1: Relation between blow count and relative density

N – value	Classification	Dr %	$(N1)_{60}$
0-4	Very loose	0-15	0-3
4-10	Loose	15-35	3-8
10-30	Medium dense	35-65	8-25
30-50	Dense	65-85	25-42
>50	Very dense	85-100	42-58

(Source Craig, 1986, Soil Mechanics p 305 After Terzaghi and Peck/Gibbs and Holtz)

3.2.3. Depth to water table

Liquefaction susceptibility decrease strongly with increasing depth to the water table (Obermeier, 1996). The extent of the control is indicated in the Table 3.2. According to this table, the lowering of water table as little as several meters can change the susceptibility from high to low. Normally liquefaction is not expected at a place where water table is greater than 10 m.

Table 3.2: Influence of age deposit and depth to water table on liquefaction susceptibility (Obermeier, 1996)

Age of deposit	Depth to water table		
	0-3 m	3-10 m	>10 m
Latest Holocene	High	Low	Nil
Earlier Holocene	Moderate	Low	Nil
Late Pleistocene	Low	Nil	Nil

3.2.4. Depth to thickness of Strata

Liquefaction during earthquake shaking frequently originate as shallow as 1.5 to 2 m below the ground surface (Obermeier et al, 1986). According to Seed (1979), the source zone for liquefaction can exceed 20 m. The most common depth however is a range between a few meters and about 10 m. Optimal depth is about 2-4 m in many field settings where the water table is within a few meters of the surface. Lacustrine sediment seems to be most favourable for the development of liquefaction effects in thin strata because of the large aerial extent to the strata. According to Ishihara (1985) and Obermeier (1996), a cap thickness exceeding 10 m prevents ground rupture even in the most favourable circumstances for liquefaction.

3.2.5. Previous Liquefaction

A great deal of information on liquefaction behaviour has come from post earthquake field investigations, which have shown that liquefaction often recurs at the same location when soil and groundwater conditions have remained unchanged (Youd, 1984a). Thus, liquefaction case histories can be used to identify specific sites or more general site conditions, that may be susceptible to liquefaction in future earthquakes.

Human made deposits (Fill) those placed without compaction are also very likely to be susceptible to liquefaction (Kramer, 1986).

3.3. Criteria for identifying and mapping Liquefaction areas

A number of guidelines are being proposed for developing liquefaction hazard map all over the world. The geotechnical earthquake engineer can systematically evaluate potential liquefaction hazards by addressing the following questions:

- Is the soil susceptible to liquefaction?
- If the soil is susceptible, will liquefaction be triggered?
- If liquefaction is triggered, will damage occur?

If the answer to the first question is no, the liquefaction hazard evaluation can be terminated with the conclusion that liquefaction hazard do not exist. If the answer is yes, the next questions must be addressed. If answer to all questions is yes then one should be ready for the mapping of liquefaction areas.

The basic criteria for identifying and mapping the liquefaction areas are:

- The areas known to have experienced liquefaction during historic earthquakes.
- Areas where uncompacted fills containing liquefaction susceptible materials are present.
- Areas underlain by saturated geologically young material mostly Holocene deposit.
- Areas where soil testing (geotechnical data) indicates probability of liquefaction.

To understand more about the liquefaction why it occurs and when, it is important to recognize the conditions that exist in a soil deposit before an earthquake. A soil deposit consists of an assemblage of individual soil particles as shown in Figure 3.1a. If we look closely at these particles, we can see that each particle is in contact with a number of neighboring particles. The weight of the overlying soil particles produce contact forces between the particles. These forces hold individual particles in place and give the soil its strength. Liquefaction occurs when the structure of loose, saturated sand breaks down due to some rapidly applied loading. As the structure breaks down, the loosely packed individual soil particles attempt to move into a denser configuration. In an earthquake, however, there is not enough time for the water in the pores of the soil to be squeezed out. Instead, the water is "trapped" and prevents the soil particles from moving closer together. This is accompanied by an increase in water pressure, which reduces the contact forces between the individual soil particles, thereby softening and weakening the soil deposit. In an extreme case, the pore water pressure may become so high that many of the soil particles lose contact with each other. In such cases, the soil will have very little strength, and will behave more like a liquid than a solid - hence; the name "liquefaction" is given to this phenomenon.

Liquefaction has been observed in earthquakes for many years. In fact, written records dating back hundreds and even thousands of years describe earthquake effects that are now known to be associated with liquefaction. Nevertheless, liquefaction has been so widespread in a number of recent earthquakes that it is often associated with them. Some of those earthquakes are Hyogo-ken Nanbu Earthquake around Kobe in 1985, Loma Prieta Earthquake, California in 1989, Mexico Earthquake in 1985, Nigata Earthquake in 1964 (Sakai, et al. 2001).

The soil liquefaction hazard cannot be prevented but can be reduced by taking the following steps:

- Avoid Liquefaction Susceptible Soils
- Build Liquefaction Resistant Structures
- Improve the Soil

These are normally applied when designing and constructing new buildings or other structures as bridges, tunnels, and roads etc. The liquefiable soil can be improved by increasing the drainage capability of soil or by applying drainage techniques for example using gravel sand or synthetic material (ABAG's Report, 2001).

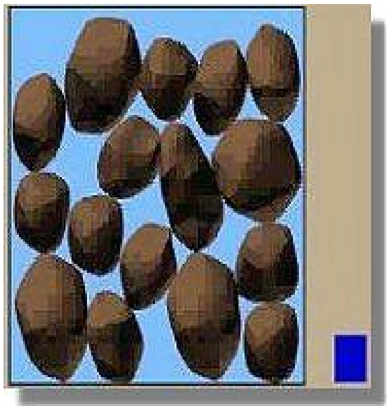

Figure 3.1 (a) Soil grains in a soil deposit. The height of the blue column to the right represents the level of pore-water pressure in the soil.
(Source: ABAG's Report 2001)

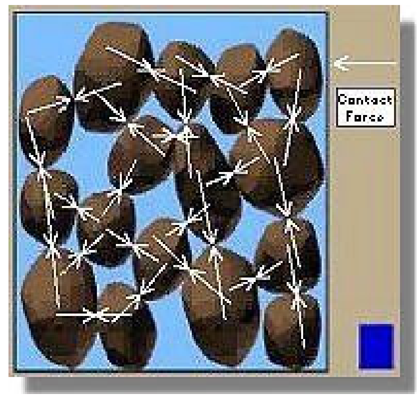

(b) The length of the arrows represents the size of the contact forces between individual soil grains. The contact forces are large when the pore-water pressure is low.

3.4. Liquefaction effects

Liquefaction-related ground failure historically has caused extensive structural and lifeline damage in urbanized areas around the world. The damage caused by liquefaction leaves very painful effects to the people. A lot of property and lives are lost due to the effects of Liquefaction. When the ground liquefies in an earthquake, sandy or silty materials saturated with water behave like a liquid, causing pipes to leak, roads and airport runways to buckle, and building foundations to be displaced. Some examples of ground failure caused by Liquefaction are shown in plates 3.1 to 3.5.

Plate 3. 1: When liquefaction occurs, the strength of the soil decreases and, the ability of a soil deposit to support foundations for buildings and bridges is reduced, as seen in the photo of the overturned apartment complex

Plate 3.2: Entire levees, dams, and other water-saturated embankments can liquefy and flow apart during strong shaking.

Plate 3.3: Buildings founded on liquefied ground will lean or topple

Plate 3.4: Commonly a soil layer on the side of a hill will liquefy during seismic shaking and flow as a landslide or mudflow, as above.

Plate 3.5: A liquefied sand layer can shoot to the surface through cracks, forming a sandblow or sandboil, and depositing a characteristic lens of sand on the ground with a volcano-like vent in the centre. With all the material in the layer forced to the surface, the surrounding area sinks unevenly.

Note: These Pictures are from a report by J.P. Bardet at USC and others at Gifu Univ.
http://www.seismo.unr.edu/ftp/pub/louie/class/100/effects-kobe.html

3.5. Methodology for Liquefaction Hazard Analysis

Various methods of defining the susceptibility of material to liquefaction theories have been proposed. Basically, there are two approaches; Qualitative method and Quantitative methods. The analysis of liquefaction susceptibility following the qualitative methods has been studied by Iwasaki et al. (1982), and Youds et al. (1978). Whereas the quantitative methods of analysis have been studied by various authors such as, Seed and Idriss (1971, 1979), Iwasaki et al. (1984), etc. Both techniques have been tested and found very useful for the liquefaction hazard assessment. Here below, both methods are discussed.

3.5.1. Quantitative analysis

The liquefaction potential of a soil layer can be determined through either laboratory tests on undisturbed soil samples or from insitu tests. However, the combination of both can also be used in the analysis. The common in situ tests for liquefaction hazard analysis are performed by using the standard Penetration Test (SPT), Cone Penetration test (CPT), Flat delatometer test (DMT), the Shear wave velocity techniques (SWV) and self boring pressure meter (SBPT).

Some of the methodologies adopted for liquefaction hazard analysis by different authors are described below.

3.5.1.1. Tsuchida - method

According to this method, a site investigation is undertaken by borings within which SPT tests are taken and from which samples are removed for particle size analysis in the laboratory. Using the particle size analysis curves the samples is classified as ‘A’ - very easily liquefy or ‘B’- easily liquefy (see Figure 3.2). The classified values are then plotted on Figure 3.3, along a vertical line corresponding to the anticipated maximum acceleration. In the case of N values from ‘A’ type samples if the values fall above the ‘A’ line on Figure 3.3, they will not be expected to liquefy; if they fall below, they may be expected to liquefy. The same procedure is adapted to ‘B’ types samples. The horizontal dotted line in the Figure 3.3 represents generalized idea of the ‘N’ limit above which occurrences of known liquefaction are rare. This method indirectly considers the number of cycles of strong motion, which is important with regard to the liquefaction process. The method is considered as an initial step to give an idea as to weather there will be a problem on a particular site or not. This method is valuable but if the analysis shows the marginal situation, more complex methods of analysis must be adopted to clarify the situation.

3.5.1.2. Seed and Idriss - method

Seed and Idriss, (1971) developed a concept of Cyclic Stress Ratio (CSR) for the analysis of Liquefaction susceptibility. According to the laboratory tests undertaken to demonstrate the liquefaction potential of any granular soil demonstrate that, at any particular point Cyclic Shear Stress (CSS) must exceed the shear strength of the ground for liquefaction to occur.

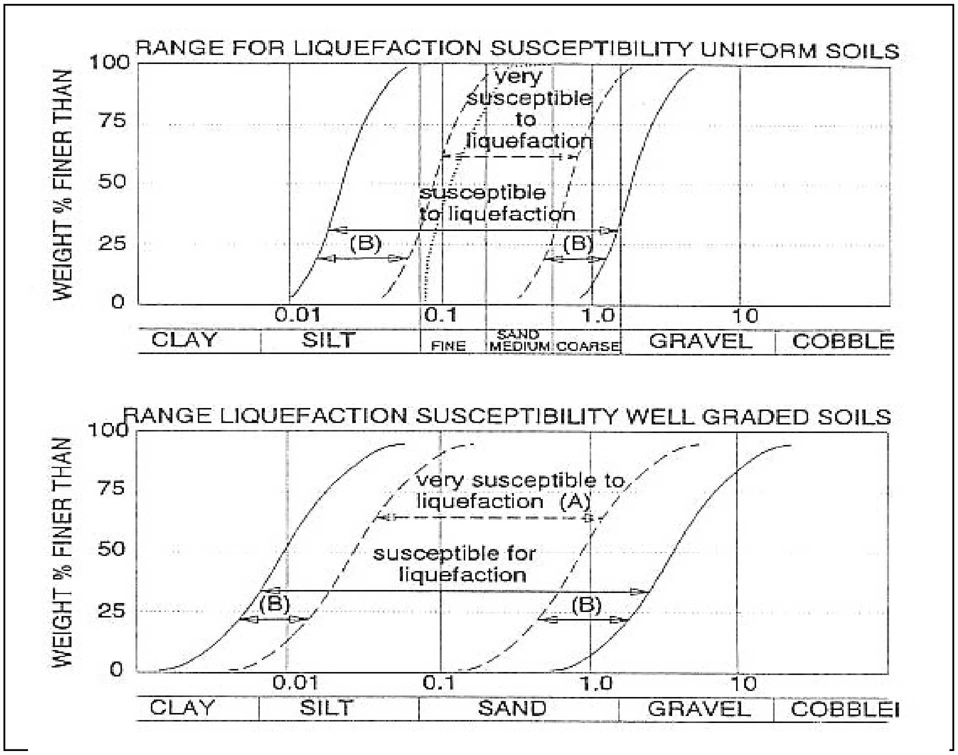

Figure 3.2: Relation between grading and Liquefaction of soil (after Tsuchida 1971, cited from, Maurenbrecher, P.M, et. al. 1998 and Obermier, 1996))

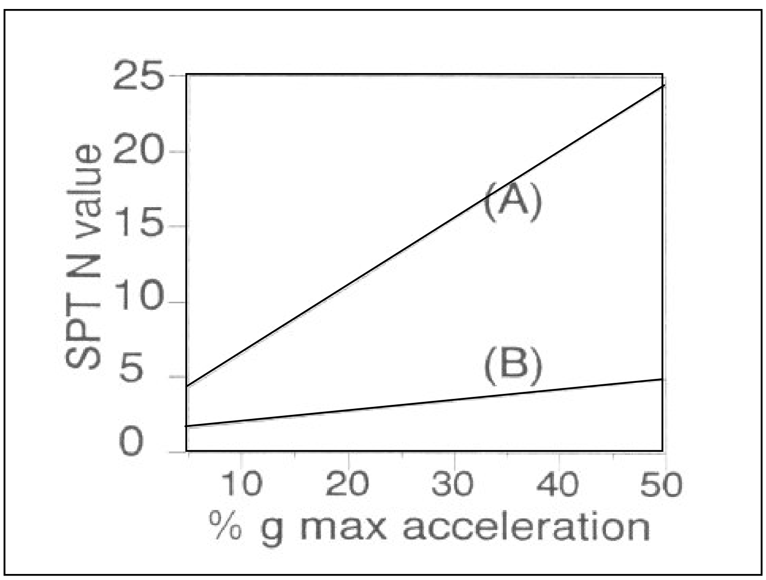

Figure 3.3: Relationship between critical N-value of liquefaction of Soil and seismic acceleration (After Tsuchida, 1971, cited from, Maurenbrecher, P.M, et. al. 1998)

The shear stress developed at any point in a soil deposit during an earthquake appears to be due primarily to the upward propagation of shear wave in a deposit. If the soil above at a depth 'h' behaved as a rigid body and the max ground acceleration is a_{max}, the maximum shear stress on the soil at depth h would be

$$T_{max} = \gamma h \times (\frac{a_{max}}{g}) \text{ -- } \quad (1)$$

γ = Unit weight of soil, g = acceleration due to gravity

Because the soil within 'h' is deformable, the actual shear stress at depth h $(T_{max})_d$ will be less than $(T_{max})_r$ so that,

$(T_{max})_d = r_d \times (T_{max})_r$, Where r_d =stress reduction factor (<1) which can be obtained by the graph as shown in the Figure 3.4 below.

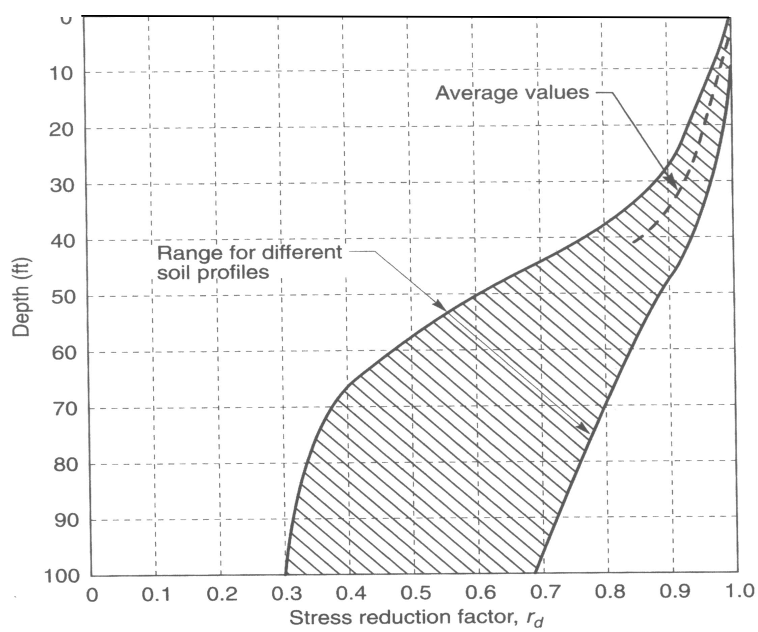

Figure 3.4: Reduction factor to estimate the variation of CSR with depth below the ground level or gently sloping ground surface (After Seed and Idriss, 1971)

Values of r_d vary for different soil profiles but down to depth of 40 to 50 ft, (12 to 18 m) average values of r_d are not so far from the extreme values. In these depths the value of the maximum shear stress (T_{max}) developed during an earthquake can be expressed by;

$$T_{max} = \gamma h \times (\frac{a_{max}}{g}) \times r_d \text{ -- } \quad (2)$$

The values of r_d being taken from the graph (Figure 3.4).

For any earthquake, the variation of shear stresses follows the same pattern as the accelerogram. For a study of a number of cases it has been found that the average shear stress T_{av} is about $0.65T_{max}$, so that the average cyclic shear stress,

$$T_{av} = 0.65 \times \gamma h \times (\frac{a_{max}}{g}) \times r_d \text{ --- } \quad (3)$$

Within the earthquake, trace there will be a number of cycles that are strong in motion. The number of significant cycles is related to the magnitude of the earthquake. The approximate relation between them are shown as in the Table 3.3,

Table 3.3: Relationship between earthquake magnitude and significant cycles of strong motion

Earthquake magnitude	Significant cycles of strong motion
7	10
7.5	20
8	30

In the laboratory, it has been found that the cyclic shear stress causing liquefaction within a number of cycles for sand of fixed relative density depends upon the grain size of the sand. The results of cyclic laboratory tests on samples at 50% relative density are expressed in terms of a stress ratio,

$$\frac{\sigma_{dc}}{2\sigma_a} \text{ -- } \quad (4)$$

Causing liquefaction under 10 and 30 cycles respectively,
Where: σ_{dc}: Cyclic deviator stress and σ_a: Overburden stress under which the sample was naturally consolidated.

A comparison with field experience has shown that at liquefaction

$\frac{T}{\sigma_o} \neq \frac{\sigma_{dc}}{2\sigma_a}$ As determined in the laboratory but is usually lower so that

$$\frac{T}{\sigma_o} = \frac{\sigma_{dc}}{2\sigma_a} \times C_r \text{ -- } \quad (5)$$

At liquefaction. It is suggested that C_r varies with relative density of the deposit.
Here: T: Field shear stress, σ_o : effective overburden pressure

Accordingly,

$$\left(\frac{T}{\sigma_0}\right)_{D_{50}} = (\frac{\sigma_{dc}}{2\sigma_a}) \times C_r \times \frac{D_r}{50} \text{ -- } \quad (6)$$

At liquefaction
Where: D_r: relative density of ground in situ and D50: relative density of 50%
C_r: reduction coefficient

3.5.1.3. Iwasaki - method

Simplified methodology to evaluate the effects of saturated sandy soils liquefaction is needed for reasonable earthquake resistant design of structures considering the surrounding soil liquefaction. Iwasaki et al. (1984) proposed two simplified methods with use of a liquefaction resistance factor $\mathbf{F_L}$ and a liquefaction potential index $\mathbf{I_L}$ to evaluate the liquefaction potential of saturated sandy soils. Based on the proposed methods, the liquefaction potential can be estimated simply by using the fundamental properties of soils, i.e. N-values, unit weights, mean particle diameters, and max acceleration at ground surface.

Liquefaction resistance factor F_L

The liquefaction potential for an individual layer is established by comparing the resistance against liquefaction of this layer (R) with the driving dynamic force that could cause liquefaction (L). With these values, the **safety factor** with respect to liquefaction F_L is determined using the relation at an arbitrary depth,

$$F_L = \frac{R}{L} \text{ --- } \qquad (7)$$

When F_L at certain soil is less than 1.0 we judge that the soil liquefies during earthquake.

R in the equation is the in situ resistance or undrained cyclic strength of the soil element to dynamic loads during earthquakes and can be simply evaluated according to numerous undrained cyclic shear stress tests results using undisturbed specimens as follows:

For $0.04 \leq D_{50} \leq 0.6mm$

$$R=0.0882* \sqrt{\frac{N}{\sigma'_v +0.7}} + 0.225 Log_{10} \frac{0.35}{D_{50}} \text{ -- } \qquad (8)$$

For $0.6 \leq D_{50} \leq 1.5mm$

$$R=0.0882 * \sqrt{\frac{N}{\sigma'_v +0.7}} - 0.05 \text{ --- } \qquad (9)$$

Where N is the umber of blows of SPT, σ'_v is the effective overburden pressure in kgf/cm^2 and D_{50} is the mean particle diameter in mm.

L is the dynamic load induced in the soil element by a seismic motion to cause liquefaction and can be simply estimated by

$$L = \frac{\tau_{max}}{\sigma'_v} = \frac{a_{max}}{g} \times \frac{\sigma_v}{\sigma'_v} \times r_d \text{ --- } \qquad (10)$$

Where τ_{max} is the max shear stress in kgf/cm^2 a_{max} is the max acceleration at the ground surface in gals, g is the acceleration of gravity = 980 gals, σ_v is the total overburden pressure in kgf/cm^2 and r_d is the reduction factor of dynamic shear stress to account for the deformation of the ground. From a number of seismic response analysis for grounds, Iwasaki et al. (1984) proposed the following relation for the factor $r_{d,}$

R_d=1.0 – 0.015Z, --- (11)

Where Z is the depth in meters.

Liquefaction potential Index I_L

An ability to resist Liquefaction at a given depth of grounds can be evaluated by the factor F_L. However, it must be noticed that the damage to structure due to soil liquefaction is considerably affected by the severity of liquefaction degree. In the view of this fact Iwasaki et al. (1984) also proposed a liquefaction Potential Index I_L defined by the following equation to estimate severity of Liquefaction degree at a given site.

$$I_L = \int_0^{20} FW(Z)dZ \,, \quad \text{---} \quad (12)$$

Where $F = 1 - F_L$ for $F_L \leq 1$ and $F = 0$ for $F_L > 1$

W (Z) = 10 - 0.5Z in meters

W (Z) accounts for the degree of soil liquefaction according to the depth.

For the case of $F_L = 0$, for the entire depth, I_L becomes 100 being the highest,

and for the case of F≥1, for the entire depth I_L becomes 0 being the lowest.

The cumulative liquefaction potential for a position at the surface (I_L) is classified according to the following scale.

$I_L = 0$ ------ Liquefaction potential is very low and detailed investigation on soil liquefaction are not needed in general.

$0 < I_L < 5$ ------ Liquefaction potential is low but detailed investigations on soil liquefaction are needed for specially important structures.

$5 < I_L < 15$ -------- Liquefaction potential is rather high and detailed investigations on soil liquefaction are needed for important structures and countermeasures for soil liquefaction are needed in general.

$I_L > 15$ ---- Liquefaction potential is very high and detailed investigations and countermeasures for soil liquefactions are needed.

In particular, such a study was done by Iwasaki et al. (1984), and developed the criteria as given above.

3.5.1.4. Evaluation of Liquefaction based on SPT data

In the United States and most other countries, the standard penetration test (SPT) has been the most commonly used insitu test for characterization of liquefaction resistance. Factors that tend to increase liquefaction resistance such as density, prior seismic straining, over consolidation ratio, lateral earth pressure, and time under sustained pressure also tend to increase SPT resistance.

Seed et al. (1983) compared the corrected SPT resistance and Cyclic stress ratio for clean sand and silty sand sites at which liquefaction was or was not observed in earthquake of M = 7.5 to determine the minimum cyclic stress ratio at which liquefaction could be expected in a clean sand of a given SPT resistance Figure 3.5.

The presence of fines can affect SPT resistance and therefore must be accounted for in the evaluation of liquefaction resistance (Seed et al. 1985), i.e. the Cyclic stress ratio (CSR) required to initiate liquefaction for given $(N_1)_{60}$ values. At higher fines contents, the fines tend to inhibit liquefaction. The plasticity of the fines also influences liquefaction resistance. The adhesion of plastic fines tends to resist the relative movement of individual soil particles and thereby reduce the generation of excess pore pressure during earthquakes. Because strong motion duration (equivalent number of uniform stress cycles) increases with earthquake magnitude. The minimum cyclic stress ratio required initiating liquefaction decreases with increasing magnitude. The minimum cyclic stress ratio for other magnitudes may be obtained by multiplying the cyclic stress ratio for M = 7.5 earthquakes by the factor shown in the Table 3.4.

Cyclic stress ratio is defined differently for different types of tests. According to Seed and Idriss, (1971),

$$CSR = \frac{\tau}{\sigma'_0} = 0.65 \times \frac{a_{\max}}{g} \times \frac{\sigma_0}{\sigma'_0} \times r_d \text{ -- } \quad (13)$$

Where τ / σ'_0 is the Cyclic Stress ratio to develop the liquefaction in the soil, a_{max} is the peak horizontal ground acceleration on the ground surface (in g), σ_0 is the total stress over the layer of interest, σ'_0 is the effective stress over the layer of interest and r_d is the reduction factor. The work of Seed and his co-workers in the form of cyclic stress versus SPT N value is presented in Figure 3.5.

Liquefaction can also be expected at depth where the loading exceeds the resistance or when the factor of the safety against liquefaction expressed as given below is less than or equal to1.

$$FS_L = \frac{\text{Cyclic Shear Stress required to cause liquefaction (graph)}}{\text{Equivalent cyclic shear stress induced by earthquake}} = \frac{\tau_{cyc,L}}{\tau_{cyc}} = \frac{CSR_L(CRR)}{CSR} \text{....}(14)$$

CRR = Cyclic resistance ratio or the Liquefaction resistance

Besides these, Liquefaction can also be evaluated based on Cone Penetration test (CPT) data and Shear wave velocity data.

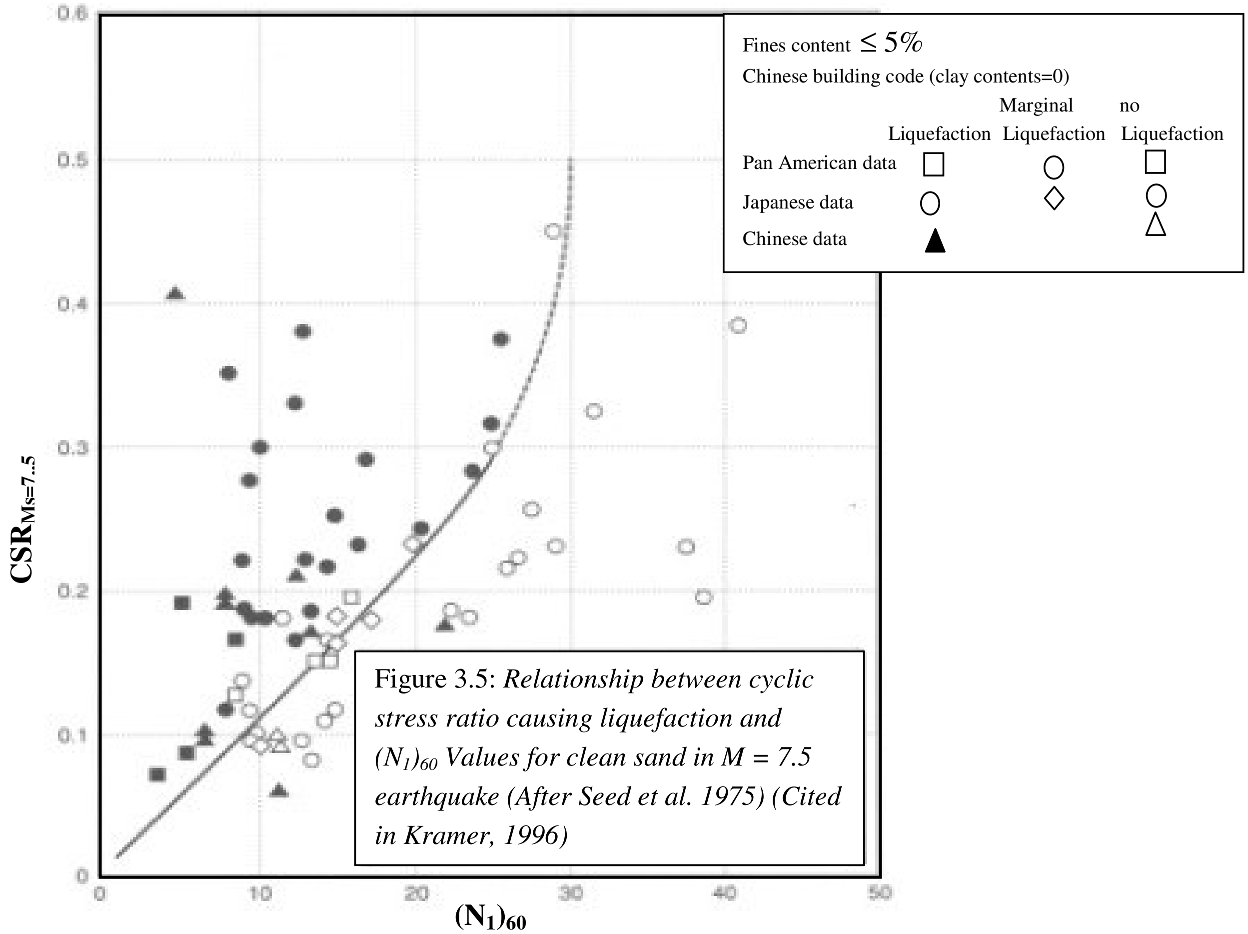

Figure 3.5: *Relationship between cyclic stress ratio causing liquefaction and $(N_1)_{60}$ Values for clean sand in M = 7.5 earthquake (After Seed et al. 1975) (Cited in Kramer, 1996)*

Table 3.4: Magnitude correction factor for Cyclic Stress Approach

Magnitude, M	$CSR_M/CSR_{M=7.5}$
5.25	1.5
6	1.32
6.75	1.13
7.5	1
8.5	0.89

3.5.2. Qualitative analysis

Quantitative analysis of liquefaction hazard assessment requires enough geotechnical parameters such as N-value, Overburden pressure, density etc, which can be only obtained by insitu measurement using field instruments. But to get such parameters is very difficult and expensive. With the lack of geotechnical data, it is not so suitable to carry out liquefaction hazard assessment in the large coverage of area using quantitative analysis method. So now a days in most part of the world including in the Unites states, Japan and in other developed countries qualitative analysis is given more importance. This method is basically based on the geological and topographical situation of the place. The qualitative analysis for liquefaction hazard assessment is generally carried out for the preliminary investigation results of the places to know whether the area is susceptible to liquefaction or not, if yes in what scale, high or low? According to this scale of susceptibility future plan can be made in the particular place for the development activities.

Basic conditions required for this process are the;

- Water table situation of the place, less than 10 m
- Holocene deposits
- Evidence for the past occurrences of Liquefaction
- Seismically active areas

If any area is met with these conditions, then the area can be considered as susceptible for liquefaction hazard.

Iwasaki et al. (1982) proposed that if a correlation is established between past occurrences of liquefaction and geologic and geomorphological criteria, then this might be used to infer the likely area of liquefaction susceptibility as shown in the Table 3.5 below.

Table 3.5: Susceptibility of geomorphological units to liquefaction (Iwasaki et al. 1982)

Rank	Geomorphological units	Liquefaction potential
A	Present riverbed. Old riverbed. Swamp, Reclaimed land, inter dune lowland	Liquefaction likely
B	Fan natural levee, sand dune, Flood plain beach Other plains	Liquefaction possible
C	Terrace hill mountain	Liquefaction unlikely

Keith I. Kelson et al. (1999) carried out liquefaction susceptibility mapping project in the Inner Rio Grande Valley near Albuquerque, New Mexico. For the construction of liquefaction susceptibility map in the Rio Grande valley, they performed very simple method called "Liquefaction Threshold Analysis" (see Figure 3.6). In this analysis, liquefaction susceptibility is based on three factors:

- The total thickness of loose sandy deposits within 40 ft (12 m) of the ground surface,
- The depth of groundwater, and
- The estimated threshold ground motions required to initiate liquefaction.

The threshold ground motions are based on available blow-count data, and calculations using the Seed Simplified Procedure and subsequent revisions (Seed and Idriss, 1971; Seed et al., 1983)

Susceptibility rating units of “very high, high, moderate, low, and very low” are designated on the basis of the estimated peak horizontal ground acceleration (PGA) required to initiate, or 'trigger', Liquefaction. They incorporated shaking duration in the analyses by considering the occurrence of a large-magnitude (M=7.0) earthquake. The susceptibility classes determined by triggering PGA-threshold values are shown in the Figure 3.6.

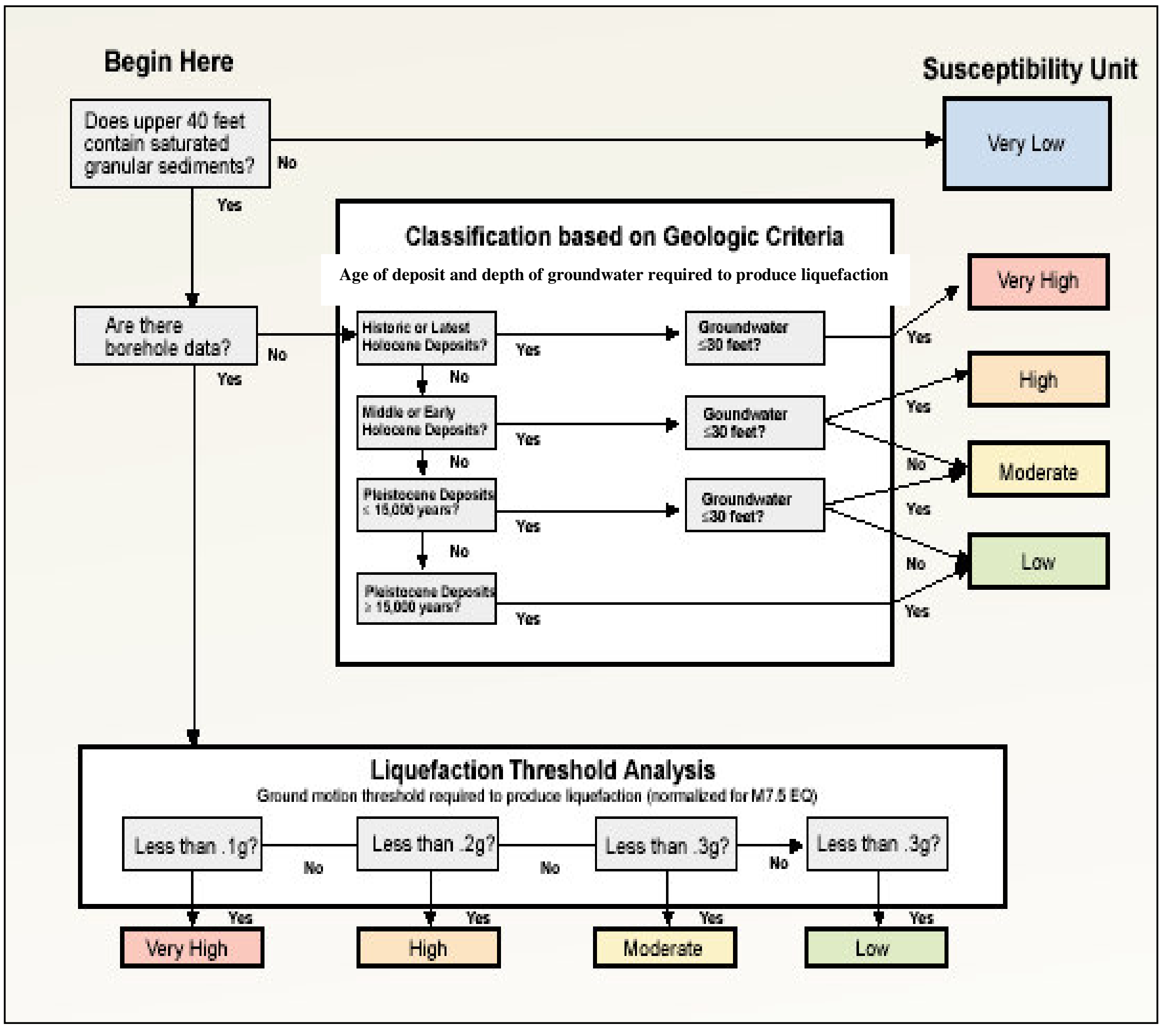

Figure 3.6: Decision flow chart for evaluation of earthquake-induced liquefaction susceptibility (after Hitchcock et al., 1999, cited at Keith, I. Kelson et al., 1999).

According to this method, the classification of susceptibilities are made as follows,

- Very High - may trigger at less than 0.1 g
- High - may trigger between 0.1 g and 0.2 g
- Moderate - may trigger between 0.2 g and 0.3 g
- Low - may trigger at levels above 0.3 g
- Very Low - unlikely to trigger at any level of acceleration

Following estimation of the liquefaction-triggering PGA threshold values, They developed a criteria matrix also for assigning liquefaction susceptibility classes as shown on Table 3.6. The criteria matrix correlates the age and type of geologic unit with depth to groundwater and threshold PGA required

Table 3.6: Criteria matrix for assigning liquefaction susceptibility based on PGA value

Description	Range in ground motion threshold (g*)	Mean ground motion threshold (g**)	Ground water depth		
			<30’	30’-40’	>40’
Artificial Fill (Recent)	No data	No data	VH	H	L
Floodplain Deposits (latest (Holocene to recent)	0.03 to 0.26	0.12 + 0.06	VH	H	L
Valley Alluvial Deposits (all facies, late Holocene)	0.03 to 0.15	0.11 + 0.03	H	M	L
Valley Alluvial Deposits (all facies, late Holocene	0.05 to 0.20	0.13 + 0.05	H	M	L
Valley Alluvial Deposits (all facies, late Holocene	0.08 to 0.21	0.14 + 0.04	H	M	L
Valley Alluvial Deposits (all facies, middle Holocene	0.20 to 0.30	0.28 + 0.04	H	M	L
Alluvial Fan Deposits (late Late Holocene	0.07 to 0.20	0.17 + 0.05	H	M	L
Alluvial Fan Deposits Early to middle Holocene	No data	No data	H	M	L
Colluvial Deposits (early to late Holocene)	No data	No data	M	L	L
Alluvial Fan Deposits (late Pleistocene)	No data	No data	M	L	L
Bedrock (Tertiary)	No data	No data	VL	VL	VL

** Estimated peak ground acceleration (PGA) required to trigger liquefaction*

*** Mean +/- 2 standard deviations, Liquefaction Susceptibility Class (VH= Very High, H= High, M= Moderate, L= Low, VL= Very Low)*

Table 3.7: Liquefaction Susceptibility of Sedimentary Deposits (from Youd and Perkins, 1978) during strong seismic action.

Type of Deposit	General Distribution of Cohesionless Sediments in Deposits	Likelihood that Cohesionless Sediments when Saturated would be Susceptible to Liquefaction (by Age of Deposit)			
		< 500 yr Modern	Holocene < 11 ka	Pleistocene 11 ka - 2 Ma	Pre-Pleistocene > 2 Ma
(a) Continental Deposits					
River channel	Locally variable	Very high	High	Low	Very low
Flood plain	Locally variable	High	Moderate	Low	Very low
Alluvial fan and plain	Widespread	Moderate	Low	Low	Very low
Marine terrace and plains	Widespread		Low	Very Low	Very low
Delta and fan-delta	Widespread	High	Moderate	Low	Very low
Lacustrine and playa	Variable	High	Moderate	Low	Very low
Colluvium	Variable	High	Moderate	Low	Very low
Talus	Widespread	Low	Low	Very Low	Very low
Dunes	Widespread	High	Moderate	Low	Very low
Loess	Variable	High	High	High	Unknown
Glacial till	Variable	Low	Low	Very low	Very low
Tuff	Rare	Low	Low	Very low	Very low
Tephra	Widespread	High	High	?	?
Residual soil	Rare	Low	Low	Very low	Very low
Sebka	Locally variable	High	Moderate	Low	Very low
(b) Coastal Zone					
Delta	Widespread	Very high	High	Low	Very low
Estuarine	Locally variable	High	Moderate	Low	Very low
Beach					
High wave energy	Widespread	Moderate	Low	Very low	Very low
Low wave energy	Widespread	High	Moderate	Low	Very low
Lagoonal	Locally variable	High	Moderate	Low	Very low
Fore shore	Locally variable	High	Moderate	Low	Very low
(c) Artificial					
Uncompacted fill	Variable	Very high	-	-	-
Compacted fill	Variable	Low	-	-	-

for initiation of liquefaction. Linking liquefaction susceptibility classes to estimated threshold triggering ground motion values allows evaluation of changes in liquefaction potential for various earthquake scenarios across the study area. Additionally, the liquefaction susceptibility classes incorporate parameters that may change with time, such as depth to groundwater, and therefore can be modified in the future to reflect additional data.

Based on liquefaction observations from historical earthquakes, Youd and Perkins (1978), estimated the liquefaction susceptibility of various sedimentary deposits as shown in Table 3.7. According to them surficial geology is an important factor controlling liquefaction susceptibility.

Protocol criteria as suggested by Nevada Earthquake Safety Council (2000) proposed a new method for liquefaction hazard analysis by considering soil type, blow count and ground water information. They assigned values based upon blow counts and other factors as follows,

Blow count less than 30 - 1 point, water present (yes/no) - 2 points if present and saturated, and type of sandy material present (non-clay -1 point; poorly graded sand-4 points; well-graded sand - 3 points; Silty sand - 2 points, and sandy clay / clayey sand – 1 point.

This shows that the key points are the soil type and water table, not only the N-value. The categories were highly liquefiable if the values were greater than or equal to 7, moderate if the values were 5 and 6, and low for values less than 5.

Juang and Elton (1991) developed general criteria for the analysis of the liquefaction hazard by assigning weight values according to their influence to liquefaction potential, as shown in the Table 3.8. The greater the susceptibility to liquefaction a factor possessed the higher the number of points that is allocated to that factor. They identified twelve factors that influence the susceptibility of a soil to liquefaction. These factors listed by their importance are as follows:

Table 3.8: Factors, weightings and criteria for rating potentially liquefiable sites

Factor	Weighting	Liquefaction Susceptibility				
		Very High	High	Medium	Low	Very Low
Depth to water table	Very important	<1.5 m	1.5-3 m	3-6 m	6-10 m	>10 m
Grain size	Very important	0.075-1 mm	1-3 mm	>3 mm	<0.075 mm	
Depth of burial	Very important	1.5-3 m	3-6 m	6-10 m	<1.5 m	>10 m
Capping layer (low k)	Very important			Good capping	Fair capping	No capping
Age of deposit	Important	<500yr	Late Holocene (1)	Holocene	Pleistocene (2)	Pre-Pleistocene
Liquefiable layer thick	Important	>2.5m	1.2-2.5 m	0.6-1.2 m	<0.6 m	

Reference: Juang and Elton (1991)

Note: 1 (Holocene): - 10,000 years old or younger

(2) Pleistocene: - 10,000 -1.6 million years

Extremely important factor**:**	Type of deposit, N-value, Soil density
Very important factors:	Depth to water table, Grain-size distribution, Depth of burial, Grain size, Arial extent of liquefiable deposit, Degree of capping by a low Permeability layer
Important factors:	Age of deposition; Ground slope; Liquefiable layer thickness

The assessment of each of these factors from borehole data can result in a relatively accurate representation of the susceptibility to liquefaction at the borehole location.

3.6. Standard Penetration Test (SPT)

The standard penetration test (SPT) is an empirical dynamic penetration test developed in USA in the 1920's and was usually carried out in 50 to 100 mm diameter wash borings. The test is most commonly used in situ test especially for cohesionless soils, which cannot be easily sampled. The test is extremely used for determining the relative density, bearing capacity and the angle of shearing resistance of the cohesionless soil. The test is performed using a split barrel sample tube of 50 mm external diameter, 35 mm internal diameter and about 65 mm in length as specified in BS 1377.

There are different methods of releasing the hammer in different countries. However, the borehole must be cleaned out to the required depth before the hammering is taken place and care must be taken to ensure that the material to be tested is not disturbed.

In this process, a hammer of 65 kg weight with a free fall height of 760 mm is used to drive the sampler. Initially the sampler is driven 150 mm into the sand to seat the sampler and by-pass any disturbed sand at the bottom of the borehole. The number of blows required to drive the sampler a further 300 mm is then recorded. This number is called the Standard penetration resistance (N) value. If 50 blows are reached before a penetration of 30 cm no further blows should be recorded. If the test is to be carried out in gravelly soils, the driving shoe is replaced by the 60^0 cone.

SPT test is very specific tool for the liquefaction hazard analysis. It also has the unique feature of supplying samples for soil classification purpose. Usually SPT is conducted at every 2 m depth or at the change of stratum.

The N-values are extensively used in determining the bearing capacity and predicting the settlement of cohesionless soil and are described by a number of authors (Meyerhof, 1956; Terzaghi and Peck, 1967). It has wide application in determining the liquefaction susceptibility of a place.

There are a number of factors involved in the SPT, which can affect the blow count, mainly related to poor testing practice. The standard penetration number is corrected for dilatancy effect and overburden effect (Craig, 1986)

3.6.1. Dilatancy correction

Silty fine sands and fine sands below the water table develop pore pressure, which is not easily dissipated. The pore pressure affects the resistance of the soil and hence the penetration number (N). Terzaghi and peck (1967) recommend the following correction in the case of silty fine sands when the observed value of N exceeds 15.

$N' = 15 + \frac{1}{2}(N - 15)$ (Craig, 1986) ……………………………………(15)

Where N' – Corrected SPT value

N – Observed SPT value.

If $N_R \leq 15$, $N_c = N_R$

3.6.2. Overburden Pressure

Skempton summarized the evidence regarding the influence of test procedure on the value of standard penetration resistance (Craig, 1986). Measured N value should be corrected to allow for the different methods of releasing the hammer, the type of anvil and the total length of boring rods. Only the energy delivered to the sampler is applied in penetrating the sand, the ratio of the delivered energy to the free fall energy of the hammer being referred to as the rod energy ratio, which varies between 45% and 78% for the operating procedures used in several countries. It has been recommended that a standard rod energy ratio of 60% should be adopted and that all measured N values should be normalized by simple proportion of energy ratios, to this standard: the normalized values are denoted $(N)_{60.}$ If a short length of boring rods (<10m) is used in a test, a reflection of energy occurs and a further loss in delivered energy results. A further correction should therefore be applied to the measured N values if the total length of rods is less than 10m.

Standard penetration resistance depends not only on relative density but also on the effective stresses at the depth of measurements. Effective stresses can be represented to a first approximation by effective overburden pressure. This dependence was first demonstrated in the laboratory by Gibbs and Holtz and was later confirmed in the field. Sand at the same relative density would thus give different value of standard penetration resistance at different depths. Several proposals have been made for the correction of measured N values. The corrected value (N_1) is related to the measured value (N) by the factor C_N, where

$N_1 = C_N N$

C_N = Correction factor and can be obtained from the graph prepared by Liao and Whitman, (1986).

Also

$$C_N = \sqrt{\frac{1}{\sigma'_{v_0}}}$$

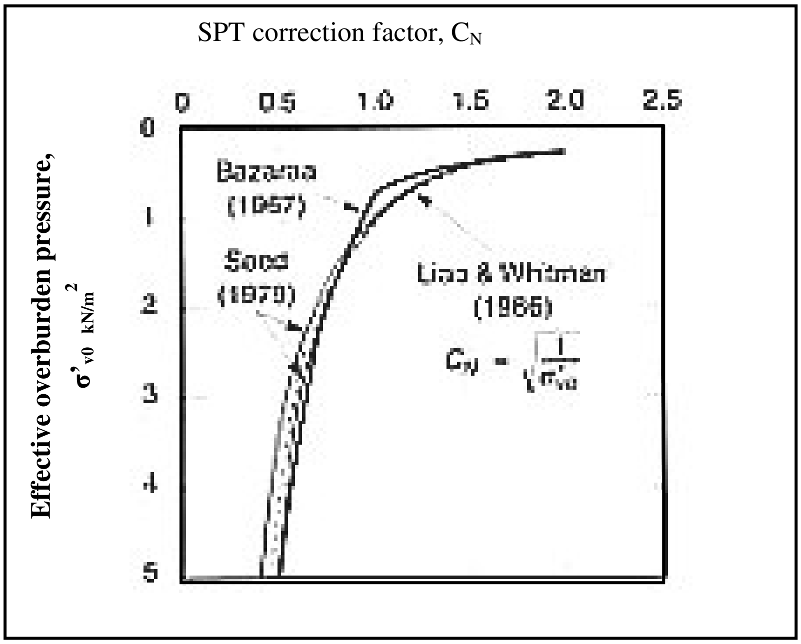

Figure 3.7: SPT overburden correction factor after Liao and Whiteman (1986)

$(N_1)_{60}$ is the standard penetration resistance normalized to a rod energy ratio of 60% and an effective overburden pressure of 100 kN/m^2.

Appropriate values of $(N_1)_{60}$ were added to the Terzaghi and Peck (1967) classification of relative density by Skempton (1986) as shown in the Table 3.1 and are considered to apply to normally consolidated sands. The relative density of sand was described by Terzaghi and Peck (1967) in general terms on the basis of standard penetration resistance, numerical values of relative density as shown in column 3 were subsequently added by Gibbs and Holtz (Craig, 1986)

3.7. Work done on Liquefaction Susceptibility analysis on Kathmandu Valley

Kathmandu valley lies in seismically hazard prone areas. The valley has been hit by number of major earthquakes in the past resulting heavy damages, injuries and deaths of people in the city. Apparently the site where the liquefaction hazard occurred has not been recorded till now, Rana (1935) in his book (**Nepal ko Mahabhukampa -"The great earthquake of Nepal")** noted that, in the Bihar-Nepal earthquake of January 15, 1934, the eastern part of Tundhikhel (Presently Parade ground for Army in the center of Kathmandu), the paddy fields and road fissured heavily forcing water to eject via the fissures. At some places, a fountain of water reaching up to 3-4 m ejected from the ground. Based on his description we can estimate that widespread liquefaction had occurred in certain places within the valley.

To date little work has been done related to liquefaction hazard assessment in Kathmandu valley. The UNDP/UNCHS in collaboration with His Majesty's Government of Nepal (HMG) did a Seismic hazard mapping and Risk Assessment for the entire country with the aim of developing building code system for Nepal. During that study, qualitative methods of liquefaction hazard assessment for Kathmandu valley was also carried using limited borehole data. The analysis for liquefaction susceptibility mapping was based on 12 factors that influence the susceptibility of soil to liquefaction as defined by Juang and Elton (1991). Out of the 12 factors determined by Juang and Elton, the project followed only six of the susceptibility factors, for the Katmandu valley including the rating value of Juang and Elton (1991). The general criteria and the scoring value developed by the project are shown in the Table 3.9 and the liquefaction susceptibility map prepared by them is shown in Figure 3.10.

Table 3.9: The table showing general criteria and score value adopted by UNDP/UNCHS/MOHPP, 1994 for liquefaction hazard assessment for Kathmandu valley.

Factor	Weighting	Liquefaction Susceptibility									
		Very High	Score	High	Score	Medium	Score	Low	Score	Very low	Score
Depth to water table	2	<1.5 m	5	1.5-3 m	4	3-6 m	3	6-10 m	2	>10 m	1
Grain size	4	0.075-1 mm	5	1-3 mm	4	>3 mm	3	<0.075 mm	2		
Depth of burial	1	1.5-3 m	5	3-6 m	4	6-10 m	3	>1.5 m	2	>10 m	1
Capping layer (low k)	2		5		4	Good capping	3	Fair capping	2	No capping	1
Age of deposit	1	<500yr	5	Late Holocene (1)	4	Holocene	3	Pleistocene (2)	2	Pre-Pleistocene	1
Liquefiable layer thick	1	>2.5m	5	1.2-2.5 m	4	0.6-1.2 m	3	<0.6 m	2		

Note: (1) Holocene: - 10,000 years old or younger, Reference: Juang and Elton (1991)
(2) Pleistocene: - 10,000 - 1.6 million years

The UNDP/UNCHS (project) categorized four levels of liquefaction susceptibility based on this scoring system, which are as follows:

High: Significant areas may liquefy under moderate to high seismic loading
Moderate: Some areas may liquefy under high seismic loading.
Low: Localized areas may liquefy under high seismic loading.
Very Low: Negligible liquefaction expected even under high seismic loading.

JICA and His Majesty's Government of Nepal (HMG) carried out detail study on Earthquake disaster mitigation in Kathmandu valley in 2000-2002. As part of their earthquake disaster mitigation study, they prepared a liquefaction potential map for Kathmandu valley (Figure 3.8, 3.9). They included some physical properties of soil, seismic motions and geological map of the valley for the liquefaction analysis. They did not mention about the number of soil samples included in this analysis.

They adopted a combination of the F_L method (Japanese design Specification of Highway Bridge, 1996) and P_L method (Iwasaki et al., 1982), which is commonly used in Japan for practical purposes, for the liquefaction hazard analysis in Kathmandu valley, which seems to be purely quantitative analysis. The map prepared by JICA is shown in Figures 3.8 and 3.9 respectively. For the determination of seismic motion, they developed a model for four earthquake scenarios as,

Mid Nepal Earthquake: This model had been set up based on the seismic gap in the middle of Nepal. This is regarded as a huge earthquake.

North Bagmati Earthquake: This earthquake model had been set based on the earthquake clusters in and around Nepal. This is regarded as a middle scale earthquake.

KV local earthquake: This earthquake model had been set based on the distinct part of the lineament in the valley. This is regarded as a local earthquake underfoot.

1934 earthquake: This earthquake model had been set up for effective comparison with the above three earthquakes, because most people in Kathmandu had impression of this earthquake. This is considered as a biggest earthquake ever occurred in Nepal during its history. This earthquake had magnitude of 8.4 Richter scale and the intensity of this earthquake reached up to MMI ‘X’ in some places of Kathmandu valley.

Besides these two large scale works for liquefaction hazard assessment carried out by UNDP and JICA, some site specific liquefaction hazard assessment works have been carried out by different consultancies for the purpose of constructing government and organizational buildings and developing infrastructures in recent days.

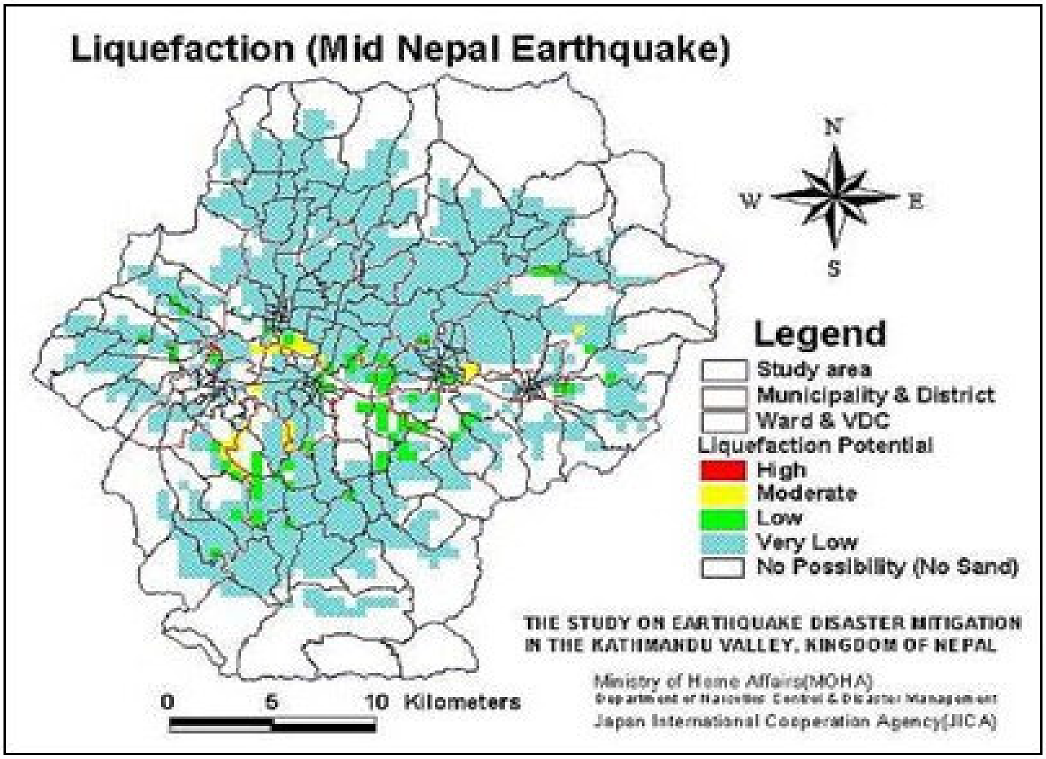

Figure 3.8: Liquefaction map prepared by JICA for mid Nepal earthquake scenario (Source: JICA, 2002)

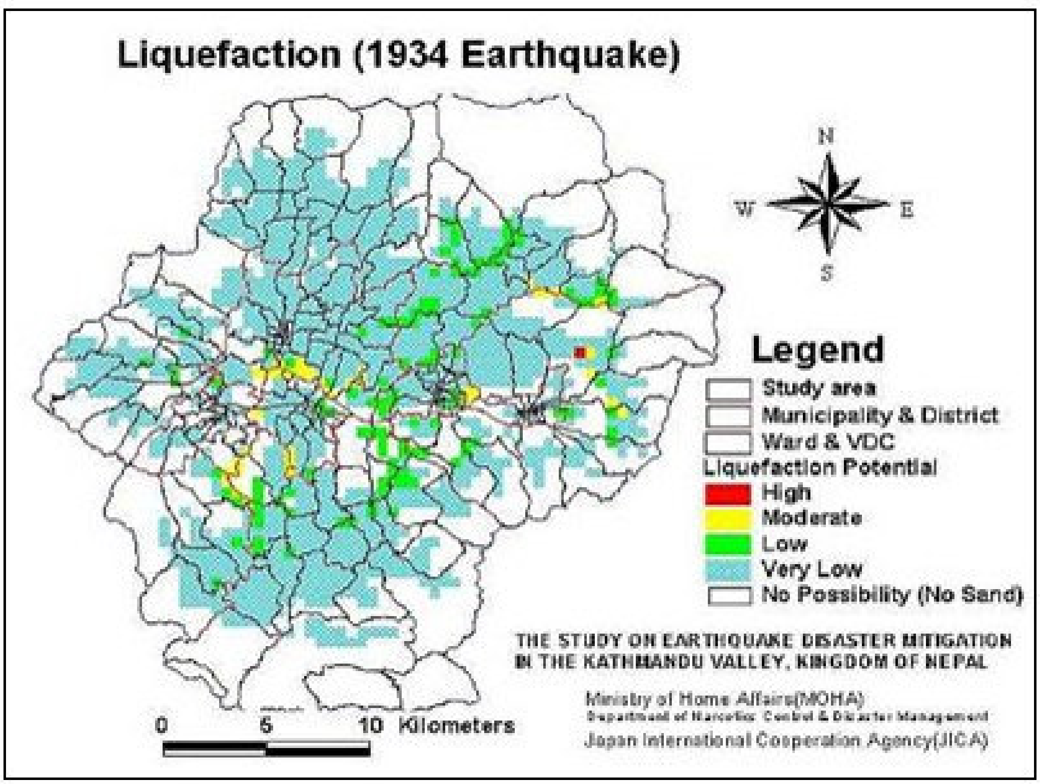

Figure 3.9: Liquefaction map of Kathmandu valley prepared by JICA for 1934 earthquake scenario (Source: JICA, 2002).

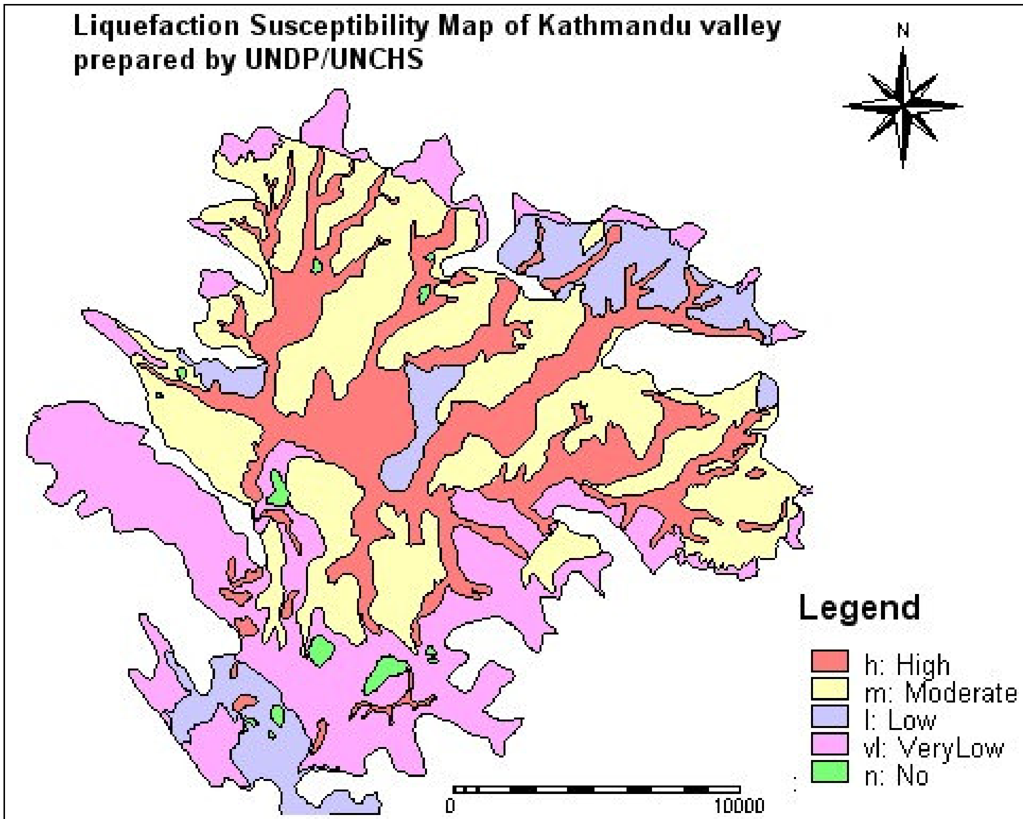

Figure 3.10: Liquefaction susceptibility map of Kathmandu valley prepared by UNDP//UNCHS/MOHPP)

4. Generation of a Subsurface database

4.1. Introduction

The effective management of borehole data is crucial for many applications in the geosciences; among which is earthquake microzonation (Houlding, 1994). The development of borehole database systems has become more important with the recent rapid developments of personal computers and GIS technology. Because borehole data are directly related to specific locations on the earth's surface, they are thus well placed for management with a GIS.

One of the objectives of this research is to develop an integrated information environment for the management of borehole data. The scope of borehole data management includes subsurface modelling, 3D-log representation, and development of GIS data layers, fence diagrams and lithological cross sections.

In a typical geological project, one must deal with hundreds of borehole logs, which may contain many different types of lithologies and may be of varying length. One also needs to deal with numerous maps in digital form, each of which may contain several points. All of this information has limited use to us unless we can integrate it in a spatial context, selectively retrieve, and display it in an appropriate way. These considerations require effective management of data location and data identity. Having all borehole logs in a standard format is an obvious advantage we need to be able to access borehole logs as a set of individual samples and observations in their correct locations.

In this section, the following topics will be discussed: data acquisition, available data, data management and processing of data in ILWIS and Rockworks.

4.2. Data aquisition

Data acquisition is one of the most difficult parts of a research work. It is time consuming and more personal relations are required, in order to contact people in institutions that might have relevant data. Till to date there was no complete inventory of subsurface lithological data of Kathmandu valley, therefore a new data acquisition was necessary.

In the Kathmandu valley to date, more than 300 deep drill holes have been made by different organizations and private companies (JICA, 1990) for various purposes. Table 4.1 summarizes the organizations and research programs conducted for the drilling of deep boreholes.

Table 4.1: Name of organizations and main research programmes with boreholes.

Organization	Program	Borehole Identification	Number	Year
Geological Survey of India (GSI)	Groundwater Resources of Kathmandu Valley	B 01 - B 25	25	1960
WHO/UNDP/Binnie & Partner	Master Plan for the Water Supply and Sewerage for Greater Kathmandu and Bhaktapur Groundwater Investigations	WHO1 - WHO10	10	1973
Japan International Cooperation Agency (JICA)	Groundwater Management Project in Kathmandu Valley	JW 1 - JW 4	4	1990
NWSC/CES (Consulting Engineers Salzgitter)	Urban Water Supply and Sanitation Rehabilitation Project for Kathmandu Valley Towns	P 1 - P 37	37	1992
DMG / Silt Consult	Detailed Feasibility Study on Kathmandu Natural Gas	DMG1 - DMG14	14	1996
Australian Geological Survey Organization & Department of Irrigation (AGSO/DOI)	The Assessment of Groundwater Pollution in the Kathmandu Valley	AG1 - AG75	75	1997
Hokaido University-Japan and Kyushu University Japan in collaboration with Central department of Geology, Kirtipur and Department of Geology Trichandra college, Kathmandu, Nepal	Integrated studies on Himalayan uplift and Climatic changes (Paleo-Kathmandu Lake project)	Paleo1 – Paleo3	3	2001
Total wells			168	

There are still many boreholes, which are drilled for private purposes such as for hotels and private houses, which are not mentioned in Table 4.1 above. Similarly, many borehole data, which are mentioned in the table, could not be obtained for this study. For the present study only 185 well logs with depths more than 30 m could be collected. Out of these 185 wells, 23 are relative shallow wells with drilling depths less than 100 m and the rest are greater than 100 m with maximum depth reaching up to 577 m located in the central part of the valley. Thirty six (36) of them have even reached up to the bedrock. The data collected so far for these boreholes contained attributes such as lithological information, depth range, altitudes and static water table. However, none of the deep wells contained geotechnical information, which will be discussed in the following sections.

On the other hand, for the liquefaction hazard analysis 328 shallow boreholes were collected. The depth of these borehole ranges from a few meters up to 30 m. The borehole records of a number of these contain both lithological and geotechnical information such as grain size distribution, Atterberg limits, N-values, moisture content, specific gravity, density, unit weight, angle of friction (ϕ), direct shear and soil type (USCS). However, it is to be noted here that only a small number of boreholes included all these types of information.

These borehole records were obtained from different sources. The main sources were reports from various organisations, such as the report of the Japanese International Cooperation Agency (JICA, 1990) for a ground water management project in Kathmandu Valley, which was obtained from the Library of Nepal Water and Sewerage Corporation (NWSC), the report of the Geological Survey of India (GSI) for groundwater resources of Kathmandu valley (1966) and the reports of the Environmental Geology Project (EGP) of the Department of Mines and Geology (DMG) for hydrogeological conditions and barrier potential sediments (Clay) in the Kathmandu valley (1998).

The data for the shallow boreholes were collected from various consultancy offices around Kathmandu, such as,

- Soil Test Lab, Balaju Kathmandu
- ESLA Soil Test Lab, Bashundhara Kathmandu
- East Drilling Company, Satdobato Lalitpur
- Soil Test Lab, Nepal Engineering College, Pulchok Lalitpur
- ITECO Consultants, Min Bhawan Kathmandu
- GEOCE Consultants, Lalitpur
- Nepal Geological Society, Kathmandu
- GEOTECH Consultant, Sinamangal Kathmandu

Figure 4.1 gives an overview of the boreholes used in the study.

4.3. Data management

4.3.1. Data management in Excel

The flow chart in Figure 4.2, explains the methodology carried out for the database generation.
Microsoft Excel 2000 and Microsoft Access were used to store the borehole data. Initially the data were entered in the Excel sheets. After the data acquisition was completed, all the boreholes were grouped according to their types and source as shown in the Table 4.2. Because most of the deep wells in Kathmandu valley were drilled for drinking water supply purposes and are clustered in a particular location, they are given specific names derived from the local name of the place. The names of the different well systems collected for this research work and their total numbers are shown in the Table 4.2.

The deep boreholes were used to study the geological evolution of the valley by generating lithological cross sections, projected stratigraphic model, fence diagrams and GIS layer models. Two types of tables were generated for this type of data storage. One containing attributes such as: Well_id, location, depth range, geological information, and thickness of the layers. The other table consisted of the following attributes: Well_id, Coordinates (UTM), Total depth, Altitude and static water table. Both these type of data were initially stored in different sheets of the same file in Excel format.

The shallow boreholes with geotechnical data were used for the liquefaction susceptibility mapping of the area. They were also stored initially in Microsoft Excel. For this purpose, also two types of tables were generated. The first table included the following attributes: Well-id, Location, Depth range, Water table, Geological information, Thickness of the layer. The second table includes the geotechnical information with the following attributes: Well-id, Location, Depth range, Grain size distribution, Atterberg limit, Moisture content, Density, Unit weight, Specific gravity, Direct shear, Coefficient of friction, and Soil type (USCS). The SPT record of the borehole was stored in a separate sheet in the same Excel file.

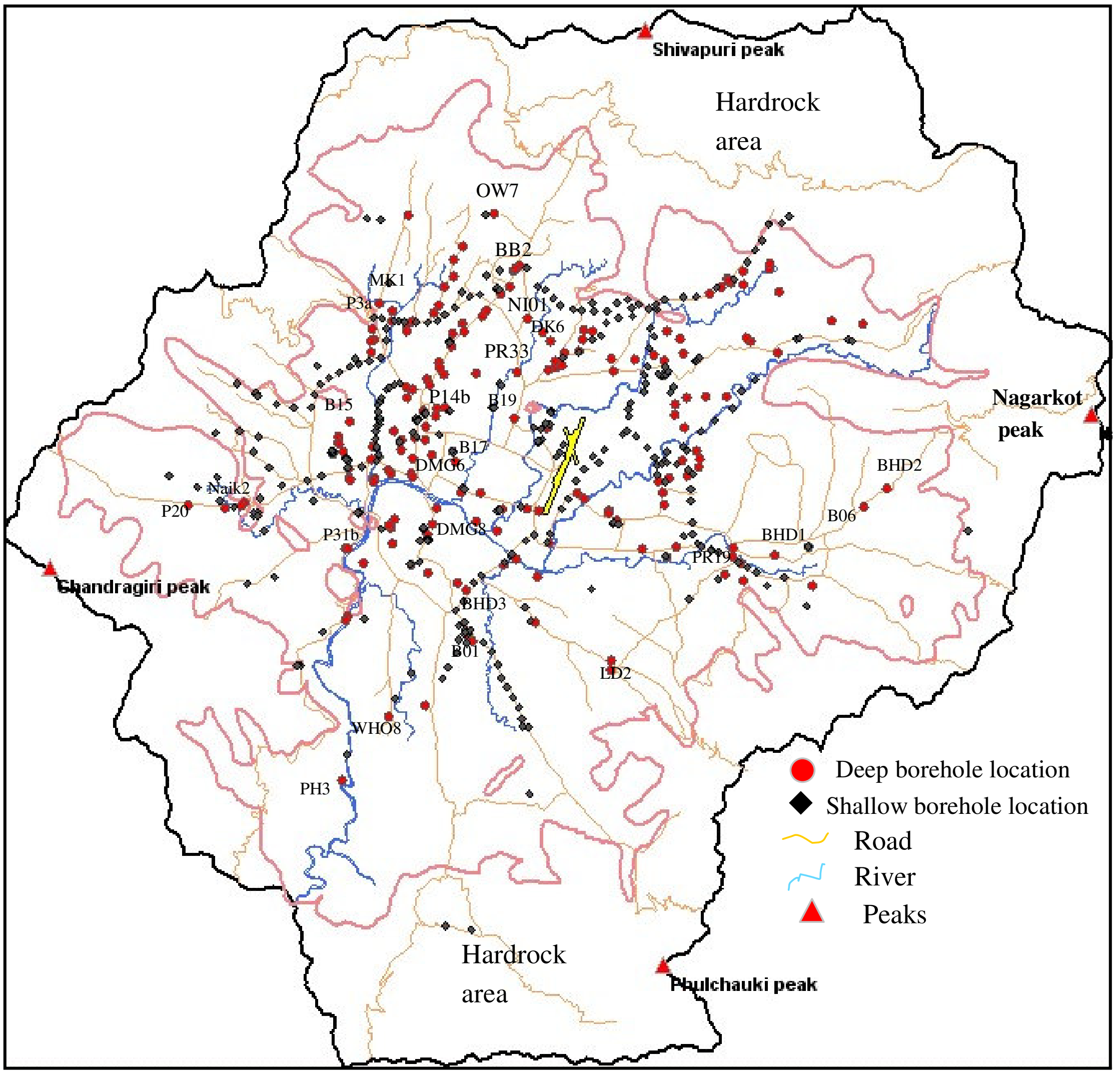

Figure 4.1: Location map for deep and shallow boreholes.

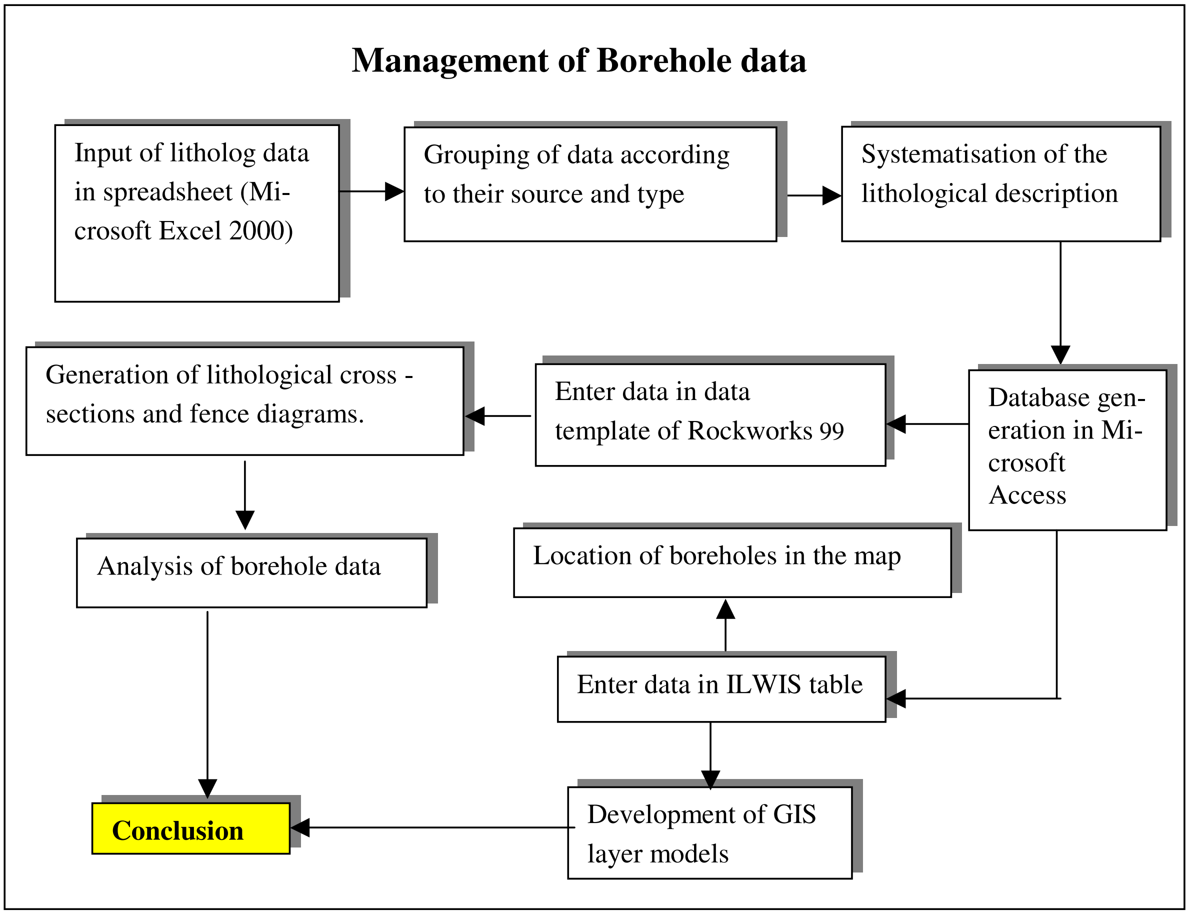

Figure 4.2: Flow chart for the borehole data management system

Table 4.2: Name of boreholes (wells) in Kathmandu valley drilled by different organizations.

Well Name	Derived from	Drilled by	Number of wells	Drilled date
B-wells	Geological Survey of India	GSI	25	1960
Balaju wells	Balaju (location name)	NWSC	3	After 1992
Bansbari wells	Bansbari (location name)	NWSC	8	After 1992
Bhaktapur wells	Bhaktapur (location name)	NWSC	12	After 1992
Dhobikhola wells	Dhobikhola (Name of a river)	NWSC	9	After 1992
DMG wells	Name of the organization,	DMG	14	1996
Gokarna Wells	Gokarna (locatioin name)	NWSC	5	After 1992
Manahara Wells	Manahara, Name of the river	NWSC	7	After 1992
OW wells	Observation wells	JICA	6	1990
WHO Wells	World Health Organisation	WHO	12	1973
PR Wells	Private wells	Private	34	Unknown
P wells	Private wells	Private	29	Unknown
Paleo-Lake wells	Paleo-Kathmandu Lake project	Project	3	2001
Kathmandu/Lalitpur Wells	Location names	Different Organization	18	Unknown

4.3.2. Data management in Access

After the initial organization of the data for the deep and shallow boreholes in an Excel spreadsheet, a database was generated using Microsoft Access, in which data were imported from Excel. In Access, a file named "*Kathmandu valley*" was created to store all types of borehole data. Under this file, seven tables were created. Three of the tables were created for deep boreholes and four for the shallow wells. The contents of the different tables are briefly described below.

Structure of the three tables used for the deep boreholes is described in Table 4.3. The tables contain information for 185 deep borehole records.

Table 4.3: Field contents of the table for the database of deep borehole in Microsoft Access.

Name of table	Name of fields	Description
DEEP-WELL_SOURCE	Source_ID	Primary Key
	Well_Name	Name of the wells, mostly derived from name of the location where boreholes are made.
DEEPWELL_SHORT	Source_ID	Primary Key, unique identifier for each borehole
	Well_ID	Primary Key
	Location	It gives name of the places where borehole is located.
	Easting	Coordinate (Modified UTM)
	Northing	Coordinate (Modified UTM)
	Altitude	The altitude of borehole location above mean sea level
	Depth	It gives total borehole depth
	Static water table	It represents the water level measured during construction.
DEEP-WELL_DETAIL	Well_ID	Primary key, unique numbers for all strata
	Strata_ID	Primary key
	Thickness	It gives total thickness of strata
	Description	It gives strata wise Lithological information of the borehole
	Modified description	It represents short description in place of long description for lithological information of the borehole.

To store the data of shallow boreholes the following four tables were created (See also Table 4.4):

- **Shallowell,** containing general information for the 328 boreholes.
- **GeoTechData,** containing geotechnical data of borehole samples taken at different depths. It has data for 119 boreholes but the data attributes it contains are not uniform. From this table only some information such as grain size analysis, density, unit weight and the soil type were used for analysis of liquefaction susceptibility mapping.
- **Shallowell_Detail,** containing geological information of boreholes for different strata. **Sptdata,** containing information for Standard Penetration Test analysis (N-values) for some boreholes.

The relationship between the different tables in Access and the contents of the tables are shown in Figure 4.3.

The purpose of database generation is to store data so that it can be retrieved and displayed when needed using SQL operations.

The data so organized in Access were transferred to ILWIS tables and to the Rockwork99 tables for further analyzing and processing.

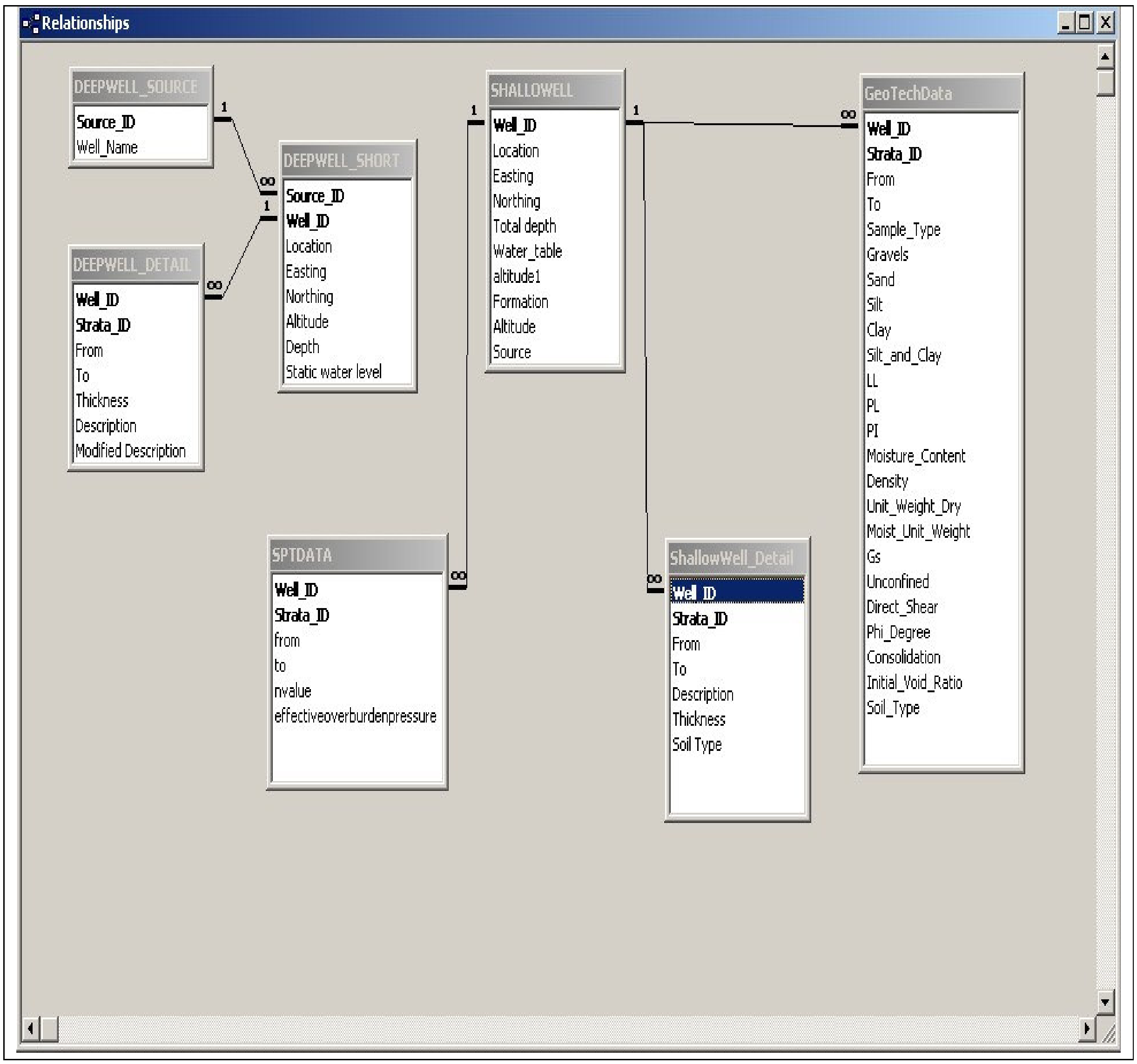

Figure 4.3: Relationship diagram of the borehole database.

Table 4.4: Field contents in Shallow borehole tables in Microsoft Access.

Table Name	Name of fields	Description
SHALLOW_WELL	Well_ID	Primary Key
	Location	Name of the place where boreholes are located
	Easting	Coordinate (Modified UTM)
	Northing	Coordinate (Modified UTM)
	Total depth	It represents total depth of the borehole
	Water_table	Measured water table at the time of construction
	Altitude	It is altitude above the mean sea level
	Formation	It represents geological formation on which boreholes are situated. This formation name is derived from the geology map prepared by DMG.
	Source	It indicates the source from which data were obtained
SHALLOW-WELL_DETAIL	Well_ID	Primary Key
	Strata_ID	Primary Key
	Description	Lithological information depth wise
	Thickness	Thickness of an individual strata
	Soil Type	Soil classification according to USCS.
	Altitude	The altitude of borehole location above mean sea level
	Water table	The water table measured for different wells
GeoTechData	Well_ID	Primary key
	Strata_ID	Primary key
	Depth range (From and To)	It represents starting and ending of strata
	Sample_Type	It indicates whether the sample type is disturbed or undisturbed.
	Sieve data (Gravel, Sand, Silt Clay, Silt_and_ Clay)	It represents percentage of gravel, sand, silt and clay contents. Silt_and_Clay indicates bulk percentage of silt and clay mixed.
	Density	It gives density value of soil samples.
	Unit_Weight (dry and moist)	It represents value of dry unit weight and moist unit weight of soil samples
	Others are Atterberg Limit (LL, PL, PI), Moisture contents, Specific gravity, Direct_shear, Angle of friction (Phi), Consolidation Initial_void_ratio.	These are different geotechnical parameters used in Engineering studies. Though they are included in database, these parameters were not used for this study purpose.
SPTDATA	Borehole-id	Primary key
	Strata_id	Primary key
	Depth range (from and to)	It gives starting and ending of strata (Soil layer)
	nvalue	It is the actual N-value obtained in the field (SPT test)
	Effective overburden pressure	It represents calculated overburden pressure for different soil layers.

4.3.3. Data management in ILWIS

In ILWIS the data was also separated for the deep wells and the shallow ones.

4.3.3.1. ILWIS database for deep wells

In ILWIS, a table was created with the Well_id as ID-domain, which was linked with a borehole point map. The structure of the ILWIS table is given in annex (annex-Table B). The column named **Action** contains the file names of the borehole logs in .JPEG format so that, when we click on anyone of the point locations on the map in the ILWIS window the respective borehole log is displayed as shown in Figure 4.4.

4.3.3.2. ILWIS database for shallow wells.

For the liquefaction susceptibility analysis, at first a spreadsheet was used in which both qualitative and quantitative methods were adopted (See Chapter 5). The result of these analyses was imported to an ILWIS table, which was linked to the shallow-borehole point map. From the columns that contained the result of the liquefaction susceptibility analysis attribute maps were generated. The structure of the table in ILWIS for liquefaction hazard analysis is given in annex (annex-Table C).

4.3.4. Data management in Rockworks99/2002

RockWorks99/2002 is software for creating boring logs, cross sections, fence diagrams, solid models, and stratigraphic layer models etc. It is a broad, integrated geological data management, analysis and visualization tool. It contains a borehole data manager for easy entry of down hole data and hence can be easily analysed using 2D and 3D visualization tools. In this study most of the work was done using Rockworks99. However, in some cases Rockworks2002 was also used. Unfortunately it was not possible to import borehole data from excel into rockworks. Therefore, first a data was created in which information required for this purpose such as coordinate, borehole-id, and elevation was copied from Excel and pasted in the Rockworks. A column Lithology was created in which the geological information for each borehole was stored in each particular row. The structure of the table in Rockworks99 is shown in annex (annex-Table D).

4.4. Data processing and analysis

This section discusses the approach in developing GIS layer models of the subsurface and the creation of lithological cross sections. Two different softwares were used for this purpose: ILWIS and Rockworks. ILWIS (version 3.2) was used for the generation of the layer models and Rockworks (versions 99 and 2000) for the generation of lithological cross sections, projected stratigraphic sections and fence diagrams.

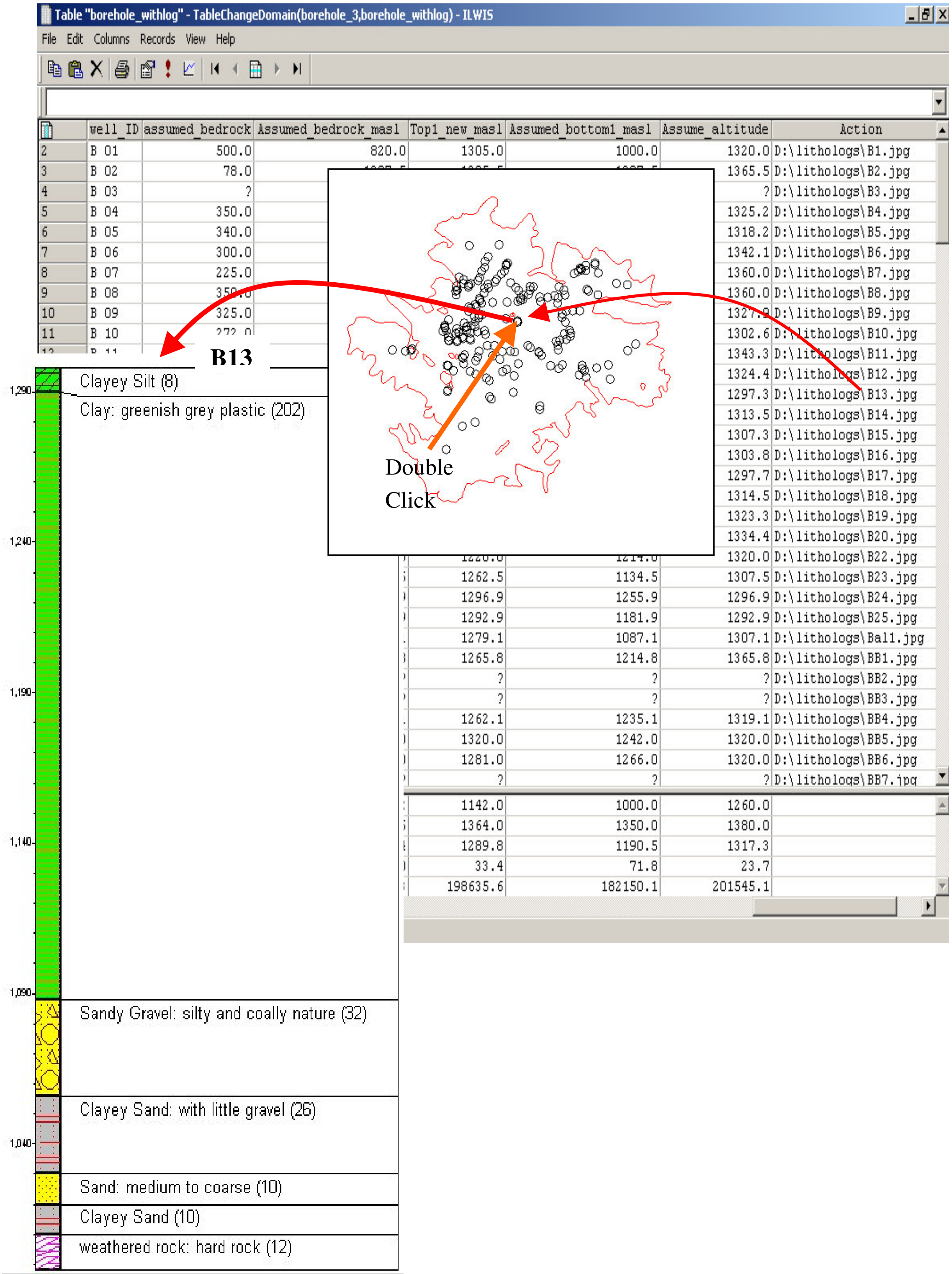

Figure 4.4: Use of Double action button in ILWIS to automatically display the borehole log, when clicking a borehole in the point map.

4.4.1. GIS Layer Modelling

The main aim of the GIS layer modelling was to determine the thickness of the various sub-surface deposits. For this purpose, data from 185 deep boreholes with depth ranging from 33 m up to 577 m below ground level were used. The sediment distribution within the valley is very complex. The valley fill sediments which were mainly formed by fluvial and lacustrine activity are distributed heterogeneously both in depth and in space as described in Chapter 2. As was discussed earlier, the basin consists of multiple stages (up to 5) of lake deposits. In order to generate layer models for such a heterogeneous environment, a certain degree of generalisation had to be accepted. In this case, a layer was classified as lake deposits if it consists of clay and has a thickness of more than 10 meters. The complexity of lacustrine depositional environment is illustrated in Table 4.5, indicating the number of clay layers per borehole. The multiple stages of thick lake deposit have taken place due to the interruption of the lacustrine environment by fluvial activity in different periods of time, as explained in Chapter 2. The layer-modelling concept is used in this study in order to separate between the lake deposits and the non-lake deposit so that the thickness of the different layers of the sediments could be determined and hence could be applied for the estimation of ground amplification during an earthquake.

However as can be seen in Table 4.5, there are multiple layers of clay in some areas of the valley. In this study only the uppermost layer of lake deposit that is present in most parts of the valley is considered for the generation of the layer models. This is because the distribution of sediments within the valley is not uniform and as shown by the boreholes many places in the valley do not possess the same multiple stages of clay deposits. Several boreholes contain thick gravel and sand beds (fluvial origin) between the clay layers, so it was not so logical to include all clay layers in a single layer. Due to this reason, the development of layer models using interpolation techniques for other lake layers was not possible. Therefore only the upper part of the lake was considered as one single lake unit. The whole sequence of sediment deposits within the valley was generalized finally into only three layers: Post Lake deposit, Lake deposits, and pre-Lake deposits demarcated by fixed altitude value (see Figure 4.5).

For the generation of the bedrock altitude map, some assumptions were made to determine depth to bedrock for some wells as only 36 of the wells have actually reached up to bedrock level and the rest of the wells are ending still in the soft sediments. The development of a layer model for the depth to the bedrock using only 36 boreholes did not give good results. The problem was encountered during the construction of cross sections as evidenced by frequent intersection of layers. Hence for the rest of the wells the depth to bedrock level was based on the depth of the neighbouring wells that have touched the bedrock level and also on the existence of rock exposure near by well locations.

During the processing and analysis of the data in ILWIS an interpolation technique was followed in order to obtain the required GIS layer models. The interpolation is the estimation of variables at unsampled locations in an area using existing observation. There are different techniques of point interpolation such as Nearest point, Moving average, Trend surface, Kriging etc. In this study Simple Kriging method was adopted.

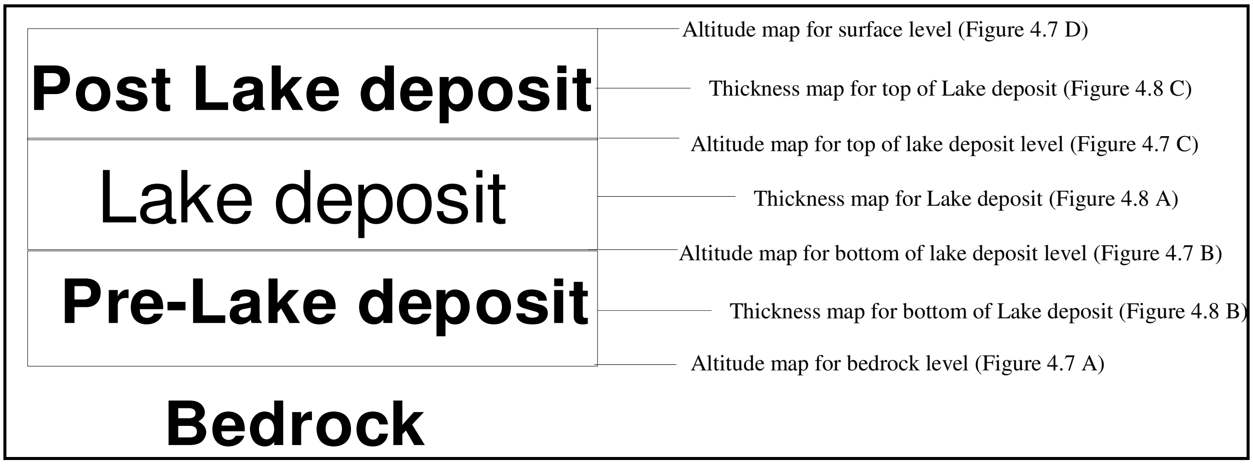

Figure 4.5: Simplified profile of different layer of sediment deposits. The boundary of each layer is represented by respective altitude maps as given in the text and also the thickness maps of each layer are indicated.

The location of the boreholes is shown in Figure 4.1. For the interpolation of soil depths, one of the most important input data consists of the locations where the soil depth is zero, and hardrock is exposed. The area of the unconsolidated sediments was masked out from the catchment map of the study area in order to separate it from hard rock area. The boundaries of the unconsolidated sediments were used as points with a soil thickness of zero value and were combined with the depth information from the boreholes. This was done because the number of boreholes was rather limited, and interpolation of these would result in large errors on the side of the valley, where there is no soil cover. Therefore, the segment boundary of the quaternary cover in the map was converted into points, and the elevation value obtained from the DEM was assigned to them. These points were then glued with borehole point map. The glued point map was then interpolated following the Simple Kriging method. Before the Kriging operation was performed, the spatial correlation operation was used for obtaining suitable (best-fit) semi-variogram models with omni-directional option and lag spacing of 300 m. In the output table obtained from the spatial correlation method semi-variogram models were plotted in a graph between Avg-lag versus semi variogram to make the best fit. The best-fitted model (spherical) was chosen for the Kriging purpose as shown in Figures 4.6. Using the same procedure, three models were prepared for the different boundaries of the sediment layers. Figures 4.6 indicates semi-variogram model for altitude of bedrock level. The semi-variogram models for other altitudes are given in annex (see in annex Figure A, B).

The Kriging operation was carried out for four different levels: bedrock level, top of the lake deposit and bottom of the lake deposit. The surface level was already available as this is the actual Digital Terrain Model of the surface. Thus, four Digital Elevation Models were representing these different layers as shown in Figure 4.7 A, B, C, D respectively. Similarly, the thickness maps of individual layers were derived by subtracting the various DEMs. Thus, three thickness maps were generated for the Post-Lake deposits, Lake deposit and Pre-Lake deposits as shown in Figure 4.8 A, B, C.

Table 4.5: Examples of the complexity of layers with clay deposits in different boreholes.

Well numbers	Number of Clay layers	Max. thickness in meter	Well_ID	First claylayer m	Second clay Layer m	Third-clay layer m	Fourth clay layer m	Fifth clay layer m	Location
92	1	304	B01	304					Harisiddhi
43	2	232	DMG4	212	19				Hyumat tole
14	3	206	DMG7	171	20	15			Teku
1	4	199	P18e	162	10	13	14		Soaltee hotel
2	5	274	DMG6	187	18	24	18	27	Bhrikutima-ndap

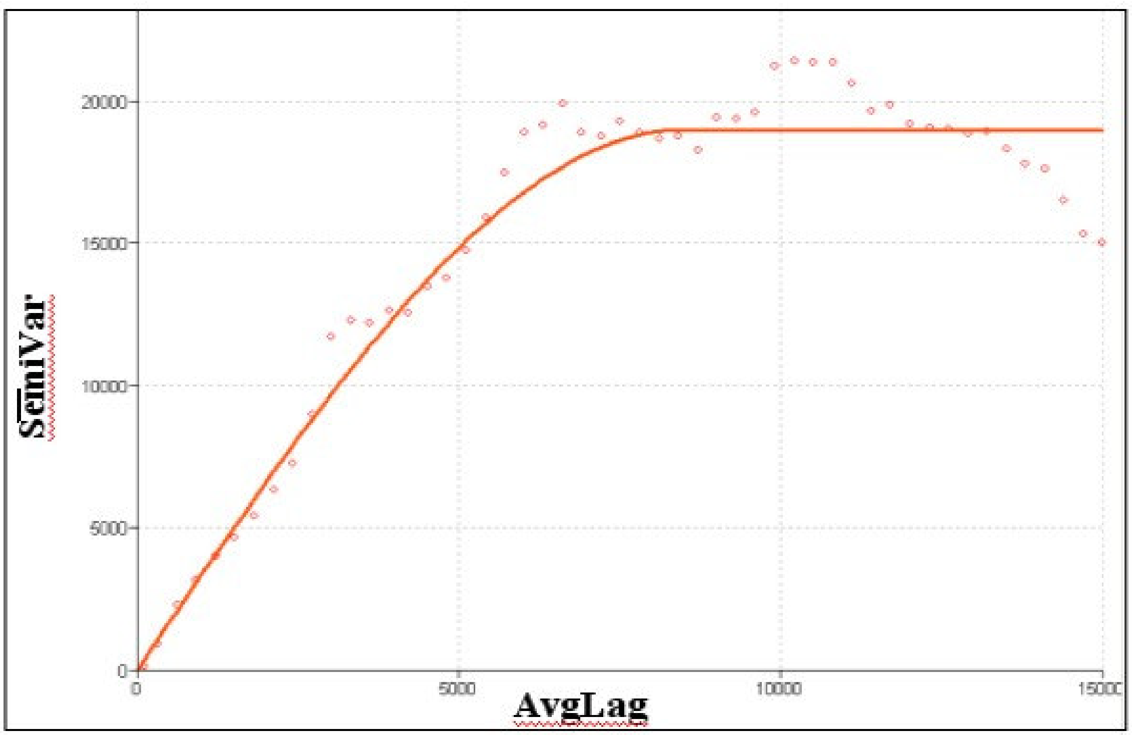

Figure 4.6: Semi-variogram model for bedrock level.
Nugget =5, Sill =19000, Range = 8000

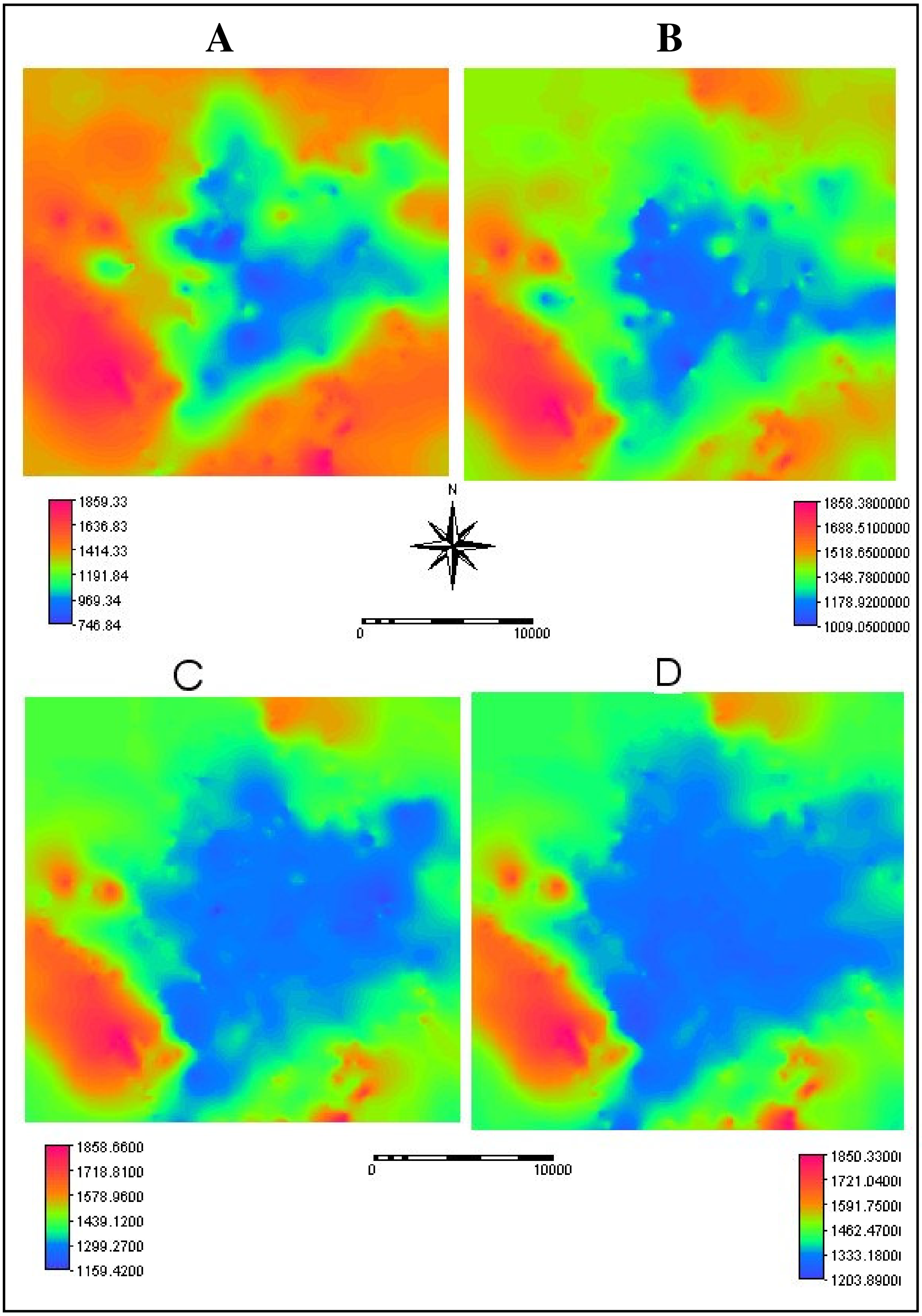

Figure 4.7: Digital Elevation Models generated for the boundaries of the layers in the four-layer model for Kathmandu valley. A: Bedrock level, B: Bottom of Lake deposits, C: Top of Lake deposits, D: Surface.

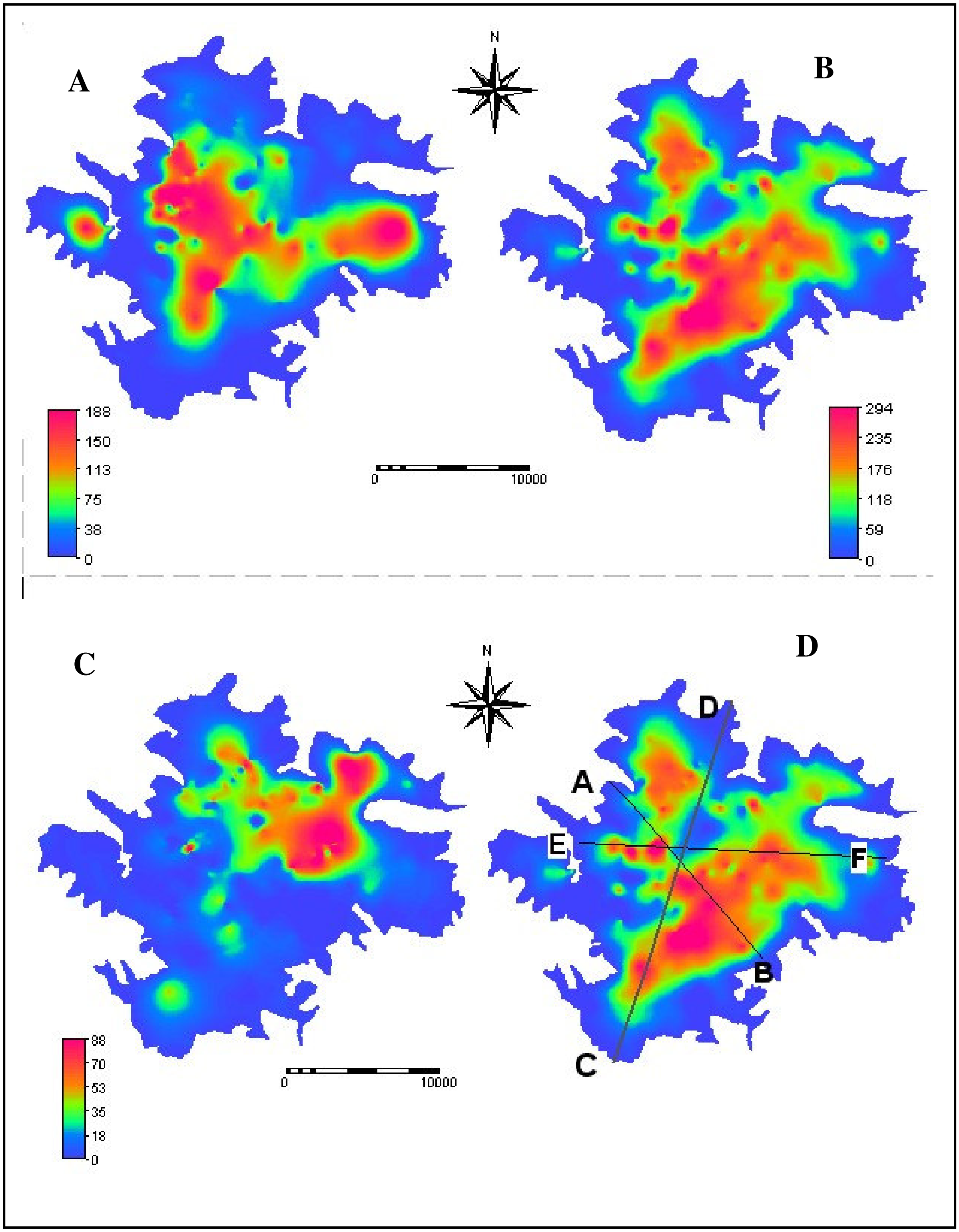

Figure 4.8: Thickness maps generated for the layers in the four-layer model for Kathmandu valley. A: Thicnkess of lake deposits, B: Thickness of Pre-Lake deposits, C: Thickness of Post-Lake deposits, D: Location of cross sections.

In Figure 4.8 A, the map shows the thickness of the lake deposits that ranges in thickness from zero to more than 188 m. The map indicates that the deepest part of the lake existed mainly in the central portion of the valley, where presently the main core of the city exists and also in the southern part of the valley in the Harisiddhi and Bungamati area (see Figure 1.1 in Chapter 1 for name of places). The deeper part of the lake can also be seen in the western part, in the Satungal area and in the East towards Bhaktapur. The Thimi and Bodegaon areas have very shallow lake deposits. Similarly in the extreme South part of the valley, very shallow or no lake deposit occurs, as is also the case in the Gokarna area towards the Northeast of the valley. From Figure 4.8 A, we can conclude that in the western part (Satungal area) and in the eastern part (Sankhu areas) two isolated lakes existed which were separated by Naikap Bhanjyang pass in the West and Changunarayan hill in the East (see Figure 1.1 for location of the place).

In Figure 4.8 B, it can be observed that the maximum thickness of the sediments below the lake deposits is greater than 294 m. The largest thickness of these sediments is found in the Harisiddhi area South-east of Lalitpur, and around the centre part of Kathmandu city (see Figure 1.1 for the location of the places)

From Figure 4.8 C, it can be concluded that the thickness of the layer of sediments above the lake deposit ranges in thickness from zero to 88 m. According to this map, the largest thickness of this type of sediment can be found in the North and northeastern part of the valley. In the South the thickness of this sediment is very small.

4.4.2 Generation of cross sections

After the data generation of the layer models, cross sections were generated for different layers along different directions following ILWIS procedures. The profile directions of the cross sections are shown in Figure 4.8 D. Lithological cross sections were also drawn using Rockworks99 by following the so-called “hole-to-hole” cross-section method. Such a technique helps to display logs of the boreholes along the desired direction and thus helps to study the subsurface geology lying along the section. One East-West striking and the other North-South striking lithological sections were prepared to study the distribution of quaternary sediments in the Kathmandu valley basin.

An example of a cross section generated by ILWIS and the corresponding cross section generated through Rockworks is shown in Figure 4.9 A and B.

The cross section generated in ILWIS (Figure 4.9 A) runs from Bungmati in the Southern part to Budhanilkantha in the Northern part (See Figure 1.1 for location of the place). The figure indicates that, the sediments above the lake deposits gradually increase to the North, in the central part, this portion is less and in some part, it vanishes as well. On the other hand, the thickness of the lake deposits gradually diminishes to the northern part and to the extreme South but increases in the central part and to the South. Similarly the sediments below the lake deposits can be observed more in the central and southern part except in Lalitpur and Pashupati area where bedrock is encountered at lower depths and hence the thickness appears less (see Figure 1.1 for location).

(A)

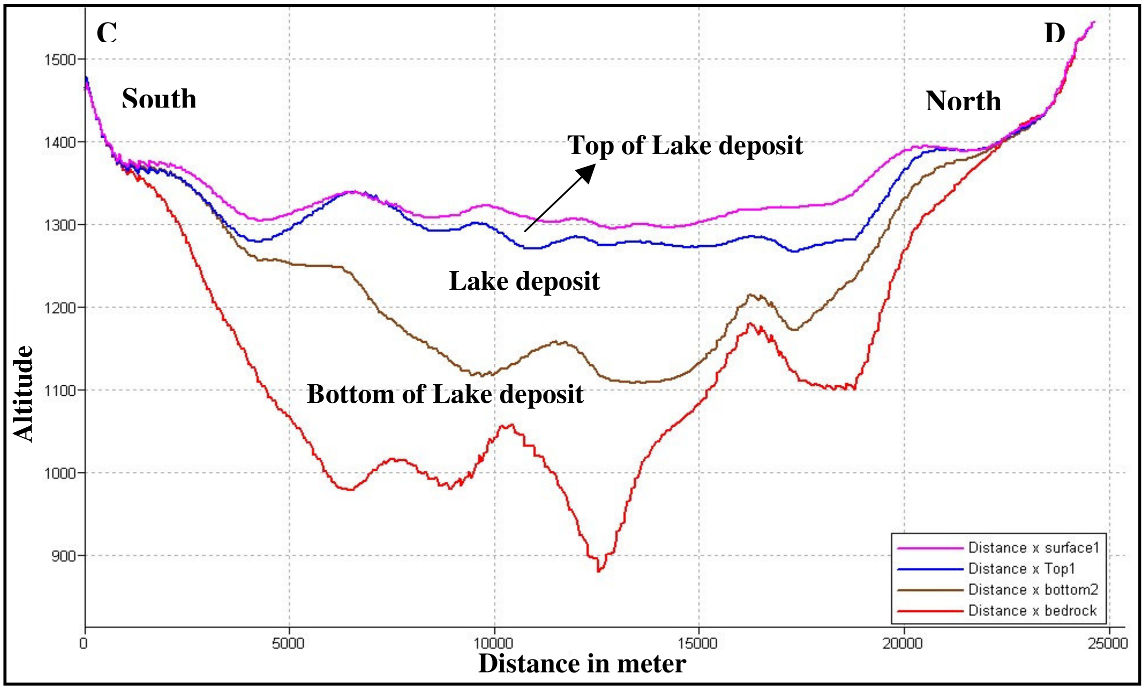

Figure 4.9: Example of a cross section. See Figure 4.8 D for the location.
A: cross section generated from the simplified layer model.
B: corresponding borehole logs for the same area.

(B)

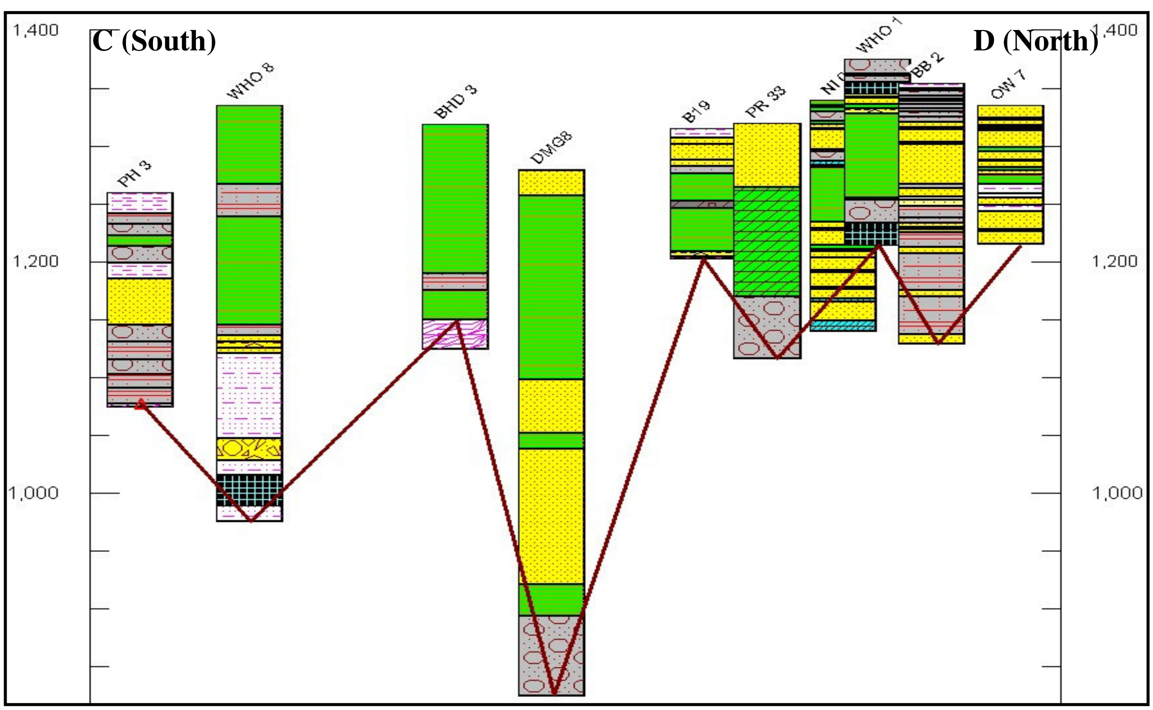

This cross section is compared with the lithological cross section drawn almost along the same direction (see Figure 4.9 B). The section also runs from South to North. It includes boreholes PH3, WHO8, BHD3, DMG9, DMG8, B19, PR33, NI01, WHO1, BB2, and OW7 (see Figure 4.1 for location of boreholes). Out of these, two of the boreholes (PH3, BHD3) have touched the bedrock and rest are still in the soft sediments. It shows that they are rather well correlated. For example in Figure 4.9 A, we can observe that the thickness of the lake deposit is more in the central part which is also represented by the boreholes WHO8, BHD3 and DMG8 (in Figure 4.9 B) respectively. In the borehole BHD3, the whole of the sequence is clay after bedrock. Similarly, if we go towards the northern part the thickness of the lake deposits gradually decreases, which is also represented by the boreholes BB2 and OW7 in Figure 4.9 B. The borehole BB2 near Bansbari indicates the marginal line for the ancient lake territory. After that place further to the North, boreholes consist of abundance of coarse sediments.

The upper most part in the cross section shown in Figure 4.9 A (Top of Lake deposit) can be correlated with the Patan Formation of Sakai (2001) which ranges in age from 29,000 BP to present (Yoshida and Igarashi, 1984), similarly the middle layer (Lake deposit) can be correlated with the Kalimati Formation as described by Kharel et al. (1998), Dongol (1985, 1987), and Sakai (2001). The age of the middle layer is believed to be from 29,000 to 2,500,000 years (Yoshida and Igarashi, 1984). The lowermost layer (Bottom of Lake deposit) is correlated with the Bagmati Formation of Sakai (2001), in the central part and the Tarebhir Formation in the extreme South consisting mainly of sand and gravels with cobbles and boulders in some places. The age of this formation is believed to be older than 2.5 million years (Yoshida and Igarashi, 1984).

The lithological information as obtained from boreholes indicates that the rocks of the surrounding mountains are the main source of the sediment material deposited in the valley. In the northern part, the Shivapuri gneiss is the main source of the sediments with coarser materials (arenaceous deposits) where as in the South the rocks of Tistung Formation, and Chandragiri Formation are the main source of the fine sediments (argillaceous deposits). The ancient drainage pattern played an important role in transporting sediments along the drainage channels and distributing them in the valley.

More examples of cross sections for other directions are shown in the annex part (Figure C, D and E).

4.4.2. Fence diagrams

Lithologs were also shown in fence diagram selecting boreholes in five different regions. The following five regions were selected: Kathmandu well colony, Gokarna well colony, Lalitpur well colony, Manahara well colony and southern part well colony. Similarly 2D lithological profiles were also created along different directions. In Rockworks99 correlation of lithology type was not possible. Only the correlation of stratigraphic layer was possible. Therefore, in order to get fence diagrams of the stratigraphic layers, the lithology of the entire area was classified into certain formation types (nine types) as mentioned in Chapter 2 (section 2.5) based on the geological information obtained from the deepest borehole logs (e.g. DMG6). According to this classification, data were entered in the Rockworks table and Patterns and colours were assigned to the various layers accordingly.

A fence diagram is a useful tool to observe lithological types of different selected boreholes at the same time, as it represents multiple logs in a single diagram. It displays cross sections in a network so that one can compare easily the sediment types among the displayed sections. Its main objective is to correlate the stratigraphic layers with the other layers through out the site. Rockworks99 and Rockworks2002 were both used for this purpose. Rockworks99 can create fence diagram only for stratigraphically defined layers whereas the Rockworks2002 can create fence diagram for lithologically defined logs also. The fence diagram generated in Rockworks2002 is different from that in Rockworks99. Rockworks99 can create fence diagram with both colors and patterns in 3D form, whereas Rockworks2002 creates fence diagram with color pattern only. Fence diagram for selected lithologs are shown in Figure 4.10 in 3D view, which was made using Rockworks99.

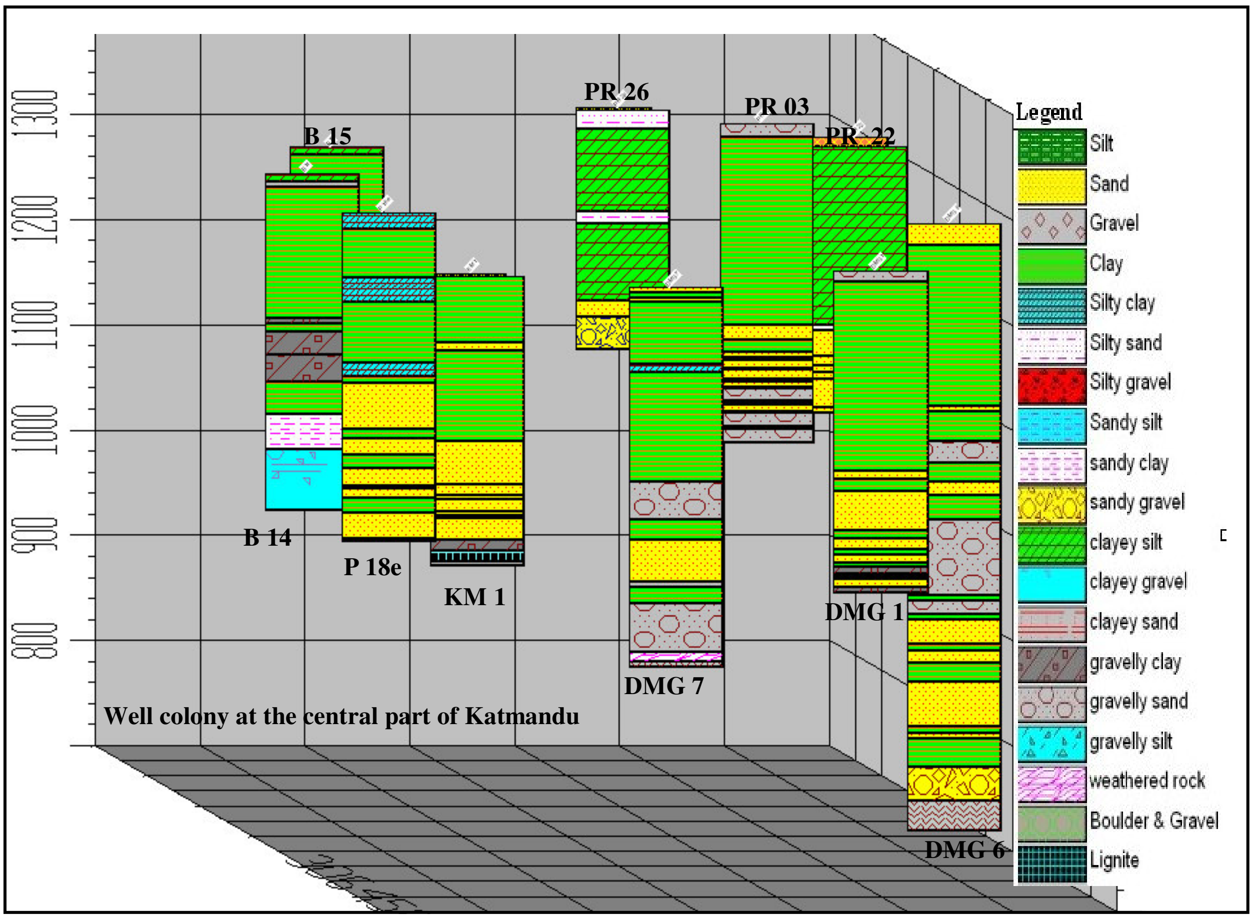

Figure 4.10: Fence diagram with lithologs, representing well colony at the central part of Kathmandu Valley.

The lithologs in Figure 4.10 have been selected from the central part of Kathmandu city. As can be seen from the diagram that the central part of the Kathmandu city is highly dominated by lake sediments (Black Clay). Similar fence diagram have been prepared for the borehole logs of Manahara well field area (northern part), Lalitpur city area (central part) and Gokarna well field area (see in annex part, Figure F-H). All these diagrams give information about the sediment types in that particular region. The location for the drawing of these sections is given in annex (Figure **I**).

The other type of fence diagram as can be seen below in Figure 4.11 is prepared for stratigraphically described logs. As mentioned before, the basin can be classified into 9 stages of depositional environment based on borehole DMG6. In Figure 4.11, a fence diagram is displayed for 5 stages of sediment deposits. The 5 stages as seen in the diagram are Proto-Bagmati deposit, Lake deposit (deep), Fluvio-deltaic deposit (3), Shallow lake deposit (3), and Post lake deposit.

A similar type of fence diagram is shown in Figure 4.12 for three stages of sediment deposits and includes boreholes, P31b, Paleo1, B13, B15, B17, MK1, P14b, P3a, BB1, DK6, and PR19. All of these boreholes have touched bedrock. The three different stages (stratigraphic layers) shown here are, Proto-Bagmati deposits, Lake deposits (deep), and Post Lake deposit which are most commonly occurring in the valley.

Besides the fence diagrams and lithological cross sections, projected stratigraphic sections (profiles) and stratigraphic models were also prepared. In a projected stratigraphic section, the program scans the location, coordinates, and borehole information, stacks them from top to bottom and displays them in a vertical profile as shown in Figure 4.13 and 4.14. Stratigraphic projections as shown in this figure indicate stages of sediment depositions in different environments. We can conclude, on the basis of the undulating contacts that the sediment depositions within the valley have been controlled by the irregular bedrock topography, for which the existing fault systems within and around the valley may have played a major role. On the other hand, the stratigraphic model simply displays multiple surfaces, stacked on top of each other for the entire area. Figure 4.15 finally represents a 3-D view from which it is possible to observe the thickness of the different stratigraphic layers.

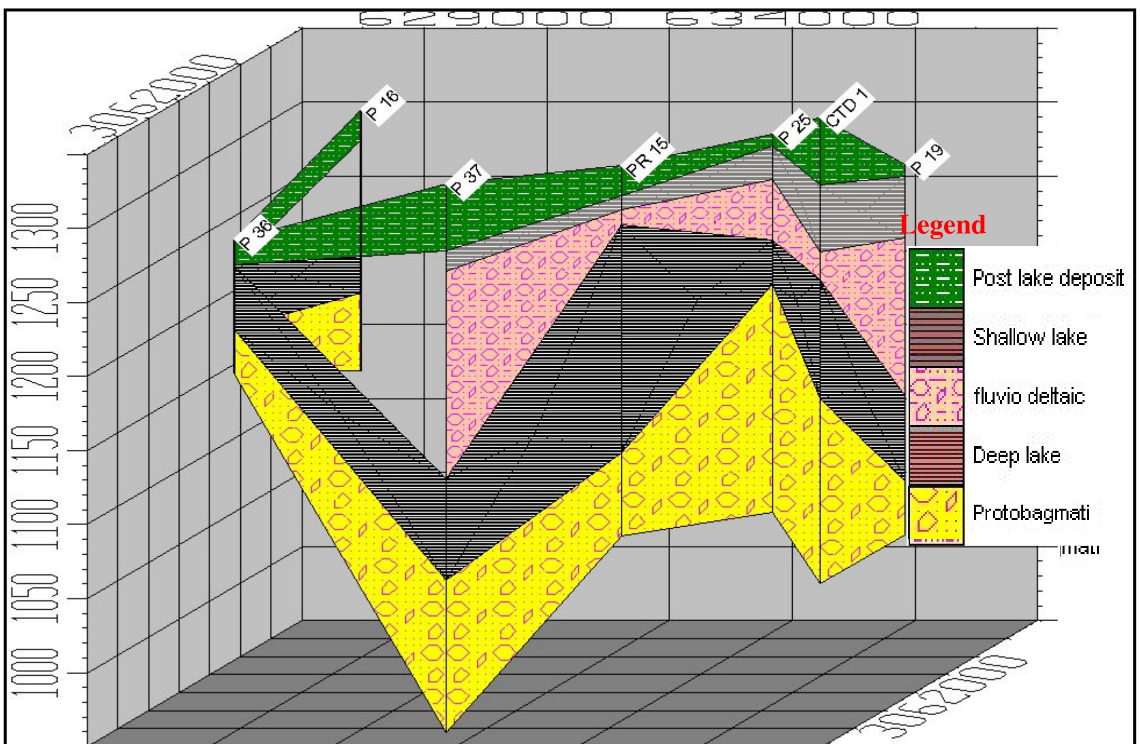

Figure 4.11: Fence diagram (for stratigraphical sequence)

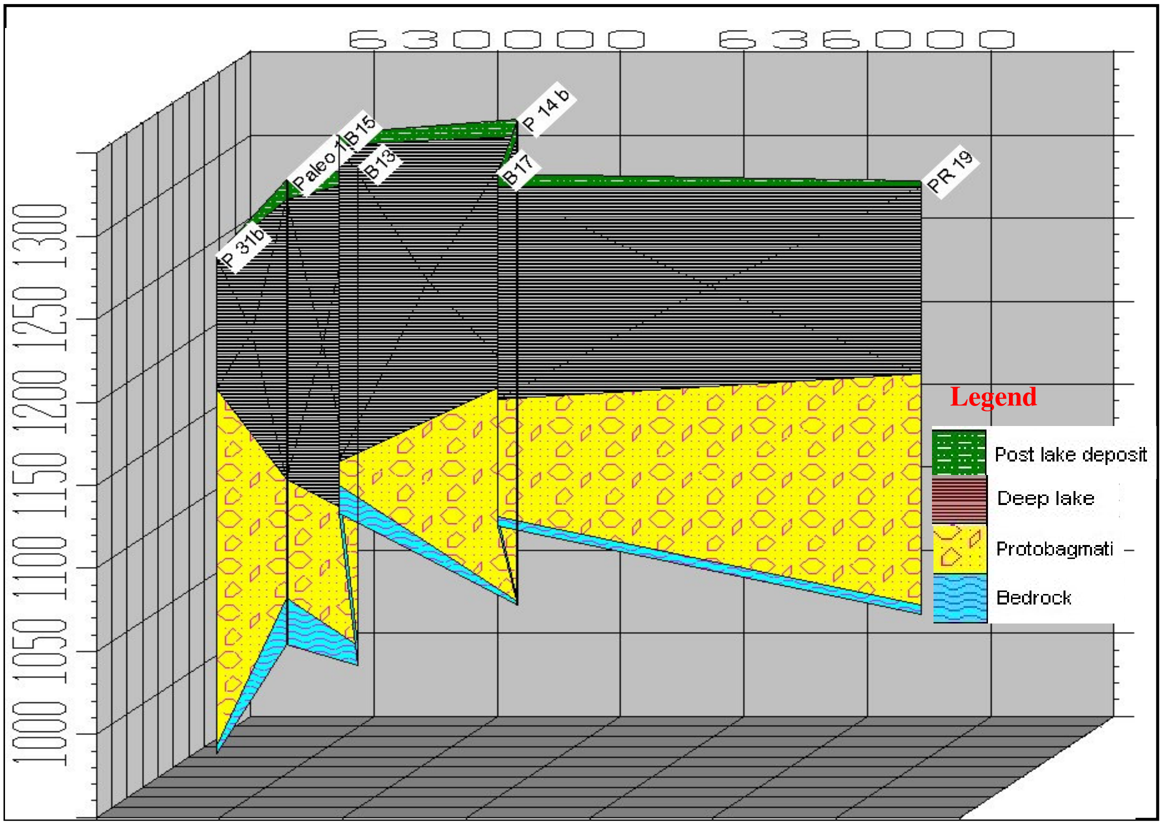

Figure 4.12: Fence diagram (for stratigraphically defined layers for the boreholes that have reached up to the bedrock level)

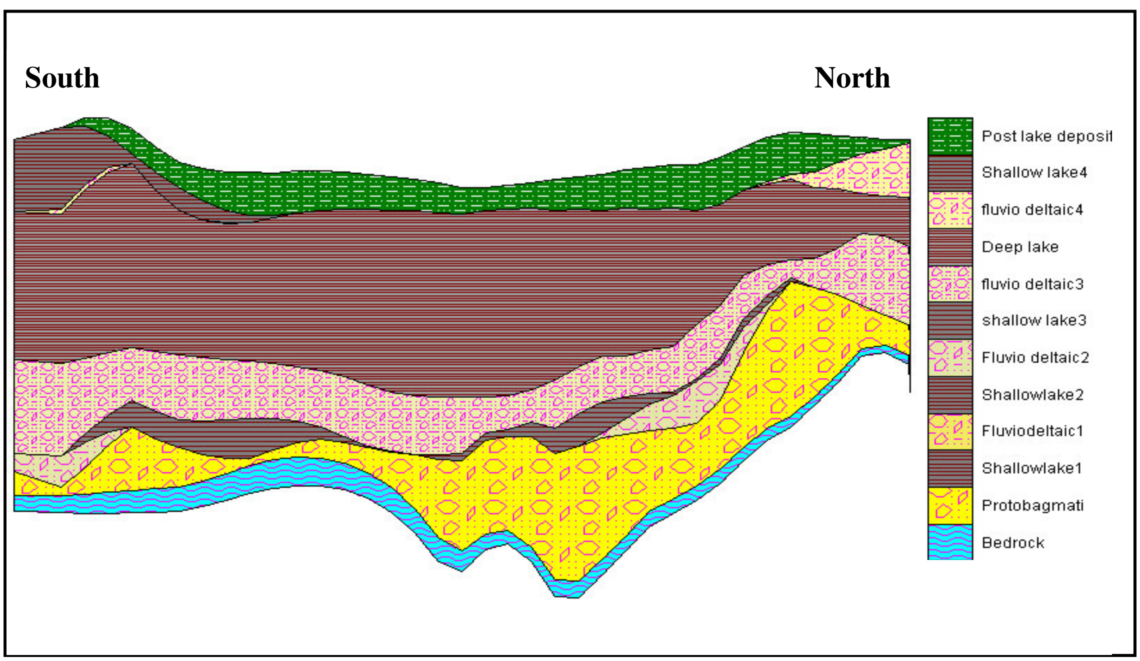

Figure 4.13: Stratigraphic profile along Bungamati in the South to Budhanilkanth in the North Crossing through the centre of the valley.

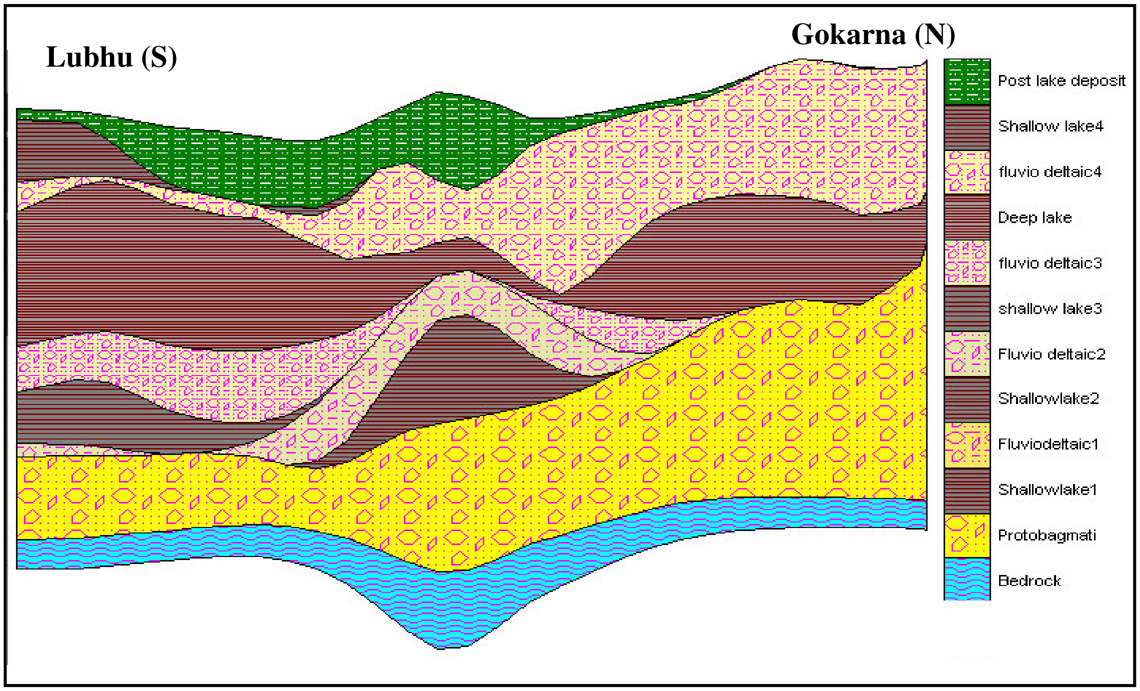

Figure 4.14: Stratigraphic profile along South to North passing through Lubhu in the South to Gokarna in the North (Eastern block)

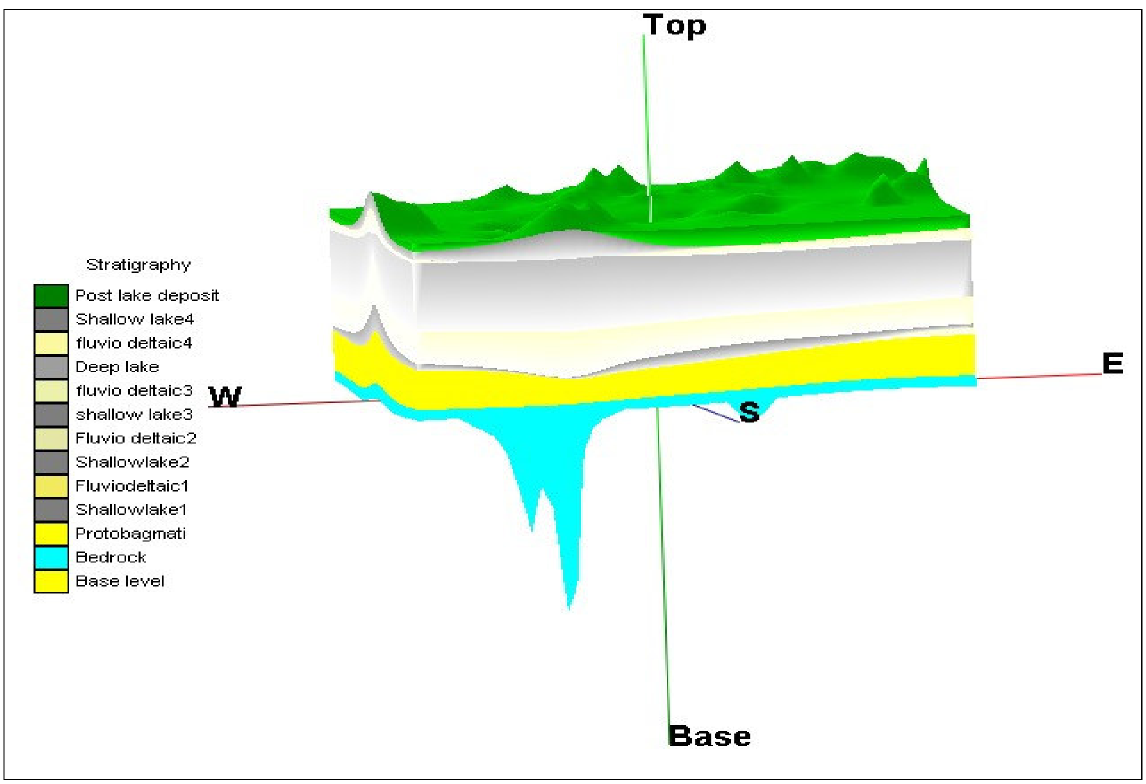

Figure 4.15: Stratigraphic model of Kathmandu valley basin

5. Liquefaction hazard assessment for Kathmandu valley

5.1. Introduction

As mentioned in chapter 1, the second main objective of this research work was to prepare liquefaction susceptibility map of Kathmandu valley using borehole data. Liquefaction phenomena have been recorded in many parts of the world, where ground shaking is frequent and soils consist of loose fine sand where the water table is shallow. Liquefaction of saturated loose sands and silty sands induce flow slides, differential settlement, and subsidence, leading damage to buildings and infrastructure and eventually to loss of life.

Kathmandu valley is a large intramontane basin filled up by fluvio-lacustrine deposit with a shallow ground water table in most areas (see Chapter 2) and is therefore considered to be potentially susceptible to liquefaction. Liquefaction in the valley is known from the 1934 earthquake (Rana, 1935).

Various methods for evaluating the liquefaction potential of sandy soils due to earthquake motions have been explained in Chapter 3. The liquefaction potential in this study will be examined using quantitative and qualitative approaches.

5.2. Methods

For the quantitative analysis of liquefaction susceptibility mapping a simplified procedure of the method developed by Seed and Idriss (1971) and Iwasaki et al. (1984) was adopted. For the qualitative analysis on the other hand, the method used was based on topographical and geological information (Iwasaki et al. 1982: and Juang and Elton 1991). The analysis and results obtained from these two methods are described and compared here in this Chapter.

The procedures followed for the liquefaction susceptibility assessment are schematically presented in Figure 5.1. In the liquefaction susceptibility study, a total of 328 shallow boreholes data were used for the qualitative analysis and around 87 boreholes with geotechnical information for the quantitative analysis. The depth of all these boreholes is limited to the top 10 m only, due to time constraints and also due to varying range of borehole depths. Besides, for the liquefaction susceptibility analysis, the sediments of the upper 10 meters depth are more important, as liquefaction is more likely to take within this depth.

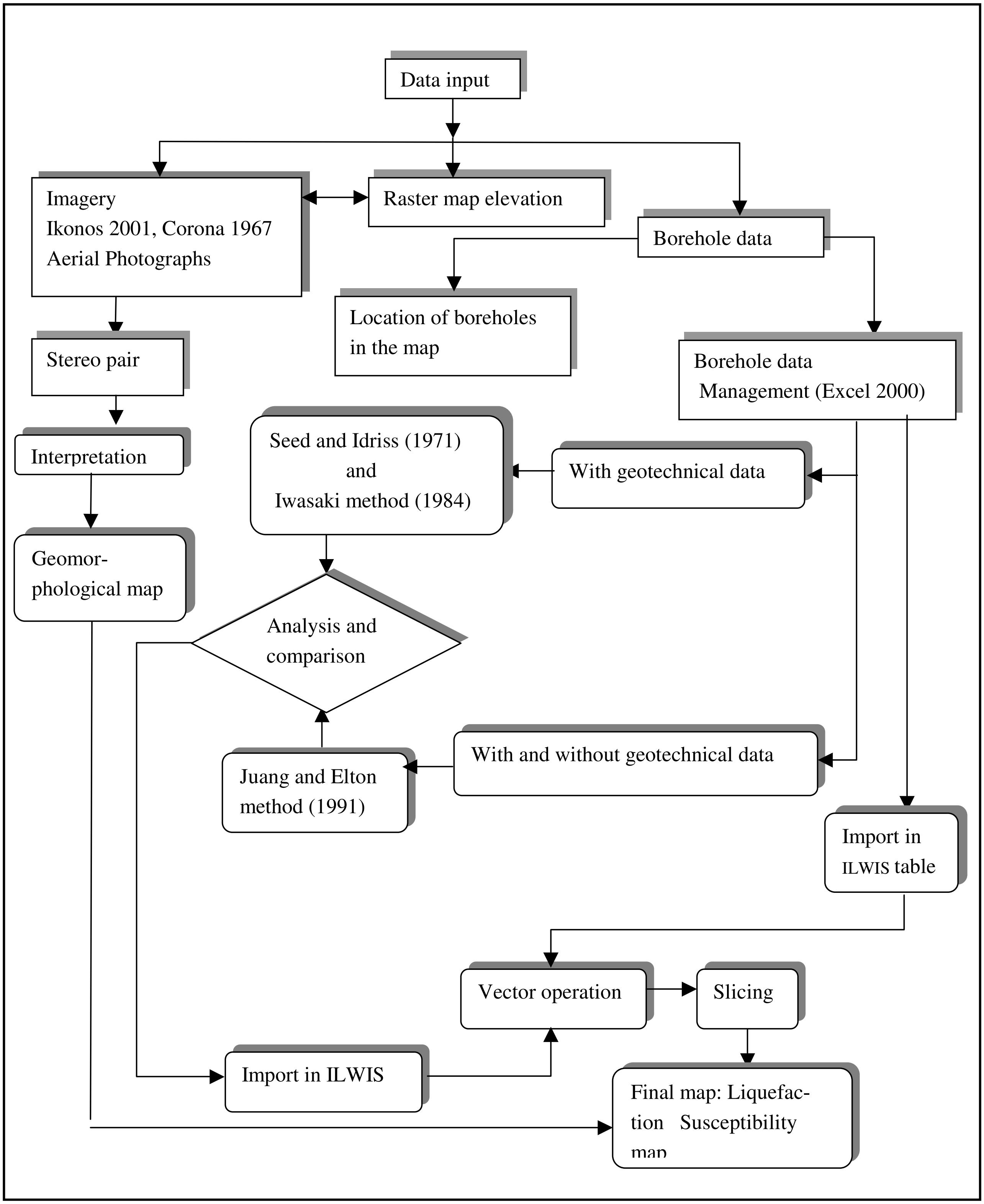

Figure 5.1: Flow chart showing the procedure for liquefaction susceptibility analysis.

Because the borehole data cover relatively a smaller portion of the Kathmandu valley (even more with respect to ones containing geotechnical information), it was not so logical to apply any of the mathematical models to map the entire Kathmandu valley. Hence the liquefaction susceptibility analysis was made following the qualitative method adopted by the UNDP/UNCHS (Habitat) Project (1994), which is primarily based on geological and hydrological factors as proposed by Juang and Elton (1991). The different susceptibility factors, the ratings attributed to them by Juang and Elton (1991), the scores and weight values adopted by the UNDP/UNCHS project are given in Table 3.9 (Chapter3).

In general, the approach of the liquefaction susceptibility mapping involved the following steps:

1. An image interpretation using digital stereo pairs constructed by combining an Ikonos image from 2001 and a DEM, a Corona image from 1967 and a DEM, Aerial Photographs (1979 and 1991) and DEM. Non of these stereo pairs covered the entire study area (Kathmandu valley).

A Geomorphological image interpretation using aerial photographs and other types of imageries, such as Ikonos (2001), and Corona (1967) was made in order to assess the liquefaction susceptibility of the sediments in Kathmandu valley. Three different stereo pairs were constructed covering most part of Kathmandu valley. Apparently some areas in the South, western, eastern and North-eastern part were not analysed due to lack of imagery. For the uncovered area, the Geomorphology map prepared by JICA (2001) and topographical map (1:50,000 scale) were used. The photo interpretation techniques applied allowed the identification of Hill, Hill slopes, Mounds, Rock outcrops, Terrace-IV, Terrace-III, Terrace-II, Terrace-I, Lake, Flood plains and Riverbeds within the Kathmandu Basin.

The terraces have been classified according to their location from the riverbed and their heights. Type-I terrace is distributed near the flood plain areas with flat to gentle plane surface. The type-II, terrace is distributed mainly in the central part of the valley. The main cities, such as Kathmandu, Lalitpur and Bhaktapur are located on this terrace formation (see Figure 5.2). JICA (2002) measured height of 20 m to 50 m for this type of terrace from the present riverbed. The type-III terrace is distributed further outwards from the centre of the valley and is situated at the higher place than that of terrace-II. The height of this terrace from the present riverbed according to JICA (2002) reaches from 50 m to 80 m. Similarly, terrace-IV is distributed along the fringe of the valley near the hilly parts and is higher than terrace-III. The height of this type of terrace reaches up to 160 m from the present riverbed (JICA 2002). The Geomorphology map prepared is shown in Figure 5.2. Hill and hill slopes can be observed in the periphery of the study area. Some mounds are locally observed within the valley. Similarly, rock outcrops can be observed in some of the areas within the valley such as in Pashupatinath, Swayambhu, Balkhu and Chobhar area (Please refer Figure 2.4 in Chapter 2, for location). One small Lake, known locally as Taudaha can be observed in the southern part of the valley. Local people believe that the lake is a remnant of the ancient lake.

2. Quantitative assessment of liquefaction susceptibility using geotechnical borehole data following a simplified procedure based on Seed and Idriss (1971) and Iwasaki et al. (1984).
3. Qualitative assessment of liquefaction susceptibility following the method of Juang and Elton method (1991).
4. Comparison of Quantitative analysis with Qualitative analysis.

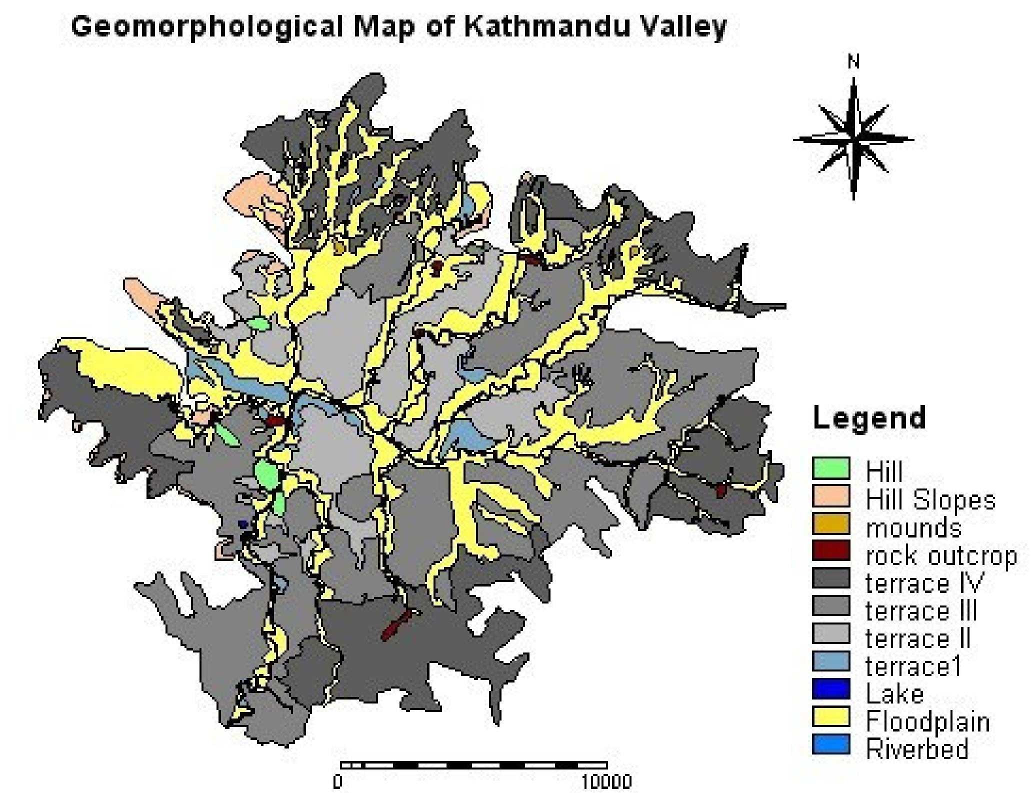

Figure 5.2: Geomorphological map of Kathmandu valley.

5.3. Qualitative analysis

Based on the surveys in earthquake affected zones in Japan, Iwasaki et al. (1982) concluded liquefaction to be more susceptible in present river beds, old river beds or flood plains and negligible in terraces and hills (see Table 3.5 in Chapter 3). Based on this hypothesis some areas were delineated with the help of stereo image interpretation techniques and classified into areas where liquefaction is likely to occur or not.

Because of the wide availability of SPT N-values and grain size distribution data, the liquefaction potential in this study area was evaluated using the method developed by Juang and Elton (1991). As mentioned in section 5.2, from the 328 borehole records about 87 were available with geotechnical properties. Out of the 87 boreholes, only 68 could be located in the map. Due to this low number the qualitative methods of Juang and Elton (1991) was used. Even these, out of the 12 factors describing the geotechnical properties only six were chosen for the analysis. These include:

- Depth to water table,
- Grain size distribution
- Burial depth
- Capping layers
- Age of deposition
- Liquefiable layer thickness.

These factors are considered to be very important for causing liquefaction at a particular place. All six factors were given appropriate score values depending on their influence to accelerate liquefaction in an area as shown in Table 3.9 (Chapter 3). Factors considered to be more influential were given greater weights. The sums were added and the final score obtained by summation of all the factors is considered to give a better indication of the soils susceptibility to liquefaction. Based on the final score obtained by summation of all the factors, four levels of liquefaction susceptibility have been selected:

- **High (score > 36):** Significant areas may liquefy under moderate to high seismic loading.

- **Medium (score between 27 and 36):** Some areas may liquefy under high seismic loading.

- **Low (score between 20 and 26):** Localized areas (Such as ribbon sands) may liquefy under high seismic loading.

- **Very Low (score ≤ 20):** Negligible liquefaction expected even under high seismic loading.

Some areas with rock outcrops were designated as not-liquefiable zones.

It is difficult to explain the quantitative terms of this classification as High, Moderate, Low and Very low. However in this classification system, High class means to say that, in moderate to strong earthquake (MMI VII-VIII), most of the sand and silt covered area with high ground water table will likely to be liquefied. On the other hand, moderate class implies, most of the areas in this category will likely be liquefied only under high seismic loading (MMI IX-X). Similarly in low class category, only the localized areas covered by sands and silts will be liquefied under violent shaking (MMI X-XI). Whereas in very low class category negligible liquefaction is expected under very high seismic loading.

Note: Modified Mercalli intensity is estimated here based on the estimation of JICA (2002) for different earthquake scenario (see Chapter 3) and Association of Bay area Government (ABAG) Earthquake Program (2001) estimation.

The relative liquefaction hazard for various combinations of liquefaction susceptibility and shaking intensity given by ABAG for example is shown in Table 5.1.

Table 5.1: Liquefaction hazard Based on Combination of Modified Mercalli Intensity and Liquefaction Susceptibility map units.

MMI Value	Description of Shaking Severity	Summary damage description used on 1995 maps	Liquefaction Susceptibility				
			Very Low	Low	Moderate	High	Very high
I							
II							
III							
IV							
V	Light	Pictures move					
VI	Moderate	Objects fall					
VII	Strong	Non structural damage			Moderately low	Moderately low	Moderate
VIII	Very Strong	Moderate damage			Moderate	Moderate	Moderate
IX	Violent	Heavy damage			High	High	High
X	Very violent	Extreme damage			High	High	High

Based on this table, ABAG Earthquake Program (2001) estimated that, only some material mapped as having high liquefaction susceptibility will liquefy when exposed to strong shaking (modified Mercalli intensity (MMI VII), while liquefaction of material mapped as comparatively less susceptible will be triggered with very strong shaking (MMI VIII).

The potential liquefaction hazard zones corresponding to these four levels of liquefaction susceptibility are shown in Figure 5.4. The map has been prepared by incorporating the following aspects: -

- Borehole points with score values that were obtained following the method mentioned above were interpolated by applying the simple Kriging method, in which a spherical semi-variogram model was chosen with semi-variogram parameters.
  Nugget =15, Sill = 99, Range = 12000.

- The interpolated raster map was then classified into four levels following the slicing operation in ILWIS 3.2.

- The preliminary zonation map of liquefaction hazard was prepared (Figure 5.3)

- A photo interpretation map, prepared by using stereo images and the geological map made by JICA (2002), was used to delineate the susceptibility zones with a consideration that low lying areas are more susceptible to liquefaction than higher terraces or hillocks located at higher elevations (Iwasaki et al. 1982).

- Regardless of the score, all recent alluvial sediments (floodplain zone) are characterized as having high liquefaction susceptibility.

- Certain areas with bedrock exposure and hillocks such as Pashupati, Gokarna, Balkhu, Swayambbhu and Chobhar gorge (see Figure 2.4, Chapter 2) are characterized as no hazard zone due to bedrock cover.

- An attribute map (point map) was created from the result obtained by the analysis of the geotechnical data (Iwaski method), which showed specific site locations with or without liquefaction susceptibility. This point map was used for validating the map prepared by qualitative method (see Figure 5.5B).

Finally, the different maps were combined to give the final liquefaction susceptibility map with four different zones, High, Moderate, Low and Very low (see Figure 5.4).

The liquefaction map produced has been prepared by adopting very simple methods and as such is not reliable (unless supported by quantitative analysis) to be used for actual development activities but as a general guide to obtain the preliminary knowledge of the areas for liquefaction susceptibility. To prepare a better and quantified liquefaction hazard map, a more detail investigation with comprehensive merging of geologic, geotechnical and seismological data is required. The map prepared in this study however, has been validated by quantitatively analysed borehole information (data sets) following Iwasaki et al. (1984) and Seed and Idriss (1971) method and the qualitatively analysed borehole data sets as shown in Figure 5.5 (A and B).

The liquefaction susceptibility map thus prepared was changed to a polygon map with identifier domains and was linked to a table that contained all the information regarding the susceptibility analysis calculated by both quantitative and qualitative methods, so that when any one polygon is clicked, it gives all the information contained on it thus helping to validate the map (see Figure 5.6).

Finally the map of liquefaction susceptibility was prepared incorporating the following components:

- The geomorphology map prepared by image interpretation.
- The result of liquefaction susceptibility obtained by following the quantitative methods of Seed and Idriss (1971) and Iwasaki et al. (1984).
- The output map prepared by adopting Juang and Elton's qualitative weighting method (1991).

The histogram table of the final map as shown in Figure 5.7 shows that the high liquefaction susceptibility area covers approximately 32 percent of the total area, mostly along the flood plain and some in the city core area. Nearly 30 percent of the area occupies moderate susceptibility, 25 percent by low, 12 percent by very low and nearly one percent by no liquefaction zone area. The low to very low region is distributed mainly in the southern part of the study area such as South of Kirtipur, Chobhar and along the hill slopes in the eastern and western part of the study area. Later, the liquefaction map with class domain was changed into identifier domain in order to give attribute values to the different polygons and was crossed with the rasterised classified point maps of the boreholes used in the liquefaction analysis.

In the confusion matrix Table (5.2) created using the classified borehole point map and classified liquefaction map, the row table represents the so-called ground truth value (represented to qualitatively assessed borehole points) and the column represents the classification result in the map. In this Table, 65 of the boreholes classified as highly susceptible to liquefaction are correctly classified as high in classified map. Similarly 51 number of borehole samples are correctly classified as moderately susceptible in classified map. Like wise 11 numbers of boreholes are correctly classified as low and 2 of the boreholes are correctly classified as very low. Rest of boreholes are labelled in wrong zones. The overall accuracy in this case is 0.46 (46 percent).

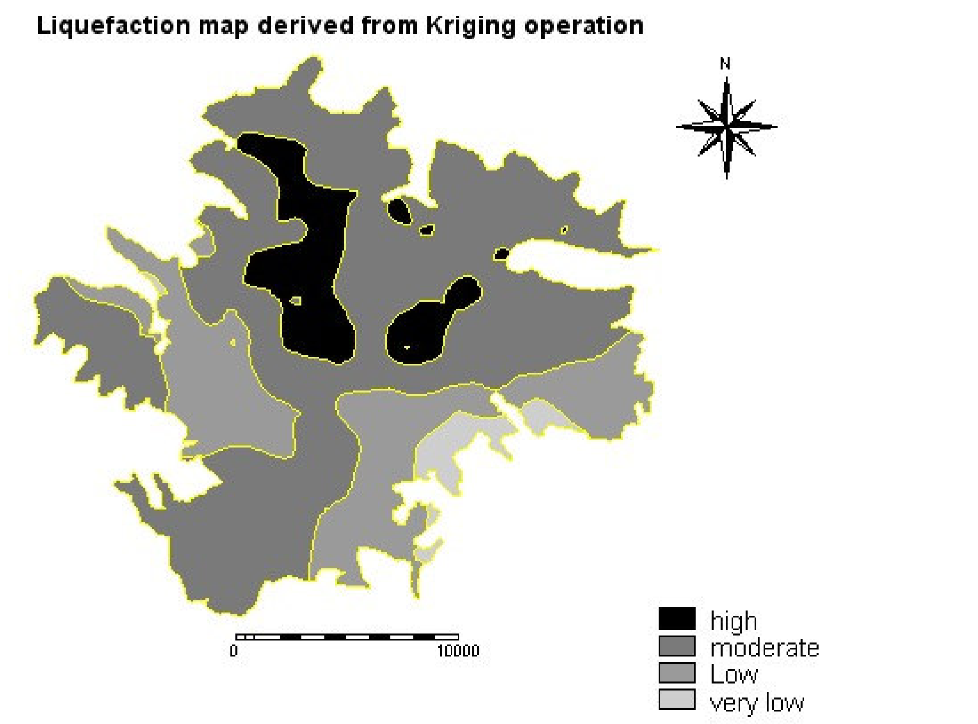

Figure 5.3: Liquefaction susceptibility map derived from Kriging operation.

The liquefaction level class assigned to different boreholes was compared with the average SPT values obtained for 10 m depth. A close agreement was found in most of the cases (boreholes), as most of the boreholes have SPT values less than 20. On the other hand some of the boreholes, which were designated as high or moderate liquefaction susceptible, have very high SPT values (greater than 30), which is rather exceptional. For example for the boreholes C 296, C 8, C 37, C 70, C 314 and C 344 which are designated as moderate have average N-values more than 30. Similarly the boreholes, C 217, C 308, C 315, and C 316 which are designated as high have average N-values greater than 33. Hence these places where N- value are greater than 30 can be considered as non liquefiable areas though they obtained high scoring values with moderate or high class during qualitative analysis. (For details please see annex in CD with file Liquefaction analysis)

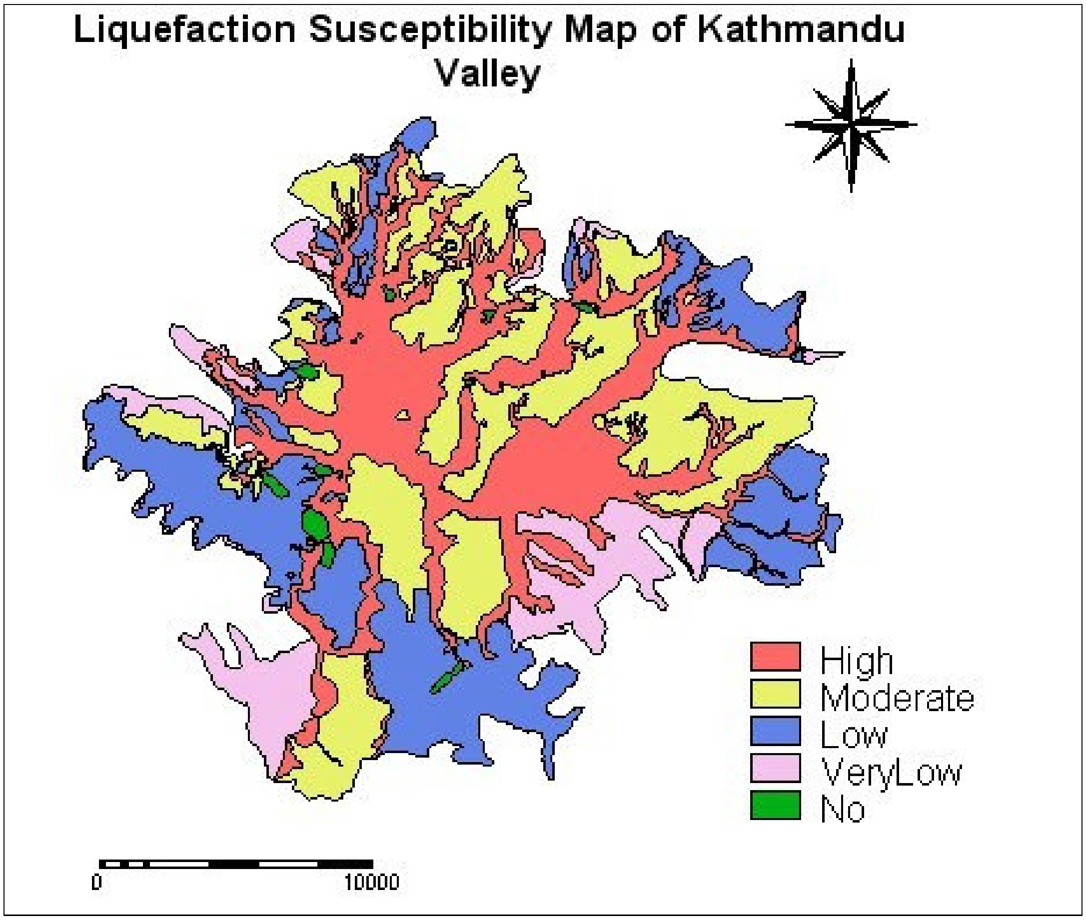

Figure 5.4: Liquefaction Susceptibility map of Kathmandu valley.

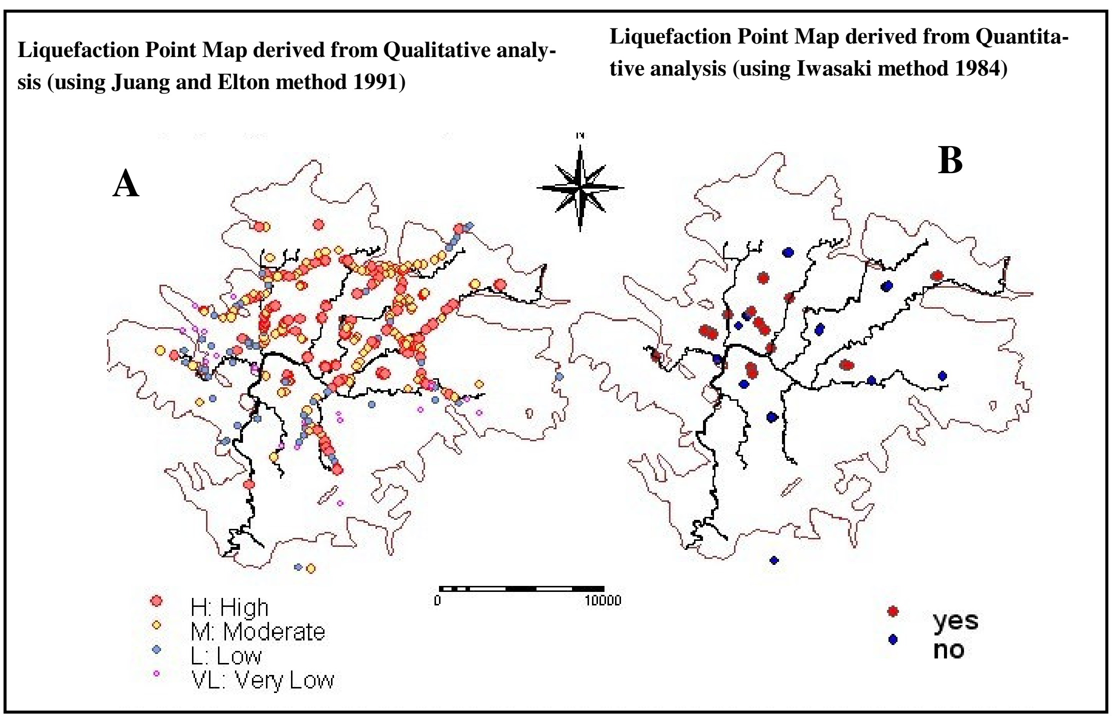

Figure5.5: Borehole wise Liquefaction Susceptibility map

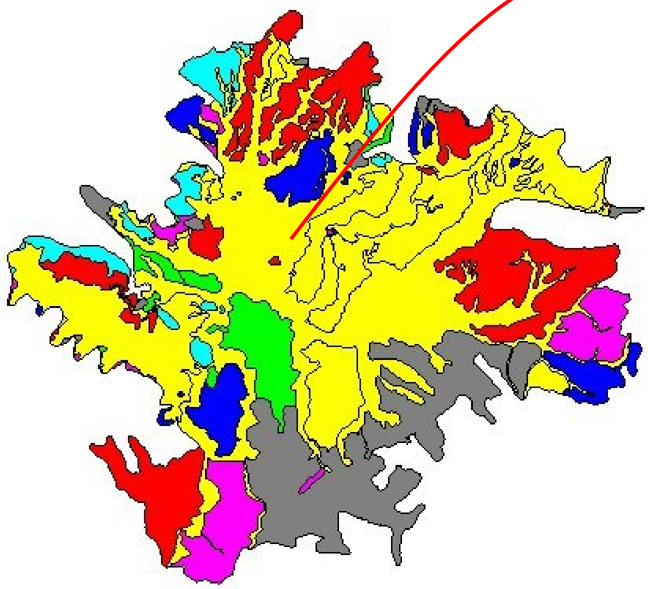

	Pol 1
lique_faction	High
Area	112787872.97
High	65
Moderate	55
Low	16
VeryLow	8
High1	65
Moderate1	55
Low1	16
Verylow1	8
Totpoint	144
Highperc	45.14
Modeperc	38.19
Lowperc	11.11
VLowperc	5.56
Iwasaki_yes	17
Iwasaki_no	5
iwasaki_yes1	17
iwasaki_no1	5
holesite_yes	9
holesite_no	3

Figure 5.6: The polygon map derived from Liquefaction susceptibility map shown with attributes.

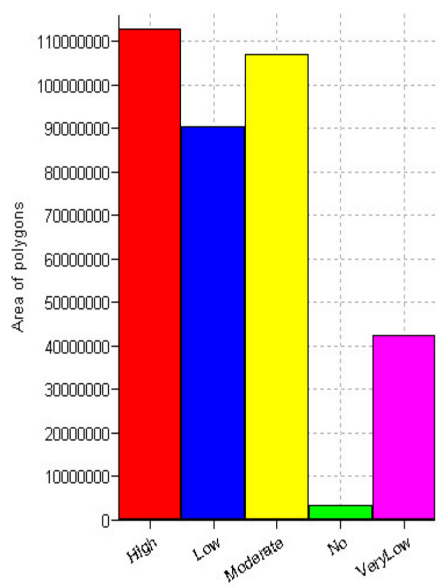

	NrPol	Perimeter	Area	areasqkm	percent_area
High	107	1172126.16	113029637.91	113.03	31.73
Low	35	329192.18	90369850.02	90.37	25.37
Moderate	37	397456.83	107123239.79	107.12	30.08
No	12	25407.54	3220106.43	3.22	0.90
VeryLow	37	188287.62	42427162.27	42.43	11.91
Min	0	0.00	0.00	0.00	0.90
Max	107	1172126.16	113029637.91	113.03	31.73
Avg	38	352078.39	59361666.07	59.36	20.00
StD	37	431870.76	51157377.05	51.16	13.21
Sum	228	2112470.33	356169996.41	356.17	99.99

Figure 5.7: Histogram table for Liquefaction Susceptibility

Table: 5.2 Confusion matrix between classified polygon map and classified borehole point map.

Sum of NPIX	LIQUE_FACTI					
LIQUE_CLASS	High	Moderate	Low	Very Low	No	Grand Total
High	65	27	2	0	0	94
Moderate	55	51	8	2	0	53
Low	16	22	11	3	1	116
Very Low	8	5	2	2	2	19
Grand Total	144	105	23	7	3	282
Overall accuracy = correctly classified pixels (sum of diagonal values)/total samples						
Correctly classified pixels	129					
Overall accuracy	0.462366					

5.4. Quantitative analysis

The quantitative analysis results were classified into two groups according to the extent of liquefaction observed, namely into liquefiable or non-liquefiable site.

The data for Liquefaction potential analysis were collected from geotechnical reports provided by different consultation companies in Kathmandu (see Chapter4). The generation of the database for liquefaction susceptibility analysis is already discussed in the previous Chapter.

The detailed calculation for the evaluation of liquefaction susceptibility using simplified procedure of Seed and Idriss method (1971) and Iwasaki method (1984) is given in an Excel file, which can be found in the CD enclosed in this thesis.

5.4.1. Iwasaki - method

A simple method suggested by Iwasaki et al. (1984) was used here to evaluate a liquefaction resistance factor, F_L. According to this method, liquefaction potential can be estimated simply by using the fundamental properties of soils, i.e. N-values, unit weights, mean particles of diameter and Peak Ground Acceleration of the ground surface (PGA). The liquefaction resistance factor was calculated using equation 8 and 9 (see section 3.5) for given samples and for given range of D50 values. However it is to be noted here that, very few data were obtained for undisturbed samples and similarly the sieve analysis curves were available only for a few soil samples. Therefore, the calculation in this case was carried out according to the given formulas only for those soil samples for which data were derived from undisturbed soil samples and for which sieve data were available. Here sieve data was required to determine D50 values. On the other hand for all other samples, which were disturbed samples and for which D50 values were not available, calculation was made using the formula of equation

9 (Chapter 3). The relation to determine the factor is given in equation 7 (see Chapter 3). According to this relation the soil of the particular site is expected to be liquefied if the calculated Liquefaction resistance factor (F_L) becomes less than 1.

The quantitative assessment following the Iwasaki method was carried out for 87 boreholes in 31 different sites using different PGA values. As mentioned before, although 87 boreholes at different places were analysed using quantitative analysis only 68 of them could be located in the map. However, It was found that out of the 87 boreholes a total of 37 boerholes in 15 different sites showed a low liquefaction resistance factor at a particular depth and thus liquefaction is likely to occur during a strong earthquake with PGA=0.1g. Similarly for a PGA 0.2g, 69 of the boreholes at a particular depth will be liquefied and for 0.3g, 80 borehole locations will be liquefied (see Table 5.3). In the rest of the boreholes, liquefaction is not expected to occur under PGA values less or equal to 0.3g. As can be expected, it is concluded that, the number of liquefiable places will increase with increasing PGA values, as shown in (Figure 5.8).

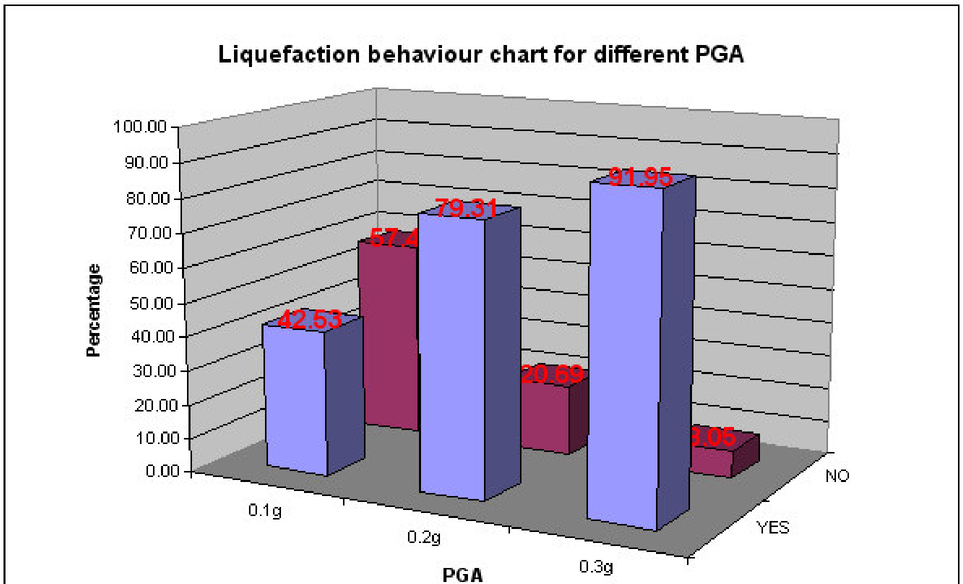

PGA value	Yes	No	Total	% Yes	%No
0.1g	37	50	87	43	57
0.2g	69	18	87	79	21
0.3g	80	7	87	92	8

Figure 5.8: Graph showing liquefaction susceptibility behaviour for different PGA values using the method of Iwasaki et al. (1984).

Table 5.3: Liquefaction potential results for different PGA values based on Iwasaki et al. (1984)

Well ID	Liquefaction potential			Well ID	Liquefaction potential		
	0.1g	0.2g	0.3g		0.1g	0.2g	0.3g
C 1	Yes	Yes	Yes	C 61	No	Yes	Yes
Hole 2	No	No	No	C 62	Yes	Yes	Yes
C 6	No	No	Yes	C 63	No	Yes	Yes
C 7	No	No	No	C 64	No	Yes	Yes
C 9	Yes	Yes	Yes	C 291	Yes	Yes	Yes
C 10	No	Yes	Yes	C 292	Yes	Yes	Yes
C 11	No	Yes	Yes	C 293	Yes	Yes	Yes
C 12	No	Yes	Yes	C 294	Yes	Yes	Yes
C 13	No	No	No	C 295	Yes	Yes	Yes
C 14	No	No	No	C 306	Yes	Yes	Yes
C 16	No	Yes	Yes	C 311	Yes	Yes	Yes
C 26	Yes	Yes	Yes	C 314	Yes	Yes	Yes
C 27	Yes	Yes	Yes	C 333	No	Yes	Yes
C 28	Yes	Yes	Yes	C 334	No	no	Yes
C 29	Yes	Yes	Yes	C 335	No	Yes	Yes
C 30	No	Yes	Yes	C 338	No	No	No
C 31	No	Yes	Yes	C 339	No	No	Yes
C 32	No	Yes	Yes	C 340	No	Yes	Yes
C 33	No	Yes	Yes	C 341	No	No	No
C 34	Yes	Yes	Yes	C 342	No	No	No
C 35	No	Yes	Yes	C 286	Yes	Yes	Yes
C 36	No	Yes	Yes	C 287	Yes	Yes	Yes
C 37	No	Yes	Yes	C 288	No	Yes	Yes
C 38	No	No	Yes	C 289	No	Yes	Yes
C 39	No	Yes	Yes	C 290	No	Yes	Yes
C 40	Yes	Yes	Yes	C 304,305,306	Yes	Yes	Yes
C 41	Yes	Yes	Yes	C 311, 312	Yes	Yes	Yes
C 42	Yes	Yes	Yes	C 313,314	No	Yes	Yes
C 43	Yes	Yes	Yes	C 317	No	Yes	Yes
C 44	Yes	Yes	Yes	C 318	Yes	Yes	Yes
C 45	No	Yes	Yes	C 319	Yes	Yes	Yes
C 46	No	Yes	Yes	C 320	Yes	Yes	Yes
C 47	No	Yes	Yes	C 321	Yes	Yes	Yes
C 48	No	No	Yes	C 322	Yes	Yes	Yes
C 52	Yes	Yes	Yes	C 323	Yes	Yes	Yes
C 53	Yes	Yes	Yes	C 324	Yes	Yes	Yes
C 54	Yes	Yes	Yes	C 325	No	Yes	Yes
C 55	Yes	Yes	Yes	C 326	No	No	Yes
C 56	No	Yes	Yes	C 327	No	No	Yes
C 57	No	No	Yes	C 328	No	Yes	Yes
C 58	Yes	Yes	Yes	C 329	No	No	Yes
C 59	No	Yes	Yes	C 330	No	No	Yes
C 60	No	Yes	Yes	C 331	No	No	Yes
				C 332	No	Yes	Yes

Note: Here Yes represents, the liquefaction is potential and No represents, liquefaction is not potential.

5.4.2. Seed and Idriss method

The quantitative analysis of liquefaction potential for a certain number of boreholes with geotechnical information was also performed using the standard method of seed and Idriss (1971). In this method, the potential maximum seismic shear stress in the ground is compared with the minimum cyclic shear stress causing liquefaction for a particular soil. The soil is susceptible to liquefaction if the maximum seismic shear stress in the ground is higher than the minimum cyclic shear stress causing liquefaction. Shear stress developed during earthquake (τ_{av}) was computed using equation 3 (see section 3.5) and similarly shear stress causing liquefaction (τ_0) was computed using the equation 13 (section 3.5) for which the value for cyclic stress ratio (CSR) was obtained from the graph in Figure 3.5 (see section 3.5).

A comparison was made between them and if τ_{av} was found greater than τ_0, then the soil would be called liquefiable. The calculation was made for an earthquake of M_s = 7.5, and for different PGA values. The result is shown in Table 5.4.

The cyclic shear stress causing liquefaction was deduced from the correlation between the cyclic shear stress causing liquefaction in the field and the $(N1)_{60}$ value given by Seed et al. (1983). The liquefaction potential was analysed for earthquake of magnitude M = 7.5. The Characteristic maximum magnitude earthquake for Kathmandu valley is M = 7.6 (UNDP, 1994). Here it is to be noted that, the earthquake of 15 January 1934 was 8.4 in Richter scale.

Following this method, the analysis was carried out for 69 boreholes located at 40 different sites. It was found that out of the 69 boreholes, in 35 of the boreholes liquefaction is likely to occur at a particular depth, and in the rest of the boreholes there will be no liquefaction for the estimated earthquake magnitude of 7.5 and PGA value of 0.1g. Similarly, for PGA value of 0.2g, 49 of the borehole locations will be liquefied and for 0.3g, 54 of the borehole locations will be liquefied. Thus we find that number of liquefying places increase with increase in PGA value.

Though the calculation for liquefaction analysis was made for different PGA values using Iwasaki et al. (1984) and Seed and Idriss (1971) methods. For the generation of a liquefaction susceptible map of borehole location (point map), peak ground acceleration of 0.1g was considered (See Figure: 5.5B). Because for Kathmandu Valley maximum PGA value is considered as 0.1g for earthquake zone V according to the Indian earthquake standard IS 1093-1984. Here it is to be noted that, JICA (2002) also has calculated PGA value for different earthquake scenario for the Kathmandu valley. The PGA value calculated for different scenario by JICA (2002) is shown in Table 5.5.

JICA's estimation for PGA value is quite higher than that of the Indian standard. If JICA's estimation is to be considered for the liquefaction susceptibility analysis, then most of the borehole locations will be liquefied as shown in Table 5.3 and 5.4. According to JICA, PGA value for Kathmandu valley ranges between 0.2g to 0.3g for all kinds of earthquake scenario.

Table 5.4: Liquefaction potential results for different PGA values for different boreholes (Seed and Idriss method 1971). (Note: Please refer annex in CD for detailed calculation procedures of quantitative analysis for both Iwasaki et al.(1984) method and Seed and Idriss (1971) method.

Well ID	Liquefaction potential			Well ID	Liquefaction potential		
	0.1g	0.2g	0.3g		0.1g	0.2g	0.3g
C 1	Yes	Yes	Yes	C 295	Yes	Yes	Yes
Hole 2	No	No	No	C 306	Yes	Yes	Yes
C 6	No	No	No	C 311	Yes	Yes	Yes
C 7	No	No	No	C 314	No	No	No
C 9	Yes	Yes	Yes	C 333	No	No	No
C 10	No	Yes	Yes	C 334	No	No	No
C 11	No	Yes	Yes	C 338	No	No	Yes
C 12	No	No	Yes	C 339	No	No	No
C 13	No	No	Yes	C 340	No	No	No
C 26	Yes	Yes	Yes	C 341	No	No	No
C 27	Yes	Yes	Yes	C 342	No	No	No
C 28	Yes	Yes	Yes	C 286	Yes	Yes	Yes
C 29	Yes	Yes	Yes	C 287	No	No	Yes
C 30	No	No	No	C 288	No	Yes	Yes
C 31	No	No	No	C 289	No	Yes	Yes
C 32	No	No	No	C 290	No	Yes	Yes
C 33	No	No	No	C-304	Yes	Yes	Yes
C 34	No	No	No	C 311	Yes	Yes	Yes
C 52	No	Yes	Yes	C 313	Yes	Yes	Yes
C 53	No	Yes	Yes	C 317	Yes	Yes	Yes
C 54	No	No	Yes	C 318	Yes	Yes	Yes
C 55	Yes	Yes	Yes	C 319	Yes	Yes	Yes
C 56	No	Yes	Yes	C 320	Yes	Yes	Yes
C 57	No	Yes	Yes	C 322	Yes	Yes	Yes
C 58	Yes	Yes	Yes	C 323	Yes	Yes	Yes
C 59	No	Yes	Yes	C 324	Yes	Yes	Yes
C 60	No	Yes	Yes	C 325	Yes	Yes	Yes
C 61	No	Yes	Yes	C 326	Yes	Yes	Yes
C 62	Yes	Yes	Yes	C 327	Yes	Yes	Yes
C 63	No	Yes	Yes	C 328	Yes	Yes	Yes
C 64	Yes	Yes	Yes	C 329	Yes	Yes	Yes
C 291	Yes	Yes	Yes	C 330	Yes	Yes	Yes
C 292	Yes	Yes	Yes	C 331	Yes	Yes	Yes
C 293	Yes	Yes	Yes	C 332	Yes	Yes	Yes
C 294	Yes	Yes	Yes				

Note: Here Yes represents, the liquefaction is potential and No represents, liquefaction is not potential.

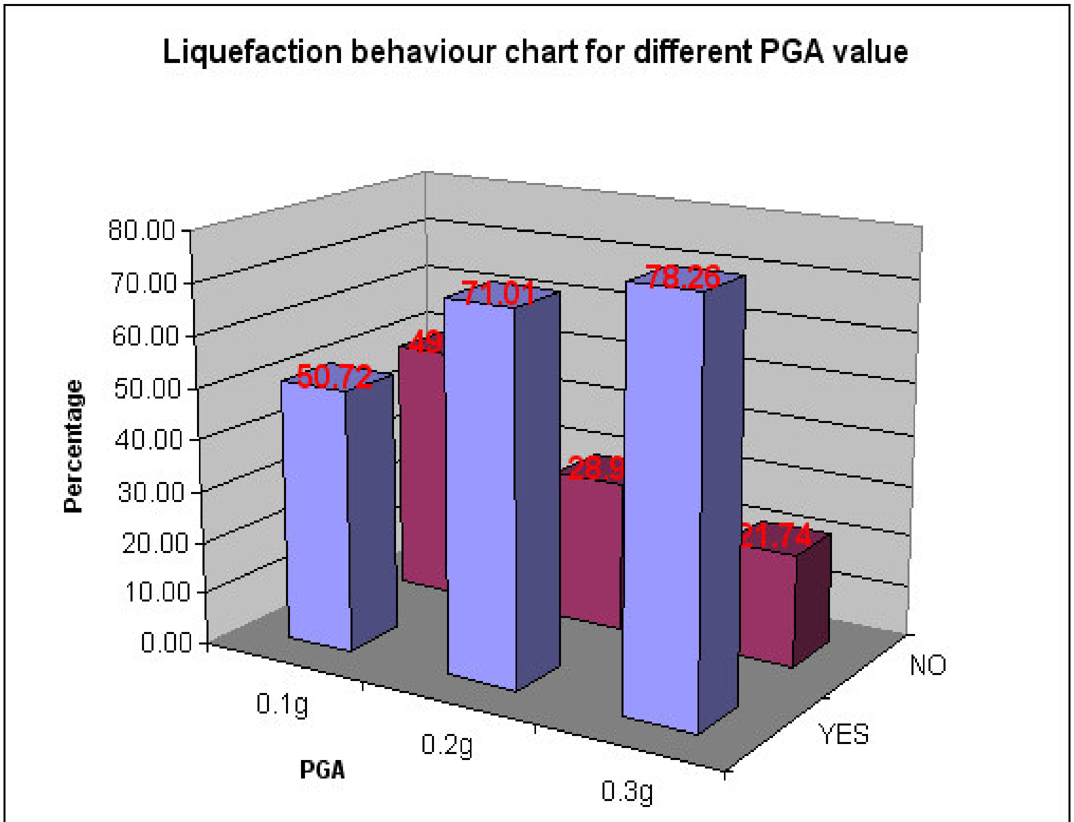

PGA	Yes	No	Total	%Yes	%No
0.1g	35	34	69	51	49
0.2g	49	20	69	71	29
0.3g	54	15	69	78	22

Figure 5.9: Graph showing liquefaction susceptibility behaviour for different PGA values using Seed and Idriss (1971) method.

Similarly, Destegul (2004) calculated PGA value for Lalitpur area, Nepal using information from some deep borehole logs of that region. She calculated PGA value for Lalitpur city (One of the main cities in Kathmandu valley) only between 0.52g to 1.42g for MMI of IX to X. She assumed earthquake hypocentral distance of 48 Km with magnitude of 8 Richter scale for this calculation. This value is even much higher than that of JICA (2002) and if this scenario earthquake is to be considered for liquefaction susceptibility analysis, then most part of the Kathmandu valley would be liquefied. Because the estimation of PGA values varies with different authors, a detail study is required to make precise determination of PGA value for different scenario earthquakes.

Table 5.5: MMI and PGA values as estimated by JICA (2002)

Earthquake Scenario	Modified Mercalli intensity (MMI)	PGA
Mid Nepal Earthquake	VIII	0.2g to 0.3g
North Bagmati Earthquake	VI to VII	<0.2g
KV Local earthquake	VII to VIII	0.3g along fault zone
1934 earthquake	VIII to IX	0.2g to 0.3g

The assessment of the liquefaction at any depth by Seed and Idriss (1971) method also involves comparison of the predicted cyclic stress ratio ($\frac{\tau_{av}}{\sigma_0}$) that would be induced by a given design earthquake (L) with the cyclic stress ratio required to induce liquefaction (R). The value of R is derived from the graph as shown in Figure 3.5 in Chapter 3. For this method, F_L is calculated for a given depth using equation 16. Liquefaction is judged to occur at that depth if F_L is less than or equal to 1. In this case

$$F_L = \frac{R}{L} = \frac{CRR}{CSR} \qquad (16)$$

The average cyclic stress ratio $\frac{\tau_{av}}{\sigma_0}$ induced by an earthquake is given by the expression (Seed and Idriss, 1971; Seed et al., 1983) as,

$$L = \frac{\tau_{av}}{\sigma'_0} = 0.65 \times \frac{a_{max}}{g} \times \frac{\sigma_0}{\sigma'_0} \times r_d \qquad (17)$$

Where σ'_0 is effective overburden pressure, σ_0 is total overburden pressure, a_{max} is estimated peak surface acceleration, g is acceleration due to gravity, r_d is reduction factor given by (1-0.015z) in which z is the depth of the ground surface in meters. The result by this method is also shown together with the previous result mentioned above. The method gives the same result as that of the previous one computed following the Seed and Idriss method (refer annex in CD for calculation procedures).

5.5. Comparison

5.5.1. Comparison of Qualitative and Quantitative methods

Both the qualitative and quantitative approaches for liquefaction susceptibility analysis were tested. 328 borehole samples were used for qualitative analysis and 68 samples (easily located in the map) were used for quantitative approach.

Table 5.6: Comparison of the results between qualitative analysis and quantitative analysis.

Hole _ID	Lique_class	Lique_Iwasaki	Hole _ID	Lique_class	Llique_Iwasaki
	Qualitative	Quantitative		Qualitative	Quantitative
C 1	High	Yes	C 13	Moderate	No
C 10	High	No	C 14	Moderate	No
C 15	High	No	C 16	Moderate	No
C 26	High	Yes	C 17	Moderate	No
C 29	High	Yes	C 27	Moderate	Yes
C 35	High	No	C 28	Moderate	Yes
C 38	High	No	C 37	Moderate	No
C 39	High	No	C 42	Moderate	Yes
C 41	High	Yes	C 44	Moderate	Yes
C 43	High	Yes	C 55	Moderate	Yes
C 45	High	No	C 286	Moderate	No
C 46	High	No	C 287	Moderate	Yes
C 47	High	No	C 288	Moderate	No
C 48	High	No	C 289	Moderate	No
C 52	High	Yes	C 290	Moderate	No
C 53	High	Yes	C 291	Moderate	Yes
C 54	High	Yes	C 292	Moderate	Yes
C 56	High	No	C 293	Moderate	Yes
C 57	High	No	C 294	Moderate	Yes
C 58	Moderate	Yes	C 295	Moderate	Yes
C 304	High	Yes	C 313	Moderate	No
C 305	High	Yes	C 314	Moderate	No
C 306	High	Yes	C 36	Low	No
C 310	High	Yes	C 320	Low	Yes
C 311	High	Yes	C 321	Low	Yes
C 312	High	Yes	C 322	Low	Yes
C 317	High	No	C 323	Low	Yes
C 318	High	Yes	C 324	Low	Yes
C 319	High	Yes	C 59	Very Low	No
C 6	Moderate	No	C 60	Very Low	No
C 7	Moderate	No	C 61	Very Low	No
C 9	Moderate	Yes	C 62	Very Low	Yes
C 11	Moderate	No	C 63	Very Low	No
C 12	Moderate	No	C 64	Very Low	No

(Note: Here in the table, “Yes” means liquefaction will occur and “No” means liquefaction will not occur at the particular earthquake scenario of 7.5 Magnitude and 0.1g PGA value).

Location map of boreholes and the result of the analysis is shown in Figure 5.5 A and B. The result obtained by both analysis are shown in Table 5.6. In qualitative analysis, four classes of liquefaction susceptibility zones are differentiated according to their score value as, high, moderate, low and very low. For certain places where rock exposure is very close to the site or at lower depth, it is classified as no liquefaction zone. On the other hand in quantitative analysis the result of the analysis is either liquefiable or not liquefiable as it was to be determined by a mathematical relation. The quantitative method of the analysis is carried out using a specific earthquake scenario and the relation for this purpose has been derived from experiments in the laboratory and verification in the field by different experts. Therefore the result obtained by this method is more accurate (reliable) than that of the qualitative one, and as such, the result obtained by this method can be directly implemented for development activities. On the other hand, the result obtained in qualitative analysis can be used to guide the possibility of occurrence of liquefaction in case of strong earthquake motion. Hence, if future development activities are to be carried out in the area where it is indicated by high susceptibility zone in a map, a specific site investigation will be necessary to carry out using quantitative analysis. From the Table 5.6, it is evident that although in some area it is indicated by high liquefaction susceptible zone, it does not indicate the possibility of liquefaction in quantitative analysis (for example in borehole C 10, C 15, C 35 etc.).

5.5.2. Comparison with 1934 Bihar-Nepal earthquake

The biggest earthquake in Kathmandu valley, which caused widespread destruction, occurred on 15 January 1934. Regarding the liquefaction phenomena at that time two different (opposing) views can be cited.

- Auden (1939), who visited the area after few weeks of the earthquake.
- Bramha Shamsher J.B.Rana (1935) who witnessed the events and the earthquake damages by himself.

According to Auden's view, the Kathmandu valley consisting of terraces bounded by steep cliffs with low ground water table did not suffer a lot from liquefaction, though he observed some sand vents near Harisiddhi village. On the other hand, Rana (1935) mentions the occurrence of widespread liquefaction within the valley. In the book entitled "Nepal Ko Mahabhukampa" (The great Earthquake of Nepal, 1935 AD) written by him, it is mentioned that, the Tundikhel (Military Parade ground in the centre of the city) was fissured heavily with the ejection of water (see Figure 1.8 and 1.9 in Chapter 1). The paddy field and road were also fissured heavily with ejection of water and most of the paddy fields were flooded (note that the time of the earthquake event was in the dry season without rain and harvesting was over). It is also mentioned that even at some places warm water with sand erupted from the fissures developed on the ground. Thus the two views contradict at this point about the liquefaction in Kathmandu valley. Here it is to be noted that, Auden visited the place after several weeks of earthquake events whereas Rana had witnessed the earthquake scene.

Auden and Ghosh (1935) prepared an intensity distribution map for Kathmandu valley for the earthquake of 1934 as shown in Figure 1.4, Chapter 1 (see also Figure 5.10 in this Chapter). He measured (MMI) intensities of 'VIII' to 'X' within the valley with maximum MMI of 'X' distributed along the South-East of the Kathmandu valley starting from Bungamati in the South to Bhaktapur in the East. According to the map, the major settlement areas that experienced the maximum MMI were Khokana, Bungamati, Sunakothi, Harisidhi, Katunje, Siddhipur, Lubhu, Godamchaur, and Bhaktapur (refer Figure 1.1 for name of places). Rana (1935) reports that about 99 % of the houses collapsed in these places. The centre part of the valley (the core area) and to the West of it towards Balambu and Thankot experienced an intensity of MMI 'IX'. The rest part of the valley experienced MMI of VIII. Thus the intensity distribution map shows that much of the destruction was taken place in and along the South-eastern part and in the central and western part of the valley. When this intensity distribution map is correlated with the destruction map of 1934 earthquake in the valley by Rana 1935 (Figure 1.3, Chapter 1), they show a high degree of agreement.

The main reason for the damage distribution pattern for the 1934 earthquake is not known yet but when we look at the subsurface sediments we find that, the area is underlain in some places by very thick unconsolidated sediments greater than 350 m (as evidence for example by borehole WHO8, B8, B6, and BHD2). Clay is dominating (more than 50%) in this region as shown in the boreholes of Figure 5.11. This would suggest that the principle factor that caused the main destruction in these places (especially in the southern part of the valley) during the 1934 earthquake might be due to the soil amplification rather than soil liquefaction. The distribution of clay in different boreholes lying within the maximum intensity zone of 1934 earthquake is shown in Table 5.7. At the same time in boreholes LD2 at Lubhu, B20 at Katunje, and BHD1, B6 at Bhaktapur consist of sand to silt at the top most layers within 10 m depth or more. This suggests that, those places might have suffered liquefaction in 1934 earthquake that was responsible for the cause of much of the destruction in those areas. However some scale of liquefaction is also reported in Harisidhi area both by Auden (1939) and Rana (1935). Both the intensity distribution map and damage map show that the destruction took place far greater in the areas underlain by thick deposit of unconsolidated sediments (Mainly Clays and silts) than the areas underlain by bedrocks and at least by coarse sand and gravel. This could be the reason that the southern part of the valley suffered more damage than in the northern part of the valley. For example, the town of Kirtipur located in the South-west of the valley suffered much less damage, as it was located on a bedrock hill.

Now, when we compare the Intensity distribution map of 1934 with the Liquefaction Susceptibility map prepared in this study (see Figure 5.10) we find that, the high intensity zone (MMI X) of Auden and Ghosh (1935) is distributed in low to very low liquefaction susceptibility classes. Whereas the Intensity zone MMI IX, is situated mainly in the high and moderate susceptible zone. Because, the intensity IX is distributed mainly in Kathmandu and Lalitpur city, we can say here that, in 1934 much of the destruction in Kathmandu and Lalitpur city might have taken place due to liquefaction phenomena. This fact is also supported by the report of Rana (1935) who had witnessed the scene and written in his book ("The great earthquake of Nepal"). On the other hand, in the southern part the destruction might have taken place due to amplification of the ground and weak construction of houses.

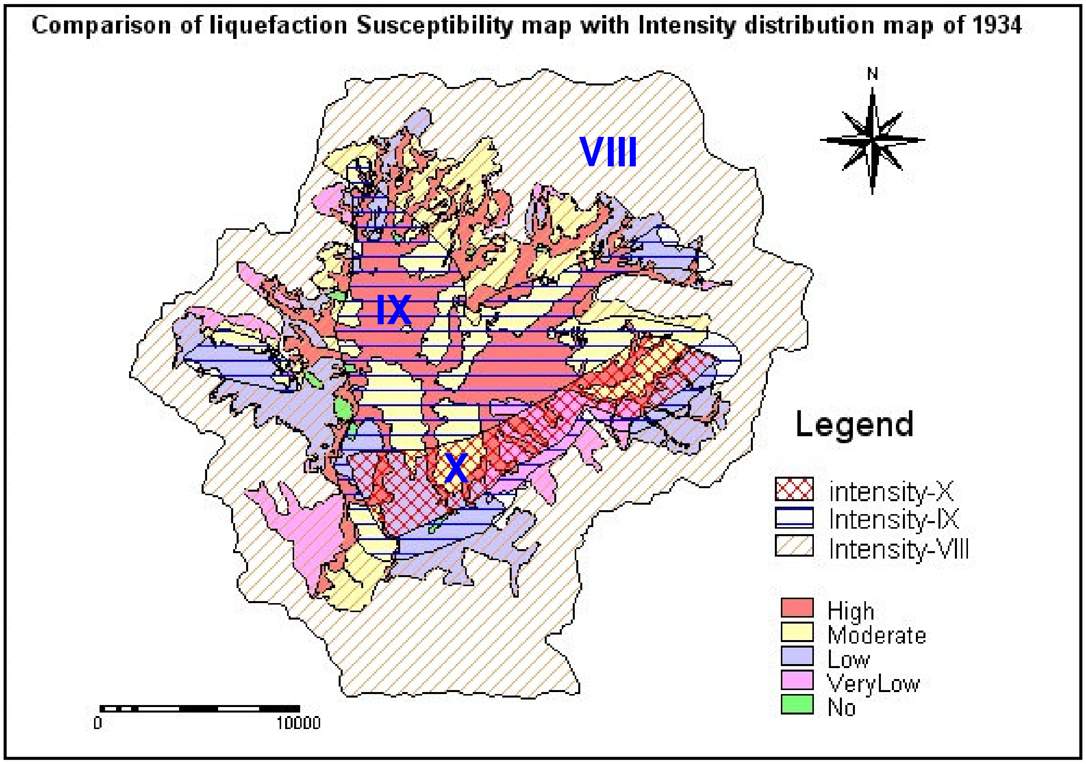

Figure 5.10: Comparison of Liquefaction Susceptibility map with Intensity distribution map of 1934.

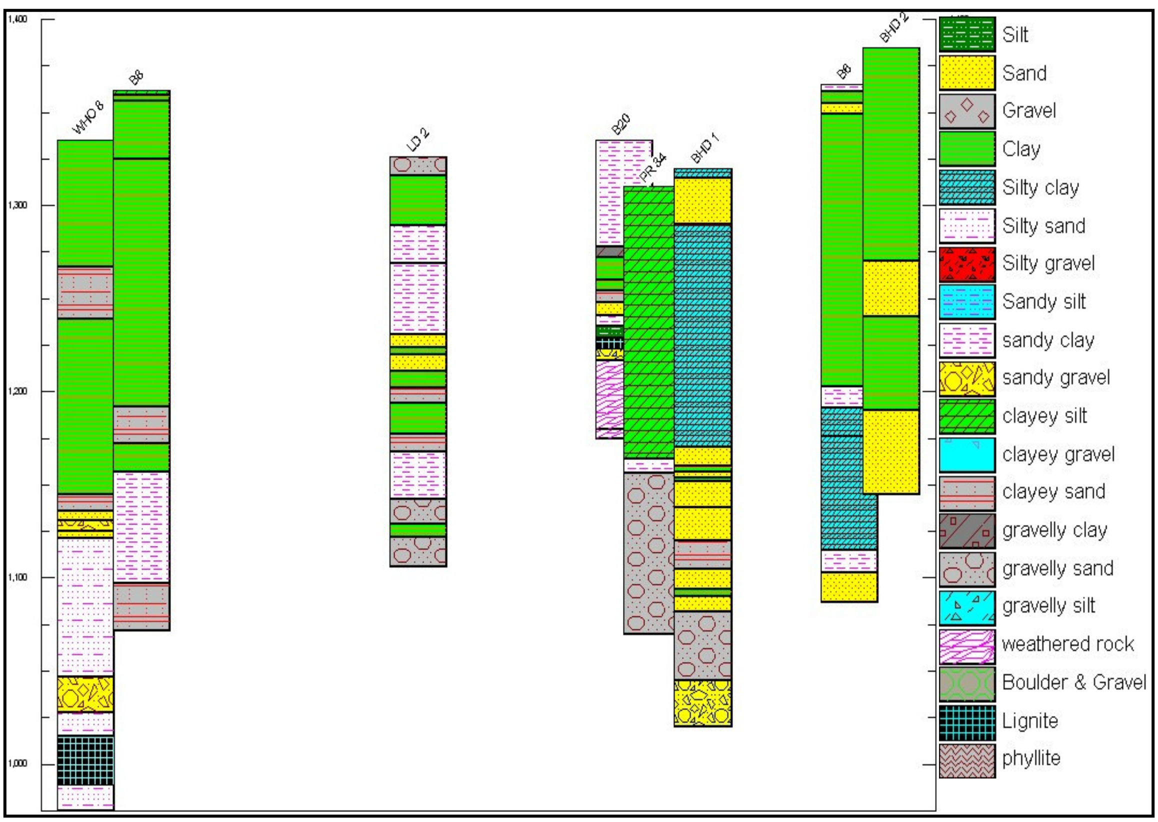

Figure 5.11: Borehole logs in high intensity zone of 1934 earthquake.

Table 5.7: Distribution of clays in boreholes that lies in the maximum intensity distribution Area of Auden & Ghosh (1935).

Borehole ID	Location	Total depth	Clay%	Others %
WHO8	Bungamati	360	55	45
B08	Sunakothi	290	85	15
B09	Lubhu	271	63	37
LD2	Lubhu	220	67	33
B20	Katunje	160	58	42
PR25	Katunje	150	40	60
PR34	Bhaktapur	240	64	46
PR19	Bhaktapur	261	48	52
PR18	Bhaktapur	253	70	30
BHD1	Bhaktapur Hospital	300	44	56
BKD2	Sipadol, Bhaktapur	150	88	12
B06	Bhaktapur	277	92	8
BHD2	Bansbari, Bhaktapur	240	68	32

5.5.3. Comparison of the JICA Liquefaction map (2001)

As part of their earthquake disaster mitigation study JICA (2002), prepared a liquefaction potential map for Kathmandu valley. They included some physical properties of soil, seismic motions and geological map of the valley for their liquefaction analysis. They did not mention about the number of soil samples included in this analysis. For the determination of seismic motion, they developed a model for four earthquake scenarios,

Based on their scenario earthquake models, they estimated PGA values and MMI classes for the valley. According to their mid Nepal earthquake scenario, Kathmandu valley would experience from 0.2g – 0.3g, with MMI 'VIII'. Similarly for their North Bagmati earthquake scenario, the whole valley would experience less than 0.2g with MMI 'VI' to 'VII'.

For the local earthquake scenario, the area along the fault would experience 0.3g (that would decrease with distance from the fault zone) with MMI 'VII' to 'VIII'.

Finally for 1934 earthquake, the valley would experience the largest PGA in which most part of the valley would experience 0.2g, the eastern part of the valley experience more than 0.3g and some parts still more than 0.4g with MMI from 'VIII' to 'IX'.

With this consideration, they prepared liquefaction potential map following Iwasaki et al. (1982) method with a consideration of high water table through out the valley as shown in Figures 3.8 and 3.9 in Chapter 3 and in Figure 5.12 in this Chapter.

These figures show that moderate potential is identified in some areas along the Bagmati river for Mid Nepal earthquake whereas most part of the valley is with low potential. Similarly for North Bagmati earthquake, they considered that no part of the valley would be liquefied.

For a local earthquake, they considered that only along the fault zone there would be some high potential with some grid cells indicating moderate liquefaction hazard along the Bagmati River. Similarly for the 1934-earthquake scenario only moderate potential is identified in some areas along Bagmati River, and at one small grid cell to the East is shown with high liquefaction potential.

Thus the team identified mostly low liquefaction susceptible areas for Kathmandu valley as a whole for all types of scenario earthquake, which does not seem to correlate well with the description of Rana, (1935) on the 1934 liquefaction phenomena. As such the map made by JICA (2002) does not seem to offer reasonable result. The liquefaction map prepared by JICA when compared with the map prepared in this study (see Figure 5.12 A), also seems completely different. In the map of JICA, it has shown moderate liquefaction susceptible areas only in some places along the Bagmati river courses and in other places it has shown by low to very low susceptible areas.

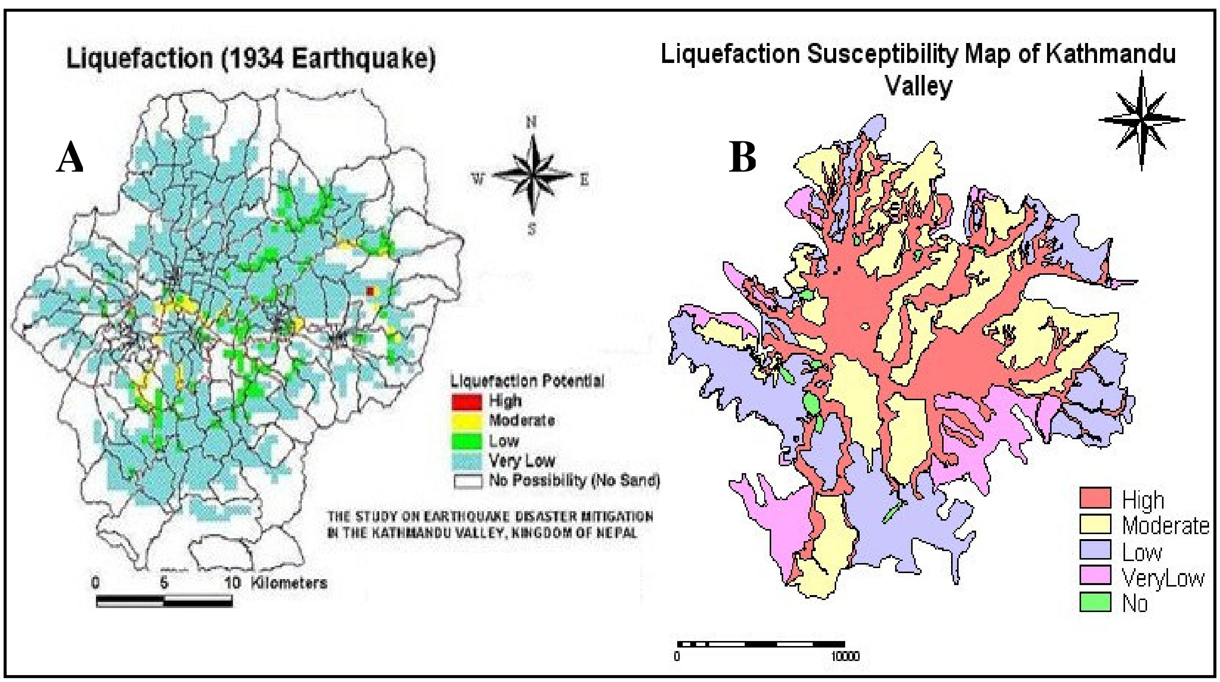

Figure 5.12: Comparison between JICA (2002) map and map prepared in this study.

On the other hand, in liquefaction susceptibility map prepared in this study (Figure 5.12 B), high liquefaction susceptible areas can be observed in most of the places, especially in the core of the Kathmandu city, along the flood plains and in the eastern part of the valley.

5.5.4. Comparison with UNDP/UNCHS Liquefaction map (1994)

As mentioned earlier a liquefaction map was also prepared by the UNDP/UNCHS/Habitat project for Seismic hazard and Risk assessment for Nepal in 1994. This map was made following the methodology of Juang and Elton (1991) based on a scoring system. The scoring system used by the project was also used in this research. Along with the scoring system, they also incorporated the surface geological mapping prepared by them for analysis, where they used lithological information from 123 borehole logs (UNDP/UNCHS report 1994). During the scoring of the parameters, sediments type like stiff clays or cobbly coarse gravels, which were unlikely to liquefy, were excluded. In this research, those sediments are scored with minimum values in order to show the place as very low potential areas. The liquefaction map prepared by UNDP/UNCHS and the map prepared in this study is shown in Figure 5.13.

According to the map of UNDP about 25 percent of the total study area is covered by high susceptible zone, about 11 percent by low, 35 percent by moderate and 29 percent by very low susceptible zone. The place where liquefaction is not possible, occupies about 1 percent. One notable point in this map is that, the airport area is defined as low liquefaction susceptible area by them, though the material contained in this area is liquefiable, the only thing is that the water table in this area is greater than 10 m. Because of this reason they might have classified it as low susceptible area. On the other hand when, the soil samples of the same area is analysed in this study using both qualitative and quantitative method, the qualitative method resulted moderate susceptible zone to this area whereas in the quantitative method using both Iwasaki et al. (1984) and Seed and Idriss (1971), it came up with the result of no liquefiable zone. However in this study, the result as obtained from qualitative analysis is followed and designated the area as moderate susceptible zone.

The comparison of the two maps UNDP and the one prepared in this study is shown in Figure 5.13. Both the maps were crossed with borehole-classified map (considered as ground truth sample) and confusion matrix was prepared (see Table 5.8 and 5.9). It was found that 52 of the boreholes were correctly classified as high in classified map of UNDP/UNCHS. Similarly 44 of the borehole samples were correctly classified as moderate, 3 as low and 6 as very low. The rest of the samples were evidently in the wrong zones. Overall accuracy in this case is calculated as 0.38 (38 %). On the other hand, 65 of the boreholes were correctly classified as high in classified map prepared in this study, 51 of the boreholes were classified correctly as moderate, 11 as low and 2 of them as very low. The rest of the samples containing in wrong zones and the overall accuracy in this case is 0.46 (46 %). A chart indicating the percentage of the area covered by different susceptible classes for UNDP map and map prepared in this study is shown in Figure 5.14.

The maps were also compared with the borehole results that were analysed quantitatively using Iwasaki method (1984). Out of 87 samples, 68 of them could be located in the map as mentioned before. For the rest (19 of them), the location could not be ascertained with precaution and as such, were not considered in this study. For the map prepared in this study however, out of 68 samples, 24 of the boreholes with liquefaction possibility matched with the high susceptible class of the map, and 14 of them matched with moderate susceptibility class. On the other hand, 6 of the boreholes with no liquefaction possibility came to lie within high susceptible class and 16 of them in moderate susceptible class (see Table 5.10). Similar type of comparison was also made between the UNDP classified map and the quantitatively analysed borehole map. The result showed that, out of 68 samples 19 of the boreholes with liquefaction possibility were laying on high susceptible class zone, the other 19 on moderate susceptible class zone and 1 in low susceptible zone. On the other hand 5 of the boreholes with no liquefaction possibility came to lie in high susceptible zone, 21 in moderate and 3 in low susceptible zone (see Table 5.11).

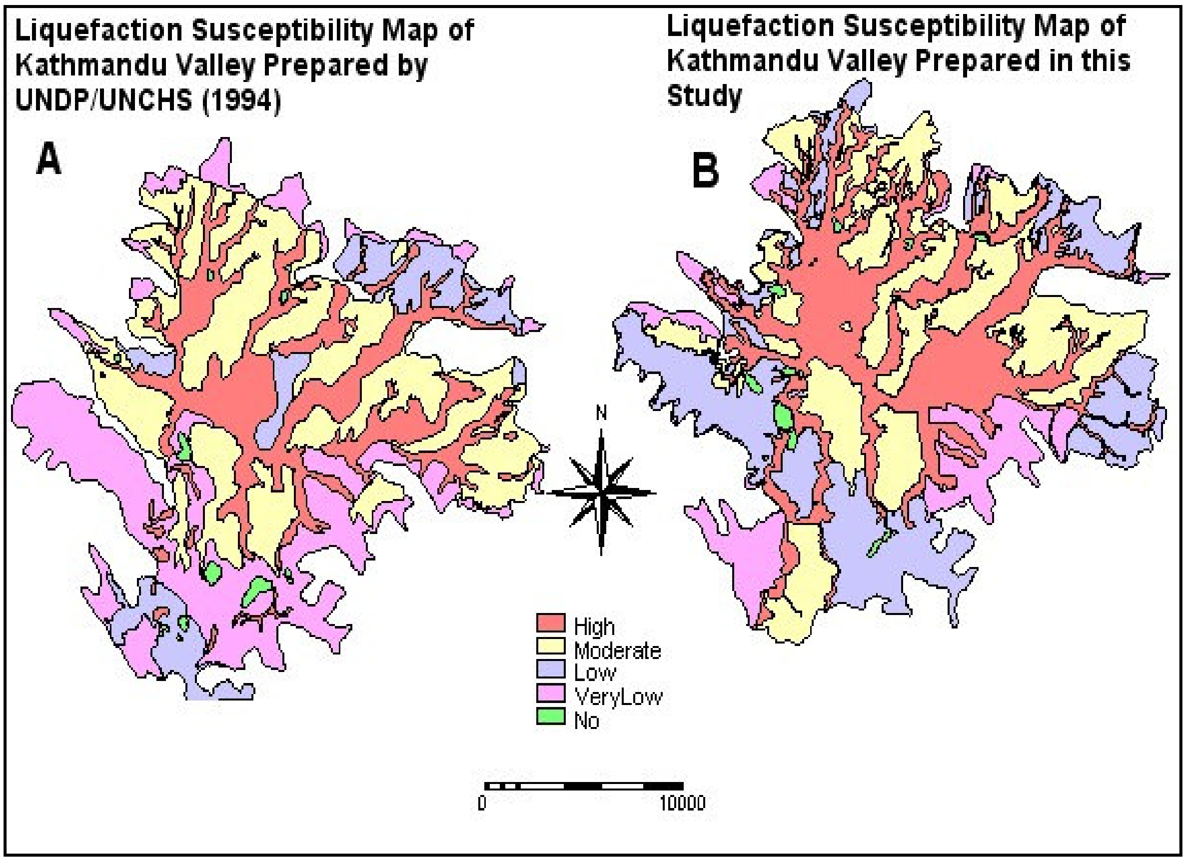

Figure 5.13 Liquefaction Susceptibility map Comparison between UNDP/UNCHS (1994) and map prepared in this study.

Table: 5.8 Confusion matrix between classified polygon map Figure 5.13A, UNDP (1994) and classified borehole point map.

Sum of Npix	Liquetype				
Lique_Class	High	Moderate	Low	VeryLow	Totals
High	52	30	4	4	90
Moderate	49	44	13	6	112
Low	19	20	3	9	51
Very Low	1	14	0	6	21
Grand Total	121	108	20	25	274
Overall accuracy=correctly classified pixels (sum of diagonal values)/total samples					
Correctly classified pixels	105				
Overall accuracy	0.383212				

Table: 5.9 Confusion matrix between classified polygon map Figure 5.13B (prepared in this study) and classified borehole point map.

Sum of NPIX	LIQUE_FACTI Polygon Map					
LIQUE_CLASS (Point map)	High	Moderate	Low	Very Low	No	Grand Total
High	65	27	2	0	0	94
Moderate	55	51	8	2	0	53
Low	16	22	11	3	1	116
Very Low	8	5	2	2	2	19
Grand Total	144	105	23	7	3	282
Overall accuracy = correctly classified pixels (sum of diagonal values)/total samples						
Correctly classified pixels	129					
Overall accuracy	0.462366					

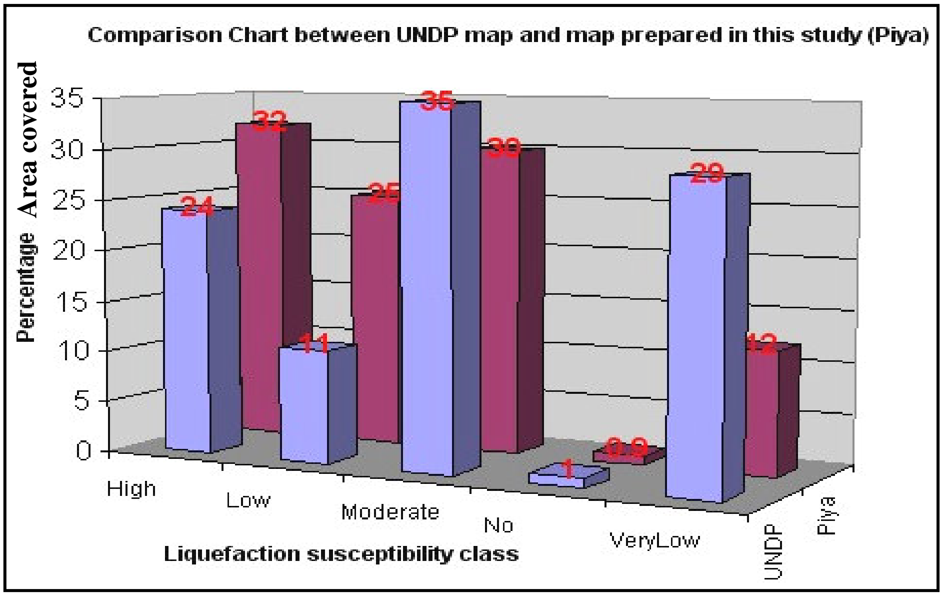

Figure 5.14: A chart showing the area covered by susceptible classes in UNDP map and map prepared in this study.

Table 5.10: Cross table between quantitatively analysed borehole map and classified map in this study.

	High	Moderate	Low	Very Low	No	Total
Yes	24	14	0	0	0	38
No	6	16	0	0	5	27
Grand total						65

(Note: Three of the samples lying outside the study area boundary)

Table 5.11: Cross table between quantitatively analysed borehole map and classified map (UNDP).

	High	Moderate	Low	Very Low	No	Total
Yes	19	19	1	0	0	39
No	5	21	3	0	0	29
Grand total						68

6. Conclusions and Recommendations

6.1. Conclusions

The main objective of the research was to generate geological database for the preparation of liquefaction Susceptibility map. For this purpose 185 deep and 328 shallow borehole logs data were collected. The deep borehole records were used to generate layer models, lithological cross sections and fence diagram, and the shallow boreholes were used for the liquefaction susceptibility analysis. The software used for this purpose were, Microsoft excel 2000, Microsoft Access, Rockworks99, ILWIS3.2.

Although the database generation is a tedious and difficult work, the GIS database resulting from it is very crucial for obtaining a better understanding of the subsurface conditions of Kathmandu valley, and the modeling of various geo-environmental aspects, such as seismic amplification, liquefaction, groundwater fluctuation, underground infrastructure planning etc.

The database, which was constructed gives the general lithological information of the various wells drilled within the valley along with some geotechnical information carried out for shallow boreholes. From the analysis of the borehole data it is found that a maximum of 5 different layers of lake deposits with a thickness greater than 10 m were found in Kathmandu valley (as evidenced by boreholes DMG6 at Bhrikutimandap and DMG12 at Tikathali Lalitpur). The greatest thickness of clay deposit (304 m) is found in well B1 at Harisiddhi.

A large part of Kathmandu valley is underlain by a sequence of thick lacustrine sediments mainly composed of black clay, locally called Kalimati Formation in the central and southern part of the valley. It is a deposit of the Paleo-Kathmandu Lake, which was formed during the last 2.5 million years, overlaying sediments that are composed of coarse sand and gravel of varying thickness formed by the so-called Proto-Bagmati River system. The northern part of the valley is dominated by medium to coarse-grained micaceous sand mixed with gravel.

From the literature survey and from the lithological information obtained from the borehole records it can be concluded that the main source of the sediments for the basin sediments are the surrounding hills. In the North and to the central part of the valley, the sediments were derived from the Shivapuri hills consisting of intrusive rocks of gneiss and granites, and in the southern part the sediments were derived from Phulchauki and Chandragiri hills consisting of meta-sediments such as limestone, schists, slates, phyllites and marbles etc. Sedimentation process within the basin has taken place through series of stages. In this study, so far nine stages of sediment deposition have been differentiated based on the deepest borehole that exist in the central part of the valley and has reached up to the bedrock.

From the analysis of borehole database, the following levels have been differentiated in Kathmandu valley.

Table 6.1: Table defining different levels of the sediments in Kathmandu Valley.

Stages	Profile	Sedimentary environment	Formation	Age range	Grouping used in the layer modeling
9	Sand and silt	Alluvial	Patan fm.	< 29,000 years BP.	Post-lake deposit
8	Clay	Shallow lake	Kalimati fm.	2.5 million years to 29,000 years BP.	Lake deposits
7	Medium to coarse sand	Fluvio-deltaic	Kalimati fm.		Lake deposits
6	Clay	Deep lake	Kalimati fm.		Lake deposits
5	Sand with gravel	Fluvio-deltaic	Kalimati fm.		Lake deposits
4	Clay	Shallow lake	Kalimati fm.		Lake deposits
3	Medium to coarse sand	Fluvio-deltaic	Kalimati fm.		Lake deposits
2	Clay	Shallow lake	Kalimati fm.		Lake deposits
1	Gravel and Sand	Protobagmati (Alluvial)	Bagmati fm.	>2.5 million years	Pre-lake deposits
Bedrock					

The ancient drainage system and the basin topography played a major role in the sedimentation process. In order to be able to carry out a GIS layer modeling for the entire valley the complex sequence of unconsolidated sediments (Fluvio-lacustrine deposit) has been simplified and classified into only three distinct layers: Pre-Lake deposit, Lake deposit, and Post Lake deposit. Each layer is of varying thickness. The layer "Pre-Lake deposit" represents the sediment deposited by fluvial activity prior to the origin of the lake. The layer named as "Lake deposits" represents black clay deposit, which is abundantly distributed in the central part of the valley (also called as "Kalimati" in local language). These layers have been used in the subsequent analysis of seismic response modeling (Destegul, 2004) and liquefaction susceptibility analysis (this study).

The evidence of neotectonic activity within the valley could not be confirmed on the basis of the borehole records due to large lateral variation of the sediments. Therefore, often borehole records of nearby sites were quite different. However, this does not exclude the existence of active faults in the valley as mentioned by previous authors who indicate the presence of neotectonic activity within the valley based on soil outcrops. In the layer modeling local displacements due to faulting therefore could not be included.

Kathmandu valley lies in an active seismic zone, which has had historical earthquakes greater than 7 Richter scale and local intensities of IX and X. Hence, the important criteria for liquefaction susceptible areas such as strong earthquake motion, shallow groundwater table, liquefiable soils (Holocene deposits) are all met in Kathmandu valley. There is also evidence of liquefaction occurrences in some parts of Kathmandu valley as a result of the 1934 Bihar-Nepal earthquake. The liquefaction study carried out by previous workers also indicated the existence of large area with high liquefaction susceptibility within the valley.

Both quantitative and qualitative analysis methods of liquefaction susceptibility in the Kathmandu valley were carried out. Quantitative analysis was carried out following the Seed and Idriss (1971) and Iwasaki et al. (1984) methods for 87 borehole samples collected from 31 different sites. It was found that 37 of the holes were subjected to liquefaction for an earthquake of 7.5-magnitude scale with a PGA value of 0.1g.

The qualitative analysis of liquefaction susceptibility following the Juang and Elton (1991) method on the other hand showed nearly 32 percent of the Kathmandu valley is classified as high liquefaction susceptibility area, 30 percent as moderate, 25 percent as low and 12 percent of the area as very low liquefaction susceptibility area. Nearly one percent of the area is occupied by rock outcrops and hence will have no liquefaction.

Peak ground acceleration value (PGA) is an important factor to trigger liquefaction phenomena during an earthquake. PGA values for Kathmandu valley have been estimated by JICA (2002) based on an earthquake scenario model that varies from 0.2g to 0.3g for 1934 earthquake, whereas it is taken as 0.1g for the characterization of the earthquake zone of V according to the Indian standard IS 1093-1934.

The quantitative geotechnical analysis of the data gives a more realistic picture of the borehole site than the qualitative analysis over larger areas. However, the availability of the geotechnical data required to do such a quantitative analysis is limited, and it is costly to collect such data over large areas.

Therefore, often a qualitative analysis is the only option. The methodology adopted in this study is considered to be suitable, if enough borehole data is available to corroborate the results. However the results obtained by following the qualitative procedure are not intended to be used as a precise tool for the detailed zoning for development planning of the urban areas. The output obtained by such a methodology just alerts the users for the possible areas of liquefaction. A more detail investigation with comprehensive merging of geologic, geotechnical and seismological data will be required to carry out precise liquefaction susceptibility mapping for each major development activities.

One of the major drawbacks of both the qualitative and quantitative methods for liquefaction susceptibility mapping is the difficulty to translate the resulting classification into quantifiable terms that can be used for the actual loss estimation of buildings, infrastructure and population. Both methods indicate high, moderate or low susceptibility but do not indicate how much of percentage of the area is likely to experience liquefaction phenomena, and in with which intensity.

The intensity distribution pattern for the 1934 earthquake in Kathmandu valley was prepared by Auden and Ghosh (1935), which has a good correlation with the damage map prepared by Rana (1935). The borehole logs located in this zone show that the zone is underlain by a very thick sequence of unconsolidated sediments mainly consisting black clay deposits, especially in the southern part of the valley. This black clay also appears close to the surface. In such conditions, soil amplification will be strong during a major earthquake. This reveals that the intense damage in that region (Southern part) might have been caused due to soil amplification, as these areas do not show high liquefaction susceptibility. On the other hand, the distribution of borehole logs in the eastern part of the valley such as in the Katunje and Bhaktapur area indicate the presence of sand and silt in the upper 10 meters and the presence of a high ground water table. Hence, in such conditions liquefaction phenomenon might occur. This observation suggests that to the South-eastern part, the damages in 1934 earthquake might have caused by liquefaction phenomena.

6.2. Applicability of the Geological database and the liquefaction susceptibility map

Besides its use in seismic risk assessment the subsurface geological database is applicable in various other fields of studies, such as in quaternary geology, neotectonics, hydrogeology, chemistry, mining, seismology, and environmental analysis.

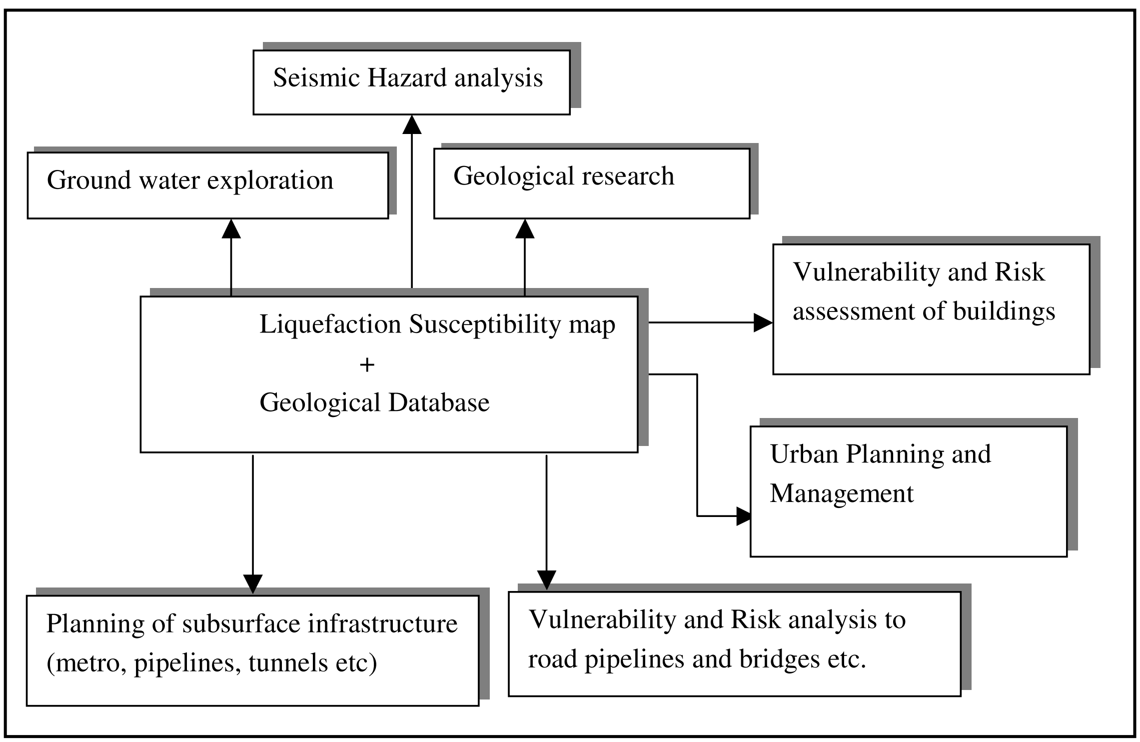

Figure 6.1: A flow chart showing the applicability of the geological database and Liquefaction Susceptibility map.

The liquefaction hazard map can be used by structural and geotechnical engineers to identify in advance areas where liquefaction potential exists especially during the designing of new and retrofitting existing facilities. Such an endeavor might minimize the risk of damage to buildings and other infrastructure due to liquefaction and allow proper design of remedial measures by local authorities during town planning and the establishment of industrial areas. The liquefaction susceptibility map can be used as a planning tool to indicate whether site-specific investigations for liquefaction susceptibility are warranted. The flowcharts given in Figures 6.1 and 6.2 indicate the applicability of the geological database and the liquefaction susceptibility map with various other fields.

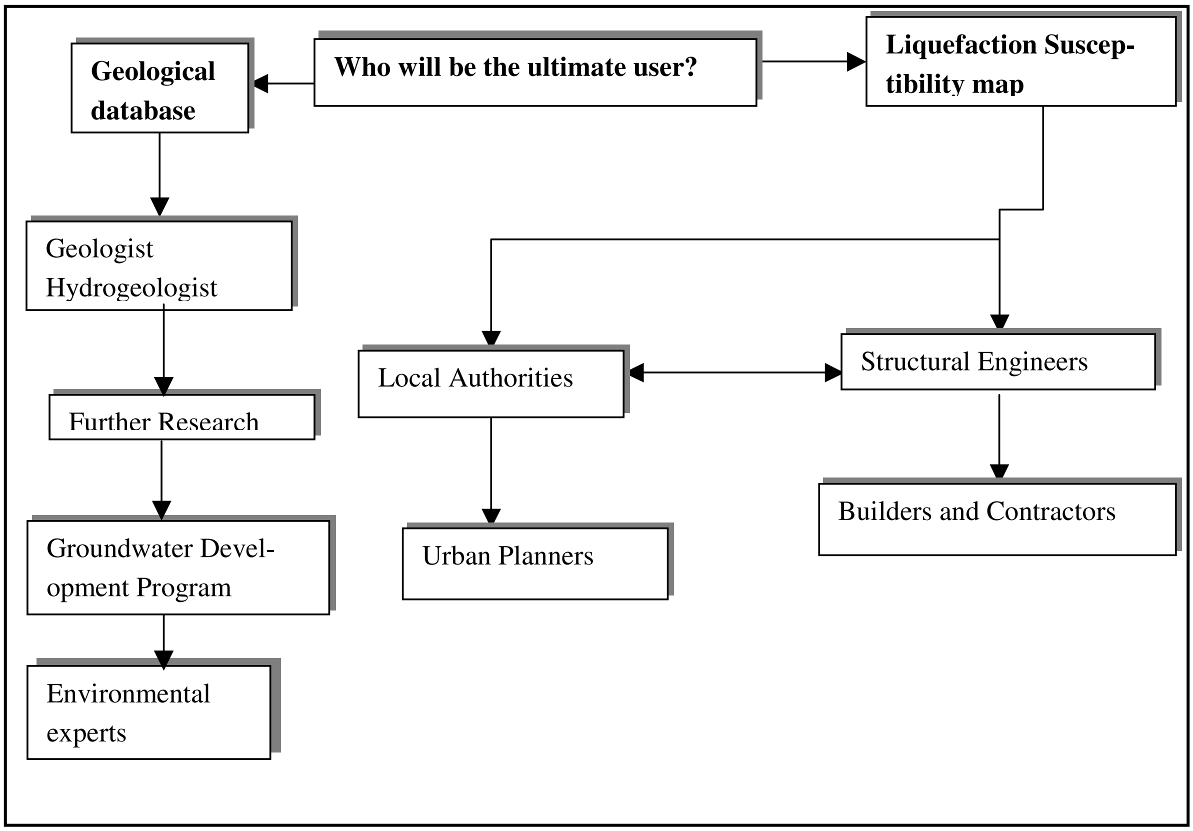

Figure 6.2: A flow chart showing the ultimate users of the geological database and Liquefaction susceptibility map.

6.3. Recommendations

Layer models for individual lake deposit could be developed if a larger number of boreholes with bedrock information were available. Hence, it is required to collect more borehole data. Government offices and private companies should be cooperative for data distribution for any type of research purpose so that the output is beneficial for all.

More deep boreholes are recommended to be made especially in the Eastern and Western side of the Manahara well field, and in the South of the study area where gaps in borehole information are noticeable. Many of the existing wells do not give adequate information about the extension of the lake deposit and bedrock topography.

It is important to carry out deep geophysical investigations in the unconsolidated sediments of Kathmandu valley, in order to obtain a better idea of the subsurface configuration, and especially on the possible fault displacements of these sediments, which could not be proven by evaluation of the borehole records, but are expected to be present.

The liquefaction susceptibility map prepared in this study is an initial attempt for the zonation of liquefaction susceptibility in the study area. The map has been basically prepared by photo interpretation (Geomorphological map) of the area and quantitative and qualitative analysis of some borehole samples. No fieldwork has been made during this study to validate this map. Future investigation must link the outcome of this research with field data. Moreover, more data regarding the geotechnical properties of the main types of materials, and their spatial variation need to be collected to carry out analysis quantitatively, so that more precise zonation of liquefaction possible areas could be made.

The photo interpretation has been made using a stereo pair formed by imageries covering only a part of the Kathmandu valley and a Digital Elevation Model created from contour lines with a fairly large interval (100m in the hillside and 20m in the valley). Hence a complete imagery covering the whole area of Kathmandu and a DEM based on the available large scale topographic map with contour interval of 2 m is required to develop a better stereo pair and thereafter to prepare a better Geomorphological map.

The borehole database prepared in this study should be updated to include new borehole data each time when new boreholes will become available.

This borehole database needs to be maintained by an organisation that has sufficient geological expertise such as the Department of Mines and Geology, and it should be made in such a way that the database can be shared by all interested organisations in the country.

References:

ABAG (2001). Bay area Liquefaction Hazard, The REAL Dirt on Liquefaction. (http://www.abag.ca.gov/bayarea/eqmaps/liquefac/liquefac.html, date of access: 30.10.2003)

ABAG (2001). Collection and analysis of Liquefaction data from the Northridge and Loma Prieta Earthquakes, Appendix C. (http://www.abag.ca.gov/bayarea/eqmaps/liquefac/Lq_techC.PDF, date of access: 30.10. 2003)

Auden, J.B. (1939). The Bihar-Nepal earthquake of 1934, Section D, Nepal, Geol.Surv. India Mem73.

Auden, J. B., and Ghosh, A.M.N. (1935). About the earthquake of first January (1934), Shock at Kathmandu valley, Rec. Geol. Surv. India, v. LXVIII, pt. 2.

Avandano, J. E. (2004). Route optimization for hazardous materials transport, M.Sc thesis, International Institute for Geo-Information Science and Earth Observation (ITC), Enschede.

Bilham, R., Gaur, V.K. and Molnar, P. (2001). Himalayan Seismic Hazard, Science, vol. 293.

Binnie and Partners, 1973. Master Plan for the water Supply and Sewerage of Greater Kathmandu and Bhaktapur. World Health Organization Programme, Nepal

Bonham-Carter, G. F. (1994). Geographic Information Systems for Geoscientists: Modelling with GIS, vol. 13 of computer methods in the geosciences. Pergamon, Kidlington U.K.

Bothara, J. K; Guragain, R., Dixit, A. (2001). Protection of Educational Buildings against Earthquakes: A manual for designers and builders. National Society for Earthquake Technology, Nepal. Book Publication series, Kathmandu.

Broughton, A.T., Van. Arsdale R.B., Broughton J.H. (2001). Liquefaction susceptibility mapping in the city of Memphis and Shelby county, Tennessee, Engineering Geology 62 (2001) 207-222, (Elsvier science direct publ.).

CBS (Central Bureau of Statistics), (2001). Statistical yearbook of Nepal, HMG, Nepal, 8th edition, Kanchan printing press, Kathmandu

Craig, R.F. (1986). Soil Mechanics (4th edition). Van Nostrand Reinhold co.ltd. (UK).

Criscionei, J. J., Werle, J. L., Slemmons, D. B., Luke, B. A. (2000). Lequefaction hazard map of the Las Vegas Valley, Nevada. (http://www.nbmg.unr.edu/nesc/lhlasvegas.pdf, date of access: 30.10. 2003)

DMG (1998). Engineering and Environmental Geology Map of the Kathmandu Valley. Department of Mines and Geology, Kathmandu (Nepal).

Destegul, U. (2004). Sensitivity analysis of Soil site Response Modelling in Seismic microzonation for Lalitpur, Nepal, M.Sc thesis, International Institute for Geo-Information Science and Earth Observation (ITC), Enschede.

Dhakal, Y.P. (2002). Study of P- & S – waves and N values in soft sediments of Katmhmandu valley for their correlation and Engineering significance, M.Sc. thesis, Tribhuwan University, Nepal.

Dill, H. G., Kharel, B. D., Singh, V.K., Piya, B., Busch, K., Geyh, M. (2001). Sedimentology and paleogeographic evolution of the intermontane Kathmandu basin, Nepal, during the Pliocene and Quaternary, Implications for formation of deposits of economic interest, Jour. of Asian Earth Sciences, v 19, issue 6. pp. 777-804.

Dixit, A. M., Dwelley, L., Nakarmi, M., Basnet, S., Pradhananga, S.B., Tucker, B. (1999). Earthquake Scenario-An effective tool for development Planning, A case study-Kathmandu valley

Earthquake Risk Management project, bull. Nepal Geol. Soc. v. 16, p 51.

Dongol, G. M. S. 1985. Geology of the Kathmandu fluvial lacustrine sediments in the light of new vertibrate fossil occurrences. Jour. Nepal. Geol. Soc., v.3, pp. 43-57.

Dongol, G. M. S. 1987. The stratigraphic significance of vertibrate fossils from the Quaternary deposits of the Kathmandu basin, Nepal. Newsl. Stratigr, v. 18, pp. 21-29.

ENPHO (Environment and Public Health Organization), (1999). Monitoring of groundwater quality in the Kathmandu valley Nepal, a report submitted to Ministry of population and Environment, HMG Nepal.

Fernandez, V.B. (1997). Evaluation of ground response spectra using a 3D GIS based model for soil deposits, a case study in Medelin, Columbia, M.Sc thesis, International Institute for Geo-Information Science and Earth Observation (ITC), Enschede.

Furusawa, W. Iwakuma, S., Nakayama, H., Imaizumi, S. (1990). Database system of boring logs and its application to drawing a geological profile, 6th international IAEG Congress, Balkema, Rotterdam, pp 39-45.

Gautam, P. Hosoi, A., Sakai, T., Arita, K. (2001). Magnetostratigraphic evidence for the occurrence of pre-Brunes (>780kyr) sediments in the north-western part of the Kathmandu valley, Nepal. Jour. Nepal geol. Soc., v 25 (sp. Issue), pp. 99-109.

Gibbs, H. J. and Holtz, W. G. (1957): 'Research on Determining the Density of sands by spoon Penetration Testing', Proceeding 4rth international Conference SMFE, London, Vol. 1, Butter worths.

Guragain. J. (2004). GIS Applicability for seismic vulnerability and risk assessment of existing building system, a case study from Lalitpur Sub-Metropolitan City area, Kathmandu Nepal. M.Sc thesis, International Institute for Geo-Information Science and Earth Observation (ITC) Enschede.

Hazus99-SR2, tech. manual, Potential Earth Science Hazard (PESH), Seismic Hazard Assessment Chapter 4.

Hagen, T. 1968. Report on the geological survey of Nepal. v.1.Denkscher, Schweiz. Naturf. Gesell., 86, Hf1. 185 p.

Houlding, S. (1994). 3D geoscience modelling, computer techniques for geological characterization, Ed. Springer-Verlag, Hong Kong.

Holzer, T. L., Bennett, M. J., Noce T. E., Padovani, A. C., and John, C. (2002). Liquefaction Hazard and Shaking Amplification Maps of Alameda, Berkeley, Emeryville, Oakland, and Piedmont, California: A Digital Database.
(http://geopubs.wr.usgs.gov/open-file/of02-296/of02-296_1.pdf, date of access: 30.10.2003)

Ishihara K. (1984). Post Earthquake Failure of a tailing dam due to liquefaction of the pond deposit, Proceeding International conference on case histories in Geotechnical Engineering, University of Missouri, St. Louis, Vol. 3, pp. 1129-1143.

Ishihara K. (1985). Stability of natural deposits during earthquakes s, Proceeding, 11th International Conference on Soil Mechanics and Foundation Engineering, vol.1, pp. 321-376.

Ishihara K. (1993). Liquefaction and flow failure during earthquakes, Geotechnique, 43 (3): 351-415.

Iwasaki, T., Tokida K., Tatsuoka., F. Watanabe, S., Yasuda, S., and Sato, H. (1982). Microzonation for soil liquefaction potential using simplified methods, 3rd Intl. Microzonation Conf. proceeding, 1939-1329.

Iwasaki, T., Tokida K., Arakawa T. (1984). Simplified procedures for assessing Soil liquefaction during earthquakes, Soil dynamics and Earthquake Engineering, 1984, vol 3, no. 1, pp. 49-58.

Japan International Cooperation agency (JICA), (1990). Groundwater Management Project in the Kathmandu Valley, Final Report, main Report.

Japan International Cooperation agency (JICA), (2002). The study on Earthquake Disaster Mitigation in the Kathmandu valley Kingdom of Nepal.- Final report, Vol - I, II, III & IV.

John N. L (1996). Earthquake Effects. (http://www.seismo.unr.edu/ftp/pub/louie/class/100/effects-kobe.html, date of access: 30.10.2003)

Juang, C. H., and Elton, D.J., 1991, Use of fuzzy sets for liquefaction susceptibility zonation, in Proc. Fourth Intl. Conf. on Seismic Zonation, v. II, Standford Univ., USA. Earthquake Engineering Research Institute, P. 629-636.

Karmacharya, S. L., and Shrestha, O., (1995). Engineering and Environmental Geological mapping of Central Part of Kathmandu Valley, Internal report, Department of Mines and Geology, HMG Nepal.

Karmacharya, S.L., and Shrestha, O. M. (1995). Report on Engineering and Environmental Geological mapping of central part of Kathmandu valley, Dept of Mines and Geology (DMG), HMG of Nepal, Unpublished report, 11p.

Kayabali. K. (1996). Soil Liquefaction evaluation using shear wave velocity, Jour. Engineering Geology, v 44 (1996), 121-127.

Kelson K.I., Hitchcock, C. S., and Randolph C. E. (1999). Final Tech. Report, Liquefaction Susceptibility in the Inner Rio Grande Valley near Albuquerque, New Mexico. (http://www.lettis.com/pdf/albuquerque/AlbuquerFTR.pdf, date of access: 3.11.2003)

Kharel, B.D., Piya. B., Singh, V.K., Shrestha, N.R., Khadka, M.S., Bhandari. R., and Muenstermann, D. (1998), Final Report, Hydrogeological Conditions and Potential Barrier Sediments in Kathmandu valley, Nepal.

Koirala, A., Shrestha, O. M., and Karmacharya, R. (1993). Engineering geology of the southern part of Kathmandu Valley, Jour. Nepal Geol. Soc., v. 3 (Sp. Issue), pp. 151-159.

Kramer, S.L., (1996). Geotechnical Earthquake Engineering, University of Washington, Prentice-hall, International series in Civil Engineering Mechanics, pp. 209-211 and 349-417.

Liao, S.S.C., and Whitman, R. V. (1986). Overburden correction factor for SPT in sand, Jour. of Geo technical Engineering, ASCE, v. 112, no. 3, pp. 373-377.

Maurenbrecher, P.M (M.Sc, Outer, A. den (ir) and EM. Prof. D. G. (1998). Foundation Engineering, Chapter 4, Lecture series, 6th edition v.1, pp. 57-71 TU Delft

Maugeri, M., Faccioli, E., Geotchnical Zonation of the Catania Soils and Evaluation of the Liquefaction Hazard. (http://gndt.ingv.it/Pubblicazioni/Faccioli/pdf2.pdf, date of access: 6.11.2003)

Mayer-Rosa, D., and Jimenez, M. J. (2000). Seismic Zoning, State-of-the-art and recommendations for Switzerland, Federal Office for Water and Geology.

Mayerhof, G.G. (1956). Penetration Test and Bearing Capacity of Cohesionless Soils. Proceeding ASCE, Vol. 82, No. SM1.

Mollamahmutoglu, M., Kayabali, K., Beyaz, T., Koly, E. (2002). Liquefaction related building damage in Adapazari during the Turkey Earthquake of August 17, 1999, Engineering. Geo. 67 (2003), 297-307.

Nakata, T. (1982). A photogrametric study on active faults in the Nepal Himalayas. Jour. Nepal Geol. Soc., v. 2 (Sp. Issue), pp. 67-80.

Nakata, T., Iwata, S., Yamanaka, H., Yagi., H., and Maemoku, H. (1984). Tectonic landforms of several active faults in the Nepal Himalayas. Jour. Nepal geol. Soc., v. 4 (Sp. Issue), pp.177- 199.

National Society for Earthquake Technology-Nepal (NSET-Nepal) and GeoHazards International (GHI) Management project, (1999). Earthquake Scenario, product of the Kathmandu Valley Earthquake Risk

National Research Council (NRC) (1985). Liquefaction of Soils During Earthquakes, Committee on Earthquake Engineering, National Research Council, Report No. CETS-EE-001.

Natori, H., Takizawa, F., montozima, K., Nagata, S. (1980). Natural gas in the Kathmandu valley, No. 1: Geology. Chisitsu News No. 312, pp. 24-35.

Obermeier, S.F. (1996). Use of Liquefaction induced features for paleo-seismic analysis-An overview of how seismic Liquefaction features can be distinguished from other features and how their regional distribution and properties of source sediments can be used to infer the location and strength of Holocene paleo-earthquakes, Engineering geology 44, issue 1-4, pp 1-76,

Pandey, M.R., Molnar. P. (1988). The distribution of intensity of the Bihar Nepal Earthquake 15 January 1934 and bounds on the extent of the rupture zone, Jour. Nepal Geol. Soc., v 5.

Pandey, M.R., Sikrikar, S.M., Chitrakar, G.R., Pierre, J.Y. (1986). Report on Microtremor Survey of Kathmandu Valley, DMG Publication, 17 pp.

Protocol criteria (Subcommittee of the Geoscience Committee on Seismic Hazard Issues), 2000. Guidelines for Evaluating Liquefaction Hazards in Nevada. (http://www.nbmg.unr.edu/nesc/liquefaction.htm, date of access: 10.11.2003)

Rana, B. S. J.B. (1935). Nepal Ko Maha Bhukampa, (The Great Earthquake of Nepal) published by the author in Kathmandu, second ed.

Ranamagar, K.B. (2002). Report on soils and foundation investigations, National Judicial academy complex (Manamaiju) and Him Shikhar Coldstore (Jorpati), unpublished report, Geotech Consultancy Kathmandu.

Saiju K., Kimora.K., Dongol.G., Komatsubara T., and Yagi. H. (1995). Active Faults in South western Kathmandu basin, Central Nepal, Jour. Nepal Geol. Soc., v 11 (sp. Issue), pp 217-224.

Sakai, H. (2001). The Kathmandu Basin as archive of Himalayan uplift and past monsoon climate, Jour. Nepal Geol. Soc., v 25 (sp. Issue), pp.1-7.

Sakai, H., Fujii, R., Kunwahara, Y., Upreti, B.N., and Shrestha, S.D. (2001). Core drilling of the basin-fill sediments in the Kathmandu valley for palaeo climatic study, preliminary results, Jour. Nepal geol. Soc., v 25 (sp. Issue), pp. 19-32.

Sakai, H. (2001). Stratigraphic division and sedimentary facies of the Kathmandu Basin group, Central Nepal, Jour. Nepal Geol. Soc., v 25 (sp. Issue), pp.19-32.

Sakai, H. (2001). Danuwargaun Fault as a trigger for draining of the Palaeo-Kathmandu Lake, Central Nepal, Jour. Nepal Geol. Soc., v 25 (sp. Issue), pp.89-92.

Sakai, T., Gajurel, A.P., Tabata. H., Upreti, B.N. (2001). Small-amplitude lake-level fluctuations recorded in aggrading deltaic deposits of the Upper Pleistocene Thimi and Gokarna Formations, Kathmandu Valley, Nepal, Jour. Nepal geol. Soc., v 25 (sp. Issue), pp 43-51.

Seed, H.B. and Idriss, I. M. (1971). Simplified procedure for evaluating soil liquefaction potential, Jour. of the Soil Mechanics and Foundation division, ASCE, v. 107, pp 1249-1274.

Seed, H.B. (1979). Soil liquefaction and cyclic mobility evaluation for level ground during earth quakes, Jour. of the Geotechnical Engineering Division, ASCE, v. 105, pp. 201-255.

Seed, H.B., and Idriss, I.M., and Arango, I. (1983). Evaluation of liquefaction potential Using Field Performance data. ASCE Journal of Geotechnical Engineering, 109(3), 458-482.

Sharma, P. N. and Sing, O.R., (1966), Groundwater Resources of Kathmandu valley, Geological Survey of India, (unpublished).

Shrestha, O. M., Koirala, A., Karmacharya, S. L., Pradhanaga, U. B., Pradhan, R., and Karmacharya, R. (1998), Engineering and environmental geological map of Kathmandu Valley (1:50,000). Dept. Mines and Geology, HMG Nepal.

Shrivastava, L. S., Professor of Earthquake Engineering University of Roorkee, Seismic Microzonation of Hilly Terrain, unpublished report.

SILT Consult, (1996). Final report of detailed feasibility study on Kathmandu Natural Gas, Dept. Mines and Geo., Kathmandu (unpublished)

Skempton, A. W. (1986). 'Standard Penetration Test Procedures and effects in Sands of Overburden Pressure, Relative Density, Particle size, Aging and Over consolidation', Geotechnique, Vol. 36, No. 3.

Stocklin, J., Bhatterai, K.D. (1977). Geology of Kathmandu Area and central Mahabharat Range, Nepal Himalaya, HMG/UNDP Mineral Exploration Project, Kathmandu

Terzaghi, K., and Peck, R. B., (1967). Soil Mechanics in Engineering Practice (2nd edition), John Wiley and Sons, New York.

Tung, P. T. (2004). Road vulnerability assessment for earthquakes, M.Sc thesis, International Institute for Geo-Information Science and Earth Observation (ITC), Enschede.

UNDP/HMG/UNCHS (Habitat), (1994). Seismic Hazard Mapping and Risk Assessment For Nepal.

Wang, W. (1979). Some findings in soil liquefaction, Water Conservancy and Hydroelectric Power Scientific Research Institute, Beizing China.

Westen, C.J.van., Rengers, N., Soeters, R., Terlien M.T.J. (1994). An Engineering Geological GIS database for mountainous terrain, presented in 7th international IAEG Congress Lisboa Portugal, OFFPRINT A.A Balkema Rotterdam, Brookfield.

Yagi, H., Maemoku, H., Ohtsuki, Y., Saiju. K., and Nakata, T. (2000). Recent activities faults distributed in and around Kathmandu valley, Lower Himalayan Zone, Active fault research for the new millinium proceedings of the Hokundan Intl. Symposium and School on Active Faulting. pp. 557-560.

Yamanaka, H., 1982. Classification of geomorphic surfaces in the Kathmandu Valley and its concerning problems. Reprint. Congress. Assoc. Japanese Geogr., 21, pp. 58-59.

Yoshida, M. and Gautam, P. (1988). Magnetostratigraphy of Plio-Pleistocene lacustrine deposits in the Kathmandu valley, central Nepal, Proc. Indian. Nat. Sci. Acad., v. 54A, pp. 410-417)

Yoshida, M. and Igarashi, Y. (1984). Neogene to Quaternary lacustrine sediments in the Kathmandu Valley, Nepal, Jour. Nepal Geol. Soc., v. 4, pp. 73-100.

Youd, T. L., (1984a). Recurrence of Liquefaction at the same site, Proceedings, 8th World Conference on Earthquake Engineering, Vol. 3, pp. 2313-238.

Youd, T. L., and Perkins, D.M. (1978). Mapping liquefaction-induced ground failure potential, Proc. ASCE Civil Eng., v.104, n0. GT4, p. 433-446.

Youd, T. L., and Hoose, S. N. (1977). Liquefaction Susceptibility and geologic setting. Proc. Sixth world Conf. Earthquake Engineering, New Delhi, India 6, 37-42.

Youd, T. L., 1991. Mapping of earthquake induced liquefaction for seismic zonation. Proc. Fourth Int. Int. Conf. Seismic Zonation 1, pp. 111-147

Annex:

Table A: Table given with depth and elevation to bedrock level.

Well_ID	Location	Easting	Northing	Altitude	Depth	D_Bedrock	B_rock Elev.
B 10 /P21	Rabi Bhawan	627776	3064610	1304	275	272	1032
B 13	Tahachal	628474	3065547	1298	300	288	1210
B -15	Swayambhunath	627793	3066279	1310	229	212	1098
B 17	Singh Durbar	630955	3065101	1300	273.7	268	1032
B 19	Gaushala	632728	3066677	1315	113	111	1204
B 2	Bansbari	632688	3070725	1370	79.25	78	1292
B 20	Katunje	639011	3061774	1335	160	155	1180
B 24	Shanta Bhawan	628982	3063517	1295	60	60	1235
B 25	Surendra Bhawan	628970	3063211	1310	136	134	1176
BAL 2	Balaju	628460	3069017	1316	72.18	69	1247
BB1	Bansbari	632581	3070260	1366	280	274	1092
DK 6	Mahankal Chaur	633791	3068653	1320	110.7	103	1217
DMG 6	Bhrikuti mandap	630250	3065300	1294	570	549	745
DMG 7	Teku Kathmandu	628518	3064492	1279	359	346	933
DMG 5	Hyumat tole	628649	3065258	1285	451	400	885
GK 5	Gokarna	639546	3070712	1345	164.7	132	1213
JP 1	Jorpati	635688	3068070	1330	151	130	1200
JP 2	Jorpati				159	136	
MH 1	Bramhakhel	640586	3068310	1335	228.2	201	1134
MK 1	Mahadev Khola	628683	3069764	1270	200	183	1087
NAIK 1	Naikap	624638	3063901	1350	230	220	1138
NAIK 2	Naikap	624541	3063799	1340	240	238	1102
P 14b	Hotel Yak & yeti	630347	3066956	1310	293	290	1020
P 31b	Hortic dev. proj.	627686	3062524	1282	300	295	987
P 4	Katmandu, hatch	628423	3068644	1316	140	137	1179
P 01	Balaju Ind Dis.	628460	3069017	1315	72	70	1245
P 03a	Bottlers Nepal	628517	3068689	1315	300	295	1020
Paleo1	Rabibhawan	627811	3064569	1303	280	252	1051
PH 3	Pharping	627575	3055700	1260	185.5	182	1058
PR 14	Rabibhawan	627808	3064561	1304	282.3	252	1052
PR 19	Bhakt.woolen ind.	639249	3062254	1330	261	255	1075
PR 16	Nursing Camp.Sanepa	629043	3063538	1295	75	48	1247
NA 14	Airport (Golf Course)	633715	3066092	1320	225	215	1105
KM 1	Kalimati, Soaltee	627766	3064886	1270	280	280	990
BHD3	B&B Hospital	631282	3061316	1319	195	169	1150
AG68	Patan Hospital	629879	3062149	1315	189	189	1126

Point map

Table B: Structure of the table in ILWIS 3.2.

Columns	Domain	Description
Well_ID	Class	It gives the name of boreholes by which we can identify them.
Location	Class	It gives the name of the place where the borehole is located.
Easting	Value	Coordinate (Modified UTM)
Northing	Value	Coordinate (Modified UTM)
Depth	Value	It gives total depth of the borehole
Geologic unit	Class	It represents the geological units on which an individual borehole is situated. The geologic unit is based on the geology map prepared by DMG (Figure 2.5 Chapter 2)
Altitude	Value	It represents measured altitude of borehole from mean sea level.
Water table	Value	It gives the Piezometric surface level of water.
Nolake1	Class	It represents the boreholes that contain or not contain lake deposit
Assume_altitude	Value	It represents the altitude value derived from a DEM
Depthbed_rocknew	Value	It represents the actual depth at which bedrock is encountered by borehole.
Assumed_bedrock	Value	It represents depth to bedrock level, in which, values are assumed for some of the boreholes.
Assumed_bedrock_masl	Value	It represents assumed altitude of bedrock level above mean sea level
Bottom1_lakenew	Value	It represents depth of bottom of the lake deposit from the surface
Assumed_bottom1_masl	Value	It represents altitude of the bottom of the lake deposit from mean sea level.
Top1_lake	Value	It represents depth of top of the lake deposit from surface.
Top1_new_masl	Value	It represents altitude of top of the lake deposit from mean sea level.
Action	String	It is a column in which all borehole logs are stored. This column helps to operate double click action in point map.

Point map (Ilwis 3.2)

Table C: Structure of table in ILWIS 3.2 for Liquefaction Susceptibility analysis.

Columns (Attributes)	**Domains**	**Description**
Location	Class	It gives the name of the places where the borehole is situated
Easting	Value	Coordinates (Modified UTM)
Northing	Value	Coordinates (Modified UTM)
Total depth	Value	It gives the depth of borehole
Water table	Value	It gives measured water table at the time of construction
Altitude1	Value	It gives altitude value of the borehole location derived from the DEM.
Formation	Class	It represents the name of geological formation at which the borehole is situated, classification is based on geology map prepared by DMG (Figure 2.5)
Altitude	Value	This is the measured altitude value of borehole location.
Depth range 0-1, 1-2, 2-3 etc.	Class	It indicates depth wise lithological information for each borehole.
Data_Source	Class	It represents consultancy name from which data were derived
Hole_ID	Class	This represents the name of the borehole by which we identify them.
Lique_Class	Class	This represents liquefaction susceptible class, which was derived from qualitative analysis of boreholes in spreadsheet.
Totscore	Value	It is total score assigned to each borehole derived after qualitative analysis in Excel
Lique_Iwasaki	Class	This represents liquefaction susceptible class, which was derived from quantitative analysis of boreholes following Iwasaki method (1984) in spreadsheet. Yes means Liquefaction is likely at that particular borehole and no means no liquefaction will occur.

Rockworks99/2002

Table D: Structure of data format in Rockworks99.

Columns	Description
Well_ID	Main identifier, It representing borehole names
Easting	Coordinates (Modified UTM)
Northing	Coordinates (Modified UTM)
Collar	It represents altitude of borehole location
Lithology	It stores lithological information for all boreholes.
Post Lake deposit	These are the stratigraphic columns and represent the altitude for the top of different stages of sediment deposit in the valley and were used for generation of fence diagrams and stratigraphic projections.
Shallow Lake (3)	
Fluvio Deltaic (3)	
Deep Lake	
Fluvio Deltaic (2)	
Shallow lake (2)	
Fluvio Deltaic (1)	
Shallow lake (1)	
Proto Bagmati	
Bedrock	

Figures:

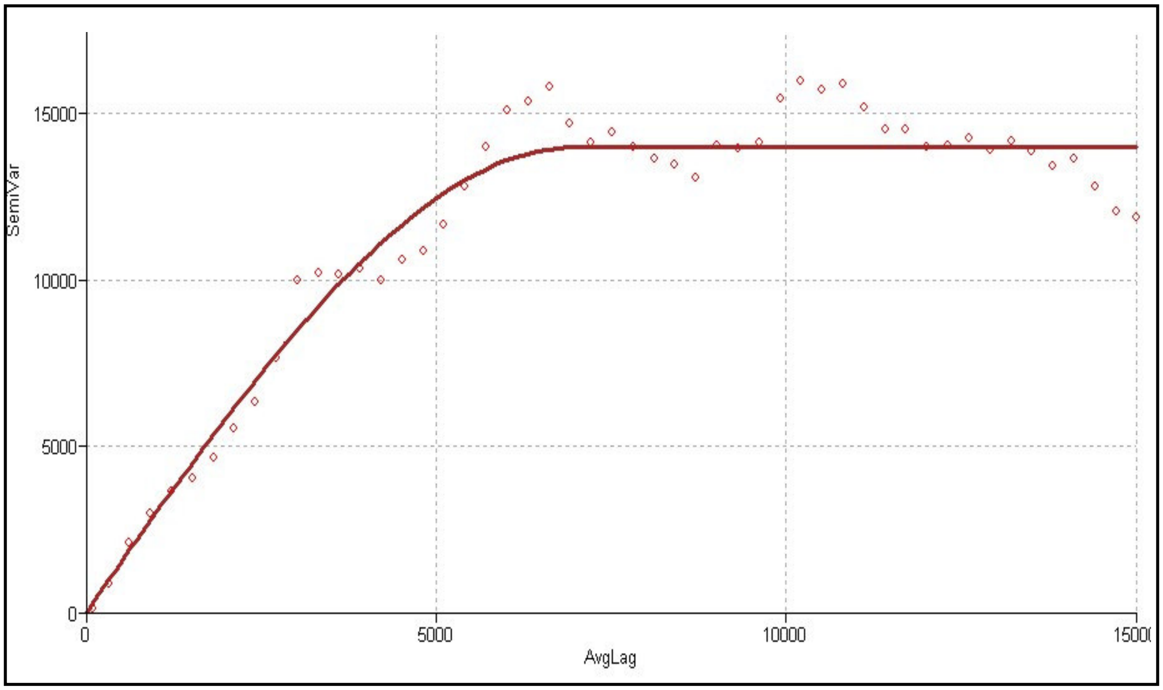

Figure A. Semi-variogram model for depth to bottom of Lake deposit
Nugget =15, Sill=14000, Range = 7000

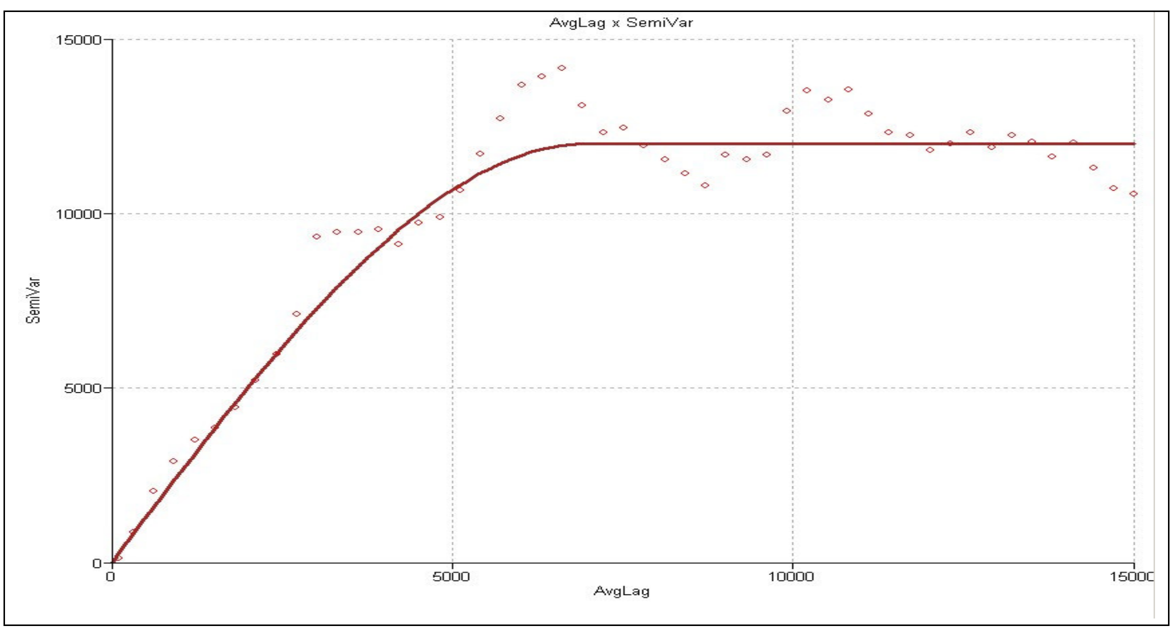

Figure B. Semi-variogram model for top of Lake deposit
Nugget =10, Sill=12000, Range = 7000

Section A - B

The section runs from Balaju (NW) to Lubhu (SE) (see Figure 1A). It shows that the lake deposit increases in the central portion of the valley and gradually fades away to the south-eastern part. Similarly the sediment above the lake deposit is more towards the north-western part (Samakhusi-Balaju area) and to the South it gradually fades away.

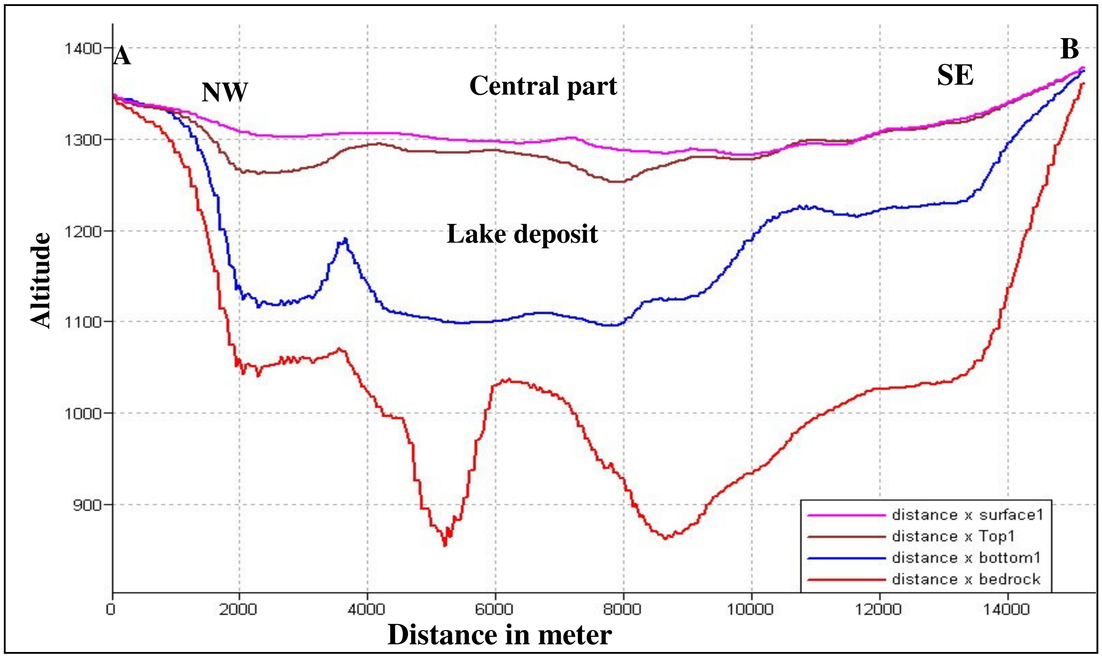

Figure C: *Subsurface Geological Cross section* along A-B

Section E – F

The section runs from Syuchatar (West) to the Bansbari, Bhaktapur East (Figure 1B). In this section we observe that the sediment above the lake deposit gradually increases to the East and decreases to the West. The lake deposit on the other hand thickens at the central part and also to the western part. Suddenly in Tigni (Bodegaon) area the thickness drops down and again further to the East the thickness increases. Similarly the thickness of the layer below the lake deposit appears more in the central and eastern part of the valley in comparison to the western part.

This cross-section is also compared with lithological cross section as shown in Figure 1 E. In this figure also the thickness of lake deposit is more towards West and to the central part, which is shown by boreholes Naik2, P29 and DMG10 (see Figure 1 E). Similarly at some places in the East the thickness of lake deposit suddenly decreases (borehole B22) and increases again further towards East, which is shown by boreholes B6, and BHD2 (see Figure 1 E). In this way we find that the layer models seem to be accurate (reasonable) when we compare them with borehole logs.

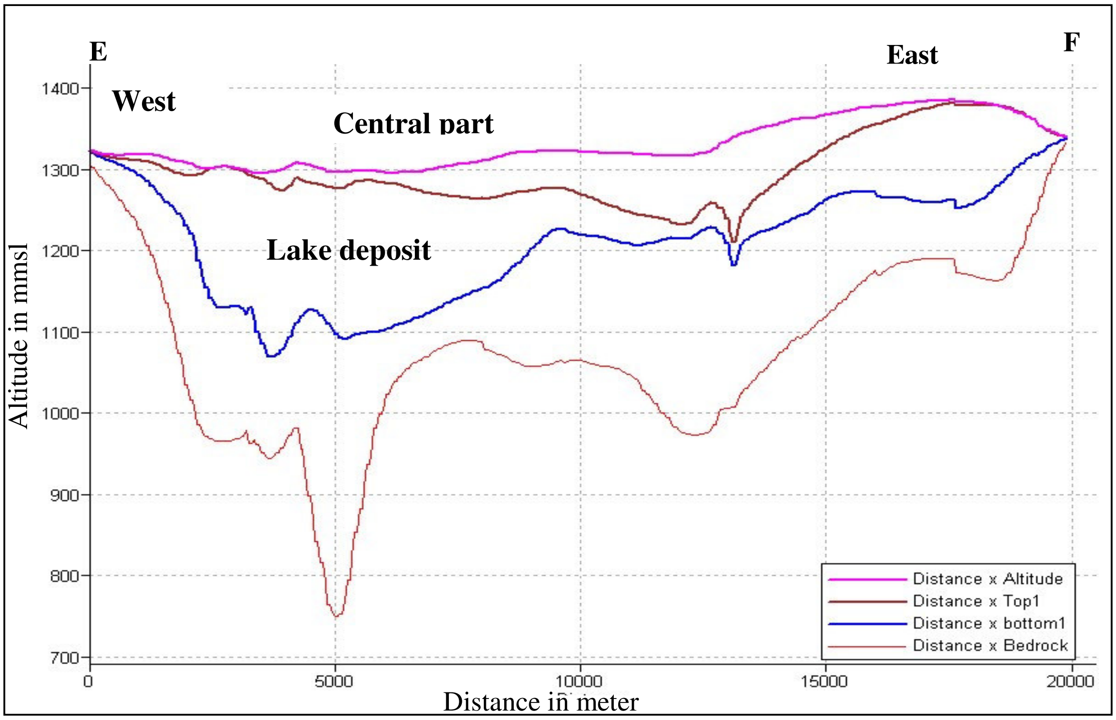

Figure D: Subsurface Geological Cross section along E- F

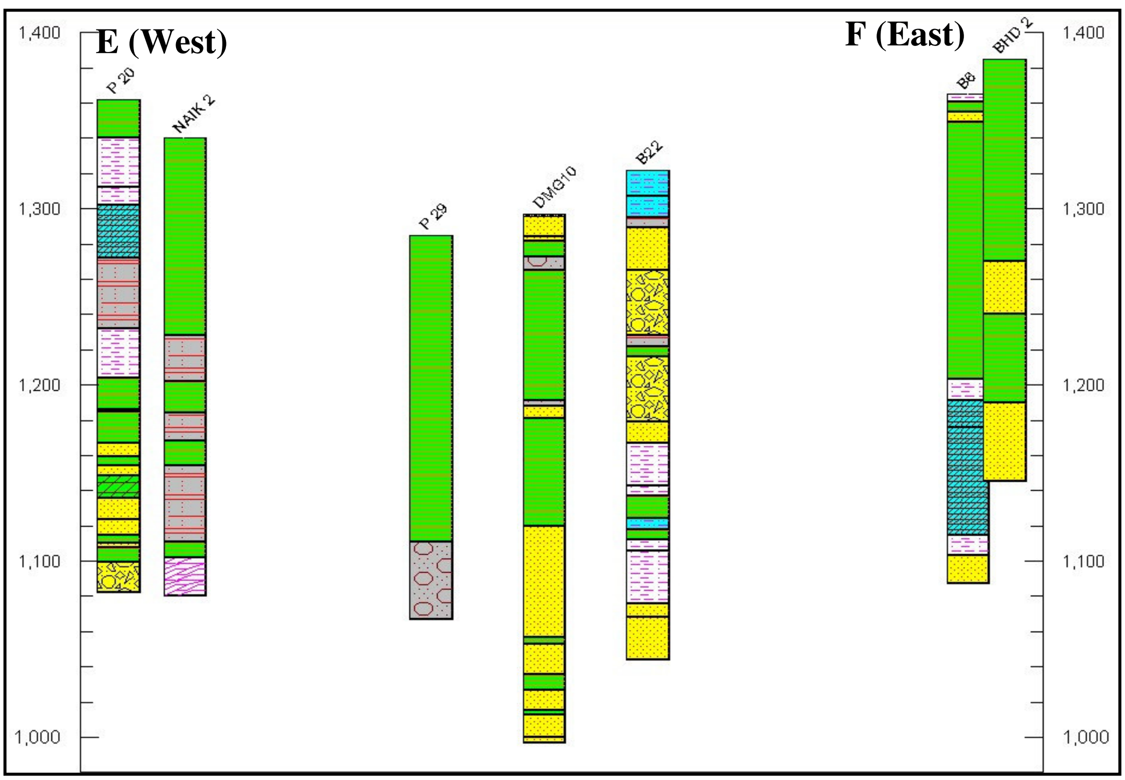

Figure E: Lithological cross section along A - B

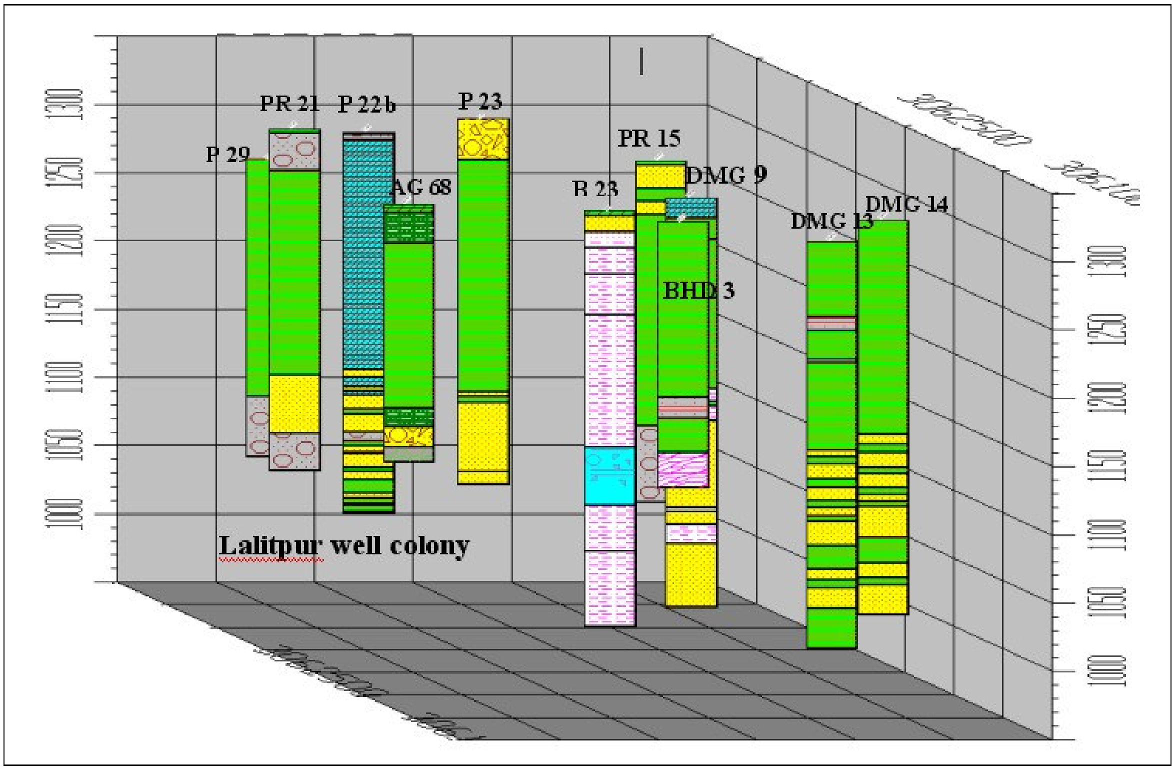

Figure F: Well colony at Lalitpur core area

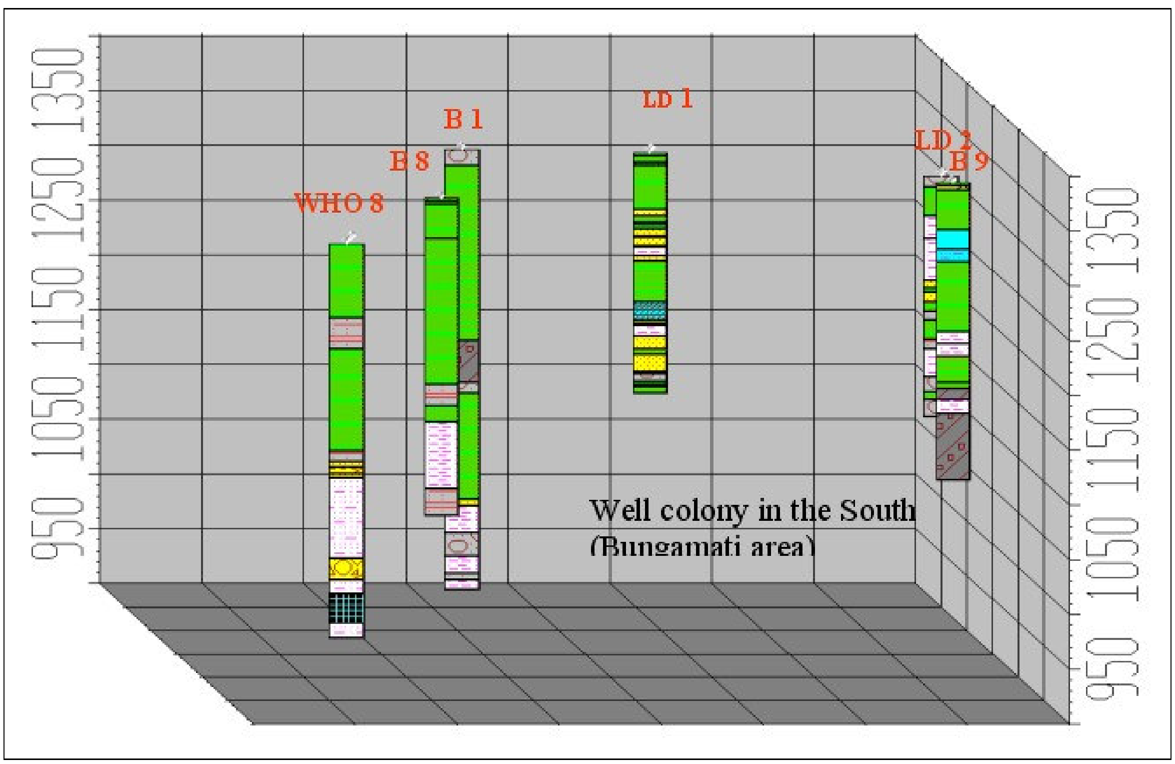

Figure G: Well colony at Southern part of the valley (Bungamati area).

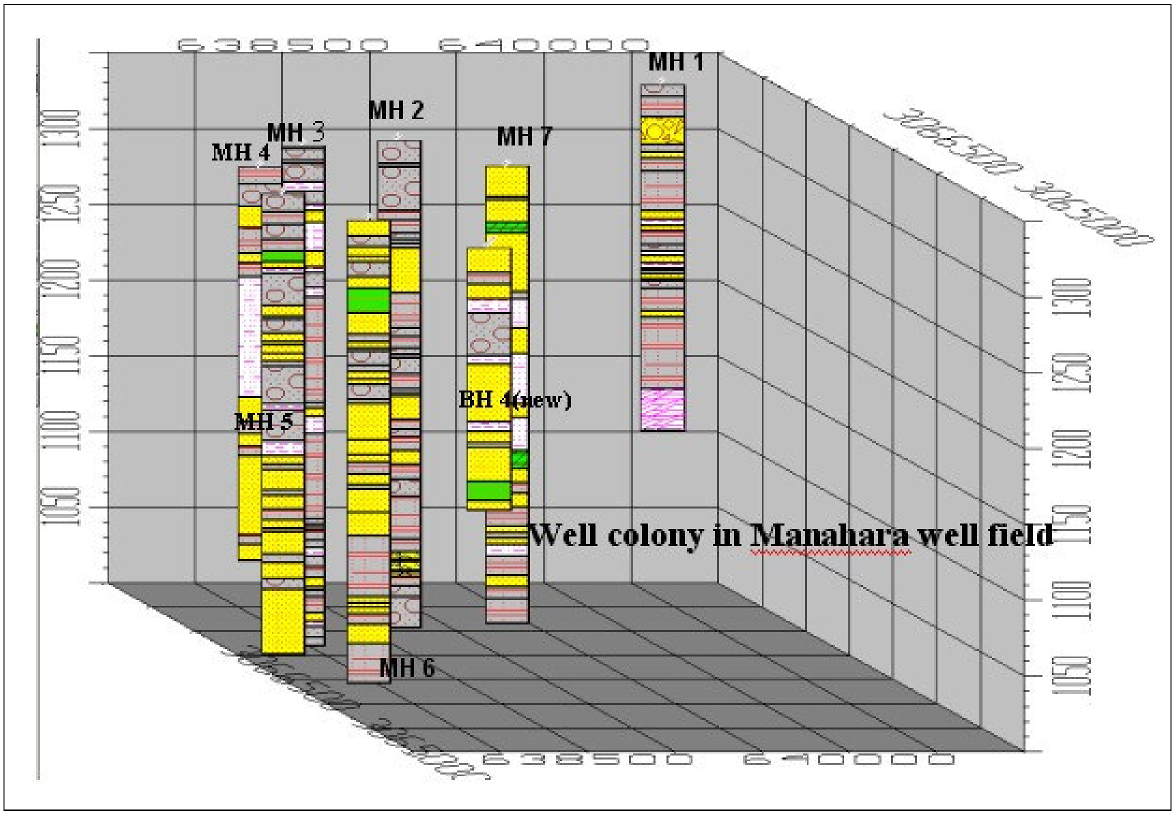

Figure H: Well colony at Manahara well field area

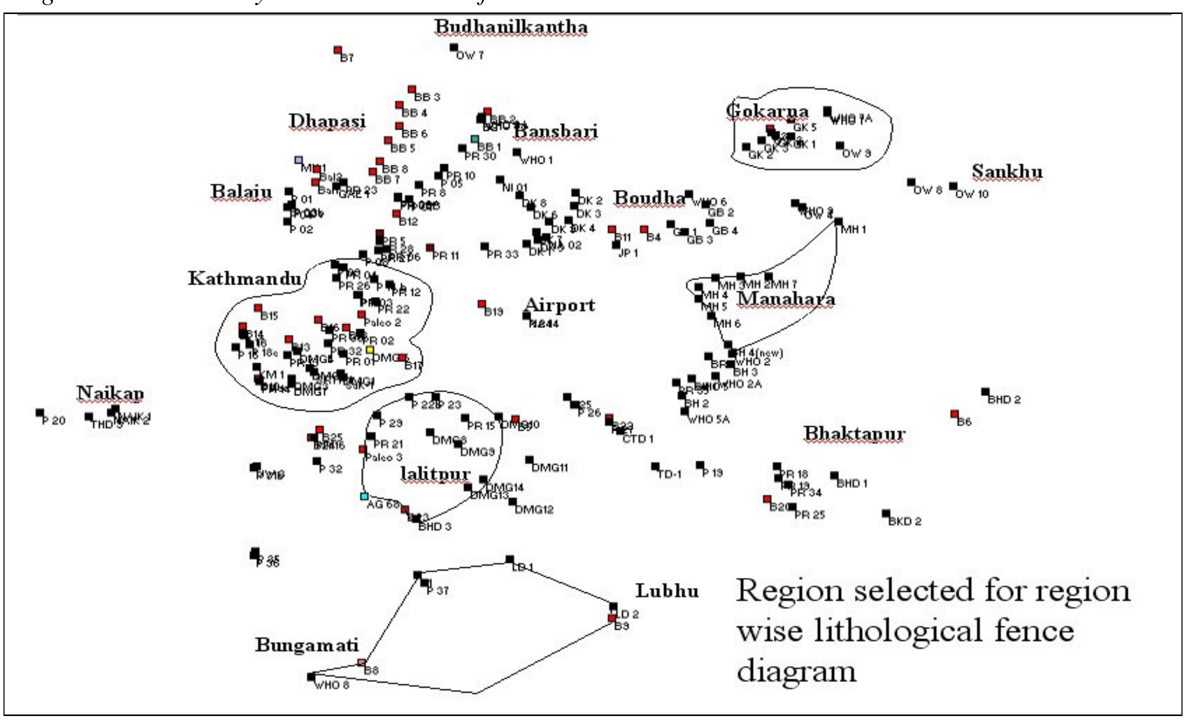

Figure I: location for region wise section.

Figure J: Legend for lithologs

Database Structure

Microsoft Access

Deep Boreholes

DEEPWELL_SOURCE: It contains the name of well group.
DEEPWELL_SHORT: Contains information such as Well_ID, Coordinates, Depth of the well, Altitude and Water level
DEEPWELL_DETAIL: Contains depth wise description of boreholes.

Shallow Boreholes

SHALLOWELL: It contains information such as borehole_ID, Coordinates, Location, Total depth of borehole, water table, Altitude1-altitude value derived from DEM. Altitude- Measured altitude value, Formation-Name of the geological formation on which borehole is situated, Source of the data.
SHALLOWELL_DETAIL: It contains strata wise lithology information.
GeoTechData: It contains attribute regarding geotechnical information.
SPTDATA: It contains information on depth wise N-value (derived from SPT test) for boreholes.

ILWIS3.2

Generation of GIS Layer Models

Point Map

Assume_altitude: Attribute map derived from elevation value.
Assumed_bedrock_masl: Attribute map derived from altitude value.
Assumed_bottom1_masl: Attribute map derived from altitude of bottom of lake deposit.
Assumed_top1_masl: Attribute map derived from altitude of top of lake deposit.
Border_100meters: Segment map border_basementnew converted into points with distance interval of 100m each.
Border_100meters_ID: Border_100meters point map converted into identifier domain
Border_100meters_zvalue: attribute map generated with altitude value of each point.
Borehole_withlog: borehole point map with log provided.
Glue_assume_altitude: Glued map between assume_altitude and Border_100meters_zvalue
Glue_Bor100Z_abedrock: Glued map between Assumed_bedrock_masl and Border_100meters_zvalue

Generation of Liquefaction Susceptibility Map

Point Map

Consultant_holes: It is borehole point map linked to attribute table.
Lique_class: Attribute map derived from column containing results from qualitative analysis of borehole samples using Juang and Elton method.
Lique_Iwasaki: Attribute borehole point map derived from column containing results from quantitative analysis using Iwasaki method.
Mask_borehole: masked out deep borehole point map, that contains sand and silt on uppermost part of a borehole.

Segment Map

Geom: A digitized map made by image interpretation
Geomor_phology: Edited segment map from Geom to generate final geomorphology map

Database structure

IlWIS3.2 CONTD.

Point map

Glue_Bor100Z_abottom1: Glued map between Assumed_bottom1_masl and Border_100meters_zvalue

Glue_Bor100Z_top1: Glued map between Assumed_top_masl and Border_100meters_zvalue

Segment Map

Border_100meters: densified segment map of bordernew_basement by distance 100m.

Bordernew_basement: A digitized segment map for unconsolidated sediment areas.

Catchment: catchment map for Kathmandu valley by DMG.

Fault: Fault map of Kathmandu valley prepared by DMG

Glue_segmaps: It is a glued map between Catchment map and subsurface geology map)

Lake_boundary: Assumed area covered by ancient lake in Kathmandu valley.

Main_river: represents main rivers in Kathmandu valley.

Road: Main roads in Kathmandu valley prepared by DMG.

Raster Map

Bordernew_base1: Rasterized from segment map Bordernew_basement.

Elevation: DEM of Kathmandu valley

Geological units: Geology (Geomorphology) map prepared by JICA.

H_surface: This is a map with altitude value derived by Kriging operation for point map Glue_assume_altitude.

H_top1: This is a map with altitude value for top of lake deposit derived by Kriging operation for point map Glue_Bor100Z_top1.

H_bottom1: This is a map with altitude value for bottom of lake deposit derived by Kriging operation for point map Glue_Bor100Z_abottom1.

H_bedrock: This is a map with altitude value for bedrock level from the surface derived by Kriging operation for point map Glue_Bor100Z_abedrock.

T_top: Thickness map for top of lake deposit

T_lake: Thickness map for lake deposit

T_top: Thickness map for bottom of Lake deposit.

Topomap Kathmandu: It is a toposheet map of Kathmandu.

Polygon Maps

Bordernew_basement: Polygonised map from segment map Bordernew_basement.

Geological Units: Geology map prepared by JICA 2002

Geology: It is also geology map prepared by DMG

Glue_segment: Subsurface geology map generated in this research work.

Segment Map

Lique_final: Edited segment map from Geom for liquefaction susceptibility map

Geom: A digitized map made by image interpretation

Geomor_phology: Edited segment map from Geom to generate final geomorphology map

Lique_final: Edited segment map from Geom for liquefaction susceptibility map

Raster Map

Elevation: DEM of Kathmandu valley

Lique_class: Rasterized map from point map lique_class

Lique_faction: Rasterized map Liquefaction from polygon map liquefaction.

Lique_Iwasaki: Rasterized map from point map lique_iwasaki.

Lique_mask_slice: Raster map derived from Kriging operation for qualitatively analyzed borehole data.

Liquetype: Rasterized UNDPmap

Lique_Polygon: Rasterized from polygon map lique_Polygon

Polygon Map

Geology: Geology map prepared by DMG.

Geomor_phology: Final Geomorphology map

Lique_faction: Polygonized Liquefaction map. The final map of liquefaction

Lique_polygon: Liquefaction map changed to identifier domain to link with attribute table.

LiquiUNDP: Liquefaction map prepared by UNDP.

Tables

Borehole_withlog: Main table consisting different attributes for deep boreholes.

Consultant: Main table consisting different attributes for shallow boreholes.

cross_iwasaki: cross table between lique_class rater map and lique_faction raster map.

Lique_cross: cross table between lique_class raster map and lique_faction map.

Lique_polygon: attribute table generated for map lique_polygon

Liquecros_final: Cross table between lique_class and lique_faction map

Database structure

Rockworks99/2002

It consists of all borehole data with lithological information, coordinate, depth and altitude values. Rockwork99 or Rockwork2002 software will be required to operate it.

ILWIS CONTD Generation of Layer models

Lake_boundary: Polygon map of Estimated lake area
Main_river: River map of Kathmandu valley

Tables

Border_100meters_ID: It is a table generated for assigning altitude values for all points generated from segment map
Borehole_withlog: It is a main table, which carries all information regarding attributes for borehole map.
Catchment: Table for catchment bound
Fault: It is a table containing information of faults (by DMG)
Glue_assume_altitude: a table generated for semi-variogram models
Glue_assume_top1: a table generated for semi-variogram models
Glue_assume_bottom1: a table generated for semi-variogram models
Glue_assume_bedrock: a table generated for semi-variogram models
Road: a table for road map

Liquefaction Analysis

It consists of following Excel files in which analysis was carried out for Liquefaction susceptibility analysis (both qualitative and quantitative)
CSR_calc: In this file, analysis is carried out according to Seed and Idriss method (1971)
Iwasaki_calc: In this file, analysis is carried out following Iwasaki et al. method (1984).
Qualitative_analysis: In this file, analysis was carried out using Juang and Elton's method (1991).
Clay thickness_for diff layers: This file contains information for deep borehole logs with thickness of clay layer deposit in each borehole.
Stratigraphic layer: This file contains information according to which, stratigraphic classification was made for different boreholes.
Earthquake_catalogue: This contains information regarding past earthquake, since 1255 AD.
Water_table data_DMG: It contains water table data measured by DMG (1998)
Watertabel_ENPHO: It contains water table data as measured by ENPHO